North Delta Food Subsidy Synthesis: Evaluating flow pulses from 2011-2019

Date: March 3, 2022

Authors: Brittany Davis, Jesse Adams, Mallory Bedwell, Aaron Bever, Dave Bosworth, Theodore Flynn, Jared Frantzich, Rosemary Hartman, Jeff Jenkins, Nicole Kwan, Michael MacWilliams, Amanda Maguire, Sarah Perry, Catarina Pien, Traci Treleaven, Hailey Wright, Laura Twardochleb

Ecosystem Monitoring, Research & Reporting Branch
Division of Integrated Science and Engineering

CALIFORNIA DEPARTMENT OF
WATER RESOURCES

Suggested Citation: Davis et al. 2022. North Delta Food Subsidy Synthesis: Evaluating Flow Pulses from 2011-2019. Department of Water Resources, Division of Integrated Science and Engineering. *Draft*.

Executive Summary

The food-limited nature of the San Francisco Estuary (SFE) is hypothesized to be a primary driver of fish declines in the area, particularly the endangered Delta Smelt. In the past, beneficial increases in phytoplankton and zooplankton have been observed following above average flow events (i.e. flow pulses) in the North Delta region of the upper SFE. These observations led to an experimental strategy led by the California Department of Water Resources (DWR), called the North Delta Food Subsidy (NDFS) Study. The NDFS study has evolved into an ongoing adaptive management action for annual consideration to improve food for Delta Smelt. Through coordinated water operations, an augmented flow pulse (i.e. a managed flow action) in summer and/or fall is sent through the Yolo Bypass with the goal to create positive net flow downstream to redistribute food through the North Delta and potentially trigger a downstream plankton bloom if nutrient ratios become more optimal for plankton growth. The following report synthesizes abiotic and biotic responses following high- and low-flow pulses in the North Delta from 2011 to 2019 that include managed (actions) and non-managed flow pulses, identifies remaining knowledge gaps in science and monitoring, and evaluates the efficacy of managed flow actions to improve adaptive management of the NDFS strategy.

Major findings

- The flow pulses succeeded in producing net positive flow out of the Yolo Bypass and Cache Slough Complex (Chapter 2).

- Chlorophyll and plankton increased in upstream regions with high-flow, managed pulses. We did not see a response in downstream phytoplankton abundance to flow pulses, but there was high variability between years, with highest biovolume in 2016 (Chapter 4).

- Zooplankton varied highly between years, with especially high abundance in 2016, but did not show clear responses to flow pulses (Chapter 4).

- Other factors such as nutrient ratios (Chapter 3), contaminants (Chapter

3) or clam grazing (Chapter 4) downstream may limit the benefits of upstream transport on downstream plankton. In particular, contaminant concentrations increase during flow pulses due to the increased flow (Chapter 3).

- We found no evidence for changes to overall fish abundance due to the flow pulses. We found no evidence for increased straying of salmonids from flow pulses; however, straying is influenced by a number of factors leading to inconclusive results. Salmon present in the bypass during flow pulses may be acutely exposed to poor water quality. More targeted research is needed on the impact of NDFS on fishes (Chapter 5).

Management Recommendations

The effects of flow pulses on downstream food web are uneven, with relatively positive responses in three high-flow pulse events (2011, 2012, 2016), but two other managed flow pulses (2018, 2019) showed only modest effects. The reasons for these differences in efficacy are unclear and worthy of continued investigation, implementation of future actions, and adaptive management. While DWR is committed to the interagency Delta Coordination Group collaborative structured decision making (SDM) process to determine implementation of summer-fall actions, we recommend future NDFS actions for consideration in the SDM process. A high priority for consideration is to conduct another summer action, redirecting Sacramento River flow and enhancing monitoring to increase our power to compare effects of flow pulse type. Alternative flow pulse types should also be evaluated to determine if longer duration, but lower magnitude flows (as in 2011, see Chapter 2) create more optimal conditions for the food web (using Sacramento River and agriculture return water). Ultimately, after several more years of adaptive management, we hope to conclude if benefits from this strategy meet the goals of improving food availability for species conservation.

Contents

Figures and Tables

Figures

Tables

Equations

Abbreviations and Acronyms

AF	Acre Feet
BiOp	Biological Opinion
CDEC	California Data Exchange Center
CDFW	California Department of Fish and Wildlife
CFS	Cubic Feet per Second
Chl a	Chlorophyll a
CPUE	Catch Per Unit Effort
CSC	Cache Slough Complex
CWT	Coded Wire Tag
DCG	Delta Coordination Group
DJFMP	Delta Juvenile Fish Monitoring Program
DO	Dissolved Oxygen
DWR	Department of Water Resources
EDI	Environmental Data Initiative (https://environmentaldatainitiative.org/)
EDSM	Enhanced Delta Smelt Monitoring Program.
FCCL	Fish Conservation and Culture Facility
FMWT	Fall Mid-Water Trawl
FTP	File Transfer Protocol
IEP	Interagency Ecological Program
KLOG	Knights Landing Outfall Gates
MA-Ag	Managed Agricultural Flow Action
MA-SR	Managed Sacramento River Flow Action
NCRO	North Central Region Office
NDFA	North Delta Flow Action
NDFS	North Delta Food Subsidies Study
NF	Non-managed Flows
NWIS	National Water Information System (https://waterdata.usgs.gov/nwis)
STN	Summer Townet Survey
QC	Quality Control
TAF	Thousand Acre Feet
USGS	United States Geological Survey
WDL	Water Data Library (https://wdl.water.ca.gov/waterdatalibrary/)
WWFRF	Wallace Weir Fish Rescue Facility
WY	Water Year
WQ	Water Quality
VIA	Visible Implant Alpha
YBFMP	Yolo Bypass Fish Monitoring Program

Chapter 1 Introduction

The North Delta Food Subsidies (NDFS) – Colusa Basin Drain Study monitors and evaluates the effects of flow pulses (and managed flow actions) in the North Delta on the food web. Flow pulses due to seasonal agricultural activities have occurred in the summer and/or fall for decades; however, routine science and monitoring activities, and assessments of food web responses began in 2011, and have occurred annually depending on water year and resources. The purpose of this synthesis report is to summarize and evaluate the ecological effects of flow pulses of varied magnitudes (low- and high-flow) and durations from 2011-2019 to increase our understanding of the efficacy of managed flow actions (e.g., high-flow pulses in 2016, 2018, and 2019) for increasing food availability in the North Delta (Figure 1-1) and inform future planning of the NDFS management strategy. This synthesis includes a series of chapters on physical and ecological responses to flow pulses: hydrodynamics, water quality, lower trophic food web levels, and fishes. Each chapter describes specific objectives, predictions, methods used to collect and integrate datasets, and summarizes the analysis of effects of pulses across the years.

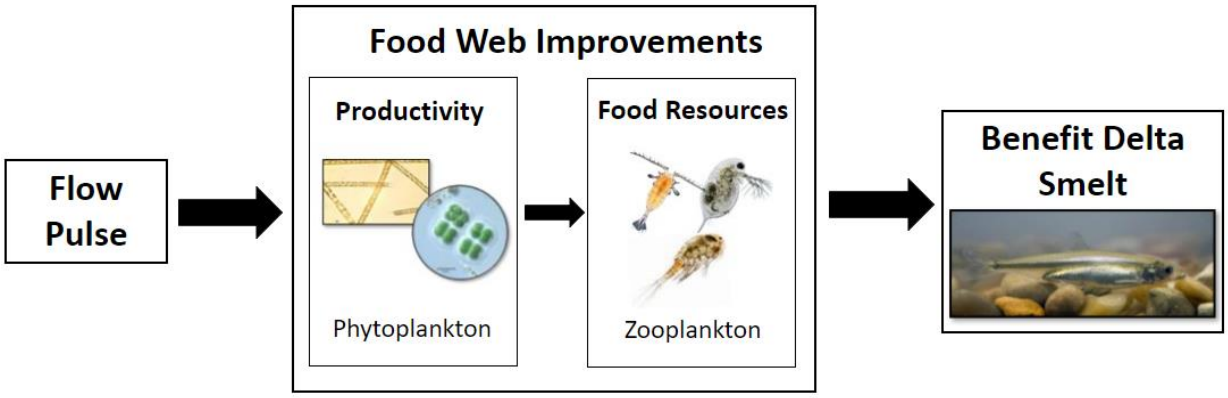

Figure 1-1. Conceptual diagram of the North Delta Food Subsidy study hypothesis; a moderate flow pulse is predicted to improve food web productivity and/or food availability in known habitat of Delta Smelt.

1.1 Regulatory Background

The California Department of Water Resources (DWR) began monitoring the lower trophic food web (phytoplankton, zooplankton, and drift invertebrates) in the Yolo Bypass in 1998 as part of the Yolo Bypass Fish Monitoring Program, a directed study of the Interagency Ecological Program (IEP). In 2011 and 2012, the program observed larger than normal summer-fall flow pulses in the bypass followed by increases in Delta plankton and food web productivity (Frantzich et al. 2018). Prior to these observations a phytoplankton bloom (>10 ug/L of chlorophyll a; Mueller-Solger et al. 2002) had not occurred for over a decade (Baxter et al. 2015). These observations led to the NDFS Study, conducting managed flow actions in the Yolo Bypass and monitoring their effects on the food web. The study was included as a food subsidy action in the Delta Smelt Resiliency Strategy (DSRS; CNRA 2016). The DSRS is a science-based document that identified a suite of thirteen applied and adaptive science strategies that could be implemented to benefit Delta Smelt by promoting resiliency to altered habitat and drought. In 2016, DWR implemented the first experimental managed flow action in the North Delta for NDFS, followed by subsequent actions in 2018 and 2019. Implementation was done in coordination and with funding from the California Department of Fish and Wildlife (CDFW), United States Bureau of Reclamation (USBR), and State Water Contractors.

Following several initial years of study (Frantzich et al. 2018, 2021; Twardochleb et al. 2021), the NDFS was listed as a food subsidy action to support Delta Smelt as part of USBR and DWR's Proposed Action for coordinated long-term operations of the Central Valley Project and State Water Projects, followed by inclusion in corresponding USFWS and NMFS Biological Opinions (BiOp; USFWS 2019; NMFS 2019), and the CDFW Incidental Take Permit (ITP; DFW 2020) issued to DWR for the State Water Project operations. The NDFS is part of a suite of potential Summer-Fall Habitat Actions to support Delta Smelt. As prescribed in the BiOp and ITP, the inter-agency Delta Coordination Group (DCG) and with support from Science and Operations technical groups will now decide on implementation of Summer-Fall actions each year. In general, the NDFS will be considered for implementation per the DCG Structure Decision Making (SDM) process evaluating the suite of actions (e.g., NDFS, Suisun Marsh Salinity Control Gates, 100 TAF, etc.) to take place in a given Sacramento Valley hydrologic

year type[1]. Implementation of NDFS would likely be considered in Above Normal, Below Normal, and Dry years with some exceptions. If Spring conditions in a Wet year bring increased plankton, there could also be an action in that summer-fall. It is important to note, that in the absence of a NDFS managed flow action (resulting in a high-flow pulse), there will still be a small to moderate flow pulse (non-managed) in the North Delta due to local agricultural activities.

1.2 Scientific Background

Around the world, coastal regions are among the most altered ecosystems due a variety of anthropogenic stressors (Lotze et al. 2006; Worm et al. 2006). Like other coastal estuaries, the San Francisco Estuary (SFE) has experienced a wide array of stressors including water diversions, channelization, diking and draining wetlands, invasive species, contaminants, and increasing urbanization (Nichols et al. 1986; Cloern and Jassby 2012). Together these stressors have led to broad changes in ecosystem functions, degradation, collapse of fish communities of the SFE, and endangered species listings (Sommer et al. 2007; Thomson et al. 2010). One species of critical concern for extinction is the endangered Delta Smelt (*Hypomesus transpacificus*), endemic to the SFE. Delta Smelt are an annual fish endemic to the SFE. They are listed as Threatened under the federal Endangered Species Act and Endangered under the California Endangered Species Act (USFWS 1993; CDFG 2010), so they are particularly important for resource management. Protections for the species can lead to alterations in water diversions and challenges to the agriculture industry in California (Moyle et al. 2018; Service 2007).

A key factor contributing to the decline of Delta Smelt is the alteration and decline in the plankton food web of the SFE (Sommer et al. 2007; Mac Nally et al. 2011). Primary productivity in the SFE has been declining to low levels since the 1970s (Jassby 2008; Cloern 2019). Compared to other estuaries, the decline in primary productivity in the SFE appears unique (Cloern and Jassby 2008) and likely due to anthropogenic stressors described above (e.g., water exports, invasive species). Concurrent with productivity declines have been declines in zooplankton (i.e. fish food). For example, densities of calanoid

[1] As determined by the Sacramento Valley Index: https://cdec.water.ca.gov/reportapp/javareports?name=WSIHIST

copepods, a key prey of Delta Smelt have decreased. Increased invasive species of copepods (*Limnoithoina, Pseudodiaptomus forbesi, Acartiella sinensis*) have increased competition and predation on native copepods, and clams (*Corbicula fluminea, Potamocorbula amurensis)* that filter plankton have contributed to the decline in the food availability for Delta Smelt and other pelagic fishes including Threadfin Shad, Longfin Smelt, and Age-0 Striped Bass in the early 2000s (Mac Nally et al. 2010; Hammock et al. 2019).

While overall productivity in the SFE is low, plankton levels can be relatively high in some regions. For example, the Yolo Bypass and Cache Slough Complex (CSC) in the upper North Delta of the SFE provide a source of phytoplankton biomass to the Delta during winter and spring when the bypass is inundated (Lehman et al. 2008; Sommer et al. 2004); however, regional contributions of the Yolo Bypass and CSC to the food web during the drier summer and fall months (Frantzich et al. 2018) are likely reduced due to changes in hydrology such as low or net negative flows from local water diversions.

The Yolo Bypass is a 24,000 hectare floodplain and tidal slough that is the primary flood control system for Sacramento, CA. During wet conditions the bypass typically has positive outflow downstream to CSC and Lower Sacramento River; however, during dry conditions the Yolo Bypass is reduced to a narrow perennial canal, called the Toe Drain. Even during these dry conditions, the bypass is known to have higher densities of plankton compared to the rest of the estuary (Mahardja et al. 2019). The CSC, a region of tidal wetlands and dead-end sloughs, is connected to the base of the Yolo Bypass Toe Drain and is one of the remaining habitats characteristic of the historic estuary. The CSC includes complex habitat such as small sloughs, channels, and open water which can influence food production and is likely why it has served as an important habitat for Delta Smelt across all life-stages (Sommer and Mejia, 2013) and other native fishes (Young et al. 2021). Together the high residence time and shallow channels of the Yolo Bypass and CSC likely promote increased plankton production. Although summer and fall lead to dry conditions in the North Delta, the problem is exacerbated with high water diversion rates in the Yolo Bypass and CSC. These diversions, for agriculture, recreation, and water management significantly change hydrology by reversing outflow to low or net negative (i.e. net flow is upstream after accounting for tidal effects) (Frantzich et al. 2018). This reversal in net flow

is likely to inhibit transport of lower trophic level biomass to downstream areas of the estuary, transporting food away from known Delta Smelt habitat.

After two decades without a fall phytoplankton bloom in the lower Sacramento River, a 5-fold increase in phytoplankton biomass occurred in 2011 and a bloom of 10-15-fold increase in 2012 occurred following larger than normal flows in the North Delta resulting from wet conditions (2011) and agriculture drainage (2012) (Frantzich et al. 2018). These flow pulses restored positive net flow (downstream) and were hypothesized to contribute to the bloom. After observing the ecological benefits of these flow pulses and complex habitat in the North Delta, DWR (with interagency collaboration) developed the NDFS, a targeted management strategy to restore net flow during summer and fall to improve the food web in Delta Smelt habitat. Managed flow actions were implemented in 2016 and subsequent years (2018 and 2019). This management strategy, was conducted using an adaptive management approach, using science to inform planning of objectives and design, implementation of monitoring, evaluation of efficacy, and inform improvements to the action in future years. Using existing infrastructure, supplemental flows from the main-stem Sacramento River were redirected through Ridge Cut Slough and Yolo Bypass in effort to restore positive net flow during the summer-fall (see Figure 1-2), redistribute food rich water downstream to habitats such as Cache Slough Complex and lower Sacramento River, and potentially increase productivity (Figure 1-1). Adaptive management strategies like managed flow actions, as well as non-managed flow pulses, can moderately change flow regimes (e.g., high or low positive net flow) and have regional impacts on lower trophic food web productivity (Frantzich et al. 2018, 2021; Twardochleb et al. 2021) that may benefit fishes such as Delta Smelt.

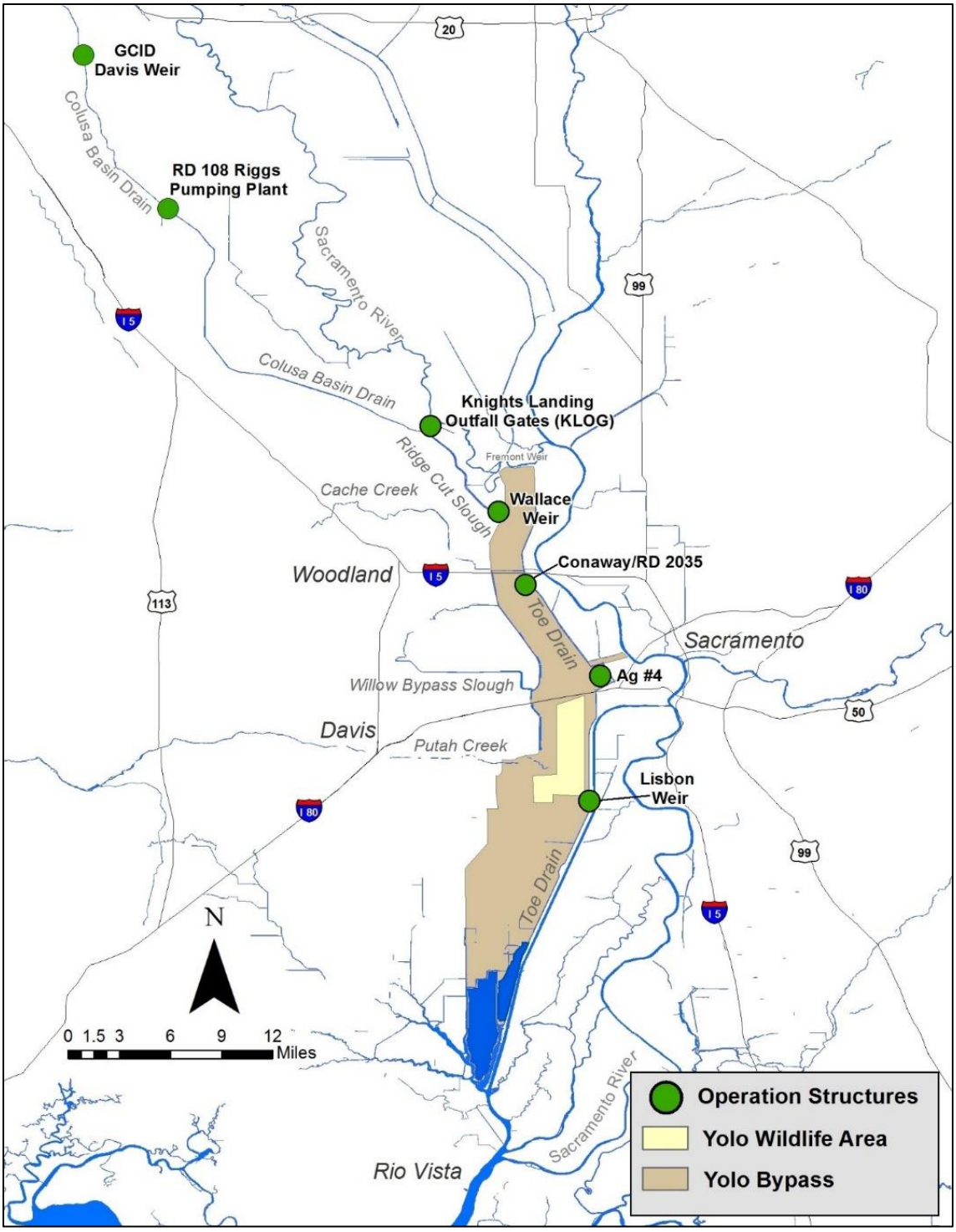

Figure 1-2 Map of Yolo Bypass tributary inputs and key operation structures used in the NDFS managed flow actions. Structures are used to redirect Sacramento River water from upstream Keswick dam releases or agriculture return drainage into the Ridge Cut Slough and Yolo Bypass.

1.3 Objectives

The goals of this study are 1) to better understand the effects of flow pulses on water quality and biota in the Yolo Bypass and downstream, 2) to evaluate where possible the efficacy of managed flow actions compared to flow pulses without intervention by assessing benefits to downstream habitat of Cache Slough Complex that may include redistributed water, transport of plankton, and overall increased food availability, 3) identify remaining knowledge gaps, and 4) use this synthesis to improve adaptive management of the North Delta Food Subsidies Study.

1.3.1 Research Questions

The overarching hypothesis for the North Delta Food Subsidies Study is that high-flow pulses resulting from managed summer or fall flow actions increase net positive flow downstream, transport of plankton downstream, and therefore food availability for juvenile and sub-adult Delta Smelt (Figure 1-1). However, with almost a decade of flow pulses now in the Yolo Bypass, habitat and food web responses to pulses have been variable, and are potentially influenced by water year, pulse magnitude, and/or antecedent Delta conditions (Table 1-1). The following are a series of general questions the synthesis addresses. Furthermore, each chapter on hydrodynamics, water quality, lower trophic food web levels, and fishes includes specific questions.

1. How do hydrology, water quality, and plankton alter along the north-south axis of the Yolo Bypass (upstream) and Cache Slough Complex (downstream) before, during, and after summer-fall flow pulses since 2011?
    a. Do flow pulses increase primary production (e.g., chlorophyll and phytoplankton) downstream or is productivity localized to the Yolo Bypass upstream?
    b. Is there evidence of downstream influences (i.e. clam grazing, ammonia-paradox) that may limit phytoplankton productivity and flow pulse benefits?
    c. Do flow pulses alter zooplankton densities and composition, and is there evidence of transport downstream?

2. What are the effects of flow pulses on water quality (nutrients and contaminants)?
    a. How do pesticide composition and concentrations in water and zooplankton vary across flow pulses and habitats?
3. Do summer-fall flow pulses in the Yolo Bypass influence fishes?
    a. Is there evidence to suggest benefits for Delta Smelt or other native species?
    b. Is there evidence to suggest negative effects on adult salmonids? For example; do flow pulses cause more adult salmonids to stray into the Yolo Bypass than would if no pulse occurred?

1.3.2 Predictions

A summary of general predictions for the effects of high and low flow pulses on the North Delta ecosystem are provided in Table 1-2. A key challenge with understanding flow pulse impacts on water quality and biota is the difficulty in differentiating changes due to flow pulses or season; however, the current synthesis report aims to untangle some of these interactions where possible.

We predict that flow pulses alter the hydrodynamics in the North Delta by temporarily restoring positive net flow during the summer-fall. However, the magnitude and duration of the pulse (high or low flows), likely influences whether pulse effects reach downstream at Cache Slough Complex where there is increased tidal forces and influence from the Sacramento River (Table 1-1). Lower magnitude pulses (without management intervention) are predicted to have more localized effects upstream in the Yolo Bypass, whereas we predict high magnitude flow pulses are large enough to influence downstream habitat.

In general, most flow pulses (with and without management intervention) result from agricultural activities and return water, therefore, it is anticipated that flow pulses will increase salinity and potentially increase water temperature marginally within the Yolo Bypass and downstream in the upper Cache Slough Complex area; however, temperature is influenced by season and while variable, should also decrease across the summer-fall season. Moreover, air temperature appears to be a stronger driver of water temperature than flow in the SFE (Wagner et al. 2011). In addition, we expect that following most high-flow pulses, downstream nutrient concentrations (i.e.

nitrogen and phosphorus) and phytoplankton biomass will increase due to initial transport from the Colusa Basin Drain and upper Yolo Bypass and/or in-situ productivity. Alternatively, we may predict neutral or decreased nutrients (and therefore phytoplankton) downstream due to suboptimal nutrient ratios from transported water upstream, or nutrient uptake by phytoplankton (Dahm et al. 2016). With potential increases in primary productivity and phytoplankton we predict increases in transport of zooplankton and/or in-situ zooplankton production both upstream and downstream. We also predict that transport of agriculture water downstream may increase detections of contaminants, as water soluble pesticides, pesticides bound in sediments, and increased concentrations of pesticides detected in zooplankton.

Managed flow pulses were designed to improve habitat conditions for Delta Smelt by increasing habitat connectivity and food availability downstream in Cache Slough Complex and the lower estuary. By similar logic, flow pulses may also improve habitat conditions for other native fishes, such as Longfin Smelt (*Spirinchus thaleichthys*), and Sacramento Splittail (*Pogonichtys macrolepidotus*). However, improved conditions from flow pulses may also increase the abundance of non-native fishes. This study explores fish assemblage from a variety of gear types during summer-fall to assess potential indirect effects of managed and non-managed actions in the North Delta. Due to the rare detections of wild Delta Smelt we do not predict to detect significant increases in Delta Smelt abundance downstream, and instead have begun to use applied experimental studies to assess how flow pulses may enhance food resources for Delta Smelt through application of caged-fish experiments.

Managed flow pulses are not expected to have significant effects on emigrating juvenile Chinook Salmon (*Onchorhyncus tshawytshca*) and steelhead (*O. mykiss*) during typical action periods (July-October). Pulses are not expected to affect listed winter- or spring-run adult Chinook Salmon migration, however, adult fall-run Chinook and steelhead can occur in the study area during flow pulses. The Yolo Bypass Fish Monitoring Program (YBFMP) has observed adult fall-run Chinook Salmon in the fyke trap catch in September, with the majority of catch in October and November (Sommer et al. 2013). Straying appears to be a long-term issue triggered by strong tidal flows at the base of the Yolo Bypass, which creates navigation issues for upstream migrating adult salmon. Specifically, tidal flows are larger through Cache

Slough Complex than the adjacent Sacramento River, likely guiding many fish towards Yolo Bypass. It is unclear how Sacramento River origin water used to generate summer-fall NDFS pulses may influence attraction signals for Chinook Salmon as the water likely undergoes dramatic chemical and physical changes. Due to the known straying of salmonids into the Yolo Bypass, CDFW has been operating an upstream fyke trap below Wallace Weir since 2014. In 2018, CDFW observed fall-run Chinook Salmon mortality in the immediate project area during late September, however, it is uncertain the correlation with the managed, high flow pulse. More investigation of the mortalities of these fish is warranted. In fall 2019, CDFW operated a new and more efficient Fish Rescue Facility at Wallace Weir. This ongoing trapping operation will allow for closer monitoring of straying effects of managed flow actions.

Table 1-1. Flow pulse magnitude and duration measured at Lisbon Weir in the Yolo Bypass (Yolo) and modeled between the Cache Slough Complex (CSC). WY indicates water year type including wet (W), below normal (BN), dry (D), and critically dry (C). Flow pulse types include high and low flows, some of which had management intervention. Flow pulse duration was measured or modeled as the number of days with positive flow at LIS in Yolo Bypass, or the number of days with net positive flow out of CSC. Flow pulse magnitude is measured in maximum daily average cubic feet per second (cfs) and thousand-acre feet (TAF). In the absence of flow pulses, net flow is negative (upstream) through the Yolo Bypass during this time. Asterisks besides year indicate pulses that were the result of planned management actions.

Year	WY Type	Flow Pulse Type	Duration		Magnitude (Yolo)			Date Range of pulse (Yolo, estimated)
			Days Net Positive Flow (Yolo, measured)	7-Day Ave Net Positive Flow (CSC, modeled)	Max Daily Ave Net Flow (cfs, measured)	Total Net Positive Flow Volume (TAF, measured)	Volume Relative to No Flow Pulse (TAF, modeled)	
2011	W	High	63	16	412	22.4	16.6	Aug 23 – Oct 24
2012*	BN	High	38	26	723	27.2	31.4	Aug 26 – Oct 2
2013	D	Low	42	-	283	11.4	18.5	Aug 22 – Oct 2
2014	C	Low	15	-	239	2.5	2.6	Sep 9 – Sep 23
2015	C	High	42	-	383	17.9	28.4	Aug 21 – Oct 1
2016*	BN	High	19	5	546	12.8	15.8	Jul 14 – Aug 1
2017	W	Low	12	2	125	1.0	2.6	Aug 29 – Sep 18
2018*	BN	High	30	14	548	19.8	23.6	Aug 28 – Sep 26
2019*	W	High	26	24	750	31.6	32.4	Aug 26 – Sep 21

Note: Flow pulse types were assigned as either high- or low-flow pulses based on the magnitude and duration of the measured flow pulses at Lisbon Weir. Flow pulses with maximum daily average net flow at Lisbon Wier exceeding 300 cfs were specified as high-flow type pulses. For all modeled years, flow pulses with at least one day above this 300 cfs threshold resulted in positive net flow out of CSC for more than a few days, and this threshold captured all years with an observed downstream phytoplankton response. Of the three years which were not modeled, 2015 was also designated as a high-flow pulse type based on this threshold. The flow pulses in 2013, 2014, and 2017 were assigned as low-flow pulse years based on the 300 cfs threshold. This 300 cfs threshold for the maximum daily average net flow at Lisbon Weir may not be an

appropriate threshold between high-flow and low-flow pulses for all years because the effectiveness of the flow pulse depends both on the magnitude and duration of the flow pulse.

Table 1-2. General predictions of ecosystem responses to low and high- flow pulses in the North Delta region. Upstream habitat stretches from the Colusa Basin Drain to the base of the Yolo Bypass Toe Drain, and Downstream habitat includes Prospect Slough, Cache Slough Complex including Liberty Island and Ryer Island, and the Lower Sacramento River at Rio Vista. Some predictions are confounded by seasonal change. Asterisks include a seasonal change.

Abiotic and Biotic Parameter Responses	Low-flow pulses		High-flow pulses	
	Upstream	Downstream	Upstream	Downstream
Habitat Conditions				
Average Daily Net Flow	Increase	Neutral	Increase	Increase
Temperature	Variable*	Variable*	Variable*	Variable*
Turbidity	Decrease	Neutral	Decrease	Decrease
Water clarity	Increase	Neutral	Increase	Increase
Conductivity	Increase	Neutral	Increase	Increase
Average Dissolved Oxygen	Decrease	Neutral	Decrease	Neutral
Average Dissolved Organic Carbon	Increase	Neutral	Increase	Neutral
Average Ammonium Concentration	Increase	Neutral	Increase	Neutral
Average Nitrate Concentration	Increase	Neutral	Increase	Neutral
Average Phosphorous Concentration	Increase	Neutral	Increase	Increase
Contaminants	Increase	Neutral	Increase	Increase
Lower Trophic Food Web				
Chlorophyll *a*	Increase	Neutral	Increase	Increase
Phytoplankton				
Phytoplankton Biomass	Increase	Neutral	Increase	Increase
Diatom Biomass	Increase	Neutral	Increase	Increase
Zooplankton				
Zooplankton Biomass	Increase	Neutral	Increase	Increase
Cyclopoid copepods	Increase	Neutral	Increase	Increase
Calanoid copepods	Increase	Neutral	Increase	Increase
Cladocerans	Increase	Neutral	Increase	Increase
Clams	Neutral	Neutral	Neutral	Neutral
Fish				
Fish assemblage	Neutral	Neutral	Neutral	Neutral
Delta Smelt	Neutral	Neutral	Neutral	Neutral
Salmonid catch	Increase*	-	Increase*	-

1.3.3 Research Approach

Our approach to evaluating effects of flow pulses on ecosystem changes in the North Delta include four types of comparisons: 1) with and without a flow pulse, 2) habitat comparisons, 3) before-during-after flow pulses, and 4) comparisons of 2 (habitat) and 3 (pulse timing) across years and pulse types (low-flow vs. high- flow) described in Table 1-1. These comparisons are intended to address general study objectives and predictions of abiotic and biotic responses to flow pulses in different regions and years of the north Delta, during and after the pulse.

1. **With and without managed flow pulse**: As in several previous years (Frantzich et al. 2021, Twardochleb et al. 2021), we use a hydrodynamic model to simulate habitat conditions in the Yolo Bypass, Cache Slough Complex, and lower Sacramento River with and without a managed flow pulse (i.e. action) to predict how hydrodynamics and outflow are changed in summer-fall. In addition, we compare results of simulations of high-flow pulses with managed flow actions to non-managed flow pulses from 2011 to 2019, excluding 2013-2015.
2. **Habitat comparisons:** We evaluate abiotic and biotic responses to flow pulses across upstream and downstream regions (Figure 1-2) and habitats in the north Delta including: Upstream regions of the Colusa Basin Drain/Ridge Cut Slough, Upper Yolo Bypass, and Lower Yolo Bypass, and Downstream regions including the Cache Slough Complex and the lower Sacramento River. These regional comparisons allow us to evaluate how flow pulses alter water quality and food web productivity and composition at the food source (Yolo Bypass) and in downstream Delta Smelt habitats. In addition, we qualitatively compare the upstream and downstream responses to those in the middle Sacramento River at a reference site that is not affected by the flow pulse (Figure 1-3).
3. **Before-During-After**: We assess abiotic and biotic responses to flow pulses by analyzing parameters before, during, and after low- and high-flow pulses. Because the study is conducted in parallel with seasonal changes, comparative analysis of flow pulses from non-managed and managed years may help unravel pulse effects from season.
4. **Different flow pulse types and habitat conditions:** The food web responses of flow pulses from 2011-2019 are qualitatively compared with varied water year (wet/dry) and other habitat conditions, flow pulse types and magnitude (low-flow vs. high-flow pulses, with and with-out

managed flow actions) (see Chapter 2). Qualitative results from these comparisons will help us understand potential food web responses to different managed flow actions under varied environmental conditions. Relevant habitat conditions for comparison include water year type, hydrology, temperature, dissolved oxygen, conductivity, nutrients, chlorophyll *a*, phytoplankton biomass and composition, and contaminants.

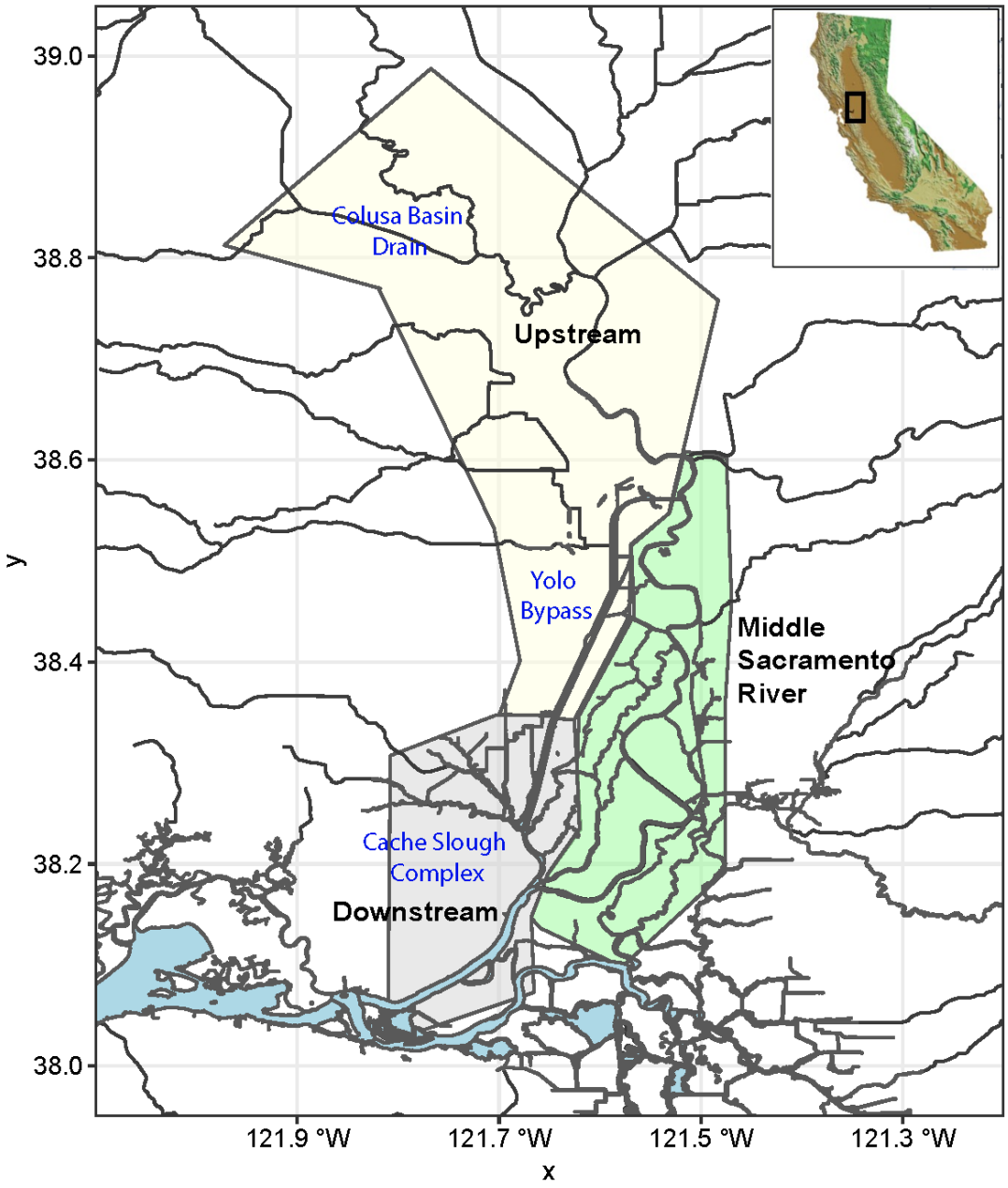

Figure 1-3. Map of North Delta area of the upper San Francisco Estuary. Colored polygons indicate comparative regions include Upstream (yellow), Downstream (gray), and the Middle Sacramento River (green) as a reference region without annual flow pulses.

Chapter 2 Hydrodynamics and habitat responses

Technical Team: Michael MacWilliams, Aaron Bever, Laura Twardochleb, Brittany Davis

2.1 Summary

Hydrodynamic modeling was used to evaluate how hydrodynamics influence the fate of water originating in the CSC and water originating from the flow pulses. A series of 3-D hydrodynamic model simulations were conducted to examine the transport of water in the CSC and downstream in 6 years with varying flow pulse magnitudes and durations: 2011, 2012, 2016, 2017, 2018, and 2019. The model predictions were analyzed to evaluate how hydrodynamics influence the fate of water originating in the CSC and water originating from the flow pulses by tracking the water through the CSC and farther downstream and by examining similarities and differences in the hydrodynamics between years.

The high-flow pulse in 2016 resulted in increased phytoplankton biomass downstream of the CSC and improved food quality (as measured by zooplankton) for fishes in the Delta (Frantzich et al. 2021). These responses are also mirrored by observations of beneficial downstream effects in 2011 and 2012, when fall flows were unusually high. However, the even larger high-flow pulses in 2018 and 2019 did not result in an increase in chlorophyll a downstream of the CSC (Frantzich et al. 2019, Twardochleb et al. 2021). This suggests that the generation or lack of generation of a downstream increase in chlorophyll *a* from a flow pulse is affected by a range of factors. Some of these factors may include differences in the flow of water within the CSC and downstream (hydrodynamic differences between the years), differences in the source of the water and associated constituent concentrations used to drive the flow pulse in each year (differences in Sacramento River versus agricultural returns between the years), or differences in phytoplankton concentration, composition, or growth rates in the flow pulse water or in the CSC (biological differences between the years).

This study applied a 3-D hydrodynamic, salinity, and water temperature model

to evaluate differences in the movement of water masses through the system during each of the 6 years analyzed. Hydrodynamic models can be used to track water originating from a specific location over time as it moves through the system, analogous to a detailed tracer study. In addition, hydrodynamic models can be applied to compare alternate conditions in a specific year and can thereby be used to predict how conditions would be different with and without the flow pulse in a specific year. Together this combination of detailed tracing of water sources with comparisons of alternate "no action" scenarios provide a way to investigate the role that hydrodynamics has in the outcomes from the flow pulses in different years.

2.2 Objectives

The overall goal of the hydrodynamic modeling was to evaluate how hydrodynamics influence the fate of water originating in the CSC and water originating from the flow pulses by tracking the water through the CSC and farther downstream. Specifically, the analysis presented in this chapter focuses on the following two topics:

1. Comparison of high- and low-flow pulses from 2011-2019 by tracing water masses during the flow pulse, determining the timing and impact of the pulse on the system, and determining upstream and downstream regional impacts on hydrodynamics.

2. Quantification of what flow pulses do to hydrodynamics by modeling conditions with and without pulses in specific years.

2.3 Methods

2.3.1 Flow Pulses

Flow pulses in 2011 and 2012 resulted from routing of agricultural water from the Colusa Basin Drain through the Tule Canal and into the Toe Drain on the eastern side of the Yolo Bypass, instead of the water returning to the Sacramento River at Knights Landing (Appendix A, Figure 3). While the 2012 flow pulse occurred with hydrologic conditions similar to later NDFS flow actions (e.g., 2016, 2018, 2019), 2011 was a particularly wet hydrologic year, with additional flows from tributaries such as Cache and Putah Creeks. In

2013 to 2015, in the middle of the historic drought (2012-2016), two low-flow pulses (2013 and 2014) and one high-flow pulse (2015) in the bypass occurred from local agriculture activities and limited water available in the Colusa Drain (Frantzich et al. 2018). In 2016, DWR worked with landowners, reclamation and irrigation districts, and interagency collaborators to generate the first managed summer high-flow pulse in the Yolo Bypass and downstream (Appendix A, Figure 2). Agricultural water was rerouted, and water was pumped from the Sacramento River into Tule Canal to create a managed flow pulse. In 2017, no managed pulse occurred due to construction on the Wallace Weir, therefore, 2017 served as a low-flow pulse baseline year (and not 2013 or 2014, dry and critically dry years that were not simulated, Figure 2-1). In both 2018 and 2019, agricultural return water, mainly from rice field drainage was rerouted down the Tule Canal and into the Toe Drain as high-flow pulses (Appendix A, Figure 3). This rerouting of water in 2018 and 2019 was similar to the mechanism that created the 2011 and 2012 high-flow pulses. Water operations for flow pulses relied on existing infrastructure, including the Knights Landing Outfall Gates (KLOG), Wallace Weir, and agriculture crossings. A summary of infrastructure operations is available in Appendix A.

The level of the flow pulse was estimated in each year based on the observed flow at Lisbon Weir (Figure 2-1). Based on this analysis, the flow pulse in 2019 was the largest volume, followed by 2012, while the flow pulse in 2017 was much smaller than the other years (Table 2-1). The flow pulse in 2011 had a lower peak flow rate than the other years simulated with substantial flow pulses (excluding 2017) but was the longest duration flow pulse (Table 2-1; Figure 2-1). The estimated volumes of the flow pulse are influenced by assumptions about when the flow pulse begins and ends and where the data for calculating the flow pulse magnitude was collected. Changing the assumed start and end dates of the flow pulses will either increase or decrease the estimated volume of the flow pulse. Because these flow pulse volumes were calculated using observed flows at Lisbon Weir, they may differ from estimates of the flow pulse based on observed flows at either Ridge Cut Slough or Wallace Weir. Because the above assumptions affect the estimated flow pulse volume, the volumes in Table 2-1 are intended to provide a relative comparison of the flows reaching the CSC but are not necessarily representative of the water volume diverted farther upstream since net water use in the Yolo Bypass between Wallace Weir and the Lisbon Weir may vary by year.

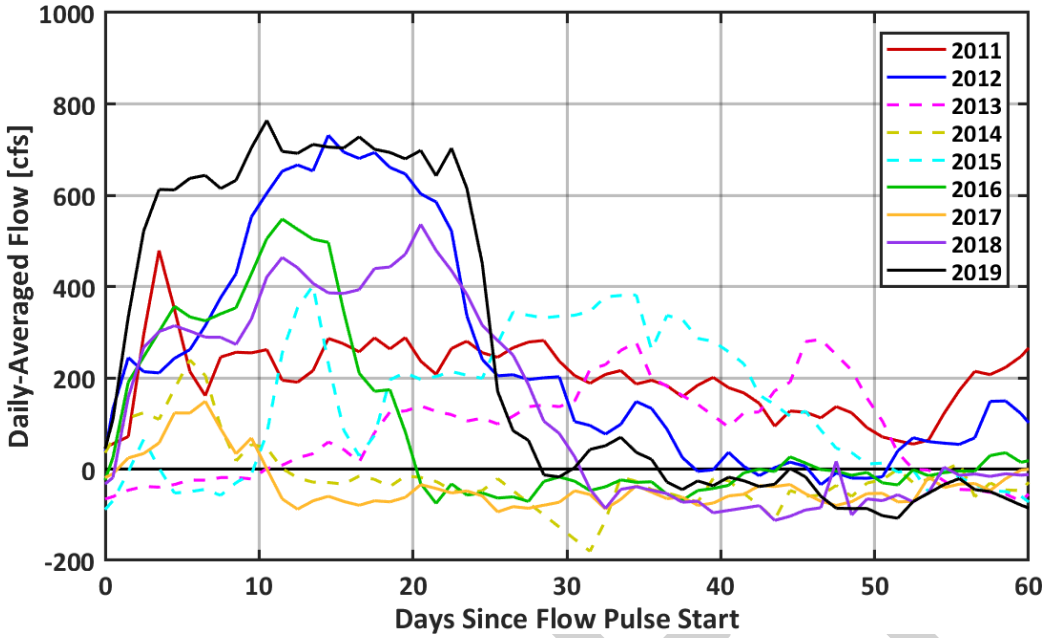

Figure 2-1. Daily-averaged observed flow past Lisbon Weir for 2011 through 2019. Dashed lines indicate years not simulated in this analysis.

Table 2-1. Flow Pulse Timing and Magnitudes at Lisbon Weir in the Upstream Yolo Bypass.

Year	Analysis Date Range	Flow Pulse Date Range	Flow Pulse Magnitude (TAF)	
			Relative to Zero Daily-Average Flow	Relative to No Flow Pulse
2011	August 15 to November 15	September 2 to October 23	NA	16.6
2012	August 15 to November 15	August 26 to October 10	27.4	31.4
2013	Not Simulated	August 11 to October 8	11.3	18.5
2014	Not Simulated	September 12 to September 23	2.5	2.6
2015	Not Simulated	August 11 to October 9	18.2	28.4
2016	July 1 to October 1	July 14 to August 3	12.8	15.8
2017	August 15 to November 15	September 8 to September 19	1.4	2.6
2018	August 15 to November 15	August 27 to September 27	19.5	23.6
2019	August 15 to November 15	August 27 to September 23	31.6	32.4

Notes:

In 2011, the daily-averaged flow was always positive; therefore, the flow pulse magnitude cannot be calculated relative to zero flow. The flow pulse magnitude relative to no flow pulse was calculated by linearly interpolating from the start to the end of the flow pulse and determining the volume of water in excess of that linearly interpolated flow (see Figure 3-5 in Anchor QEA 2020 for an example). Years 2013, 2014, and 2015 have not been simulated using the hydrodynamic model and thus do not have an analysis date range.

2.3.2 3D Hydrodynamic Model

We used the three-dimensional UnTRIM Bay-Delta model (MacWilliams et al. 2015, Anchor QEA 2020) to evaluate hydrodynamics of the high- and low-flow pulses in 2011, 2012, 2016, 2017, 2018, and 2019. These model scenarios include 2017, which served as a low-flow pulse baseline year. The flow pulses in 2013, 2014, and 2015 have not been simulated so they are not included in this analysis. For the six years evaluated, hydrodynamic model simulations were conducted for the low-flow summer period spanning periods before, during, and after the flow pulses (Table 2-1). The wet water years of 2011, 2017, and 2019 generally had higher Delta outflow and lower X2 than the below normal water years 2012, 2016 and 2018 and the dry and critical water years from 2013 to 2015 (Figure 2-2).

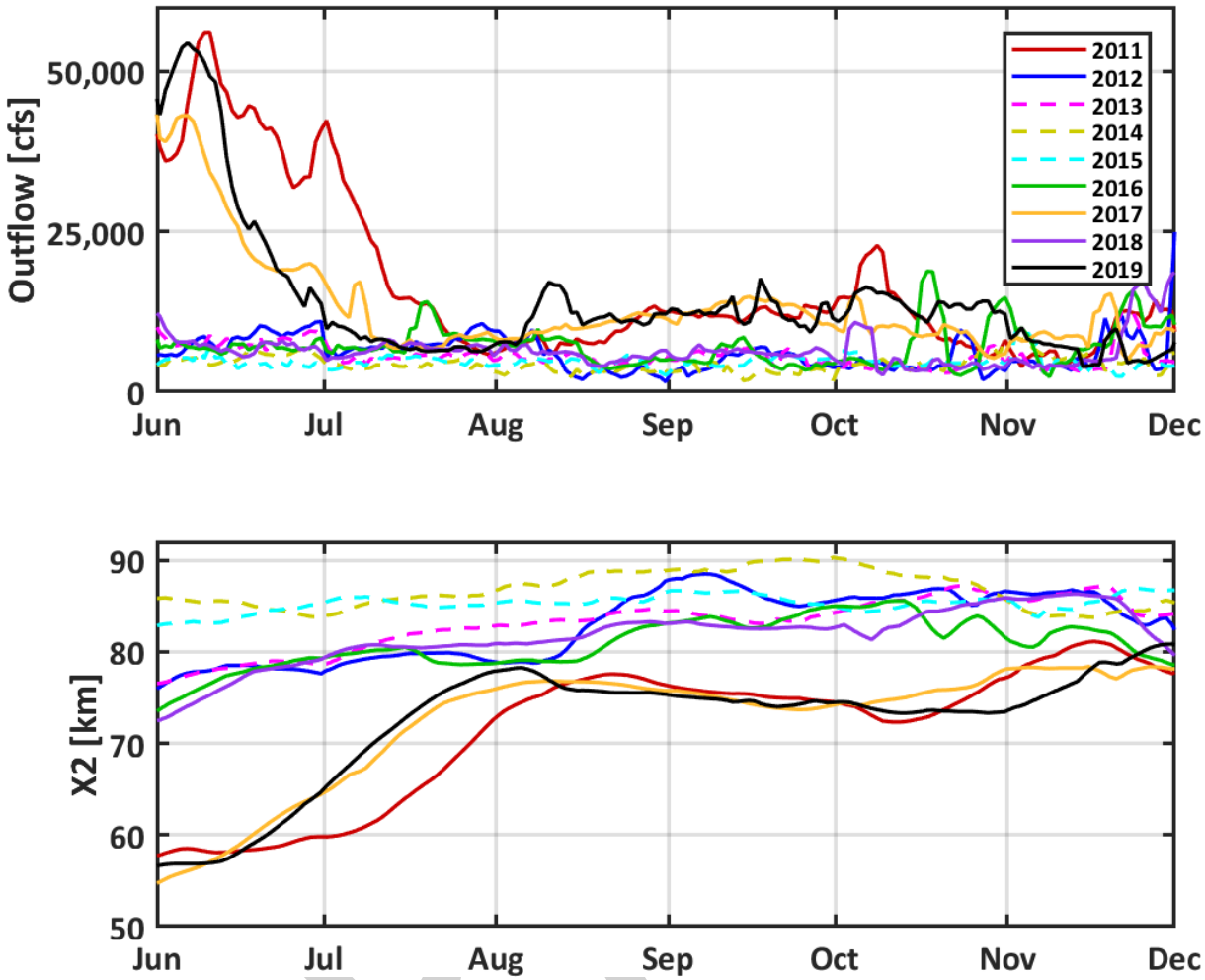

Figure 2-2. Time series of outflow and X2 from DAYFLOW for 2011 through 2019. Dashed lines indicate years not simulated in this analysis.

The UnTRIM model predicts water flow and transport throughout the Bay-Delta and has been validated using time series of flow, stage, and specific conductance in the Yolo Bypass and CSC (MacWilliams et al. 2015, Anchor QEA 2020). We previously used this model to evaluate both high- and low-flow pulses during 6 years between 2011-2019 (Anchor QEA 2020). Simulations incorporated observed inflow (daily averaged), water temperature, and salinity in the Yolo Bypass. We simulated the movement, age and fate of water originating from the flow pulse and other water masses such as CSC to downstream stations, and the Lower Sacramento River at Rio Vista (Anchor QEA 2020). Our prediction was that the flow action would increase net downstream transport through Cache Slough. To evaluate this prediction, we performed tracer analysis to estimate the percentage of water originating from the flow pulse across locations. We also used water age

analysis to assess the average number of days required for the water originating from the flow pulse to reach locations within the study area.

One of the challenges associated with large-scale adaptive management actions is assessing the effect of the action relative to the conditions that would have been presented if the action was not implemented. Data collected during a managed flow pulse can be compared to data from a year when a managed flow pulse was not conducted, but this comparison can be influenced by other differences between the years that are independent of the management action. One advantage of using a hydrodynamic model is that the same historical period can be simulated with and without the management action to help understand the direct effect of the management action.

For both 2016 and 2019, two simulations were evaluated to allow for a comparison of conditions with and without the action. In this report, these comparisons for 2016 and 2019 are presented to evaluate differences between: 1) Action, including the high-flow pulse, and 2) No Action, with the flow pulse removed from the inflow hydrograph. For the Action alternatives, measured historic flows at Lisbon Wier were used. For the No Action alternatives, we removed the flow pulse by assuming a linear change in inflow past Lisbon Weir, from the observed flow immediately prior to the flow pulse period to the observed flow immediately following the flow pulse period. Identical observed flows were used at Lisbon Weir before and after the flow pulse for both the Action and No Action simulations. It is important to note that the No Action alternatives had negative inflow during the flow pulse period; that is, simulated flow through the Toe Drain was net negative (toward the north away from the CSC), because observed flow was net negative both before and after the 2016 and the 2019 flow pulses. Comparing the results of the Action and No Action simulations allowed us to directly evaluate the effects of the flow pulse on water transport and age.

A total of eight model simulations were used to examine the hydrodynamics around the CSC before, during, and after the flow pulses in 6 years (Table 2-2). The first six simulations represented hindcasts of historical conditions. The seventh and eighth simulations removed the flow pulse from the specified inflow at Lisbon Weir to examine the effect of the flow pulse water on hydrodynamics.

Hydrodynamic modeling focused on the Yolo Bypass and North Delta,

extending from Lisbon Weir south through the CSC to the Sacramento River near Sherman Island (Figure 2-3). Analysis of the hydrodynamic model predictions focused on water flow between different portions of the study area and the proportion of water from various sources at discrete locations in the study area.

Table 2-2. Hydrodynamic model scenarios

Scenario Number	Year	Scenario
1	2011	Hindcast of historical conditions
2	2012	Hindcast of historical conditions
3	2016	Hindcast of historical conditions
4	2017	Hindcast of historical conditions
5	2018	Hindcast of historical conditions
6	2019	Hindcast of historical conditions
7	2016	2016 hydrodynamics with the flow pulse removed from the inflow specified at Lisbon Weir
8	2019	2019 hydrodynamics with the flow pulse removed from the inflow specified at Lisbon Weir

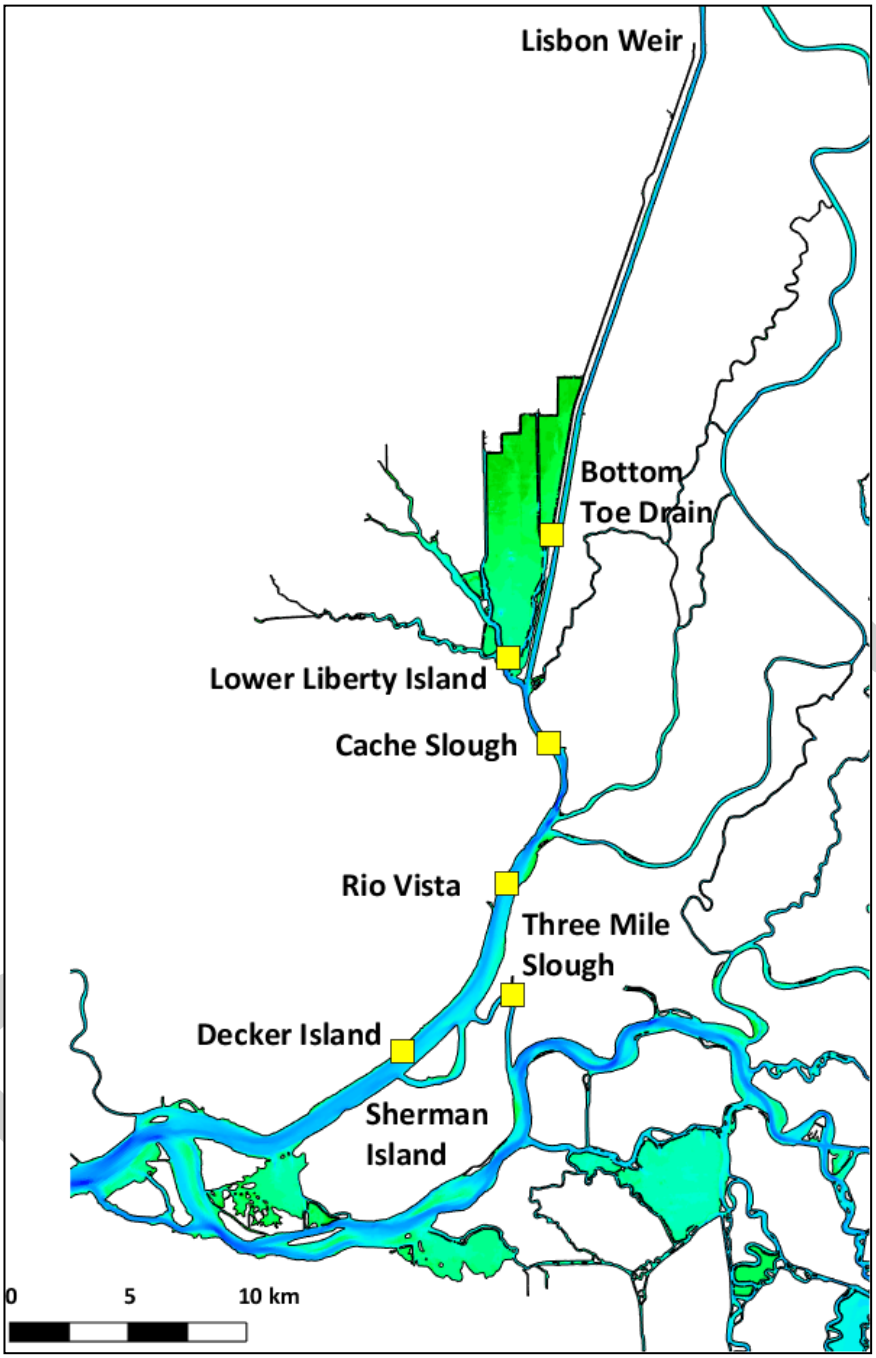

Figure 2-3. Extent of the hydrodynamic modeling focus area and discrete locations where water age and tracers were analyzed as time series (yellow squares).

2.4 Results

The similarities and differences in the water flow and tracer transport during the flow pulse were evaluated for each of the six years simulated. Since the flow pulses occurred during different days each year, comparisons between years are shown relative to the number of days after the start of the flow pulse to facilitate the comparison. This analysis focusses on conditions at Lower Liberty Island and Rio Vista (Figure 2-3). Similar comparisons for additional locations (shown on Figure 2-3) are discussed in Anchor QEA (2020).

2.4.1 Comparison of Flow Pulse for Six Years between 2011 and 2019

The flow pulse magnitude and duration were different in each of the years simulated (Figure 2-1). Each of the years simulated were predicted to have different net flow between the CSC and Cache Slough. In each of the years, the 7-day running-average flow was out of the CSC for at least part of the period during the flow pulse (Figure 2-4). In 2012, 2018, and 2019, the flow was into the CSC at the start of the flow pulse and then transitioned to southward out of the CSC as the flow pulse ramped up. As the flow pulses decreased in these years, the time-averaged flow transitioned back to northward into the CSC. The time-averaged flow in 2016 showed a similar pattern to 2012, 2018, and 2019, with the flow northward into the CSC at the start of the flow pulse, transitioning to southward out of the complex, and then transitioning again to northward into the complex. However, the southward flow out of the complex was of shorter duration and lower magnitude than in 2012, 2018, and 2019. The flow pulse in 2011 was longer duration with lower peak flow rates than 2012, 2016, 2018, and 2019 (Figure 2-4). The predicted time-averaged flow was northward into the CSC until about 30 days after the start of the flow pulse. The predicted time-averaged flows then switched to southward out of the CSC but trended toward more northward flow until the end of the flow pulse. The low-flow pulse in 2017 was much smaller than the other years and the predicted time-averaged flow was only toward the south out of the CSC for a very short duration.

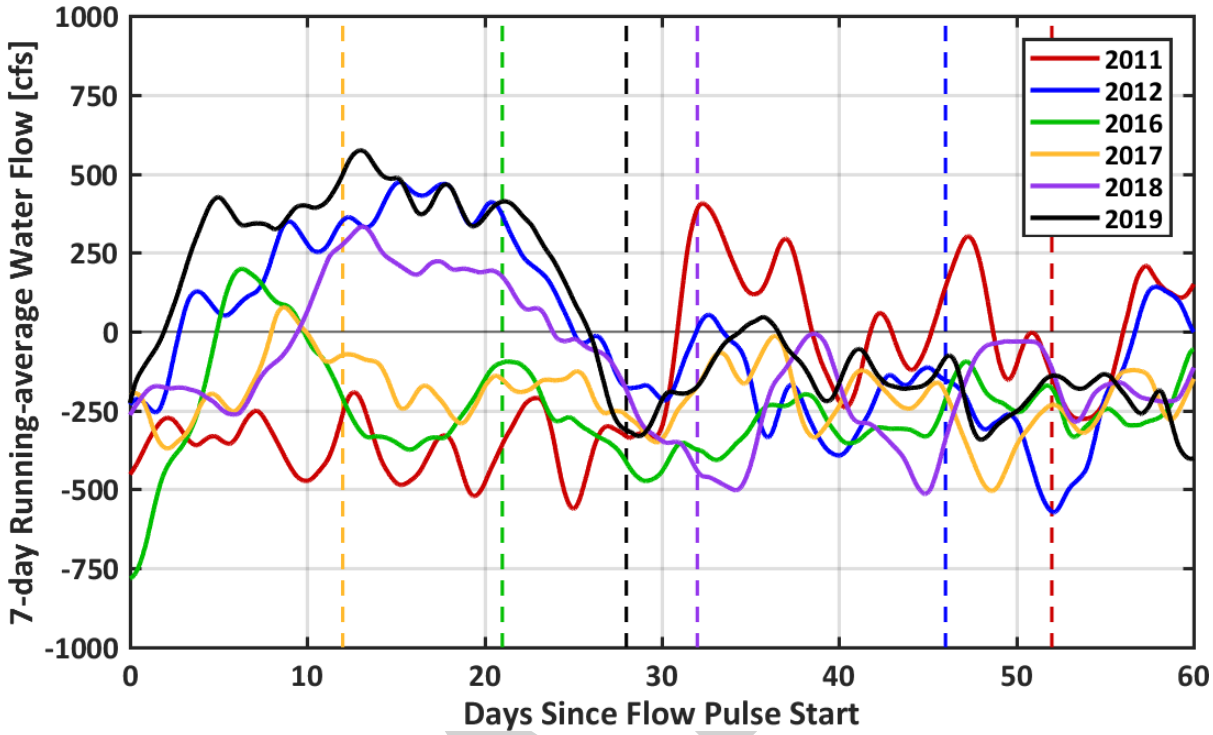

Figure 2-4. 7-day running-average water flow southward out of the Cache Slough Complex in each year simulated. Vertical dashed lines indicate the end of the flow pulse in each year.

Table 2-3. Number of Days the 7-Day Running-Averaged Net Flow Out of Cache Slough Complex Was Southward During the Flow Pulse.

Year	Days
2011	16
2012	26
2016	5
2017	2
2018	14
2019	24

These similarities and differences in the predicted time-averaged flows result from a combination of differences in the magnitudes of the flow pulses and other factors, such as meteorological, tidal spring-neap, and larger Delta-wide forcing on the net flows between the CSC and Cache Slough. The relatively large flow rate at Lisbon Weir (Figure 2-1) during 2012, 2018, and 2019 flow pulses helped generate the relatively large time-averaged flows out of the CSC. The relatively short duration of the flow pulse in 2016 relative to 2012, 2018, and 2019 likely limited the southward transport out of the CSC relative to 2012, 2018, and 2019. In 2011, the relatively lower-magnitude inflow rate

of the flow pulse limited the effectiveness of the flow pulse to generate a net flow southward out of the CSC during the first 30 days of the flow pulse, relative to 2012, 2016, 2018, and 2019. However, around 30 days after the start of the flow pulse, conditions other than the magnitude of the flow pulse changed that resulted in a predicted net flow southward out of the CSC in 2011. Possible factors that affected the net flow between the CSC and Cache Slough near Ryer Island were a decrease in the North Bay Aqueduct intake rate and rain near the beginning of October in 2011.

The flow pulse water initially reached the analysis locations (Figure 2-3) at a percentage of 0.01% or higher after a similar amount of time in each of the simulated years, except for 2017 (Table 2-4). With the largest magnitude flow pulse and the largest average flow down Cache Slough during the flow pulse, flow pulse water reached the analysis locations the fastest in 2019.

Table 2-4. Day After the Start of the Flow Pulse That Flow Pulse Water Reached A Given Location. Locations are shown on Figure 2-3.

Year	Days Since Start of Flow Pulse					
	Bottom of Toe Drain	Lower Liberty Island	Cache Slough	Rio Vista	Decker Island	Three Mile Slough
2011	3	5	5	7	9	11
2012	3	5	6	7	10	11
2016	3	5	5	7	8	10
2017	5	7	10	23	32	33
2018	3	6	7	8	10	11
2019	2	3	4	5	7	8

The maximum percentage of flow pulse water at Lower Liberty Island was highest in 2019, then 2012, 2018, 2011, 2016, and 2017 (Table 2-5; Figure 2-5, top). Very little flow pulse water reached Lower Liberty Island in 2017, since the net water flow was generally into the Cache Slough Complex (indicated by negative values on Figure 2-4). A lower water age indicates that the flow pulse water was predicted to reach Lower Liberty Island on average faster than higher water ages. The relative order of the age of the water at Lower Liberty Island (Figure 2-5, bottom) indicates that the years with the higher flow pulse magnitudes have lower water age and higher flow pulse water percent than the years with lower flow pulse inflow magnitude.

Table 2-5. Maximum Percentage of Flow Pulse Water at Lower Liberty Island and the Number of Days After the Start of the Flow Pulse the Maximum Was Reached.

Year	Flow Pulse Water at Lower Liberty Island		Flow Pulse Water at Rio Vista	
	Maximum Percent	Days	Maximum Percent	Days
2011	10.5	61	2.0	64
2012	18.9	24	4.0	27
2016	6.0	19	1.0	23
2017	0.08	24	0.02	32
2018	12.3	23	2.1	27
2019	21.9	24	3.4	29

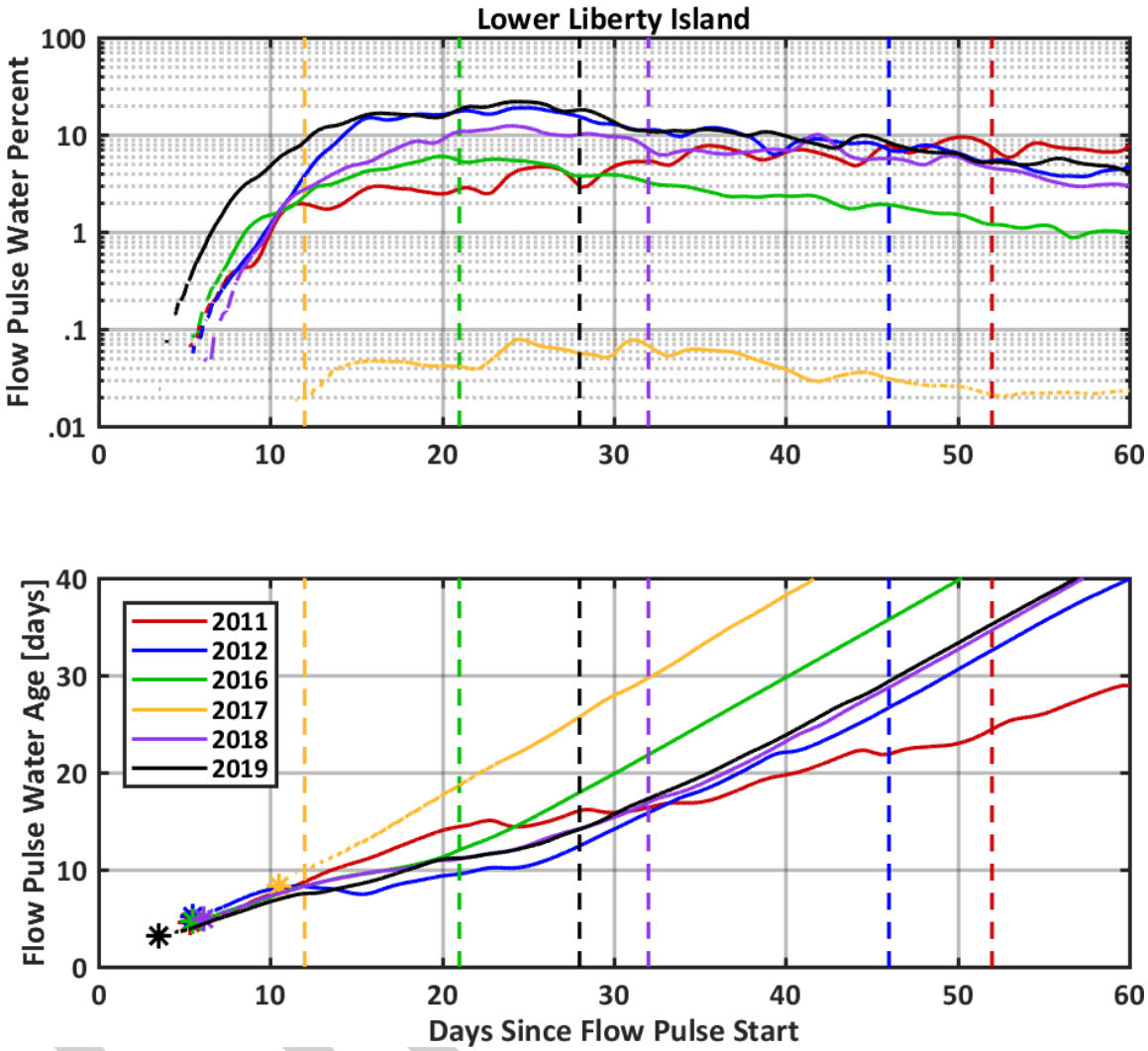

Figure 2-5. Tidal-averaged flow pulse water percent and flow pulse water age at Lower Liberty Island in the six years simulated. Stars mark when flow pulse water first reached the location and vertical dashed lines represent the end of the flow pulse.

The maximum percentage of flow pulse water downstream at Rio Vista was highest in 2012, then 2019, 2018, 2011, 2016, and 2017 (Table 2-5; Figure 2-6, top). Very little flow pulse water reached Rio Vista in 2017. In 2012 and 2018, the maximum percentage of flow pulse water at Rio Vista occurred during the flow pulse and about 27 days after the start of the flow pulse. In 2011, 2016, 2017, and 2019, the maximum percentage of flow pulse water at Rio Vista occurred after the flow pulse. The relative order of the age of the water at Rio Vista (Figure 2-6, bottom) indicates that the years with the higher

flow pulse magnitudes have lower water age and higher flow pulse water percent than the years with lower flow pulse inflow magnitude. The lower water age indicates that, on average, flow pulse water was predicted to reach Rio Vista faster than higher water ages.

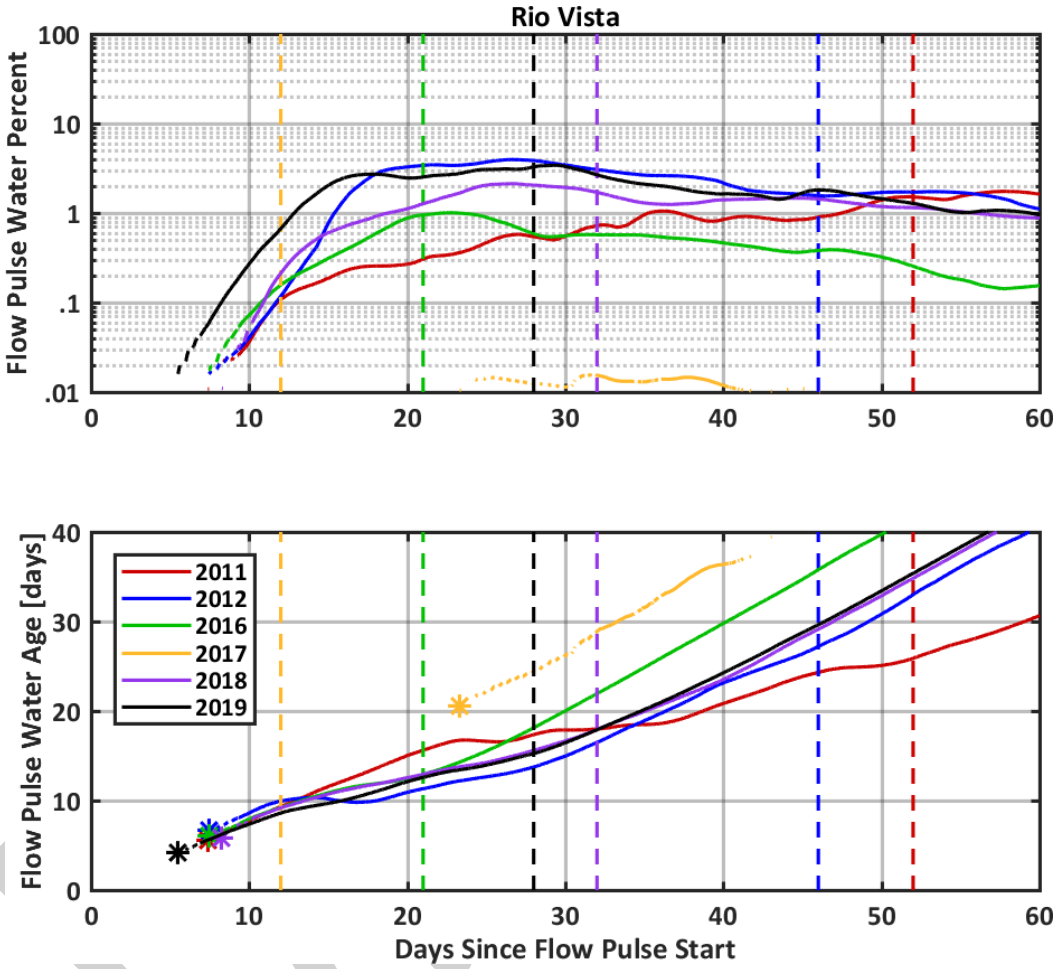

Figure 2-6. Tidal-averaged flow pulse water percent and flow pulse water age at Rio Vista in the six years simulated. Stars mark when flow pulse water first reached the location and vertical dashed lines represent the end of the flow pulse.

2.4.2 Comparison of 2016 With and Without Flow Pulse

Two additional "No Action" model scenarios were used to evaluate the effects of the flow pulses through the Toe Drain on net flows and on the transport of water initially in the CSC to downstream areas in Cache Slough and the Sacramento River. These No Action scenarios simulated 2016 and 2019 with the flow pulse removed from the inflow hydrograph (

Figure 2-7 and Figure 2-8). Outside the period of the flow pulse, the flow past Lisbon Weir was either toward the north or essentially zero throughout the analysis period. Comparison of the historical simulations that included the flow pulse with these No Action simulations allow for direct evaluation of the effects of the flow pulse on water transport.

Flow pulse water age and water percent were not compared for the Action and No Action simulations because there is no flow pulse water in the No Action scenario. However, running-averaged net flows through the study area and the percent of the water at any location composed of water initially in the CSC were compared between the simulations.

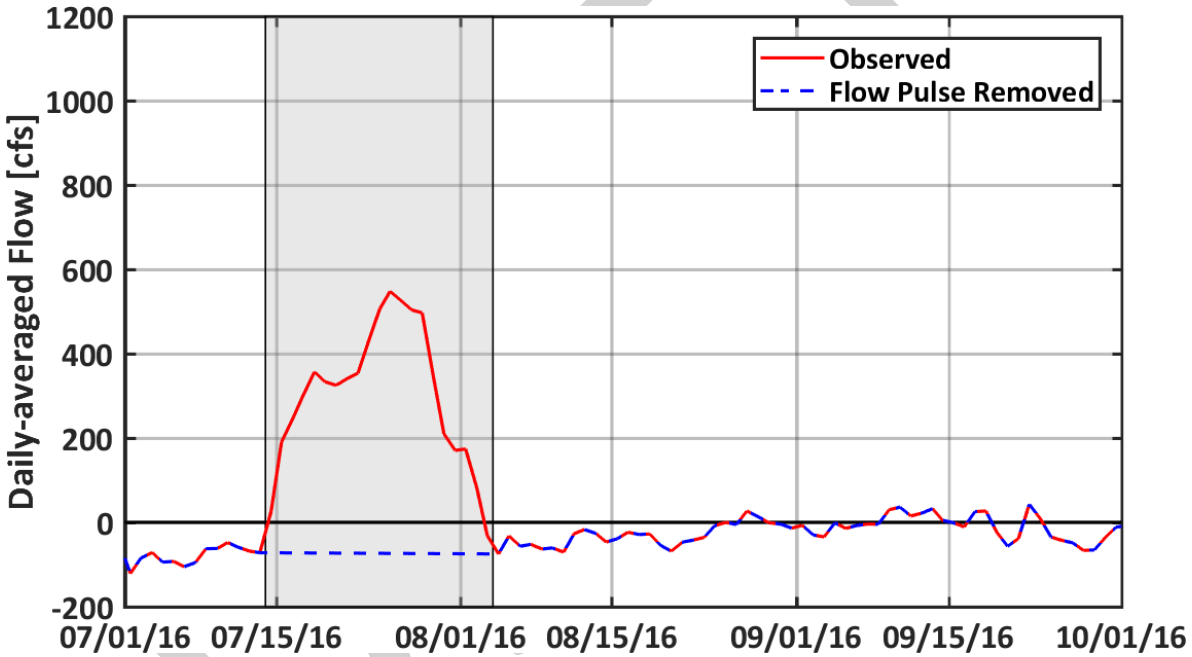

Figure 2-7. Daily-averaged observed flow past Lisbon Weir around the 2016 flow pulse and the daily-averaged flow with the pulse removed (No Action). Shaded area denotes the estimated flow pulse period.

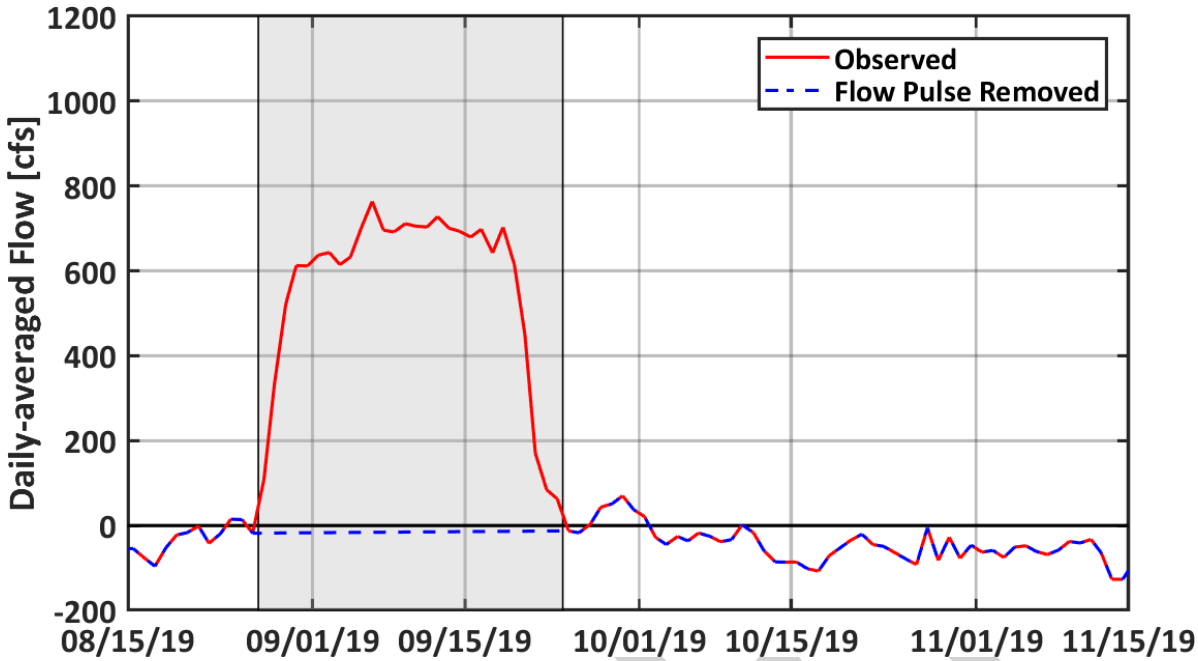

Figure 2-8. Daily-averaged observed flow past Lisbon Weir around the 2019 flow pulse and the daily-averaged flow with the pulse removed (No Action). Shaded area denotes the estimated flow pulse period.

2.4.2.1 Effect of 2016 Flow Pulse on Flow and Tracer Transport from the Cache Slough Complex

Before the flow pulse in 2016, the net water flows throughout the study area were the same with and without the flow pulse (Table 2-6). With the flow pulse in 2016, the 7-day running-average water flow between the CSC and Cache Slough was predicted to be toward the south out of the CSC for a short period during the flow pulse (Figure 2-9). However, without the flow pulse, the 7-day running-average flow was predicted to always be toward the north into the CSC. The result of the additional water from the flow pulse was to increase the time-averaged flow in the southward (out of CSC) direction. This increase resulted in a short duration of flow out of the CSC and overall smaller time-averaged flow into the CSC over the remainder of the flow pulse period. However, the effects on the time-averaged net flow from the CSC did not last long after the flow pulse ended, with the time-averaged flows from the scenario without the flow pulse quickly converging with the time-averaged flows from the historical scenario with the flow pulse.

Table 2-6. Time-Averaged Predicted Water Flow Rate South from the Cache Slough Complex

Simulation	Time-averaged Predicted Water Flow Rate (cfs)		
	Before Flow Pulse	During Flow Pulse	After Flow Pulse
2016	-535	-110	-263
2016 Without Pulse		-514	-265
2019	-444	293	-209
2019 Without Pulse		-310	-211

Note:
Negative values represent flow toward the north.

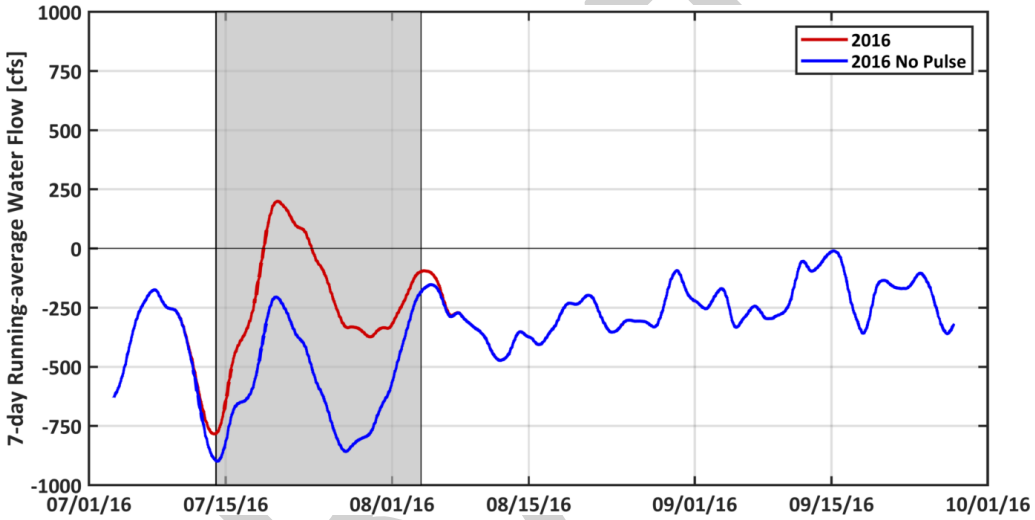

Figure 2-9. Water flow southward out of the Cache Slough Complex in 2016. Shading denotes flow pulse period. Positive flow is toward the south out of the CSC. The figure shows some effect before the flow pulse because the 7-day running average includes a few days at the start of the flow pulse in the averaging before the flow pulse.

The proportion of the flow pulse water at a given location can be added to the proportion of water at that location that originated in the CSC at the start of the flow pulse. Combining the flow pulse and CSC water allows for analysis of how the flow pulse affected the combined downstream movement of water from the CSC. When the 2016 flow pulse water is considered together with the water initially in the CSC, the flow Action scenario had a higher proportion of flow pulse plus CSC water than the No Action scenario throughout the study region, indicating more downstream transport in the flow Action scenario (Figure 2-10). The proportion of flow pulse and CSC water at any location in the study area diverged the most between the two scenarios during the flow pulse. The difference in the proportion of the water at the analysis locations persisted after the end of the flow pulse.

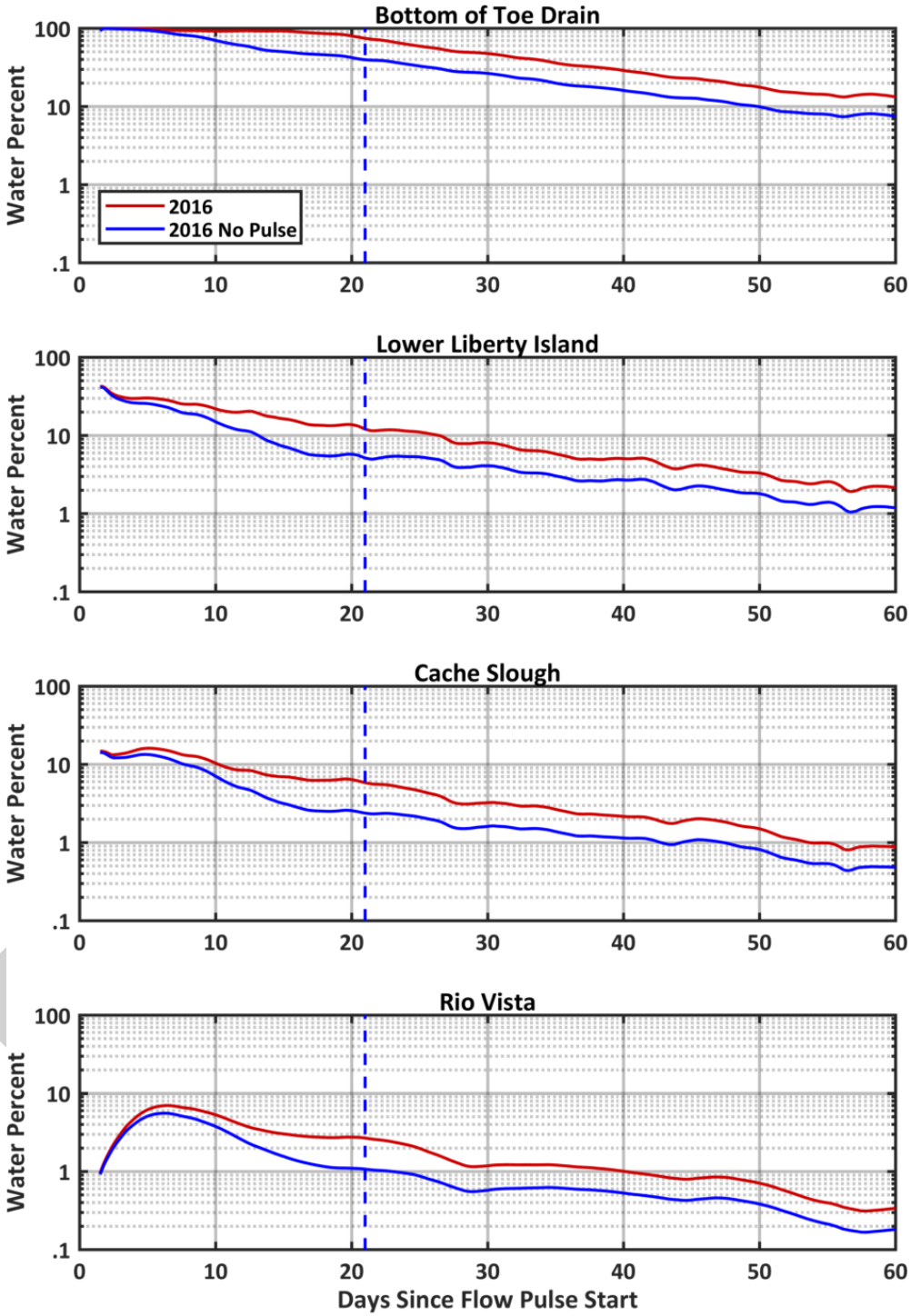

Figure 2-10. Tidal-averaged percent flow pulse water plus Cache Slough Complex water at four locations in 2016 with and without the flow pulse. Vertical dashed lines represent the end of the flow pulse.

2.4.2.2 Effect of 2019 Flow Pulse on Flow and Tracer Transport from the Cache Slough Complex

Before the flow pulse in 2019, the net water flows throughout the study area were the same with and without the flow pulse (Table 2-6). With the flow pulse in 2019, the 7-day running-average water flow between the CSC and Cache Slough was predicted to be toward the south out of the CSC for a long duration of the flow pulse (Figure 2-11). However, without the flow pulse, the 7-day running-average flow was predicted to nearly always be toward the north into the CSC, except for a very short period of time after the flow pulse around October 1, 2019. The result of the additional water from the flow pulse was to increase the time-averaged flow in the southward (out of CSC) direction. This increase resulted in the long duration of flow out of the CSC and the flow averaged over the entire flow pulse being out of the CSC. However, the effects on the time-averaged net flow from the CSC did not last long after the flow pulse ended, with the time-averaged flows from the scenario without the flow pulse quickly converging with the time-averaged flows from the historical scenario with the flow pulse.

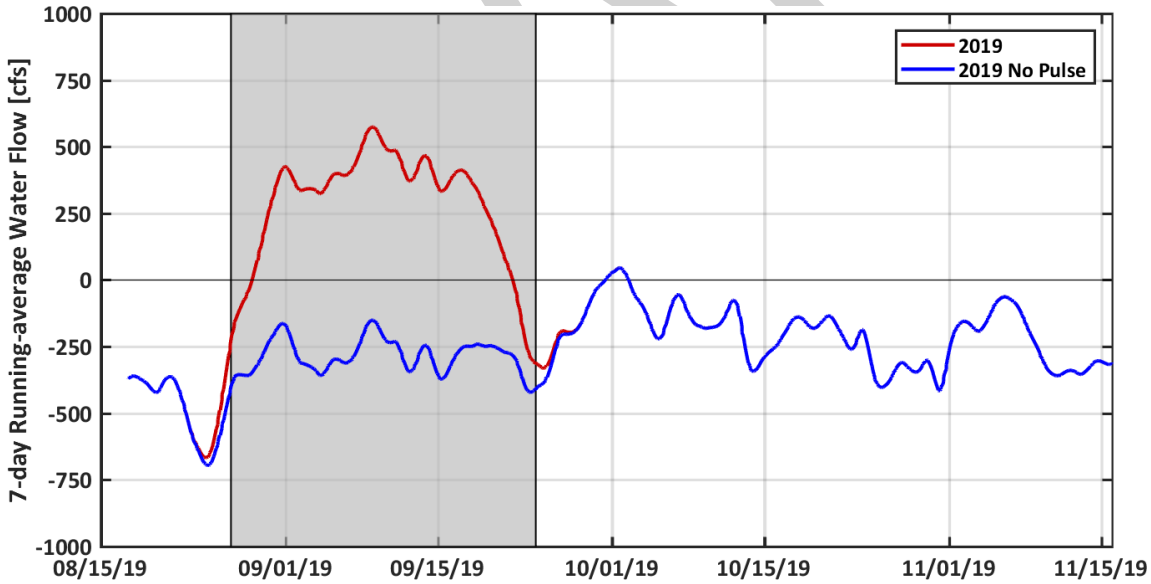

Figure 2-11. Water flow southward out of the Cache Slough Complex in 2019. Shading denotes flow pulse period. Positive flow is toward the south out of the CSC. The figure shows some effect before the flow pulse because the 7-day running average includes a few days at the start of the flow pulse in the averaging before the flow pulse.

The proportion of the flow pulse water at a given location can be added to the proportion of water at that location that originated in the CSC at the start of the flow pulse. Combining the flow pulse and CSC water allows for analysis of how the flow pulse affected the combined downstream movement of water from the CSC. When the 2019 flow pulse water is considered together with the water initially in the CSC, the flow Action scenario had a higher proportion of flow pulse plus CSC water than the No Action scenario throughout the study region, indicating more downstream transport in the flow Action scenario (Figure 2-12). The proportion of flow pulse and CSC water at any location in the study area diverged the most between the two scenarios during the flow pulse. The difference in the proportion of the water at the analysis locations persisted after the end of the flow pulse.

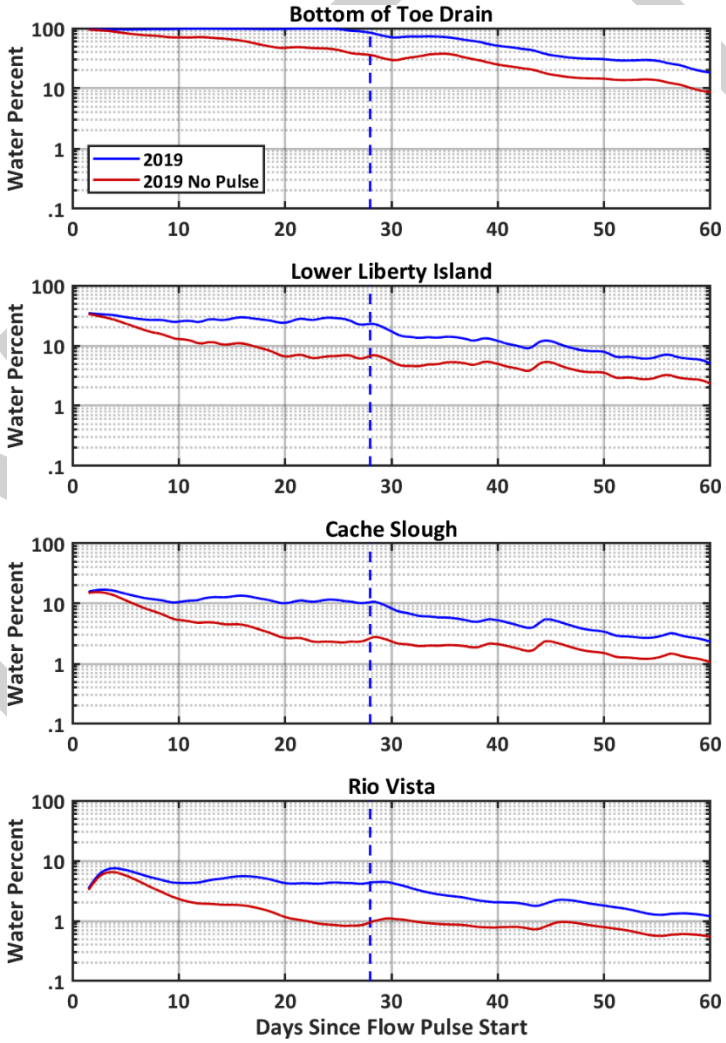

Figure 2-12. Tidal-averaged percent flow pulse water plus Cache Slough Complex water at four locations in 2019 with and without the flow pulse. Vertical dashed lines represent the end of the flow pulse.

2.5 Discussion

The analyses of the transport of flow pulse water and water originating in the CSC demonstrate that the magnitude and duration of the flow pulses affect the hydrodynamics of the CSC and the transport of flow pulse water and CSC water out of the CSC and downstream. Larger-magnitude flow pulses with longer periods when the net flow was southward out of the CSC resulted in more transport of both flow pulse water and CSC water out of the CSC downstream past Lower Liberty Island and Rio Vista.

The evaluation of water flow and water transport through the study area demonstrates that the high-flow pulses and hydrodynamics in 2018 and 2019 were the most similar to the high-flow pulse in 2012. The shape of the flow pulse hydrographs and inflow rates were most similar between 2012 and 2018 and 2019, and these three years were most successful at achieving the goal of positive outflow from CSC (Figure 2-4). The effects of the 2018 and 2019 flow pulses on net water flow out of the CSC and the transport of both flow pulse water and CSC water downstream to Lower Liberty Island and Rio Vista were also the most similar to 2012. One difference between the years is that the flow pulse ramped down more slowly in 2012 than in 2018 and 2019, which may have effects on the average age of the water at Lower Liberty Island and residence time in Liberty Island during the trailing end of the flow pulse.

Using a hydrodynamic model, the same historical period can be simulated with and without the management action to help understand the direct effect of the management action. Analysis of simulations with and without flow pulses from 2016 and 2019 indicates that the flow pulses affected the hydrodynamics in the CSC such that there was an increased net flow out of the CSC in the southward direction relative to conditions that would have been present if the flow pulse had not occurred (Table 2-6; Figure 2-9 and Figure 2-11). There was also more southward transport of water from the CSC to Cache Slough and Rio Vista as a result of the flow pulse. Due to the assumptions used to develop the No Action alternative, there is zero or net negative flow past Lisbon Weir during the flow pulse period in the No Action scenarios simulated for 2016 and 2019. However, even in the low-flow pulse years (such as 2017) there is a short period of net positive flow past Lisbon Weir (Figure 2-1). This suggests that the No Action scenarios may be overly conservative in terms of positive outflow relative to low-flow pulse years which can include a short

period of positive flow past Lisbon Weir. The flow pulse in 2019 was larger than the flow pulse in 2016 (Table 2-1; Figure 2-1). As a result of the larger flow pulse in 2019, a larger amount of the CSC water was transported downstream out of the CSC during the flow pulse in 2019 than in 2016. The analysis indicates that although the flow pulse in 2016 and in 2019 did not completely flush out the water from Little Holland Tract or the CSC, the flow pulse did modify the hydrodynamics and resulted in increased transport of the CSC water downstream relative to the conditions which would have existed if the flow pulse had not occurred in these years.

Chapter 3 Water Quality

Technical Team: Dave Bosworth, Sarah Perry, Traci Treleaven, Amanda Maguire, Jared Frantzich, Laura Twardochleb

3.1 Summary

This chapter examined continuous and discrete water quality to provide a comprehensive look at the habitat conditions in the North Delta Food Subsidy Study area before, during, and after summer-fall flow pulses. We assessed how physical and chemical water quality changes with high- and low-flow pulses, and whether these changes mediate responses in chlorophyll *a* (productivity).

Discrete sampling provides a snapshot of water conditions over a wide spatial range, while continuous monitoring enables high-resolution accounting of water quality at specific locations. Continuous and discrete water quality sampling together provide insight to the quality of the source water, whereas continuous water quality monitoring provides baseline conditions and can detect changes in water conditions not detected by discrete sampling. Continuous data investigated in this chapter includes temperature, turbidity, dissolved oxygen, conductivity, and chlorophyll fluorescence. Discrete data investigated in this chapter includes the same parameters as continuous sampling with the addition of chlorophyll *a*, nutrients, organic carbon, and contaminants. Contaminant sampling contributes to our robust suite of water quality measurements by providing important information about how flow pulses affect pesticide concentrations in water and zooplankton.

3.2 Objectives

We analyzed responses of water quality to low-flow and high-flow pulses across years and between upstream and downstream regions of our study area. Our specific objectives were:

1. Describe how water quality parameters including temperature, turbidity, dissolved oxygen, conductivity, and chlorophyll fluorescence change across years between the upstream and downstream regions before, during, and after flow pulses.
2. Compare primary productivity responses in the upstream and

downstream regions following flow pulses.

3. Examine changes in pesticide composition and concentration in water and zooplankton across years and flow pulse periods at upstream and downstream sites.
4. Determine whether individual pesticide concentrations exceed EPA benchmarks for toxicity to invertebrates and fish.

3.3 Continuous Water Quality

3.3.1 Methods

Data Overview

Twelve stations (Table 3-1) were included for analysis of continuous water quality within the upstream and downstream regions of our study area (Figure 3-1). The station furthest upstream is located at Colusa Basin Drain at Rominger Bridge, while the furthest-downstream station is Sacramento River at Rio Vista. We downloaded water quality data collected at 15-minute intervals from 2011-2019 from three sources: United States Geological Services (USGS), which is stored in the National Water Information System (NWIS), Department of Water Resources (DWR) North Central Region Office (NCRO) stored in DWR's Water Data Library (WDL), and DWR's Continuous Environmental Monitoring Program (CEMP), also stored in WDL. The time frame used in quality control (QC) and analysis was filtered based upon the study period for the corresponding year (Table 3-2). Parameters of interest for the study included: Water Temperature (°C), Dissolved Oxygen (DO; mg/L), Specific Conductance (µS/cm), pH (total units), Turbidity in Formazin Nephlometric Units (FNU), Chlorophyll Fluorescence (expressed as µg/L), Fluorescent Dissolved Organic Matter (fDOM) in Quinine Sulfate Equivalent Units (µg/L as QSE), and Nitrate plus Nitrite (mg/L as N). We standardized all continuous datasets to identify collection site, collection dates, and the state of data cleaning, using Microsoft Excel (Microsoft Corporation, Redmond Washington) and R (R Core Team 2020). Additional procedures used to format the datasets in preparation for QC and analysis included removing duplicate records and missing values and rounding all time stamps to the nearest 15-minute interval. The final dataset will be uploaded to Environmental Data Initiative (EDI).

Table 3-1. Continuous Water Quality Stations Used in Analysis

Station Name	Station Code	Station ID (WDL or NWIS)	Project/Agency	Region
Colusa Basin Drain at Rominger Bridge	RMB	WDL: A0C85051515	DWR – NCRO	Upstream
Ridge Cut Slough	RCS	WDL: A0D84761435	DWR – NCRO	Upstream
Toe Drain at Road 22	RD22	WDL: A0D84061386	DWR – NCRO	Upstream
Toe Drain at I-80	I80	WDL: A0D83441350	DWR – NCRO	Upstream
Toe Drain at Lisbon Weir	LIS	WDL: B9D82851352	DWR – NCRO	Upstream
Toe Drain at Screw trap	STTD	WDL: A0D82120386	DWR – NCRO	Upstream
Toe Drain at Liberty Island Near Courtland CA	TOE	NWIS: 11455140 NWIS: 11455139	USGS	Upstream
Liberty Cut at Little Holland Tract near Courtland	LIBCUT	NWIS: 11455146	USGS	Downstream
Cache Slough at Liberty Island Near Rio Vista	LIB	NWIS: 11455315	USGS	Downstream
Cache Slough at Ryer Island	RYI	NWIS: 11455350 NWIS: 11455385	USGS	Downstream
Sacramento River at Rio Vista Bridge	RVB	WDL: B9D80960412	DWR – CEMP	Downstream
Sacramento River at Hood	SRH	WDL: B9D82211312	DWR – CEMP	Middle Sacramento River

Table 3-2. Before and after flow pulse date designations (45 days before and after the flow pulse) across years and flow types.

Year	Flow Pulse Type	Before Flow Start	Before Flow End	After Flow Start	After Flow End
2011	High	7/8/2011	8/22/2011	10/25/2011	12/9/2011
2012	High	7/11/2012	8/25/2012	10/3/2012	11/17/2012
2013	Low	7/7/2013	8/21/2013	10/3/2013	11/17/2013
2014	Low	7/25/2014	9/8/2014	9/24/2014	11/8/2014
2015	High	7/6/2015	8/20/2015	10/2/2015	11/16/2015
2016	High	5/29/2016	7/13/2016	8/2/2016	9/16/2016
2017	Low	7/14/2017	8/28/2017	9/19/2017	11/3/2017
2018	High	7/13/2018	8/27/2018	9/27/2018	11/11/2018
2019	High	7/11/2019	8/25/2019	9/22/2019	11/6/2019

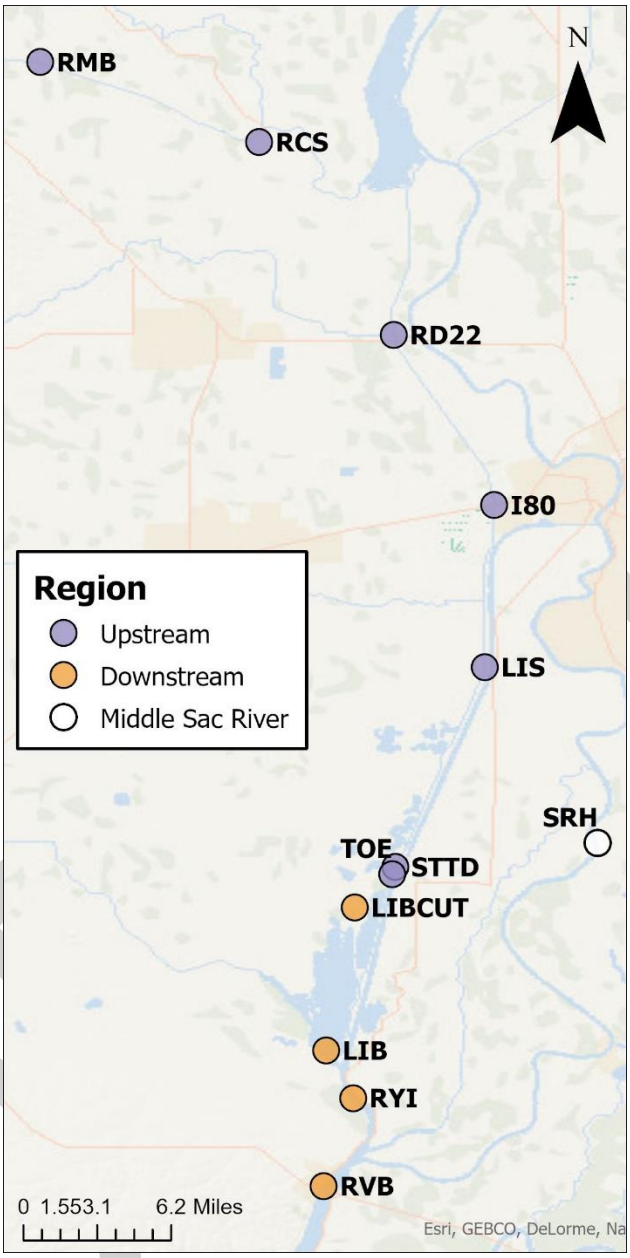

Figure 3-1. Map of continuous water quality stations. The Upstream region (purple) extends from the Colusa Basin Drain at Rominger Bridge (RMB) to lower Yolo Bypass Toe Drain (TOE, STTD). The Downstream region (orange) extends from Prospect Slough to the Lower Sacramento River at Rio Vista Bridge (RVB). The Middle Sacramento River, a comparative control region included Sacramento River at Hood (SRH). See Table 3-1 for site details.

Data Quality Control

Following standardization of collection sites and dates of continuous data (Table 3-1 and Table 3-2), we evaluated additional data quality limitations given data were acquired from different programs and agencies across 9 years, 12 stations, and a variety of parameters. Due to the lack of standardization and consistency within and among agency datasets such as levels of review and quality codes associated with the data, we developed our own data quality control objectives for continuous water quality datasets. We created a series of continuous datasets that: 1) contained all available data; 2) were checked for QA/QC; and 3) were formatted/cleaned so that they can easily be integrated with each other and with datasets from other subgroups. All data that were considered unreliable based on our QA/QC criteria were flagged as such and excluded from any analyses. All data management and metadata information were documented in a Data Management Plan and a metadata document, and data processing steps were documented using R scripts. All metadata, data management plans, and review methods are available upon request.

With the goal of having a clean and validated data set to be analyzed and published to EDI, multiple methods were used to review the data in a way that caused the least amount of subjectivity. Generally, our data QC process involved:

1. Visual inspection of timeseries to identify possible outliers and suspicious patterns that may have resulted from equipment failure, sensor fouling, and/or environmental interference.
2. Investigation of suspected outliers and suspicious patterns by reviewing all available field and calibration records and collaborating with data collection teams.
3. Classification of outliers and suspicious data using the best available information on data quality.

Analysis

We visually inspected processed data to evaluate variability of most water quality parameters across years and directional changes (i.e. increases or decreases) before, during, and after flow pulses. Grouped by region, we examined evidence for water transport from upstream to downstream regions. Continuous water quality trends of the NDFS study area were visually

compared with the middle main stem Sacramento River, a region adjacent to the Yolo Bypass that is not influenced by flow pulses.

To determine which abiotic factors influenced continuous water quality, we used type II Analysis of Variance (ANOVAs) using the 'car' package in R (version 3.0-10) after defining the model structure using the 'lme4' package (version 1.1-26). We included year (2013-2019), flow pulse period (e.g., before, during, after), and region (Table 3-1) as fixed effects and station as a random effect to account for the autocorrelation within stations. We restricted our analyses to include data from the years 2013-2019 since monitoring started in 2013 at most stations. This meant that we excluded two relatively important high-flow years, 2011 and 2012, since continuous sensors were not installed at most sites in those years. In addition, we did not include the Middle Sacramento River region or interaction terms in the models. The Middle Sacramento River region contained only one representative station (SRH), and the models were unable to converge on a solution when interaction terms were included.

To prepare the data for the models, we log-transformed the data and binned it in daily intervals via averaging to meet ANOVA assumptions of normality, homoscedasticity, and independence. In addition, we included lag terms in the models to address autocorrelation among the residuals. We determined the number lag terms needed for each model via exploratory analysis of autocorrelation function (ACF) diagrams and Ljung-Box Portmanteau tests to examine autocorrelation within 20 lags. We defined significant results as $p<0.05$.

After determining which fixed effects were statistically significant via ANOVA F-tests, we performed pairwise comparisons of estimated marginal means (EMM) using the 'emmeans' package in R (version 1.5.4; Length et al. 2021) to determine inter-group significance. P-values were adjusted using the Sidak correction.

3.3.2 Results

Chlorophyll

Overall, flow pulse periods did not significantly affect continuous chlorophyll fluorescence values across all years and sites (ANOVA, $F_{2,5507} = 0.35$, $p=0.71$). However, daily average chlorophyll values were visibly lower and less variable during the flow pulse at some of the upstream stations during some of the years with high-flow pulses (2015, 2018, and 2019) (Figure 3-3; Figure 3-4 and Figure 3-5). In contrast, both year ($F_{6,4955} = 2.85$, $p<0.01$) and region ($F_{1,13} = 29.2$, $p<0.001$) significantly affected continuous chlorophyll concentrations. The upstream region had higher chlorophyll values than downstream throughout the study period ($p<0.001$), while chlorophyll was significantly lower in 2018 than in 2013 and 2016 ($p<0.05$) (Figure 3-2). While we were unable to test for statistical interactions between the fixed effects of year, region, and flow pulse period, visual trends in boxplots of interaction terms (Figure 3-3) and the daily time-series suggest that there may be interactions between these fixed effects.

During most of the years with high-flow pulses, chlorophyll was transported from the stations in the upper Yolo Bypass (RCS, RD22, and I80) downstream to the lower bypass sites (LIS and STTD) during flow pulses (Figure 3-4 and Figure 3-5), and supported by hydrodynamics Figure 2-10 and Figure 2-11 (top panel). This was most apparent in 2016. There were brief increases in daily average chlorophyll values at the beginning of the flow pulses in 2018 and 2019 at LIS and STTD; however, concentrations quickly decreased to <10 µg/L at most of the stations in the upstream region for the remainder of these flow pulses. Interestingly, 2015 was the only dry water year with a high-flow pulse that occurred within our study period. The 2015 pulse had a lower magnitude and longer duration than the other high flow pulses, and the daily average chlorophyll values remained slightly elevated at LIS and STTD throughout the 6-week pulse (Figure 3-5).

Chlorophyll values increased at RVB after the high-flow pulses in 2011 and 2012, and most notably at all downstream stations (LIB, RYI, and RVB) after the high-flow pulse in 2016 (Figure 3-4 and Figure 3-5). Daily average chlorophyll increased by about 6 µg/L at RVB in 2011, 15 µg/L at RVB in 2012, and 7-11 µg/L at LIB and RYI in 2016. The region-wide increase in chlorophyll at the downstream stations in 2016 followed the apparent downstream transport of chlorophyll from the upper to the lower Yolo Bypass stations.

Additionally, chlorophyll values increased at all downstream stations in 2016 for about a 2-week period prior to the flow pulse (Figure 3-5). Continuous chlorophyll data was not collected at the upstream stations in 2011 and 2012, so we were unable to examine whether there was possible downstream transport of chlorophyll during those years. During the remaining three years with high-flow pulses (2015, 2018, and 2019), flow pulses did not appear to transport higher chlorophyll levels in the upstream region to the stations in the downstream region (Figure 3-4 and Figure 3-5). Overall, chlorophyll values were between 0.5-4 µg/L during and after the flow pulses at all downstream stations in 2015, 2018 and 2019.

Daily average chlorophyll values were more variable during the years with low-flow pulses (2013, 2014, and 2017); however, there appeared to be some downstream transport of chlorophyll to LIS and STTD during flow pulses in 2013 and 2014 (Figure 3-6). During all years with low-flow pulses, the downstream region consistently had low chlorophyll values that fell between 1-4 µg/L with the comparatively highest values at LIB.

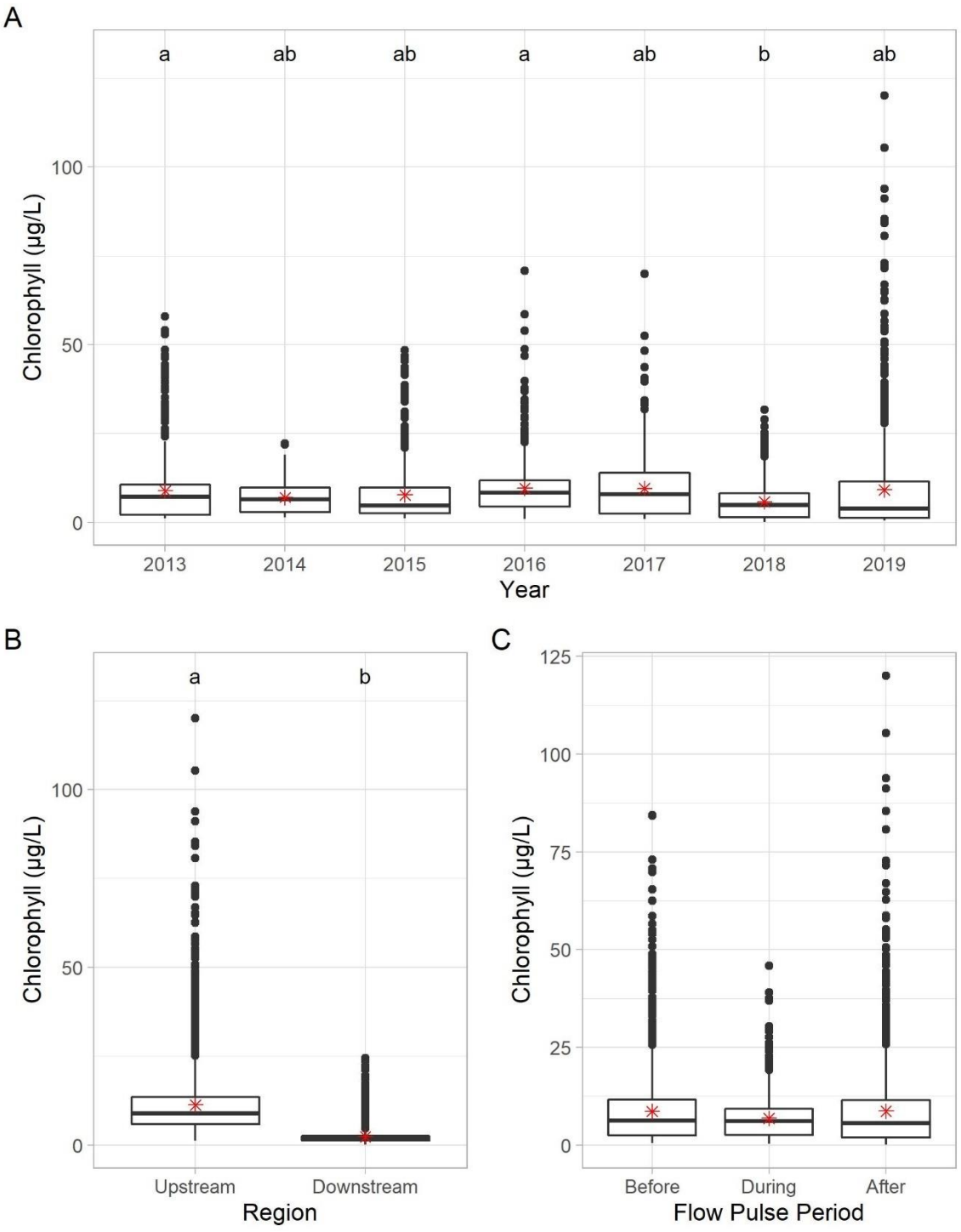

Figure 3-2. Boxplots of medians and quartiles of daily average chlorophyll fluorescence values by model predictors A) year, B) region, and C) flow pulse period. The red asterisks represent the mean of each group. The letters above boxes in A) and B) indicate significant differences in chlorophyll values among years and regions, respectively, according to post-hoc tests. Different letters above boxes indicate significant differences.

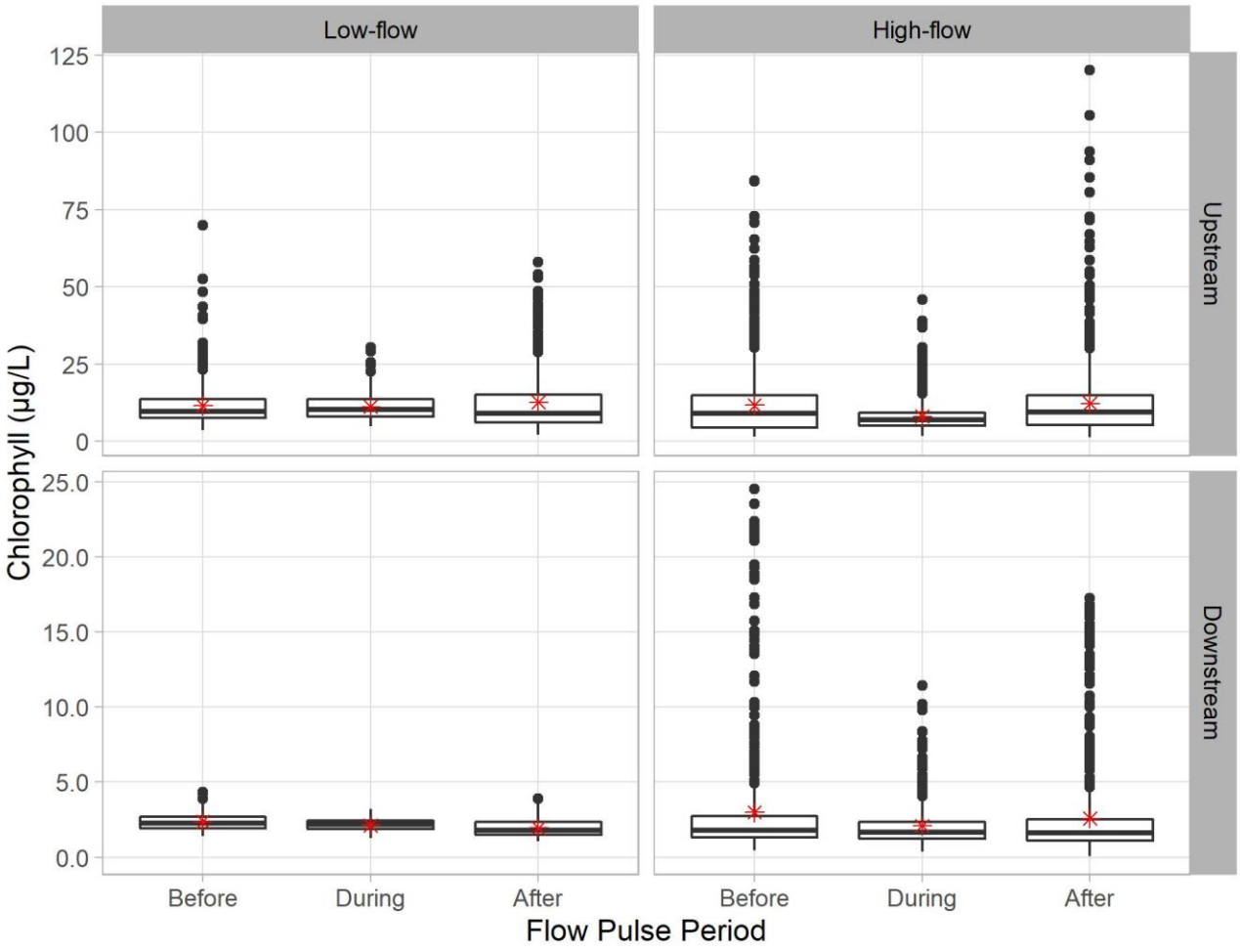

Figure 3-3. Interaction boxplots of medians and quartiles of daily average chlorophyll fluorescence values between flow pulse type (low-flow or high-flow pulses), region (upstream or downstream), and flow pulse period (before, during, after). The red asterisks represent the mean of each group.

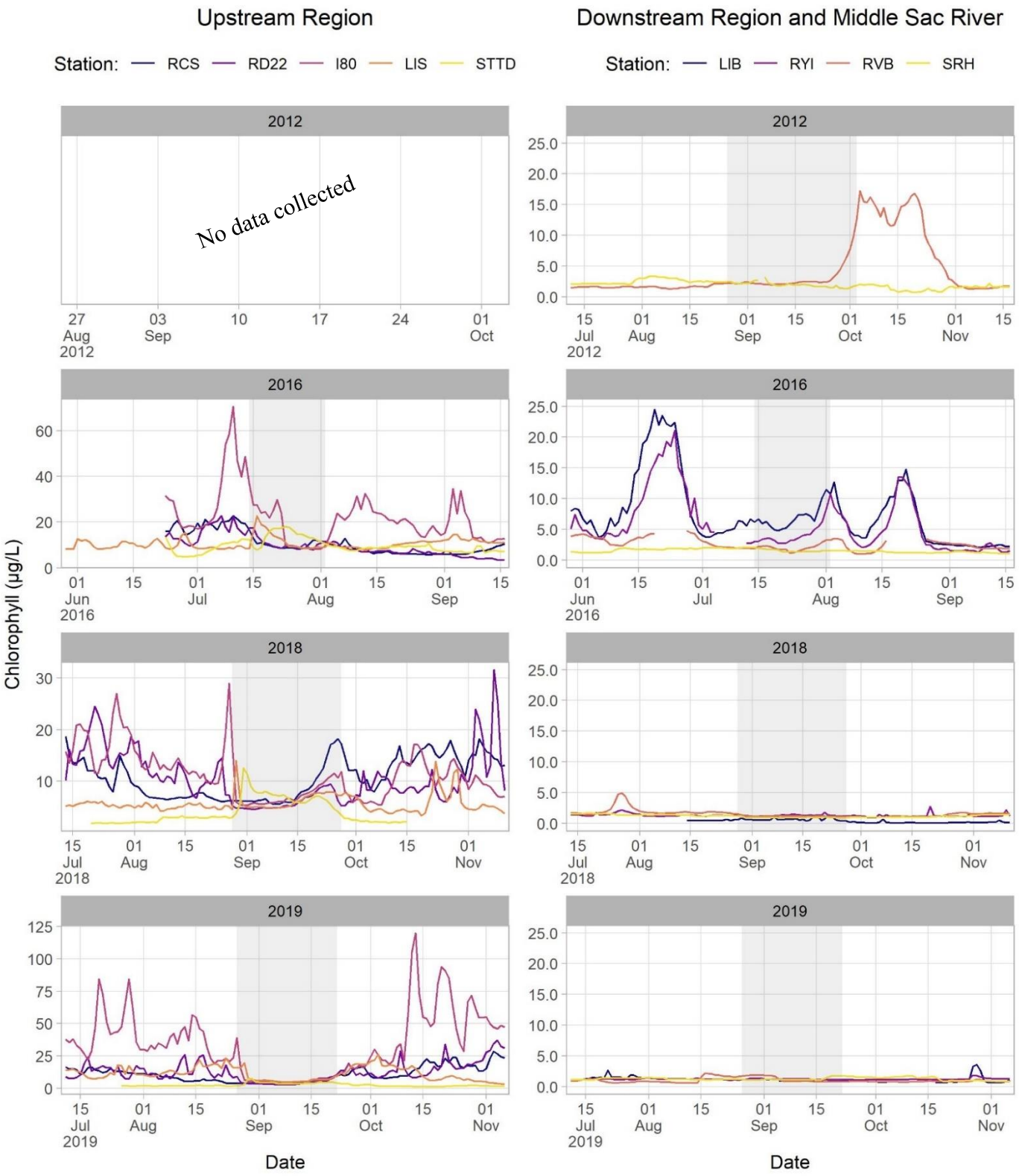

Figure 3-4. Daily average chlorophyll fluorescence values in the upstream region, downstream region, and middle Sacramento River in the years with high flow, high magnitude, and short duration flow pulses (2012, 2016, 2018, and 2019). The light grey shaded box represents the flow pulse period, and each plot for the upstream region has a different y-axis scale.

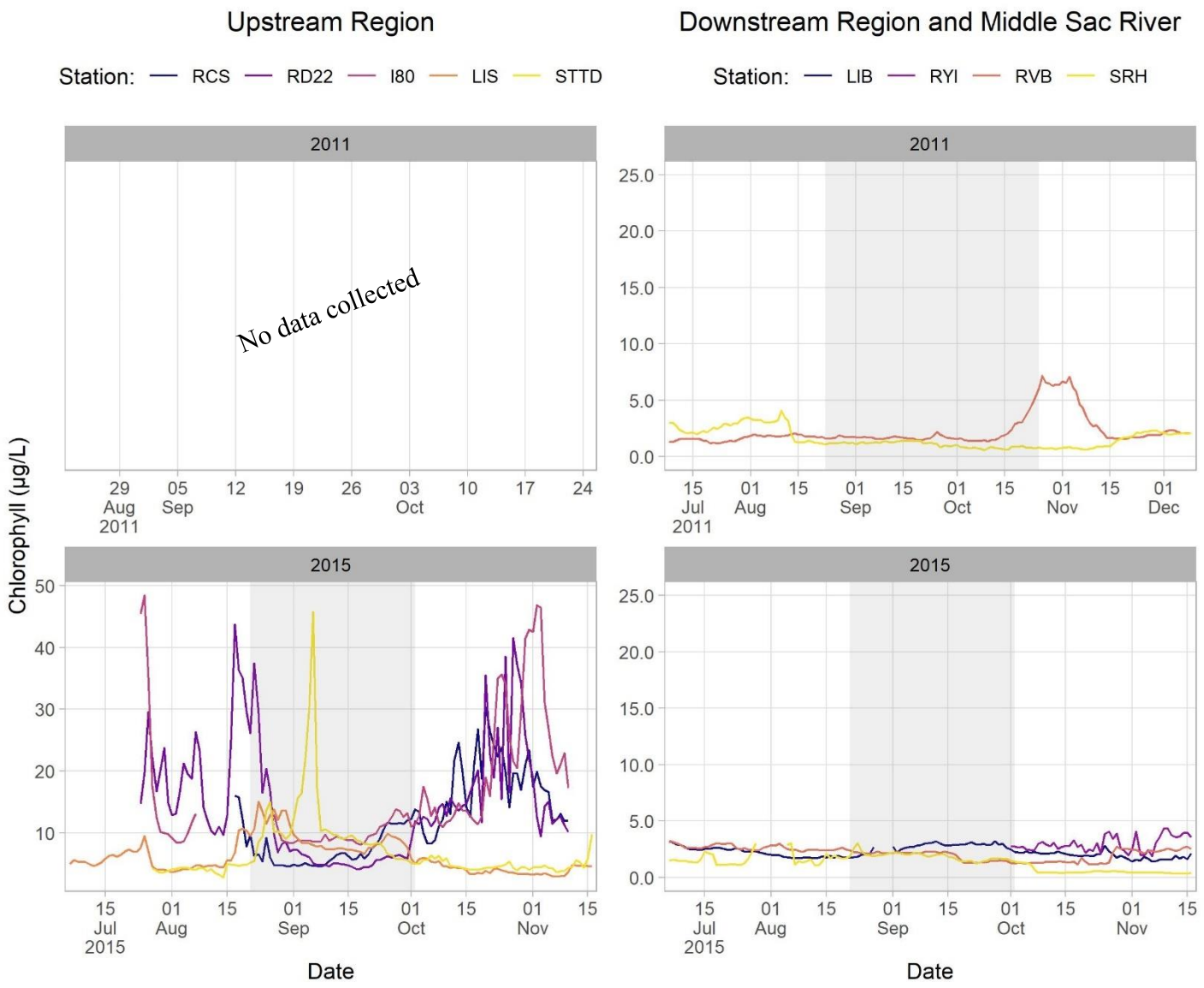

Figure 3-5. Daily average chlorophyll fluorescence values in the upstream region, downstream region, and middle Sacramento River in the years with high flow, low magnitude, and long duration flow pulses (2011 and 2015). The light grey shaded box represents the flow pulse period, and the plots for each region have different y-axis scales.

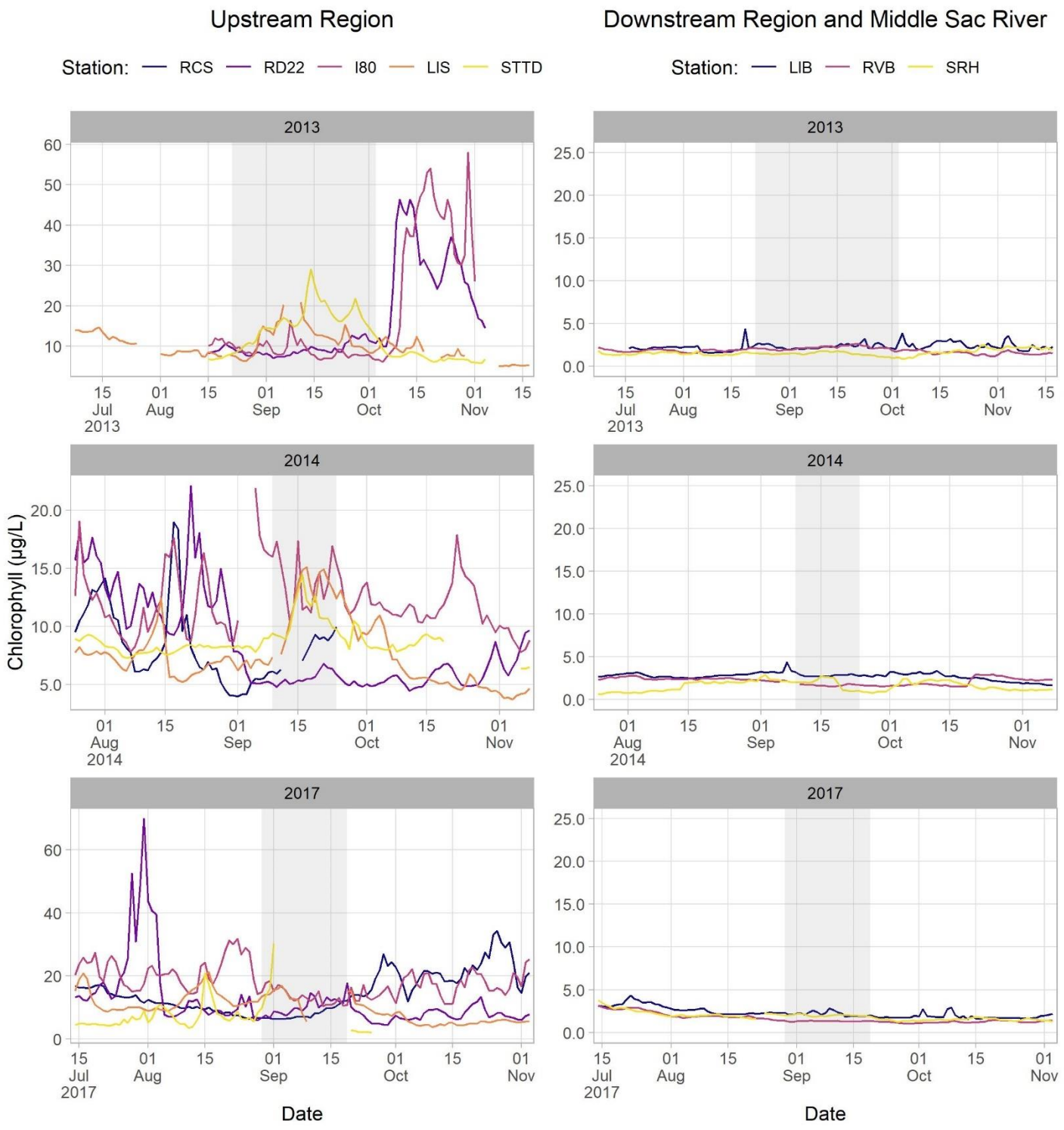

Figure 3-6. Daily average chlorophyll fluorescence values in the upstream region, downstream region, and middle Sacramento River in the years with low-flow pulses (2013, 2014, and 2017). The light grey shaded box represents the flow pulse period, and each plot for the upstream region has a different y-axis scale.

Dissolved Oxygen

The main effects of year ($F_{6,5527}$ = 2.49, p<0.05), region ($F_{1,9}$ = 6.63, p<0.05), and flow pulse period ($F_{2,5786}$ = 9.67, p<0.001) all significantly affected DO. DO concentrations were significantly higher in 2019 than in 2015 (p<0.01). Spatially, the downstream region had significantly higher dissolved oxygen than the upstream region (p<0.05) (Figure 3-7). Dissolved oxygen concentrations were significantly higher after flow pulses than before (p<0.001) and during (p<0.01) flow pulses across all years and sites; however, visual assessments of boxplots of flow pulses indicate potential interactive effects between pulse type (low- or high-flow pulses), regions, and flow pulse periods (Figure 3-8).

In years with high-flow pulses (2015, 2016, 2018, and 2019), daily average DO concentrations at all stations in the upstream region were less variable during the flow pulses (Figure 3-9 and Figure 3-10). In addition, DO levels decreased during these flow pulses in the upstream region (Figure 3-8), particularly at stations in the lower Yolo Bypass (LIS and STTD). Two of the years with high-flow pulses (2018 and 2019) had sudden declines in DO values that coincided with the start of the flow pulse (Figure 3-9). It appears that during the years with high-flow pulses, lower DO water in the upper Yolo Bypass (RCS and RD22) may have been transported downstream to LIS and STTD during the flow pulse.

For the years with low-flow pulses, DO concentrations appeared to decrease during flow pulses at some of the stations in the upstream region (I80, LIS, and STTD) (Figure 3-11). However, these declines were shorter in duration and the daily averages were not as low as the decreases observed during the high-flow pulse years. DO concentrations at the stations in the downstream region (LIB, RYI, and RVB) were not impacted by the flow pulses in any year during the study period (Figure 3-9, Figure 3-10, and Figure 3-11). In fact, the trends in daily average DO values at all downstream stations closely followed the trend of the Middle Sacramento River station (SRH) in all years, suggesting DO may also be confounded with seasonal effects. Consistent with the ANOVA results, DO levels were higher and less variable at the downstream stations than they were at the upstream stations across all years.

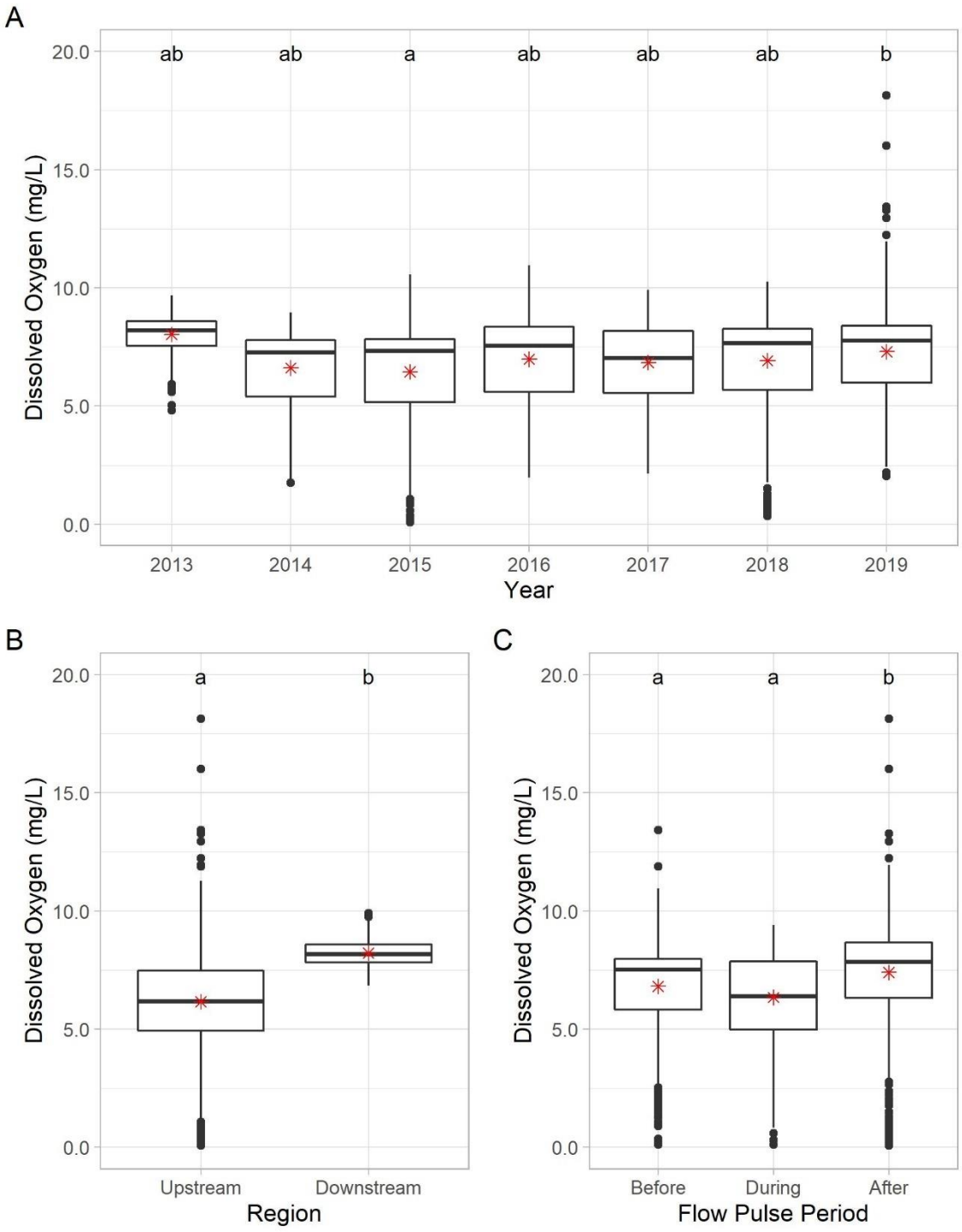

Figure 3-7. Boxplots of medians and quartiles of daily average dissolved oxygen (mg/L) values by model predictors A) year, B) region, and C) flow pulse period. The red asterisks represent the mean of each group. The letters above boxes in A), B), and C) indicate significant differences in dissolved oxygen values among years, regions, and flow pulse periods, respectively, according to post-hoc tests. Different letters above boxes indicate significant differences.

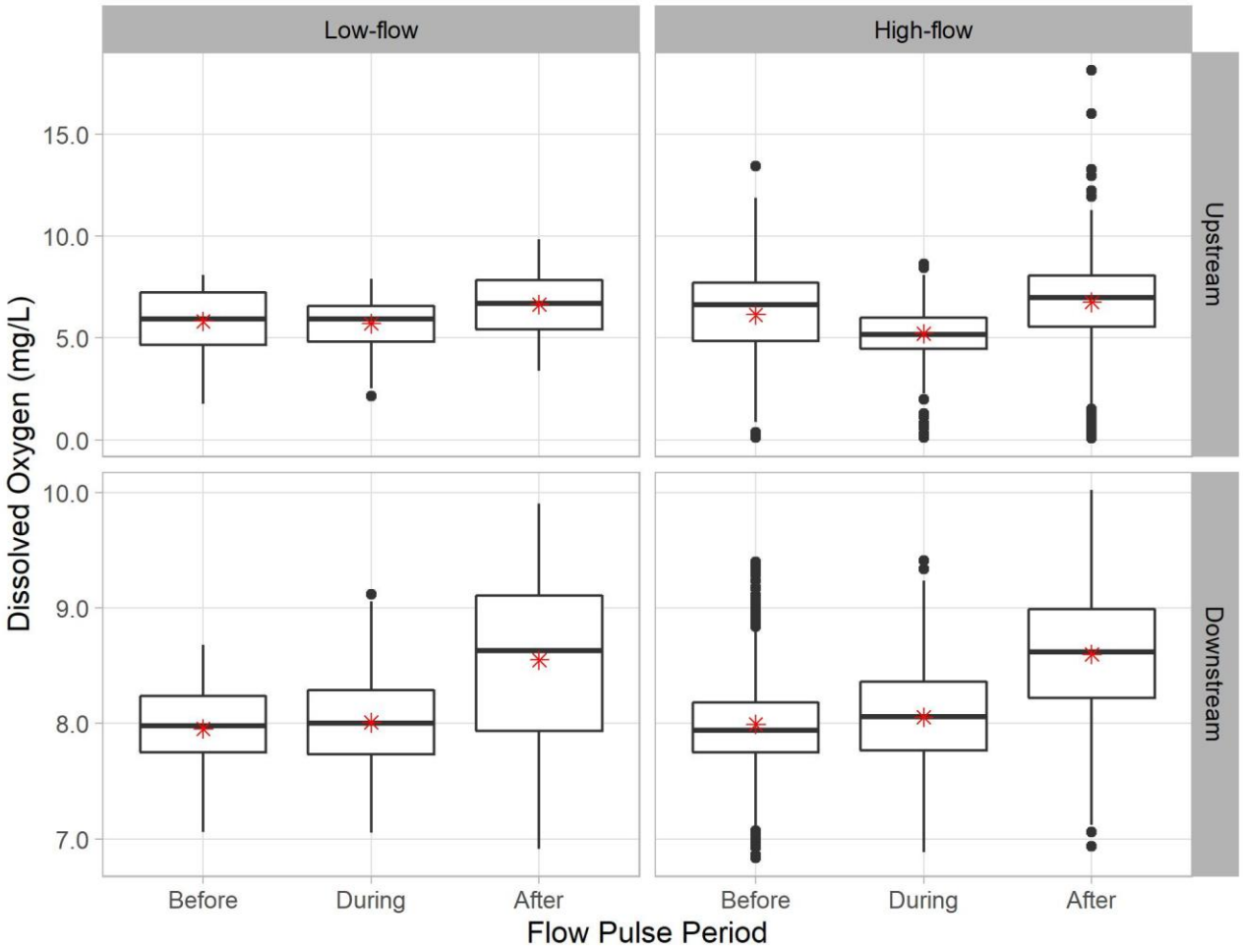

Figure 3-8. Boxplots of medians and quartiles of daily average dissolved oxygen (mg/L) values displaying potential interactions between flow pulse type (low-flow or high-flow pulses), region (upstream or downstream), and flow pulse period (before, during, after). The red asterisks represent the mean of each group.

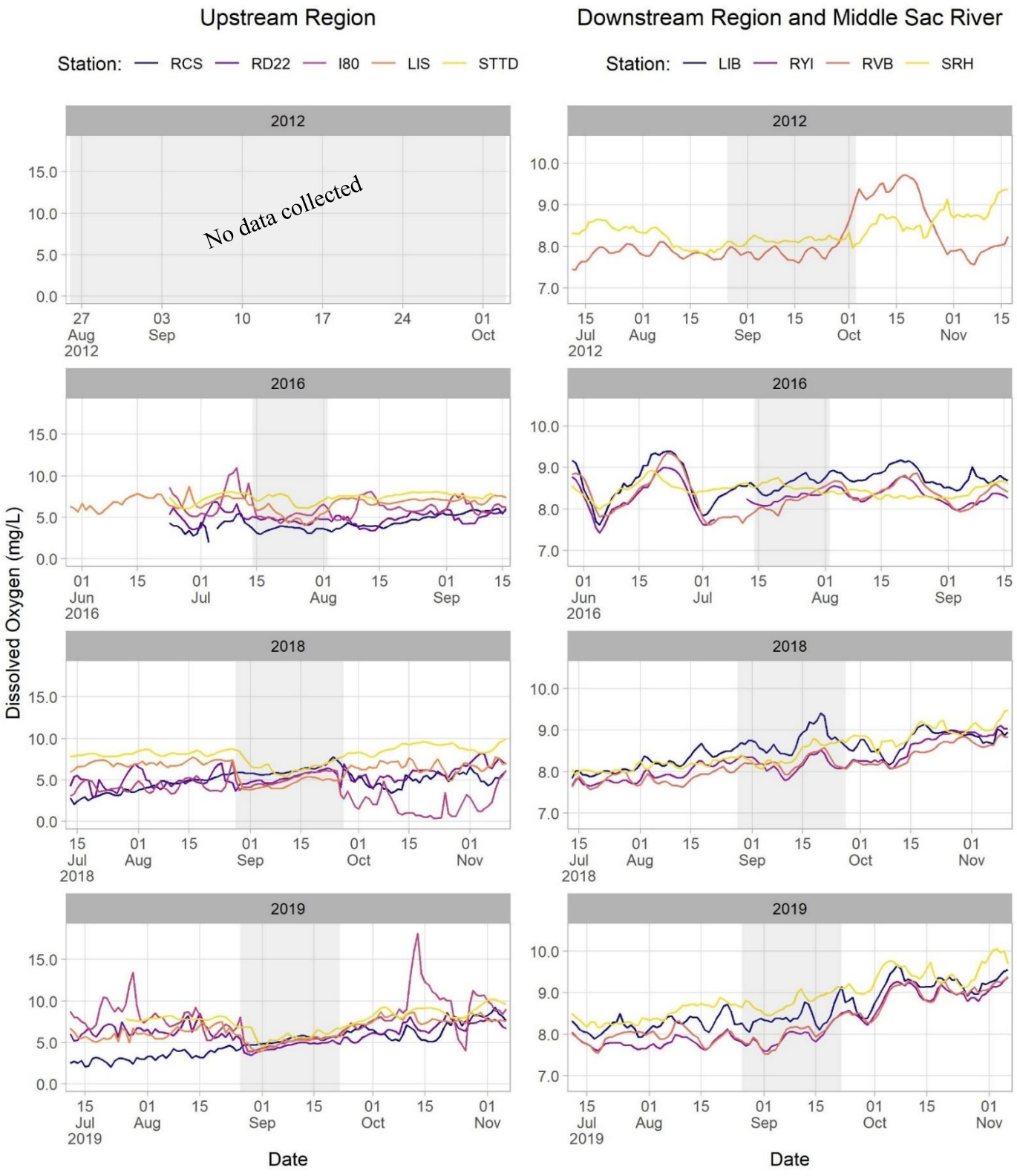

Figure 3-9. Daily average dissolved oxygen values in the upstream region, downstream region, and middle Sacramento River in the years with high flow, high magnitude, and short duration flow pulses (2012, 2016, 2018, and 2019). The light grey shaded box represents the flow pulse period, and the plots for each region have different y-axis scales.

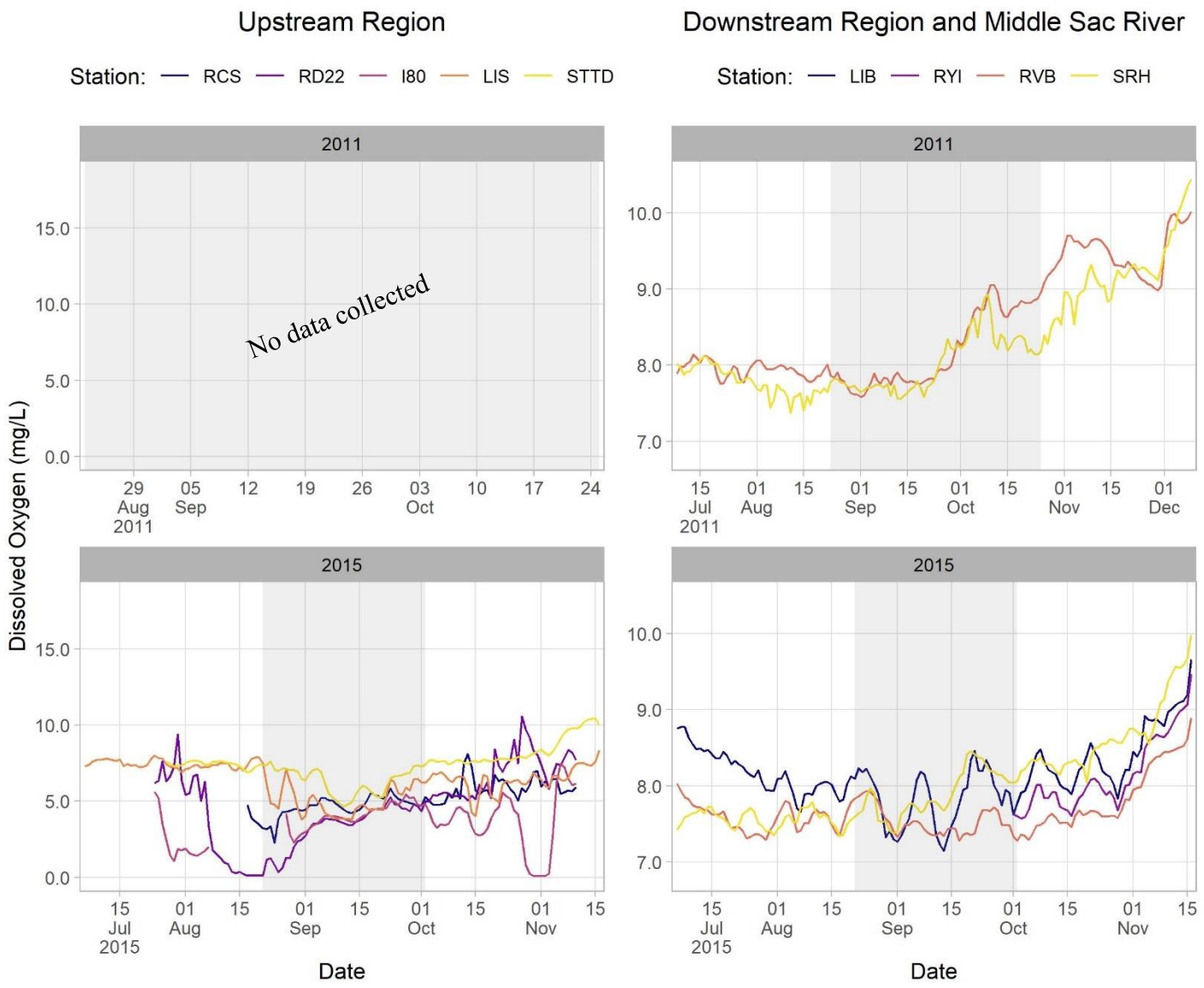

Figure 3-10. Daily average dissolved oxygen values in the upstream region, downstream region, and middle Sacramento River in the years with high flow, low magnitude, and long duration flow pulses (2011 and 2015). The light grey shaded box represents the flow pulse period, and the plots for each region have different y-axis scales.

Figure 3-11. Daily average dissolved oxygen values in the upstream region, downstream region, and middle Sacramento River in the years with low-flow pulses (2013, 2014, and 2017). The light grey shaded box represents the flow pulse period, and the plots for each region have different y-axis scales.

Nitrate plus Nitrite

Nitrite+Nitrite was collected at a minimal number of stations from 2013-2019 (Figure 3-12 and Figure 3-13). As a result of this limited data, we did not analyze continuous Nitrate+Nitrite using ANOVA. Visually, Nitrate+Nitrite concentrations at TOE spiked during the flow pulse in 2018 and 2019 (Figure 3-12). The two downstream stations (LIB and RYI) followed a similar trend of increasing concentration throughout time (excluding 2016) regardless of flow pulse magnitude (low- or -high-flow), duration, or year (Figure 3-12 and Figure 3-13).

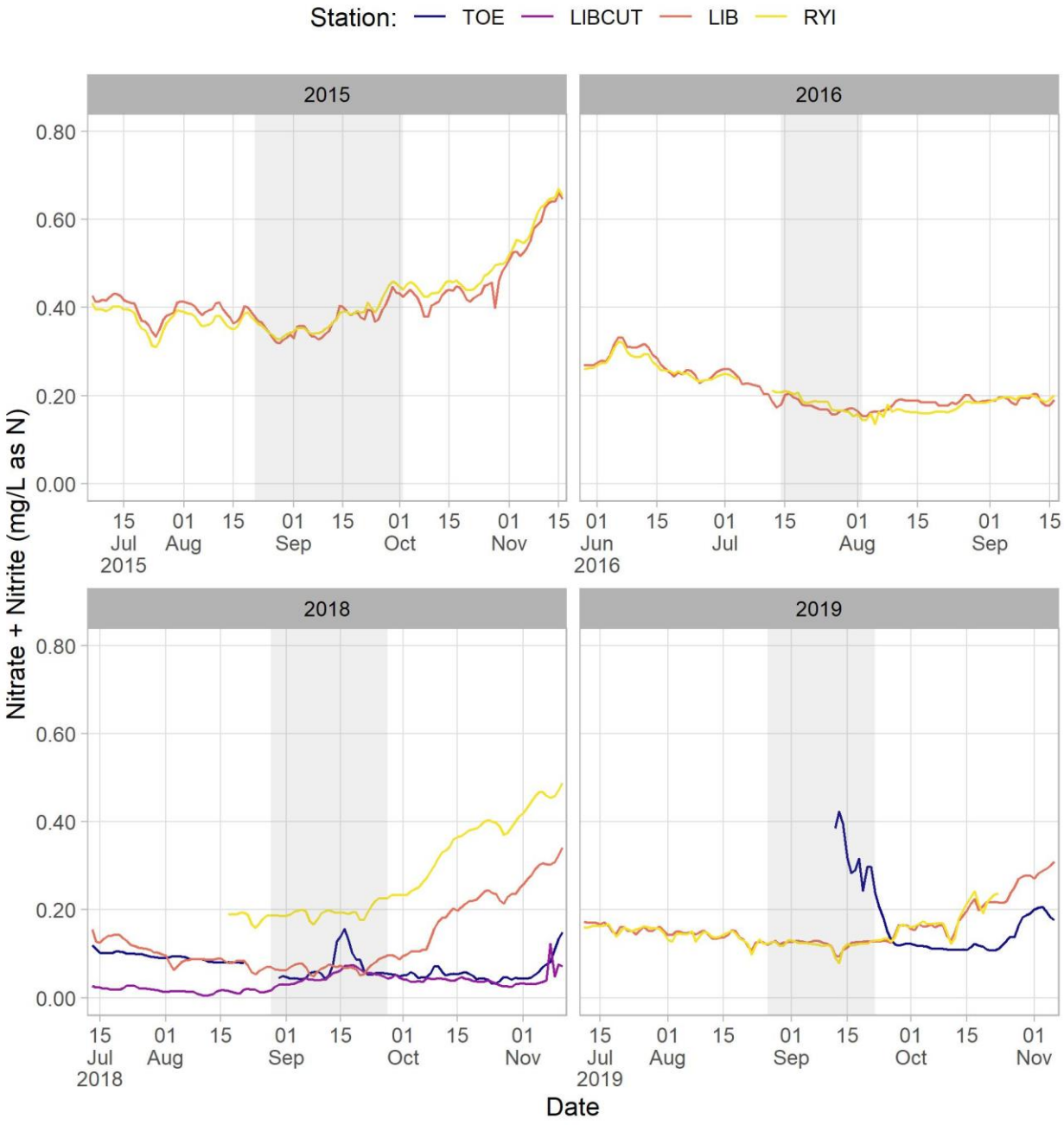

Figure 3-12. Daily average nitrate plus nitrite values in the years with high-flow pulses (2015, 2016, 2018, and 2019). The light grey shaded box represents the flow pulse period.

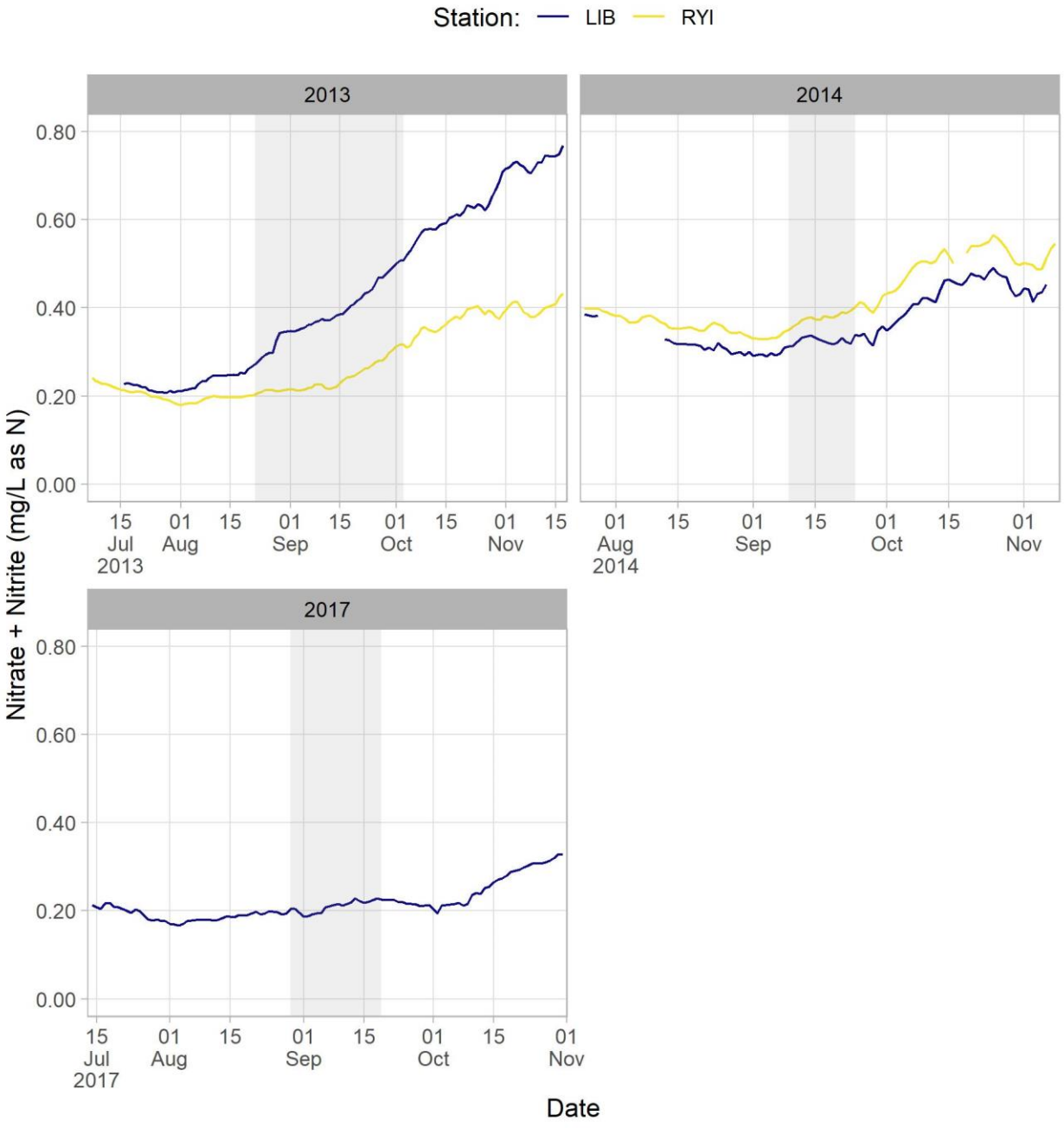

Figure 3-13. Daily average nitrate plus nitrite values in the years with low-flow pulses (2013, 2014, and 2017). The light grey shaded box represents the flow pulse period.

pH

Overall, pH differed significantly across years (ANOVA, $F_{6,5526} = 2.76$, $p<0.05$), while the region ($F_{1,9} = 1.92$, $p=0.20$) and flow pulse period ($F_{2,5756} = 1.31$, $p=0.27$) main effects were not significant. Post-hoc comparisons indicated that pH was significantly higher in 2019 than in 2015 ($p<0.05$) and 2017 ($p<0.05$) (Figure 3-14).

Comparative assessments of low- and high-flow pulses by region and flow pulse period are provided in Figure 3-15. Like chlorophyll and DO, pH values in the upstream region appeared to have less variability during flow pulse periods in two years with high-flow pulses (2018 and 2019) (Figure 3-16). Across all years in the upstream region, pH values were frequently > 8.0 before and after the flow pulse, suggesting uptake of carbon dioxide resulting from photosynthetic processes (Figure 3-16, Figure 3-17, and Figure 3-18; ICF 2020). In contrast, pH in the downstream region was lower except for LIB which had consistently higher pH values than the other downstream stations (RYI and RVB) (Figure 3-16, Figure 3-17, and Figure 3-18). In addition, pH at LIB exceeded 8.0 during high flow years 2018 and 2019. In 2018, LIB exceeded 8.0 for about one week during the flow pulse and three times in 2019 (Figure 3-16).

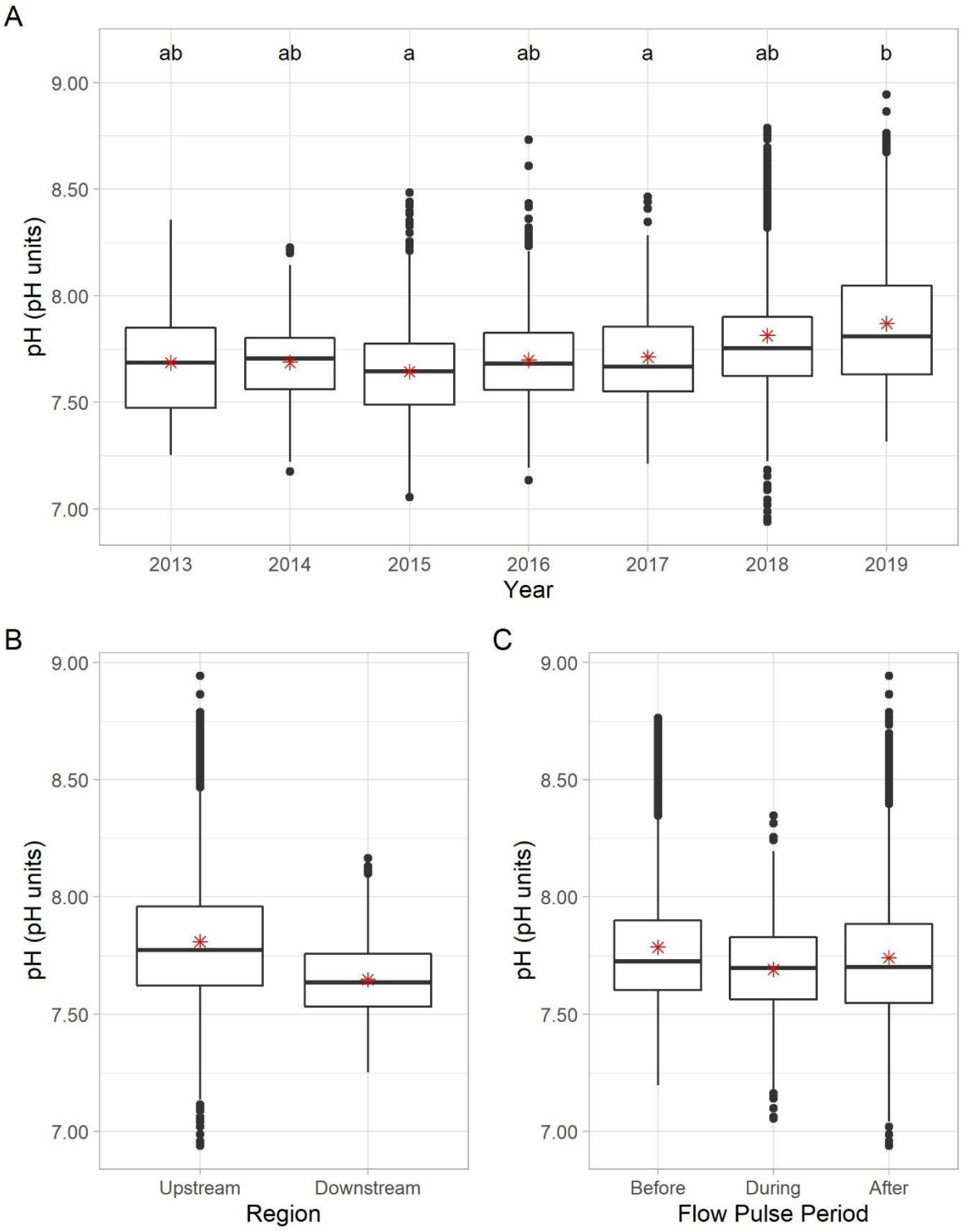

Figure 3-14. Boxplots of medians and quartiles of daily average pH values by model predictors A) year, B) region, and C) flow pulse period. The red asterisks represent the mean of each group. The letters above boxes in A) indicate significant differences in pH values among years according to post-hoc tests. Different letters above boxes indicate significant differences.

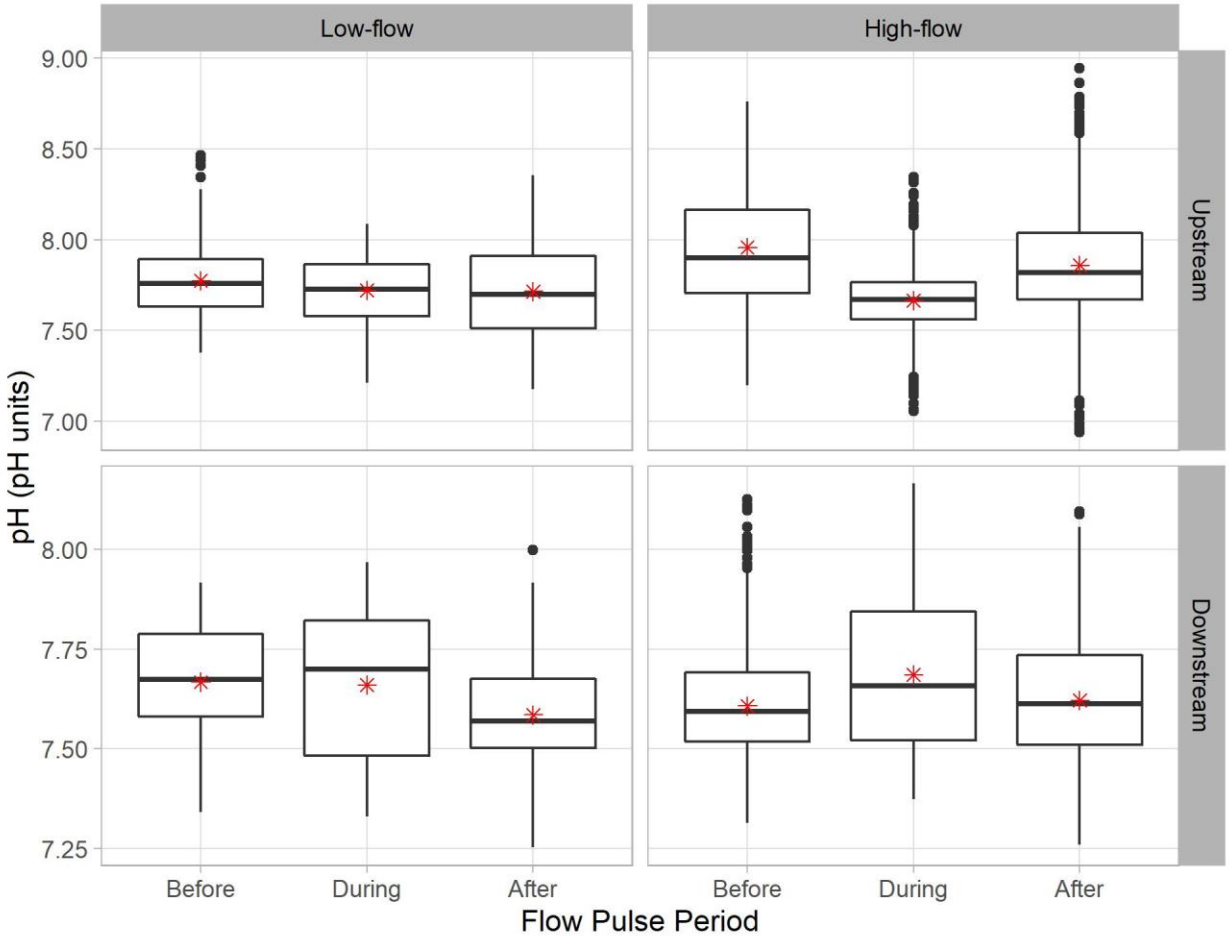

Figure 3-15. Interaction boxplots of medians and quartiles of daily average pH values between flow pulse type (low-flow or high-flow pulses), region (upstream or downstream), and flow pulse period (before, during, after). The red asterisks represent the mean of each group.

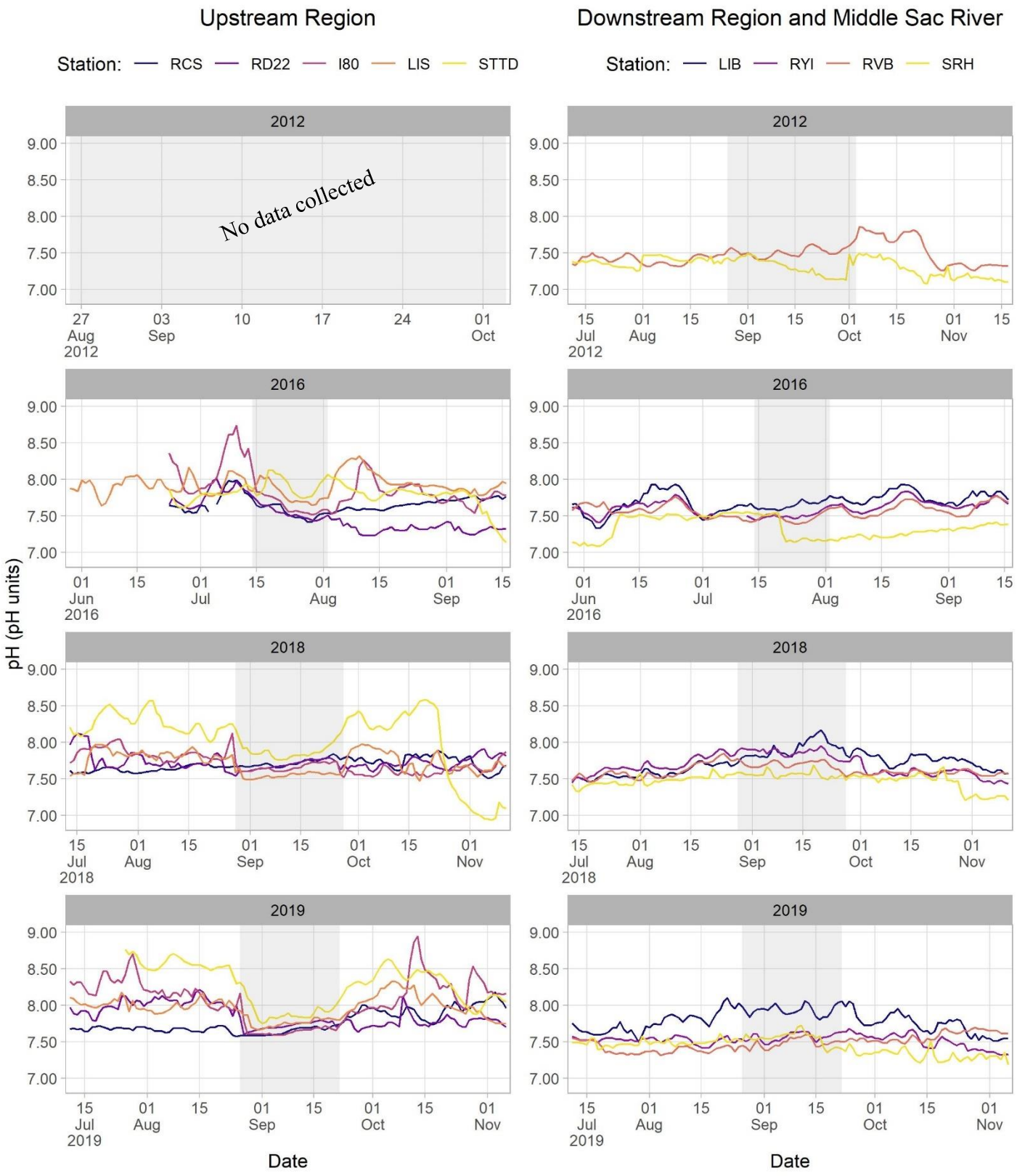

Figure 3-16. Daily average pH values in the upstream region, downstream region, and middle Sacramento River in the years with high flow, high magnitude, and short duration flow pulses (2012, 2016, 2018, and 2019). The light grey shaded box represents the flow pulse period.

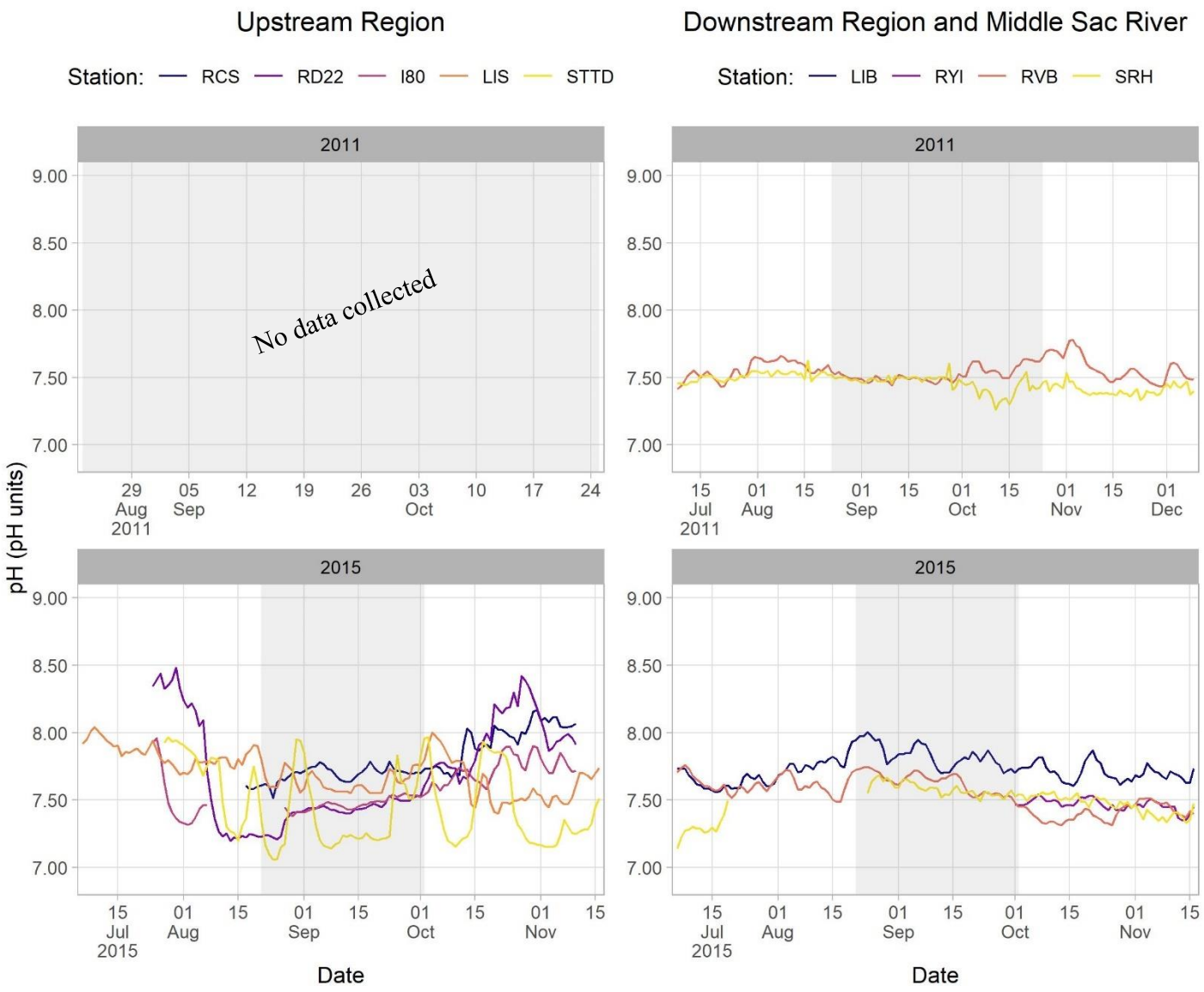

Figure 3-17. Daily average pH values in the upstream region, downstream region, and middle Sacramento River in the years with high flow, low magnitude, and long duration flow pulses (2011 and 2015). The light grey shaded box represents the flow pulse period.

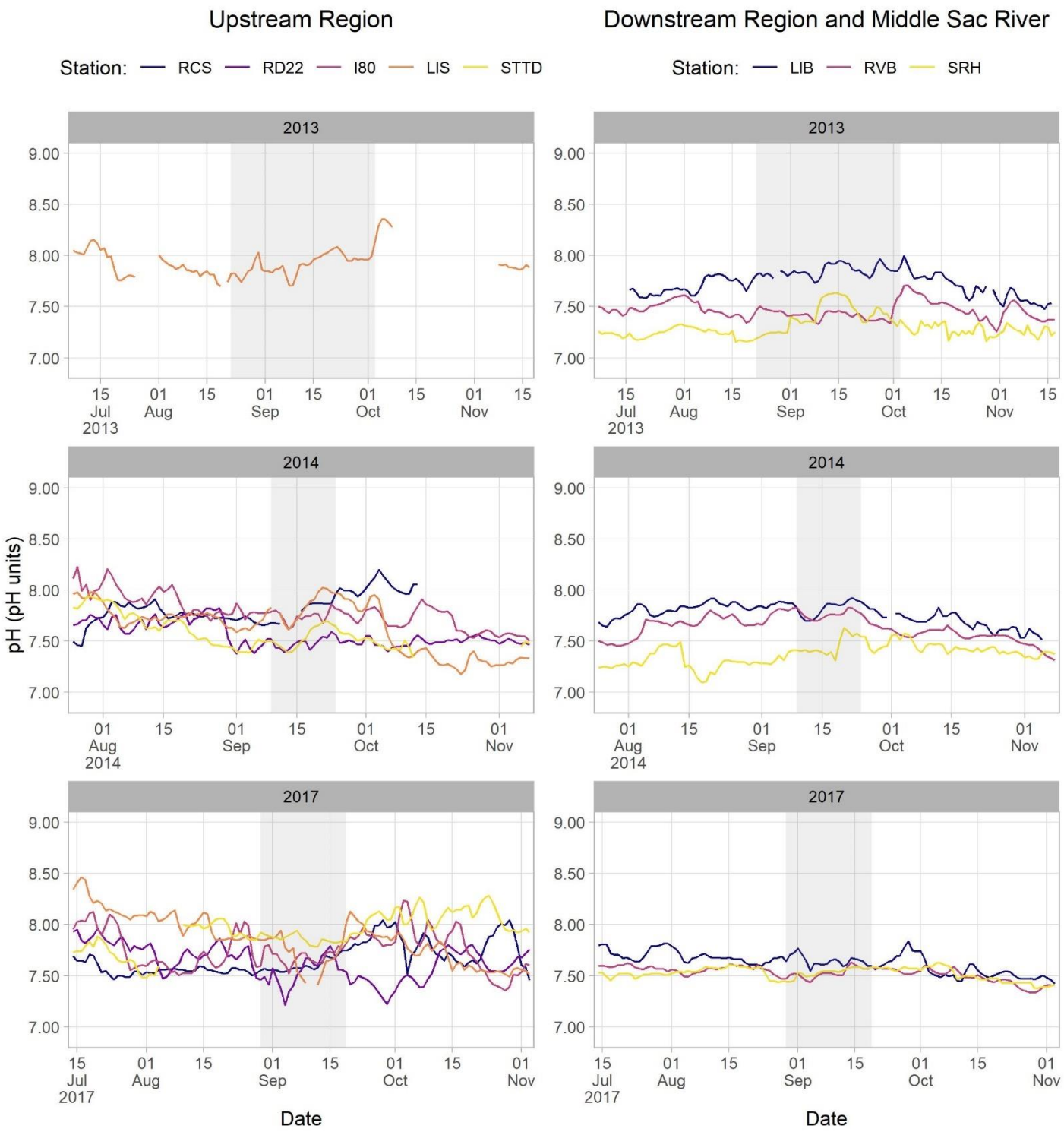

Figure 3-18. Daily average pH values in the upstream region, downstream region, and middle Sacramento River in the years with low-flow pulses (2013, 2014 and 2017). The light grey shaded box represents the flow pulse period.

Specific Conductance

The main effects of year ($F_{6,5960}$ = 4.56, p<0.001), region ($F_{1,10}$ = 10.3, p<0.01), and flow pulse period ($F_{2,6054}$ = 21.1, p<0.001) significantly affected specific conductance. The upstream region had significantly higher specific conductance values than the downstream region (p<0.01), while specific conductance was significantly higher during flow pulses than before (p<0.001) and after (p<0.001) pulses across all years (Figure 3-19; Figure 3-20). Specific conductance values were significantly higher in 2015 than in 2016 (p<0.05), 2017 (p<0.001) and 2019 (p<0.01), and values were higher in 2014 than in 2017 (p<0.01) (Figure 3-19).

Daily average specific conductance values varied widely between the stations in the upstream region with generally lower values at the stations in the lower Yolo Bypass (LIS and STTD) and higher values in the upper Yolo Bypass (RCS, RD22, and I80) (Figure 3-21, Figure 3-22, and Figure 3-23). However, during all years with high-flow pulses (2015, 2016, 2018, and 2019), specific conductance values at the upstream stations converged during the flow pulses (Figure 3-20, Figure 3-21, and Figure 3-22). This trend was particularly obvious during the flow pulses in 2018 and 2019 when specific conductance at all upstream stations was influenced by the station located furthest upstream (RCS). Moreover, before the flow pulses in 2018 and 2019, specific conductance values at the stations in the downstream region (LIB, RYI, and RVB) were similar to the values in the Middle Sacramento River (SRH); however, towards the middle and end of these flow pulses, values at the downstream stations increased to levels that exceeded those at SRH, and became more similar to values at upstream stations (Figure 3-21).

In contrast, daily average specific conductance values at the upstream stations did not strongly converge during the flow pulses in the years with lower flows (2013, 2014, and 2017) (Figure 3-23). Specific conductance increased during the flow pulses in these low-flow years at LIS and STTD to values closer to those observed at the stations in the upper Yolo Bypass, but there was a lot of variation between the upstream stations during the flow pulses. At the stations in the downstream region, specific conductance values did not change in response to the flow pulses in the low-flow years (Figure 3-23).

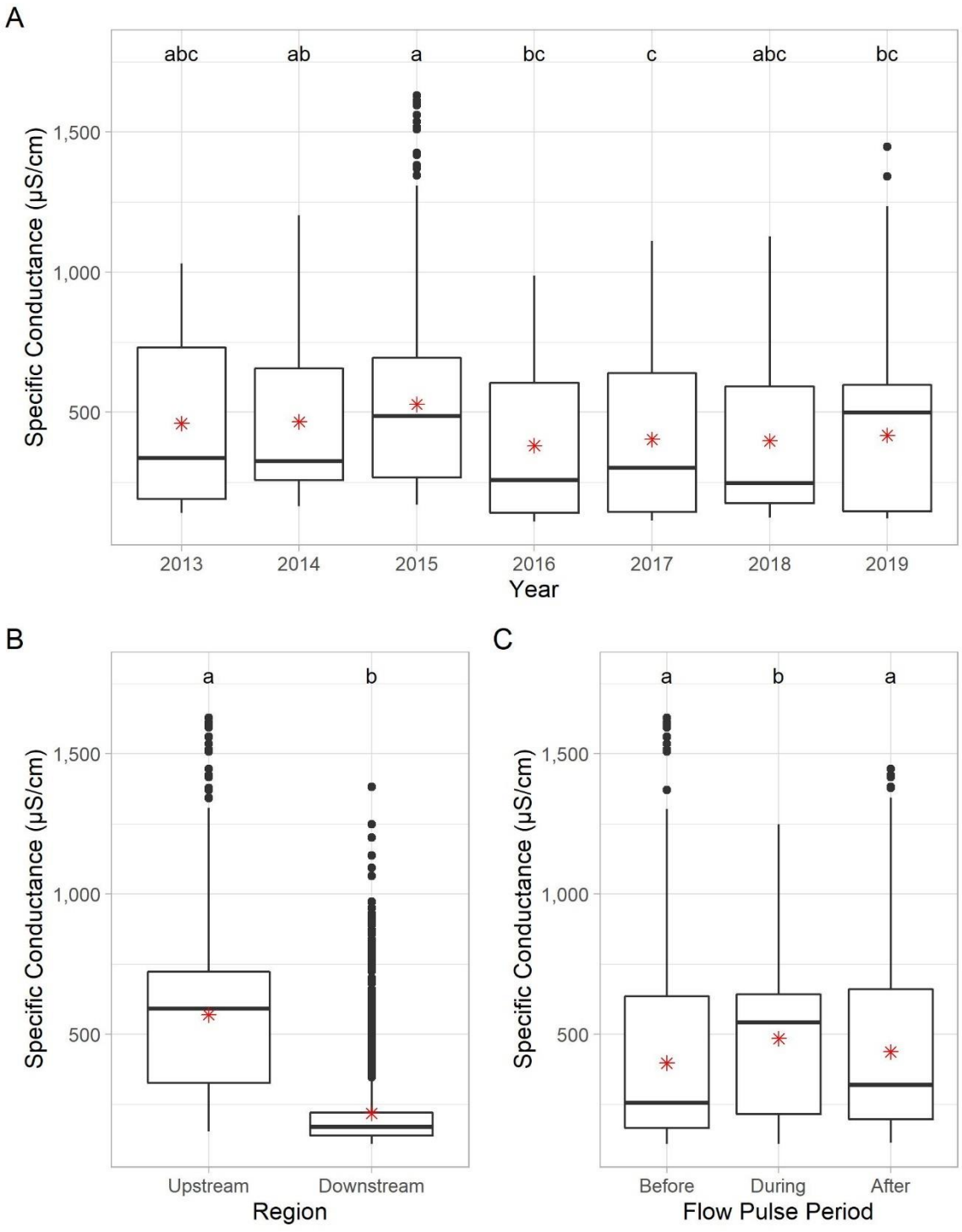

Figure 3-19. Boxplots of medians and quartiles of daily average specific conductance values by model predictors A) year, B) region, and C) flow pulse period. The red asterisks represent the mean of each group. The letters above boxes in A), B), and C) indicate significant differences in specific conductance values among years, regions, and flow pulse periods, respectively, according to post-hoc tests. Different letters above boxes indicate significant differences.

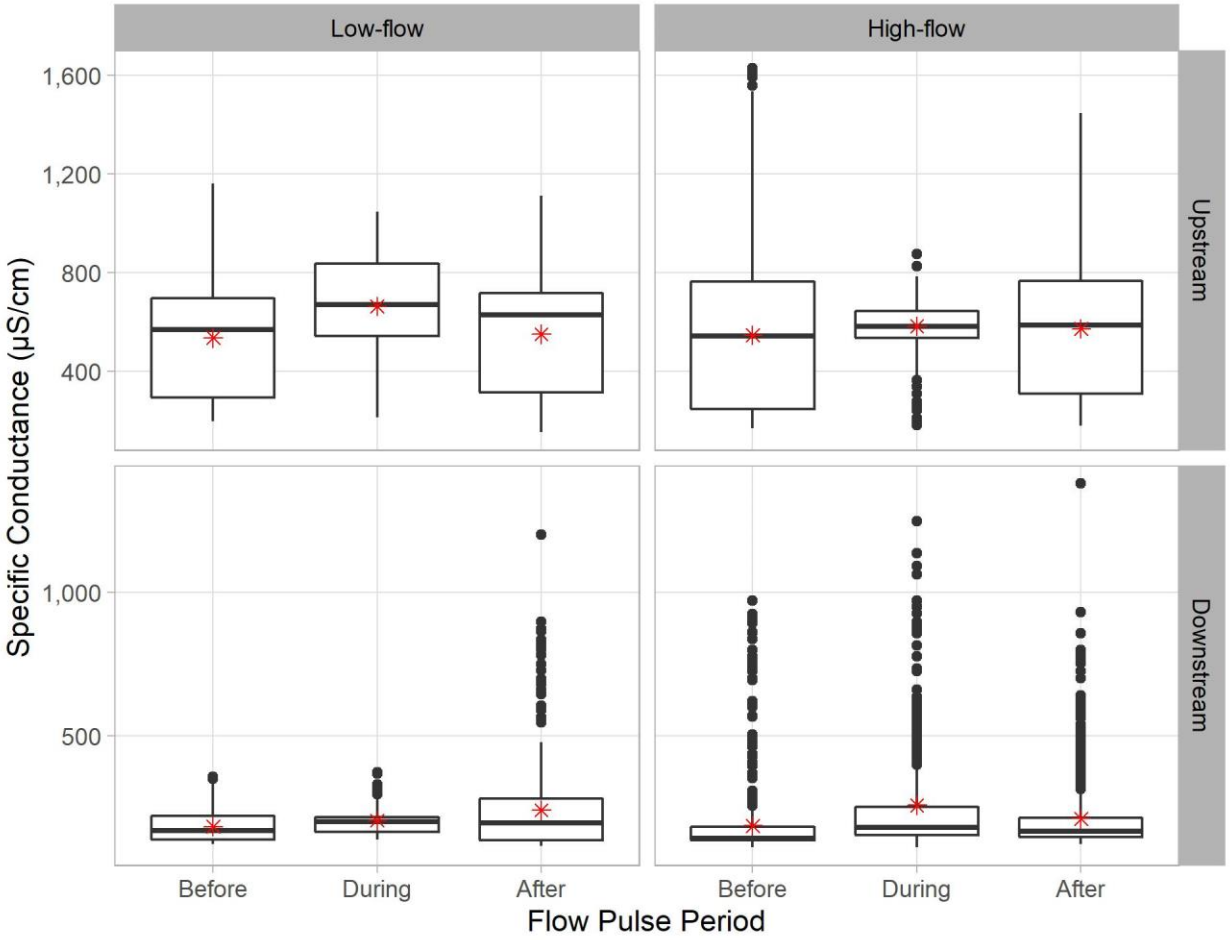

Figure 3-20. Interaction boxplots of medians and quartiles of daily average specific conductance (µS/cm) values between flow pulse type (low-flow or high-flow pulses), region (upstream or downstream), and flow pulse period (before, during, after). The red asterisks represent the mean of each group.

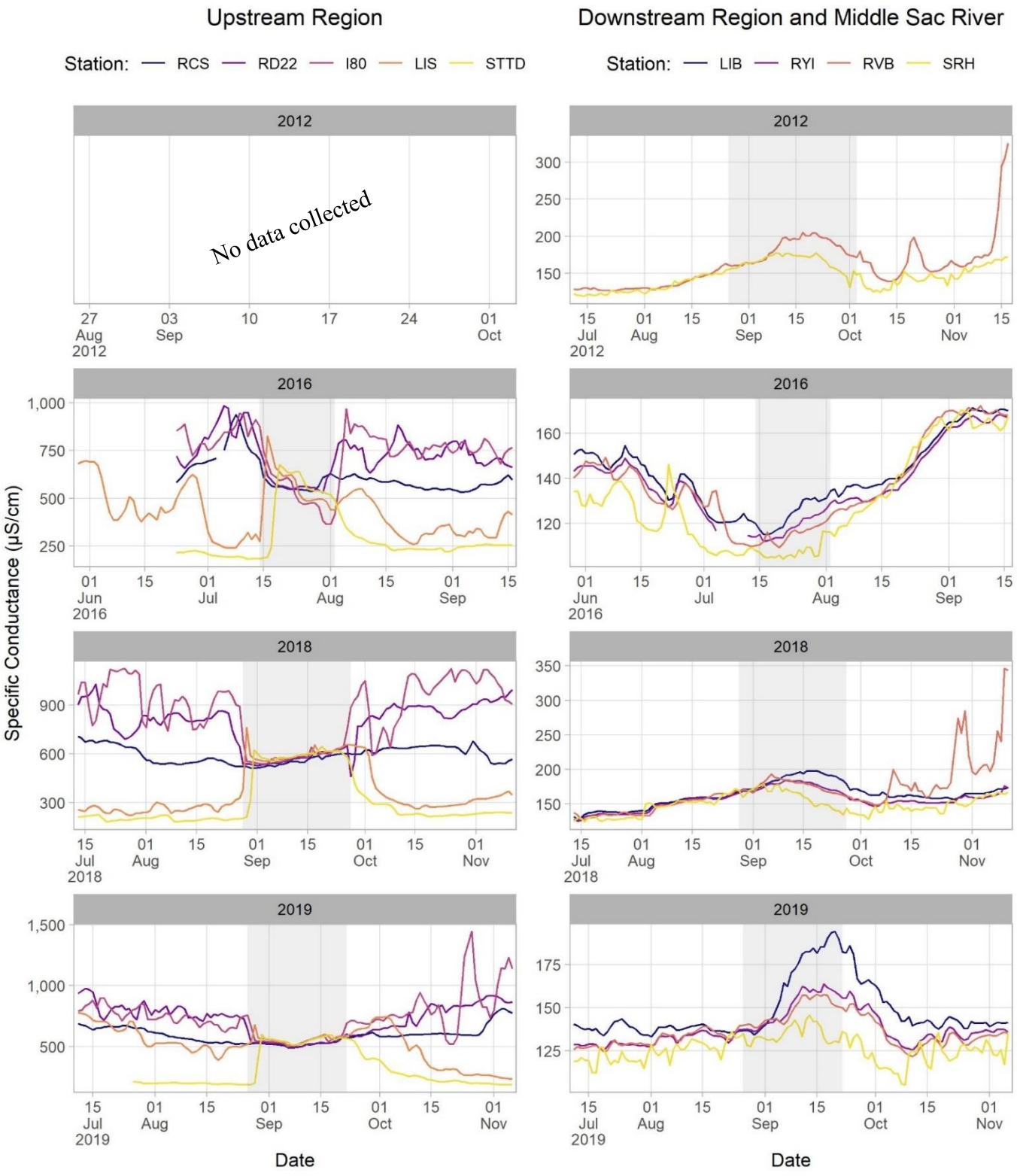

Figure 3-21. Daily average specific conductance values in the upstream region, downstream region, and middle Sacramento River in the years with high flow, high magnitude, and short duration flow pulses (2012, 2016, 2018, and 2019). The light grey shaded box represents the flow pulse period, and each plot has a different y-axis scale.

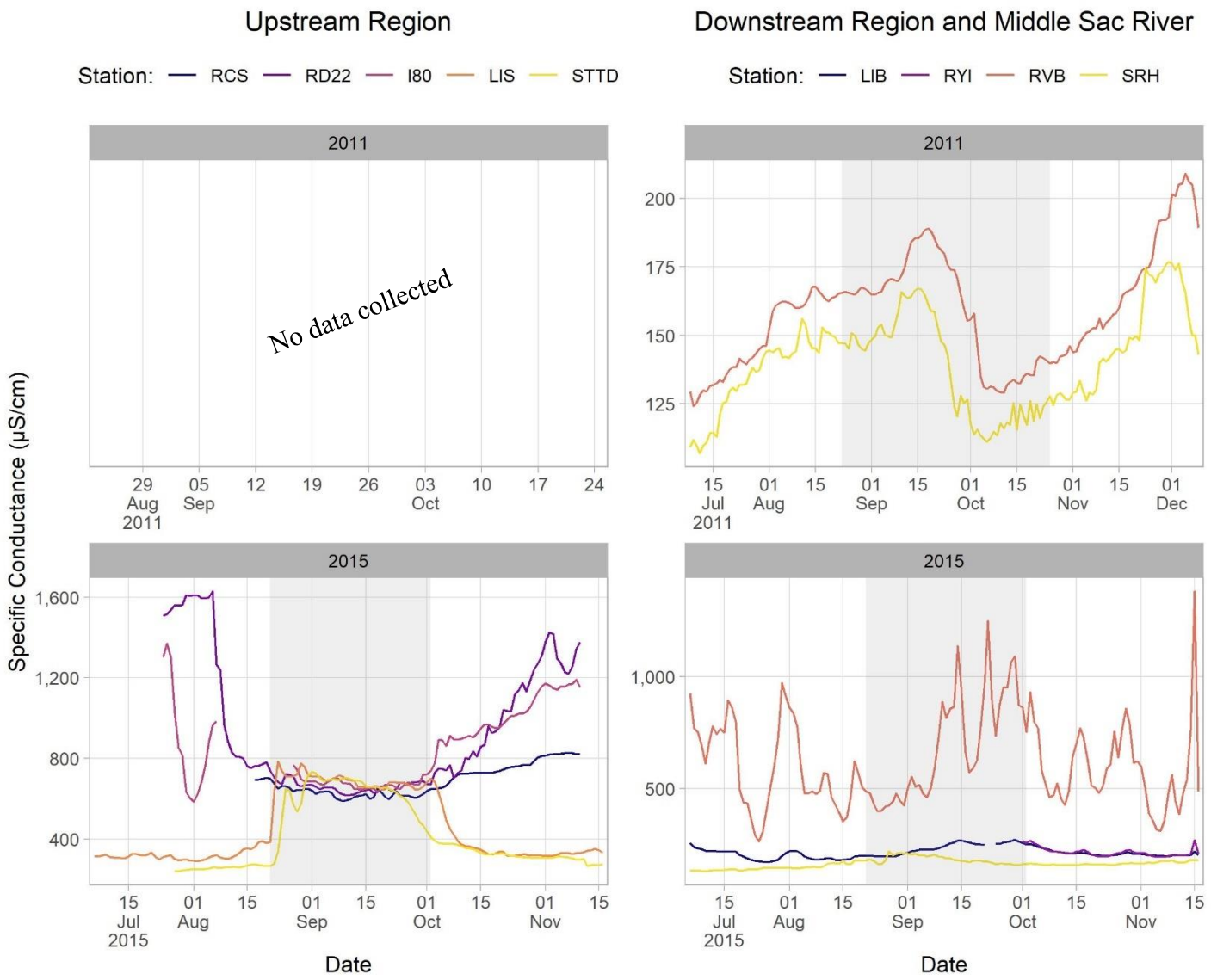

Figure 3-22. Daily average specific conductance values in the upstream region, downstream region, and middle Sacramento River in the years with high flow, low magnitude, and long duration flow pulses (2011 and 2015). The light grey shaded box represents the flow pulse period, and each plot has a different y-axis scale.

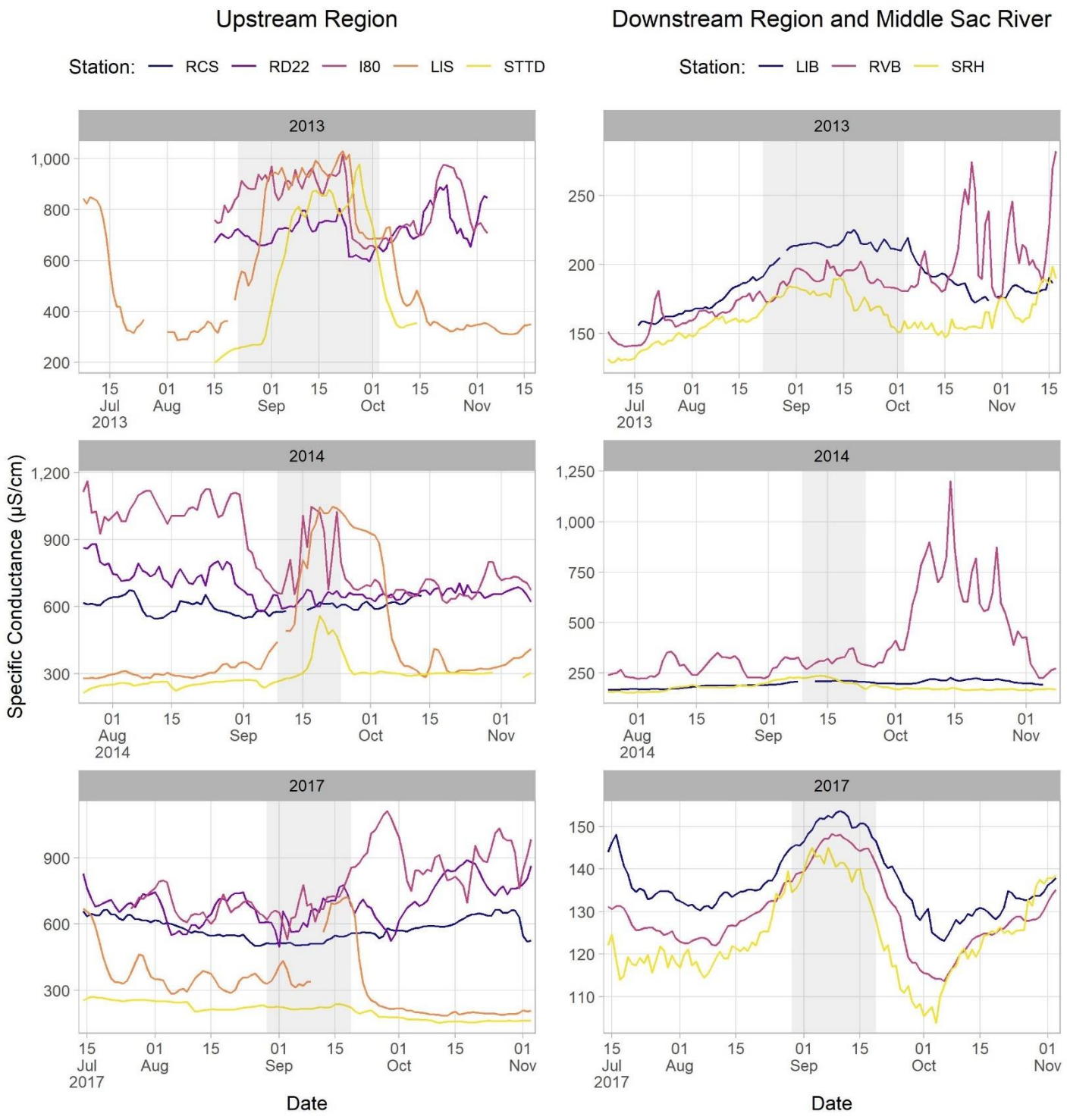

Figure 3-23. Daily average specific conductance values in the upstream region, downstream region, and middle Sacramento River in the years with low-flow pulses (2013, 2014 and 2017). The light grey shaded box represents the flow pulse period, and each plot has a different y-axis scale.

Turbidity

Turbidity was significantly different across years ($F_{6,4462}$ = 10.7, p<0.001), flow pulse periods ($F_{2,4939}$ = 7.80, p<0.001), and regions ($F_{1,12}$ = 28.7, p<0.001). Spatially, turbidity of the upstream region was higher than downstream (p<0.001). Temporally, turbidity values before flow pulses were significantly higher than during (p<0.05) and after (p<0.001) flow pulses (Figure 3-24), however, spatial and temporal interactions are uncertain (Figure 3-25). Turbidity in both 2014 and 2016 was significantly higher than 2017, 2018, and 2019. Overall, turbidity was significantly lower in 2018 than all other years.

Similar to trends with specific conductance, daily average turbidity values in the upstream region converged during the high-flow pulse periods (Figure 3-26). However, turbidity was not measured consistently at all stations and during all years, so region-wide trends are difficult to determine for some years. Apparent responses to flow pulses varied between the upstream stations during years with high flows. In 2015 and 2016, turbidity values at LIS decreased at the onset of the high-flow pulse (Figure 3-26 and Figure 3-27). In contrast, turbidity increased when the flow pulse began in 2018 and 2019 at STTD (Figure 3-26). After the flow pulses in 2015 and 2018, turbidity generally returned to levels resembling those before the pulses, but only LIS returned to levels observed before the pulse in 2016 (Figure 3-26 and Figure 3-27). In addition, 2019 was the only high-flow year that had a general decreasing trend in turbidity values across most stations in the upstream region (Figure 3-26). The stations in the downstream region typically had lower turbidity levels at <25 FNU across all years. LIB had a few isolated spikes in turbidity (15-25 FNU) during the flow pulse in 2017 and 2018 (low-flow year and high-flow year, respectively), but this pattern was not apparent at the remaining stations in the downstream region (Figure 3-26 and Figure 3-28).

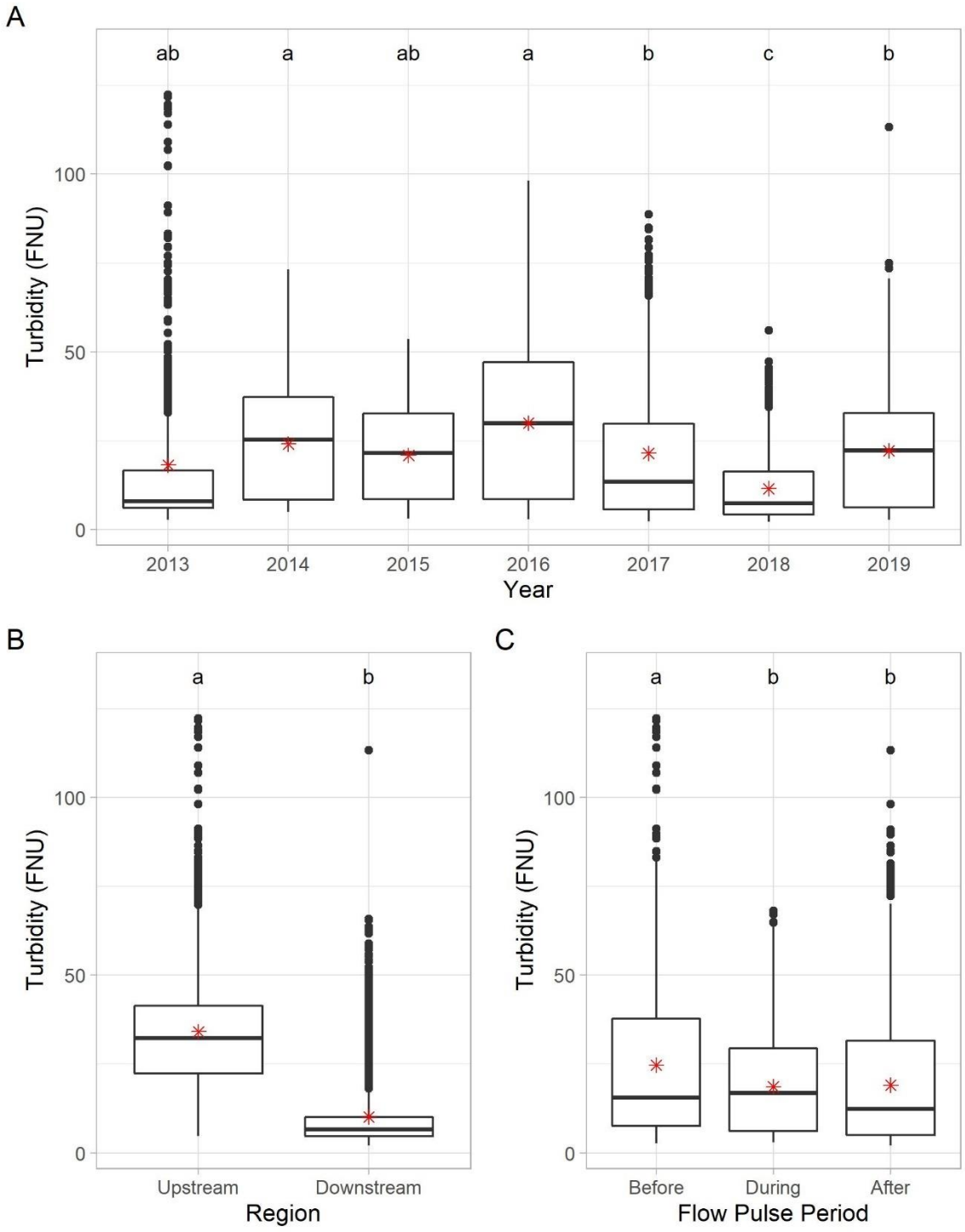

Figure 3-24. Boxplots of medians and quartiles of daily average turbidity values by model predictors A) year, B) region, and C) flow pulse period. The red asterisks represent the mean of each group. The letters above boxes in A), B), and C) indicate significant differences in turbidity values among years, regions, and flow pulse periods, respectively, according to post-hoc tests. Different letters above boxes indicate significant differences.

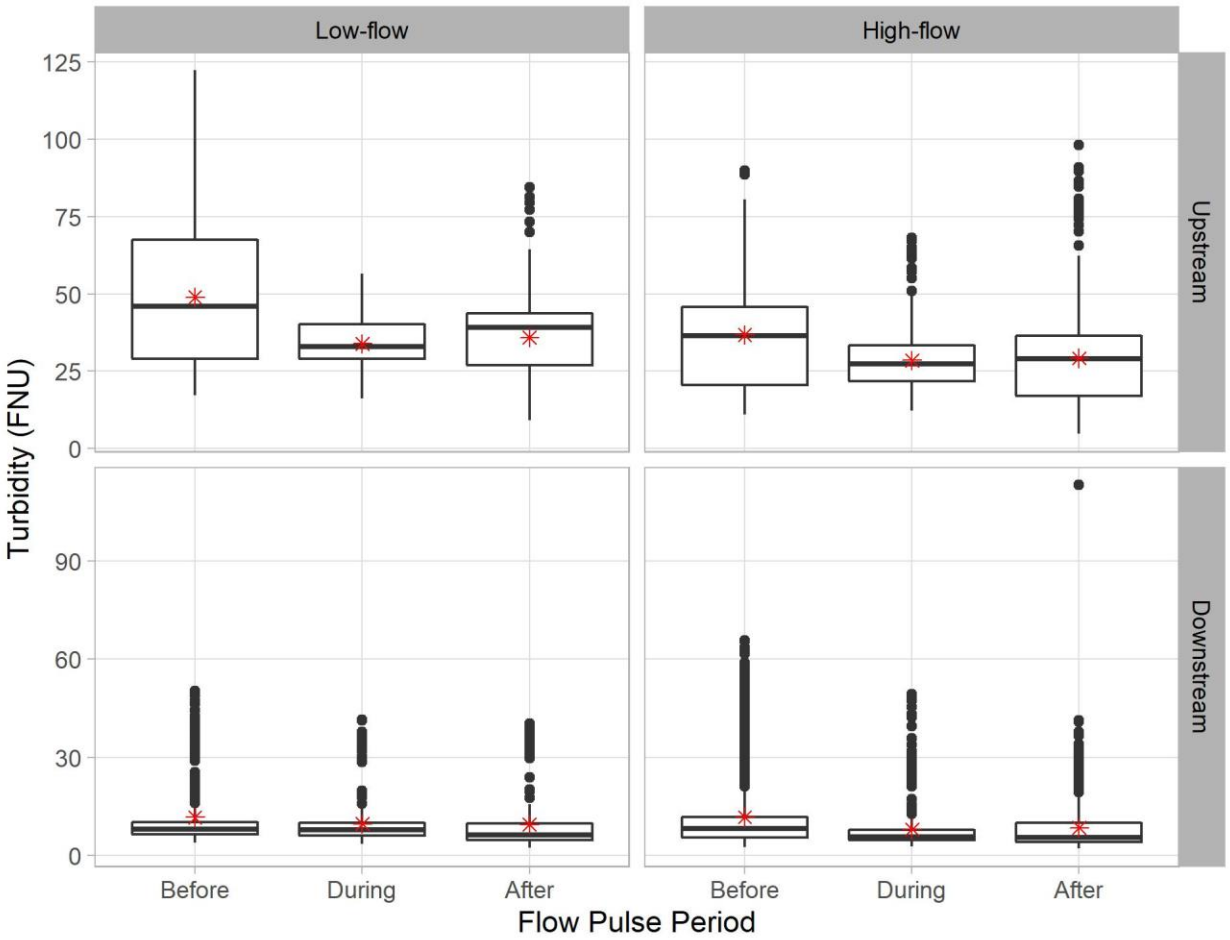

Figure 3-25. Interaction boxplots of medians and quartiles of daily average turbidity (FNU) values between flow pulse type (low-flow or high-flow pulses), region (upstream or downstream), and flow pulse period (before, during, after). The red asterisks represent the mean of each group.

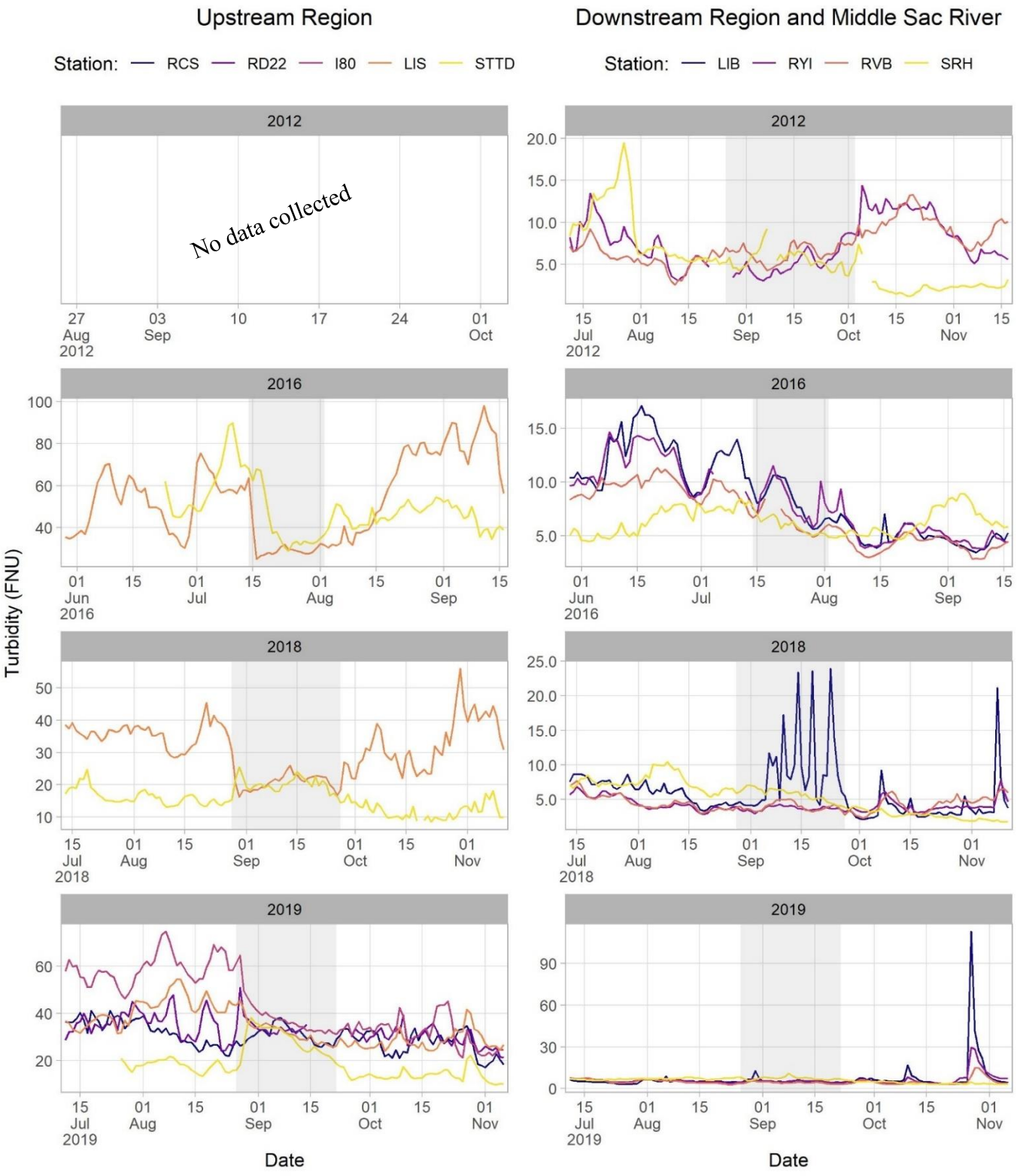

Figure 3-26. Daily average turbidity values in the upstream region, downstream region, and middle Sacramento River across all flow pulse periods in the years with high flow, high magnitude, and short duration flow pulses (2012, 2016, 2018, and 2019). The light grey shaded box represents the flow pulse period, and each plot has a different y-axis scale.

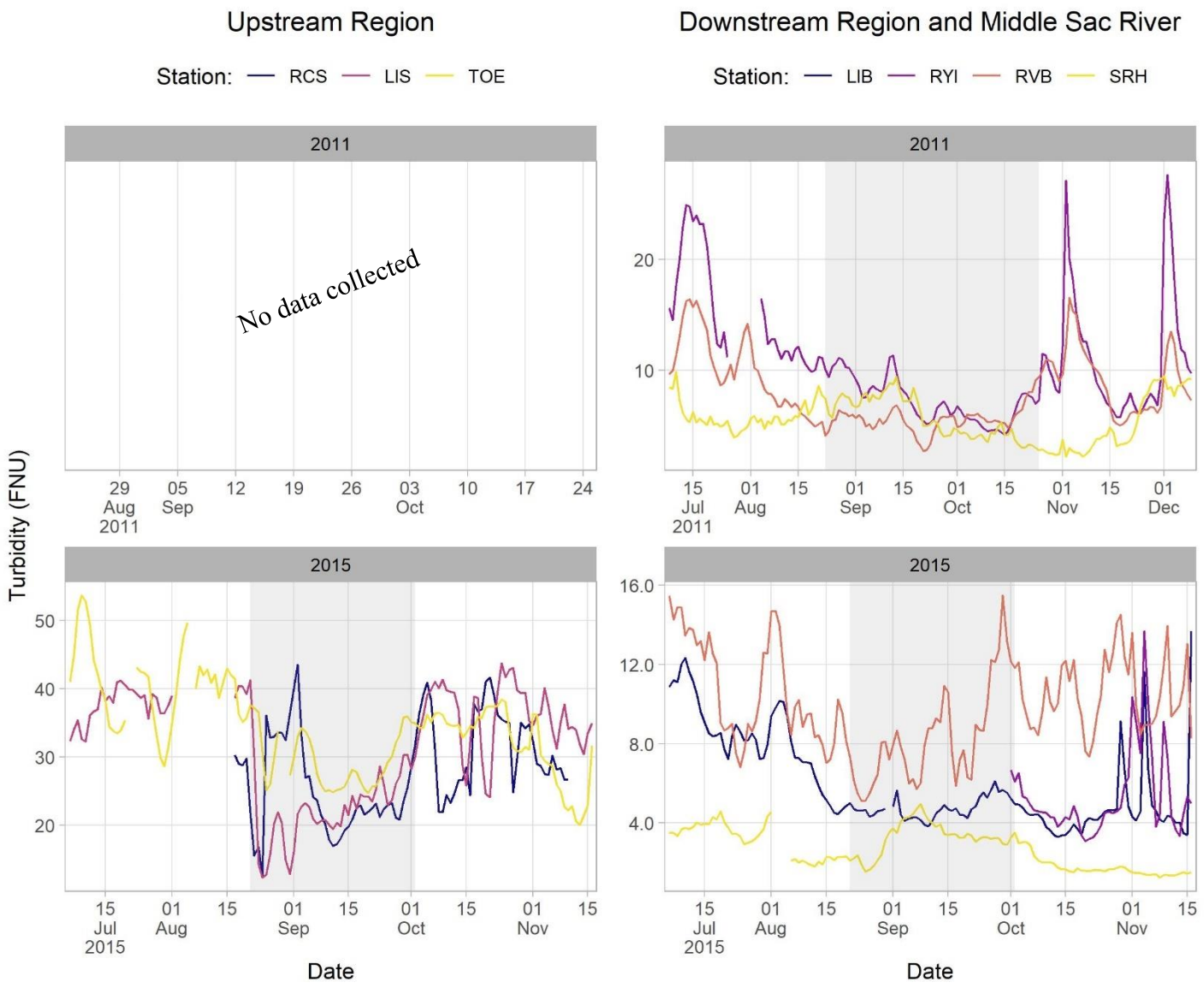

Figure 3-27. Daily average turbidity values in the upstream region, downstream region, and middle Sacramento River in the years with high flow, low magnitude, and long duration flow pulses (2011 and 2015). The light grey shaded box represents the flow pulse period, and each plot has a different y-axis scale.

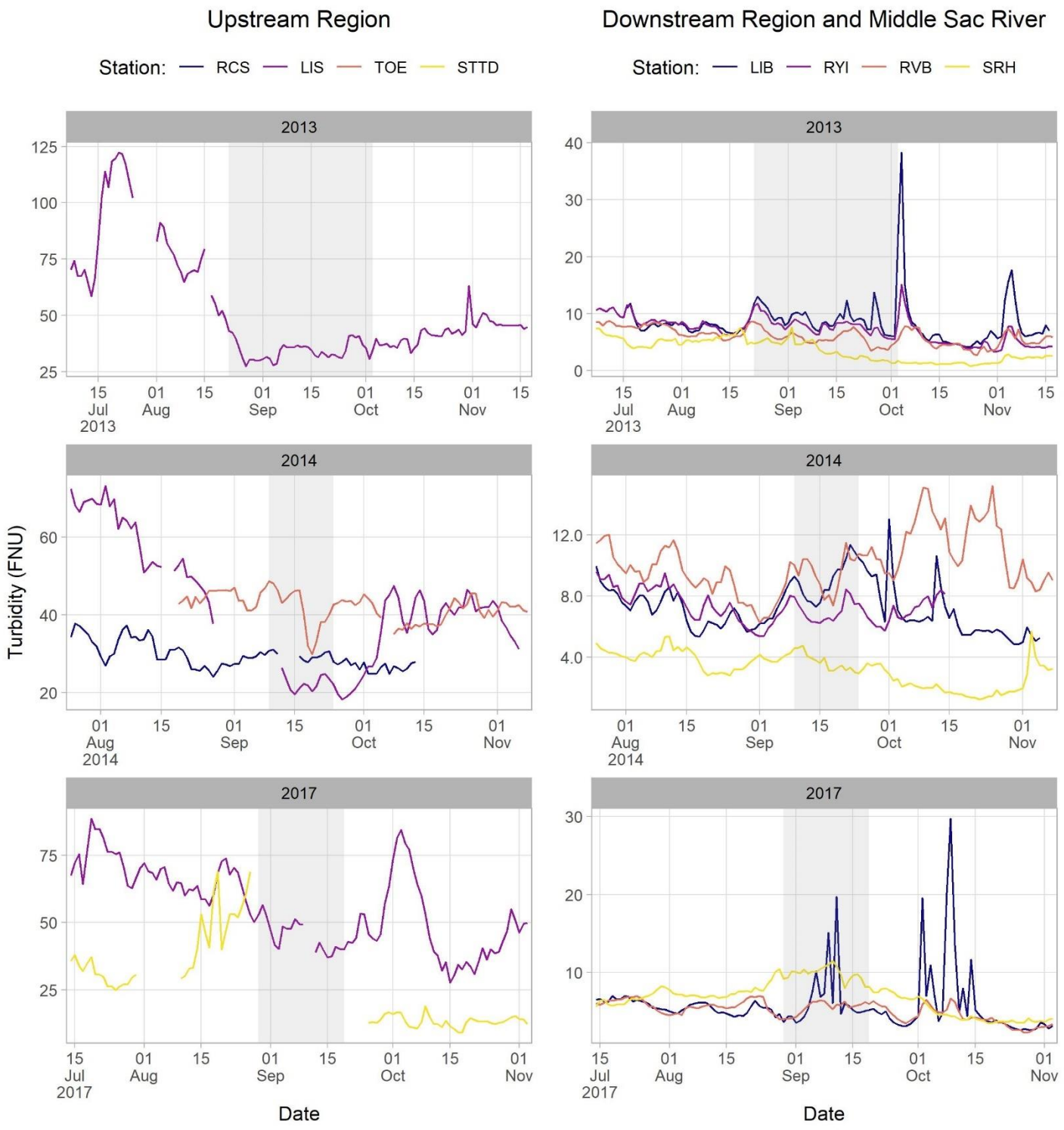

Figure 3-28. Daily average turbidity values in the upstream region, downstream region, and middle Sacramento River in the years with low-flow pulses (2013, 2014 and 2017). The light grey shaded box represents the flow pulse period, and each plot has a different y-axis scale.

Water Temperature

Water temperature is strongly influenced by seasonality, indicating ANOVA models used to evaluate the effects of flow pulses on water temperature would likely be confounded by season. In addition, results of exploratory models varied based on how we accounted for seasonality. Therefore, we did not analyze continuous water temperature data using ANOVA and instead relied on visual assessments of time-series. Daily average water temperatures were generally higher at stations in the upstream region compared to the downstream stations (Figure 3-29) and were similar during both low- and high-flow pulses (Figure 3-30). In general, all stations were very similar to each other and decreased over time following seasonal trends (Figure 3-31, Figure 3-32, and Figure 3-33).

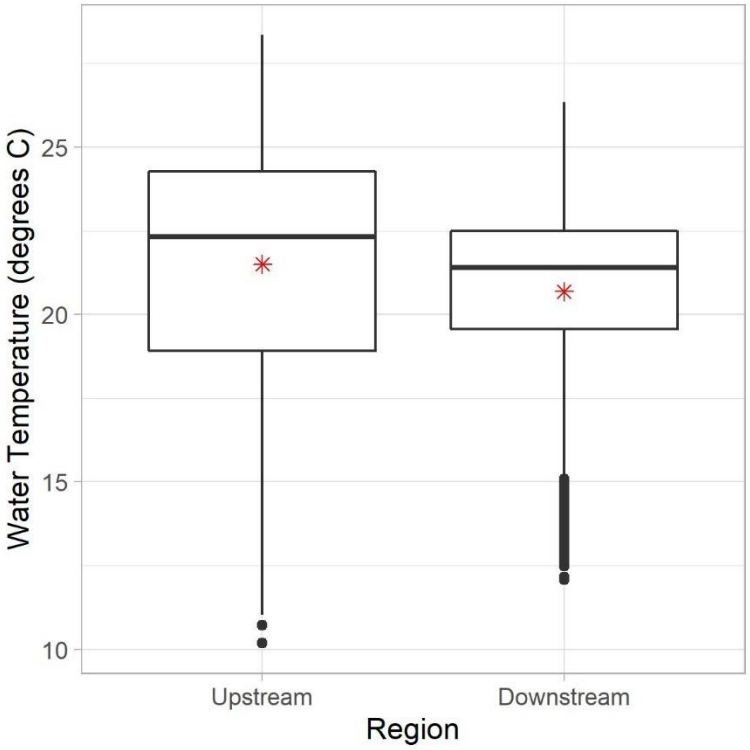

Figure 3-29. Boxplot of medians and quartiles of daily average water temperature values by region from 2013-2019. The red asterisks represent the mean of each group.

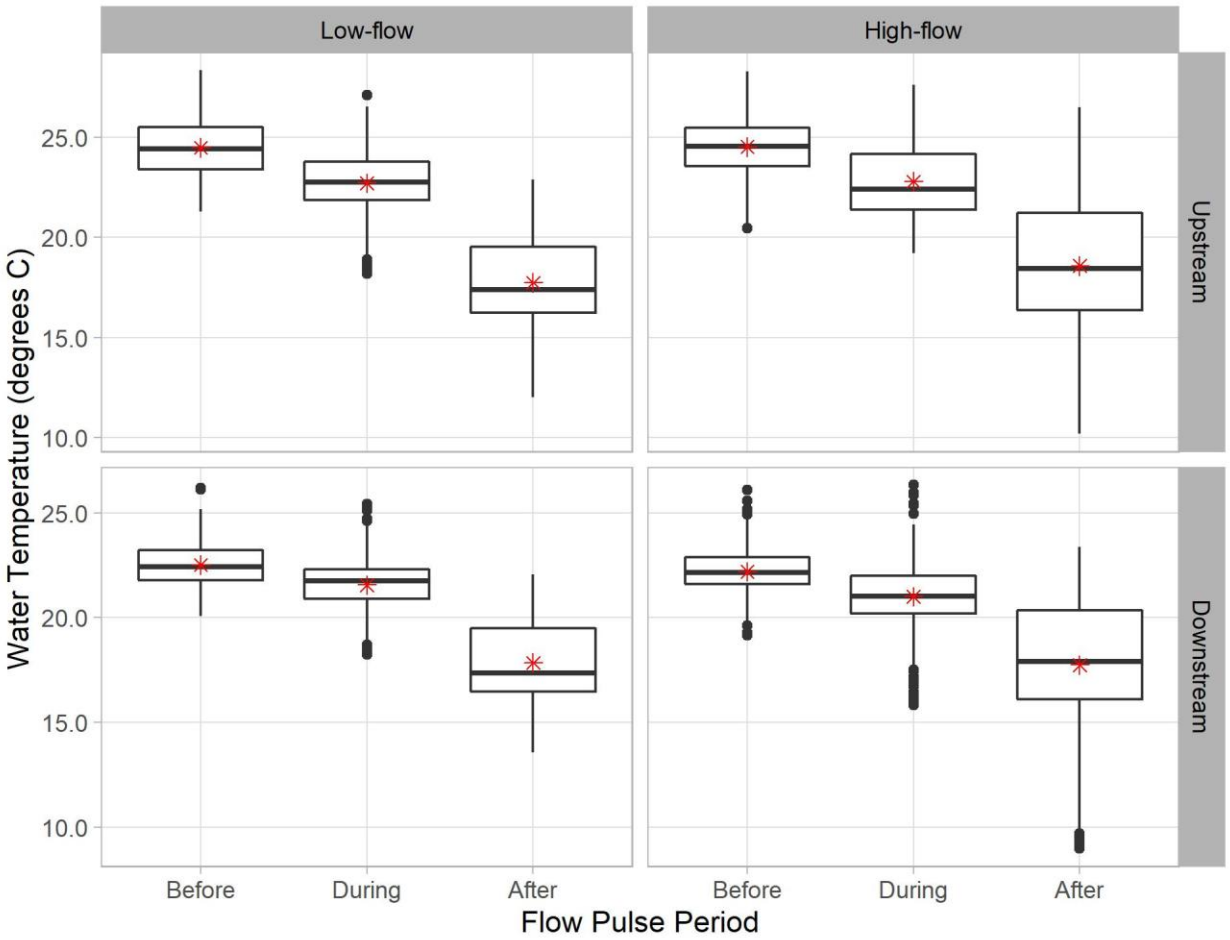

Figure 3-30. Interaction boxplots of medians and quartiles of daily average water temperature (°C) values between flow pulse type (low-flow or high-flow pulses), region (upstream or downstream), and flow pulse period (before, during, after). The red asterisks represent the mean of each group.

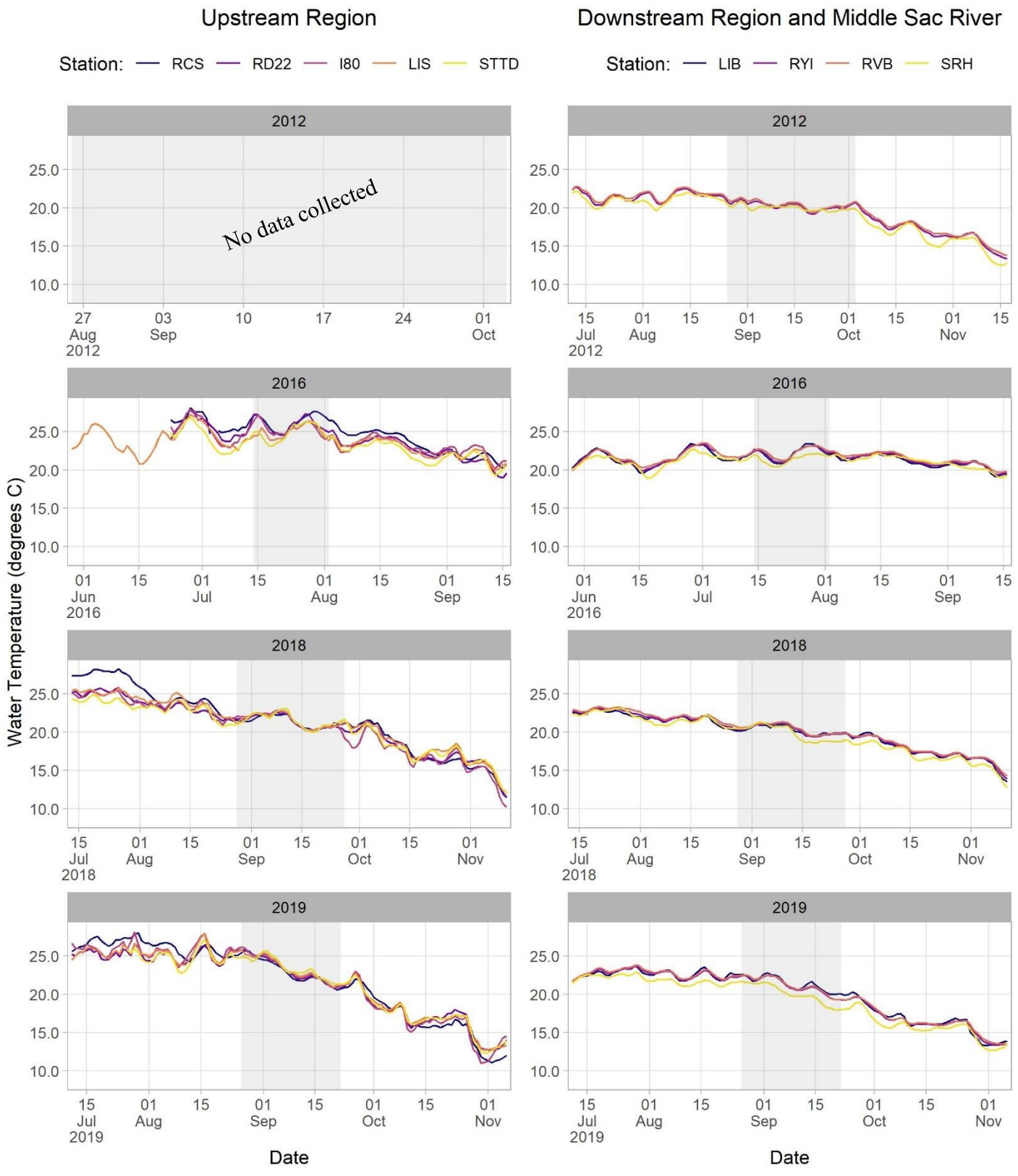

Figure 3-31. Daily average water temperature values in the upstream region, downstream region, and middle Sacramento River in the years with high flow, high magnitude, and short duration flow pulses (2012, 2016, 2018, and 2019). The light grey shaded box represents the flow pulse period.

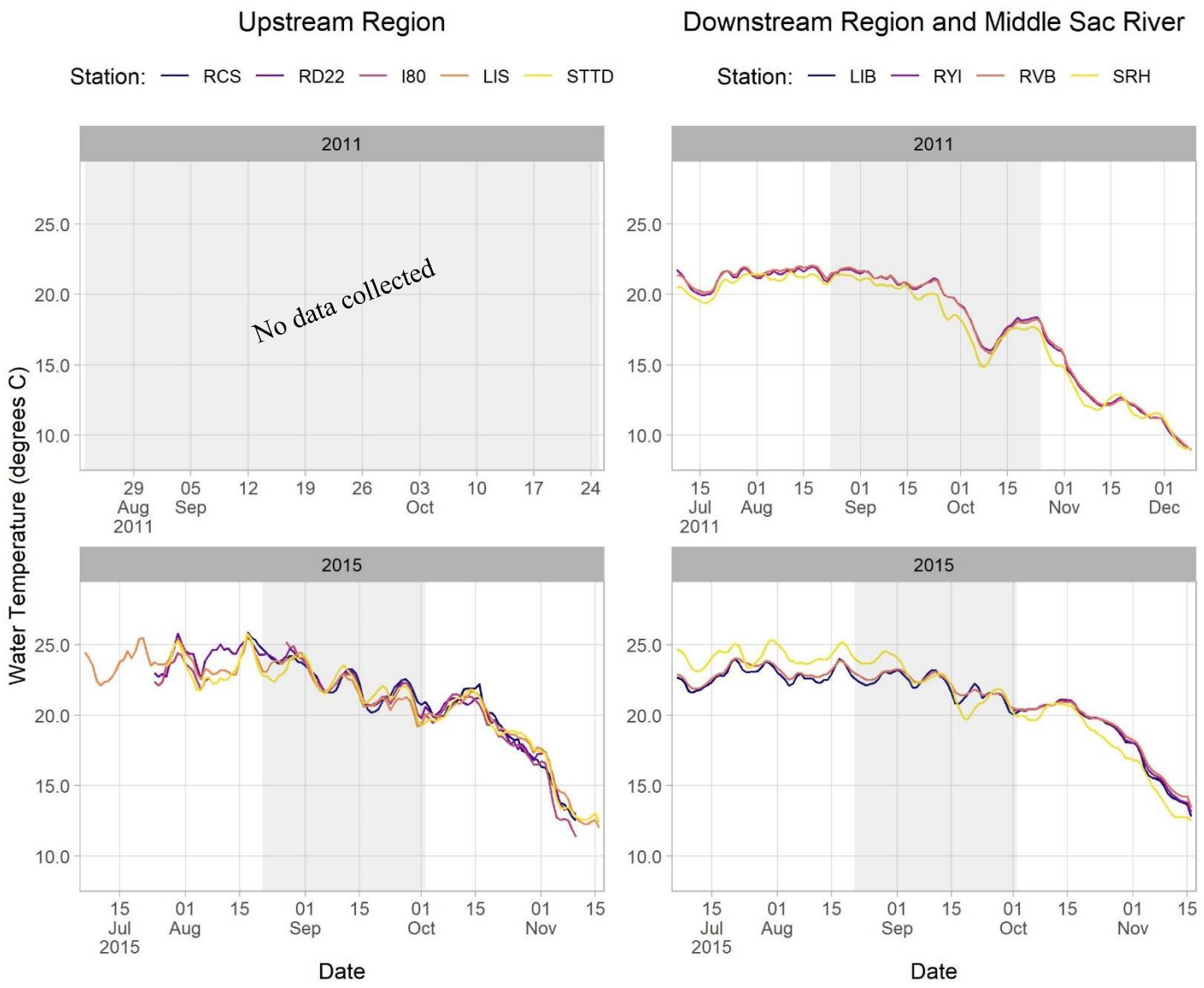

Figure 3-32. Daily average water temperature values in the upstream region, downstream region, and middle Sacramento River in the years with high flow, low magnitude, and long duration flow pulses (2011 and 2015). The light grey shaded box represents the flow pulse period.

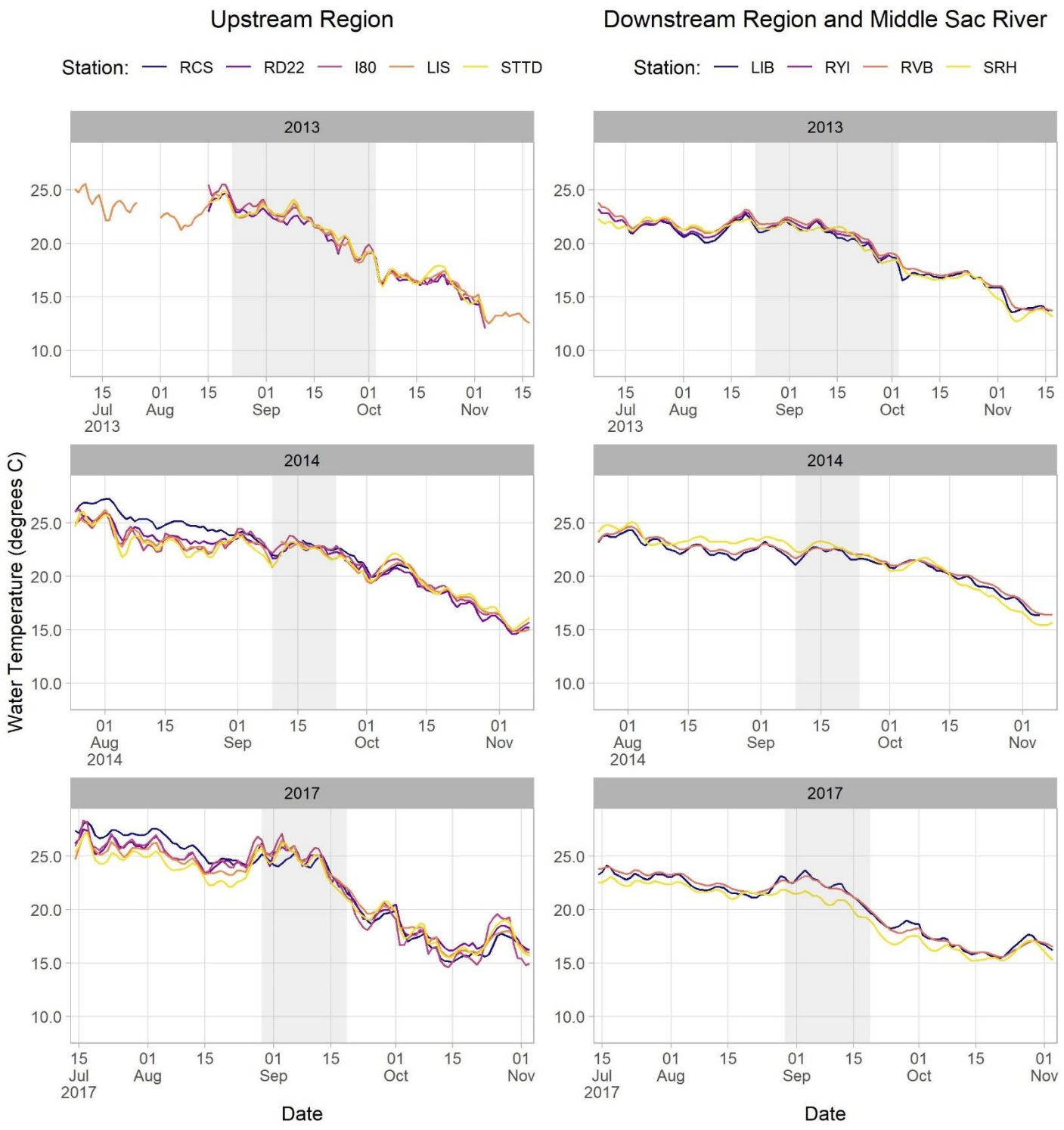

Figure 3-33. Daily average water temperature values in the upstream region, downstream region, and middle Sacramento River in the years with low-flow pulses (2013, 2014, and 2017). The light grey shaded box represents the flow pulse period.

Fluorescent Dissolved Organic Matter

Fluorescent dissolved organic matter (fDOM), a proxy for total organic carbon, was monitored at limited stations from 2013-2019 (Figure 3-34 and Figure 3-35). As a result of limited data, we did not analyze fDOM using ANOVA but assessed qualitative changes during and after flow pulses and across years. fDOM increased during flow pulses in the high-flow pulse years of 2018 and 2019 at all stations (Figure 3-34). The magnitude of these increases was higher at the upstream stations (TOE and LIBCUT) than the downstream stations (LIB and RYI). In addition, fDOM values increased during the flow pulse in 2015 at LIB, but this was the only station with data available during the flow pulse in this year (Figure 3-34). fDOM also increased slightly at LIB during years with low-flow pulses, but again this was the only station with data available during these years (Figure 3-35). Consequently, we were unable to determine if these trends observed at LIB in 2013-2015 and 2017 occurred elsewhere.

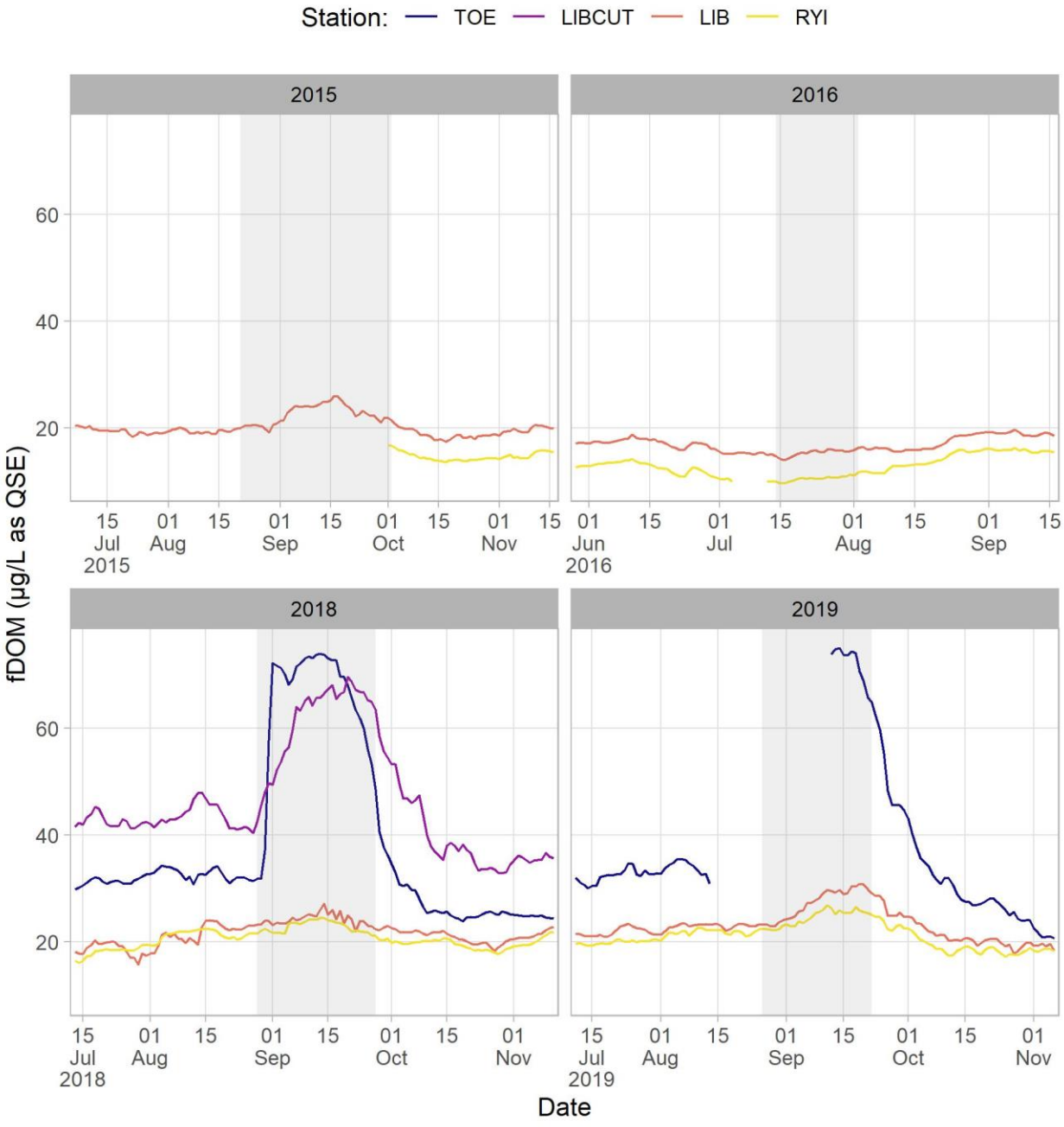

Figure 3-34. Daily average fDOM values in the years with high-flow pulses (2015, 2016, 2018, and 2019). The light grey shaded box represents the flow pulse period.

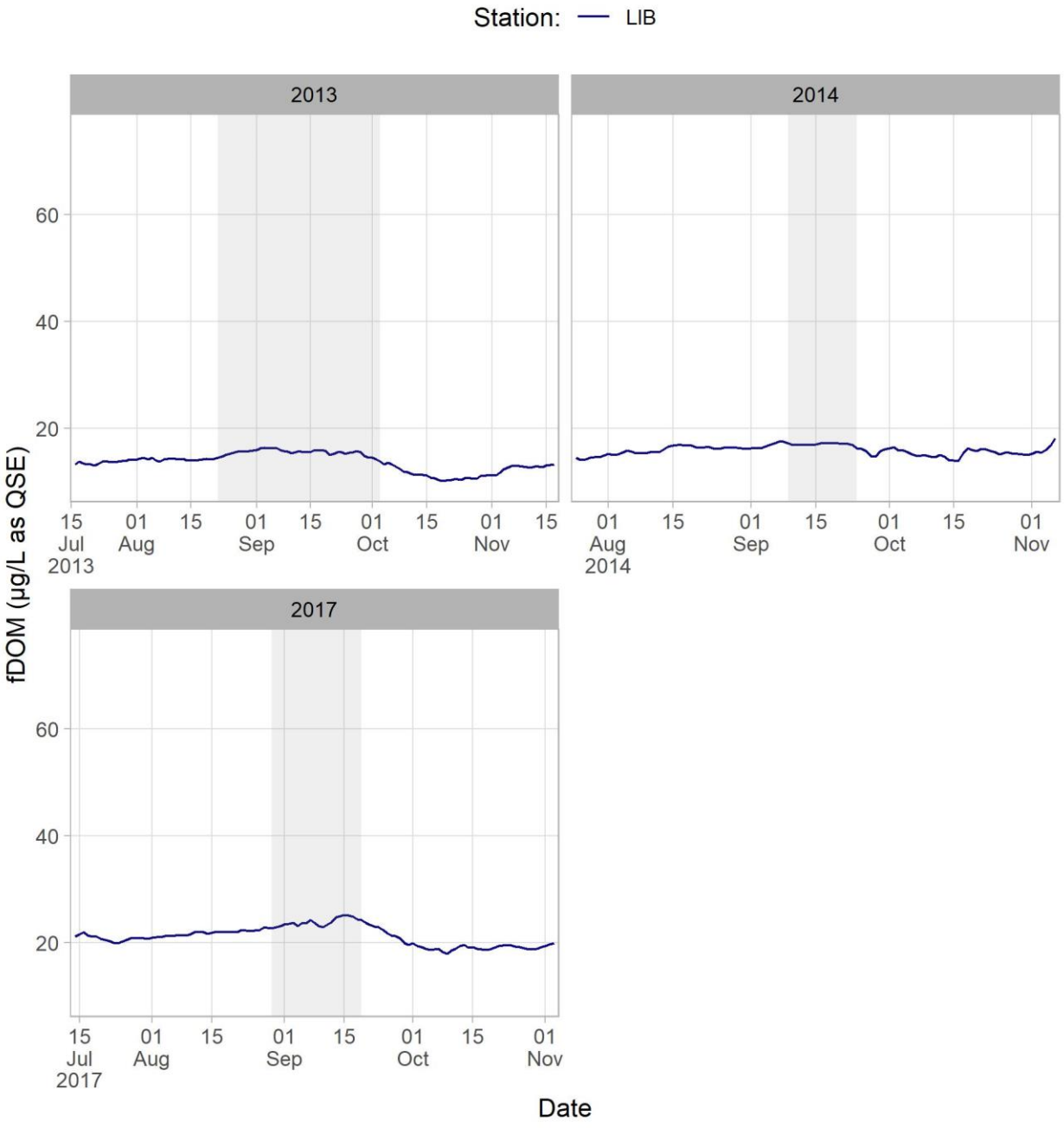

Figure 3-35.Daily average fDOM values in the years with low-flow pulses (2013, 2014, and 2017). The light grey shaded box represents the flow pulse period.

3.3.3 Discussion

Daily average specific conductance values suggest that water in the upper Yolo Bypass was transported downstream along the Toe Drain during flow pulses in the high flow years of 2015, 2016, 2018, and 2019. Agricultural drainage water from the upper Yolo Bypass and Colusa Drain are normally higher in specific conductance because salts within the water are concentrated by evapotranspiration in the agricultural fields (Schoups et al. 2005). Additionally, upstream water with higher specific conductance traveled far enough downstream to mix with the water at the downstream stations including RVB, particularly in 2018 and 2019, both of which were years with managed flow actions. For example, hydrodynamic modeling (Chapter 2) showed a maximum of 3% flow pulse water at the Rio Vista Bridge in 2019 (Table 2-5), and we saw an increase in specific conductance from a mean of ~120 to ~150 uS/cm (Figure 3-22). Given that specific conductance in the Bypass was ~600 uS/cm during the flow pulse, the modest increase we observed in Rio Visa may not have been due solely to the flow pulse, but the pulse was likely a major contributor.

Additional observations of daily average DO, pH, and turbidity values all showed evidence of water transport downstream from the Yolo Bypass to Cache Slough Complex (CSC) during high-flow pulse years (2015, 2016, 2018, and 2019). In addition, large increases in fDOM values in the upstream bypass and smaller increases downstream in CSC during the flow pulses in 2018 and 2019 suggested downstream transport of organic carbon and mixing of waters from upstream and downstream sources. Cumulatively, this evidence demonstrates that high-flow pulses in the North Delta transport water from the upper Yolo Bypass downstream into the lower Bypass, Cache Slough Complex, and Lower Sacramento River near RVB. Low-flow pulses (primarily during non-managed flow years) did not consistently appear to transport water from upstream Yolo Bypass to the downstream region, and instead had localized effects on water quality within the upstream region.

Continuous chlorophyll sensors measure fluorescence reflected from chlorophyll, a proxy for phytoplankton biomass and primary productivity. Fluctuations in chlorophyll concentrations over time can indicate changes in productivity rates. Our modeled results indicated that flow pulses did not significantly affect chlorophyll values in the Yolo Bypass and Cache Slough Complex across all years, which suggests that flow pulses did not increase

productivity downstream. However, daily average trends in chlorophyll fluorescence suggest that instead of in situ primary production (i.e. phytoplankton bloom), chlorophyll was likely transported downstream during the flow pulses of high-flow years (with net positive flows in 2015, 2016, 2018, and 2019; Figure 3-4, Figure 3-5), which is consistent with the trends observed in specific conductance and other parameters. The spatial and temporal extent of transport varied between years, with more substantial transport of chlorophyll in 2016, while 2015, 2018, and 2019 were much more limited. Downstream transport of chlorophyll was also more limited temporally and spatially during the years with low-flow pulses (2013, 2014, and 2017). While high-flow pulses resulted in transport of pulse water and other water masses down the Yolo Bypass Toe Drain as evident from hydrodynamic modeling (Chapter 2), it's important to acknowledge alternative hypotheses for the increases in chlorophyll fluorescence downstream such as differential in situ grazing, local productivity, or other mechanisms unrelated to the flow pulse.

If transport was the main mechanism underlying the observed increases in chlorophyll fluorescence (phytoplankton biomass) downstream in 2016 (Chapter 3), it remains unclear why localized phytoplankton production did not occur (see Chapter 4), but it may have been due to suboptimal nutrient ratios for phytoplankton growth in the study region (described below in Discussion of discrete water quality). This lack of response in situ primary production also could have been related to antecedent conditions, such as hydrology or phytoplankton community composition (see Chapter 4). Regardless, our results indicate that managed flow pulses are most likely meeting one of our objectives of transporting phytoplankton downstream to Delta Smelt habitats, but it remains difficult to untangle transport and in situ production.

Downstream transport of chlorophyll was most apparent in 2016 when there was a region-wide increase in chlorophyll at the downstream stations following the flow pulse. The high-flow pulse in 2016 was notably different from other years in three ways: it was the only year with water sourced from the Sacramento River from additional releases from the Keswick dam, it occurred earlier in the year at the end of July, and it was preceded by a Delta-wide phytoplankton bloom (Frantzich et al. 2018, 2021). It may be pragmatic to conduct another managed, high-flow pulse with water from the Sacramento River or modify the timing of the pulse to observe if these factors (water

source or timing) affect phytoplankton transport and primary productivity in the downstream region. In addition, conducting more managed, high-flow pulses using Sacramento River or agricultural source water would improve our assessment of the effects of antecedent conditions, such as the Delta-wide plankton bloom observed prior to the flow pulse in 2016, on changes in water quality in response to managed high-flow pulses. A comprehensive assessment of the effects of antecedent conditions was impractical for this report due to limited data: we have conducted a limited number of managed, high-flow pulses, and have few years with low-flow pulses for comparison.

From 2013 to 2019, the upstream region had significantly higher chlorophyll fluorescence values than the downstream region in the Cache Slough Complex and the Sacramento River near Rio Vista. These regional differences could be caused by multiple factors including differences in water temperature, light availability, nutrient concentrations, and residence time (Cloern, 2014). The stations in the upstream region appeared to have higher water temperatures than the downstream stations (Figure 3-29), which could be a result of the generally shallower water column of the Yolo Bypass Toe Drain within the upstream region as compared to the more open water habitat and deeper channels of Liberty Island and lower Cache Slough, respectively (Frantzich et al. 2018). In addition, a shallower water column could allow for more light and nutrients in the upstream region. The upstream region also has higher water residence times before and after flow pulse periods when compared to the downstream region, which is likely a result of the physical channel characteristics and low-flow dynamics (Frantzich et al. 2018). Together, increased water residency, nutrients, light-availability, and temperature in the upstream region provide more favorable conditions for phytoplankton growth.

Light availability, usually measured as photosynthetically available radiation (PAR), varies with turbidity, as well as incident solar irradiance and depth of the mixed layer (Cloern, 2014; Wofsy, 1983). Turbidity from suspended sediments reduces the photic zone to shallow depths and leads to light limitation for photosynthesis in the water column, slowing nutrient uptake by phytoplankton (Cloern 2014). Spatially, turbidity values were higher in the upstream region than in the downstream region for the entire study period. Temporally, turbidity was lower in 2018 than all other years, and higher in 2016. The continuous chlorophyll data also followed these regional and interannual trends of higher values in the upstream region and generally lower values in 2018 and higher values in 2016; however, this outcome is the

opposite of what would be expected if light availability strongly affected primary productivity in the North Delta. In the upstream region, light availability may not be a limiting factor of primary productivity due to regionally shallow waters allowing for more nutrients and light penetration into the water column. Additionally, the longer water residence times and warmer water temperatures within the upstream region can increase primary productivity relative to the downstream region during periods with lower flows.

Continuous chlorophyll fluorescence, pH, and DO tend to follow similar trends when photosynthesis is actively occurring because of the chemical changes in water during photosynthetic processes. Higher rates of photosynthesis during the day cause an increase in DO levels and a decrease in carbon dioxide, increasing aqueous pH levels (ICF 2020). At night, increased respiration and reduced photosynthesis lowers DO levels and introduces more carbon dioxide into the water, causing it to become more acidic as indicated by lower pH values (ICF 2020). Daily average pH trends remove the daily variation that occurs naturally, allowing us to observe general trends in pH over time. Lower pH during flow pulses may indicate water transport while higher pH before and after flow pulses may result from uptake of carbon dioxide, a potential result of new algal and/or phytoplankton growth. Similar trends of elevated chlorophyll, pH, and DO before and after the flow pulses in 2016, 2018, and 2019 in the upstream region suggest that some of these increases in primary productivity could have resulted from blooms occurring locally. Coinciding increases were most notable at I80 in 2016, 2018 and 2019, at RCS and RD22 in 2018, and at LIS in 2019 (Figure 3-4, Figure 3-9, Figure 3-16). In addition, chlorophyll, DO, and pH values all increased at RVB after the flow pulses in 2011 and 2012 and at all downstream stations after the flow pulse in 2016 (Figure 3-4, Figure 3-5, Figure 3-9, Figure 3-10, Figure 3-16, and Figure 3-17) suggesting higher rates of local primary productivity in the Cache Slough Complex and lower Sacramento River during these times. However, not all periods with elevated chlorophyll fluorescence levels had corresponding increases in pH and DO values, such as in 2014, 2015, and 2017 (Figure 3-5, Figure 3-6, Figure 3-10, Figure 3-11, Figure 3-17, and Figure 3-18). Advection could have been responsible for the increased primary productivity during these instances. Future analyses should consider including saturated DO levels to assess rates of productivity (photosynthesis and respiration processes), since photosynthesis is the only biological process that will cause measured DO to exceed DO saturation.

Daily average DO concentrations decreased below the fall-run Chinook Salmon stress threshold of 6 mg/L (NMFS 2008) at LIS during the flow pulses (managed and non-managed, low- and high-flow pulses) in all years of the study period (Figure 3-9, Figure 3-10, Figure 3-11). These periods of low DO values occurred for longer periods of time in the years with high-flow pulses (2015, 2016, 2018, and 2019). Daily average DO values were also below the Chinook Salmon stress threshold at STTD during the flow pulses in 2015, 2018, and 2019, but for shorter time periods. The periods with decreased DO values at LIS and STTD may have resulted from the transport of water with lower DO concentrations from the stations upstream (RCS, RD22, and I80) during the flow pulse periods. It is important to note that while the daily average values were low, it is likely that instantaneous DO values exceeded 6 mg/L at times during the periods with lower DO at LIS and STTD. Further information about temperature and DO thresholds as a function of Chinook Salmon health can be found in Chapter 5, section 5.6, Chinook Salmon and Central Valley Steelhead.

It is important to mention that the technology used to measure in-situ chlorophyll fluorescence improved during the study period. Gaps in the continuous record resulted from failed or fouled sensors or other interference. Data gaps appeared to occur more often during earlier years of the study but improved in recent years. For these periods of poor quality and missing data it may be best to reference the discrete chlorophyll *a* data. In addition, increasing future collection of fDOM data in the upstream region will expand spatial and temporal coverage and further our understanding of how flow pulses affect organic carbon in the Delta.

3.4 Discrete Water Quality

3.4.1 Methods

To determine the concentrations of various analytes (Table 3-3), ten stations, grouped into upstream (Yolo Bypass) and downstream (Cache Slough Complex) regions (Table 3-4; Figure 3-36), were selected for discrete water quality sampling. From 2011 to 2019, data were collected during the summer-fall flow pulse and the 45 days preceding/succeeding it at roughly two-week intervals. Water sample collection for nutrients followed methods established by the IEP Bay-Delta Monitoring and Analysis Section (DWR, 2011). For each batch of samples, a blank sample was analyzed as a control for collection and laboratory procedures. Samples were typically collected at a 1-meter depth using a Van Dorn sampler (downstream sites and STTD) or using Nasco 12' Extendible Swing Sampler (upstream sites, except STTD). Samples were collected in required containers, using preservation techniques and holding times as required by Standard Methods for the Examination of Water and Wastewater (APHA, 2005). Sample analyses were conducted by the DWR Bryte laboratory. Final data set(s) will be uploaded via the Environmental Data Initiative (EDI).

Table 3-3. Discrete water quality analytes collected for study.

Water Quality Analyte	Abbrv.	Units	Method
Chlorophyll *a*	--	µg/L	Std Method 10200 H
Pheophytin	--	µg/L	Std Method 10200 H
Dissolved Ammonia	--	mg/L as N	EPA 350.1
Dissolved Chloride	--	mg/L	EPA 300.0 28d Hold
Dissolved Silica	--	mg/L	EPA 200.7 (D)
Dissolved Nitrate Nitrite	--	mg/L as N	Std Method 4500-NO3-F (28Day)
Dissolved Calcium	--	mg/L	EPA 200.7 (D)
Dissolved Organic Phosphorous	DOP	mg/L as P	EPA 365.1 (DWR Modified)
Dissolved Organic Nitrogen	DON	mg/L as N	EPA 351.2/EPA 350.1 (Dissolved
Dissolved Organic Carbon	DOC	mg/L as C	EPA 415.1 (D) Ox [PS-3]
Total Organic Carbon	TOC	mg/L as C	EPA 415.1 (T) Ox [PS-3]
Total Organic Phosphorus	TOP	mg/L as P	EPA 365.4
Total Kjeldahl Nitrogen	TKN	mg/L as N	EPA 351.2
Total Dissolved Solids	TDS	mg/L	Std Method 2540 C
Total Suspended Solids	TSS	mg/L	EPA 160.2
Volatile Suspended Solids	VSS	mg/L	EPA 160.4

Table 3-4. Discrete water quality stations used in analyses.

Station Name	Station	Region	Years
Colusa Basin Drain at Rominger Bridge	RMB	Upstream	2019
Ridge Cut Slough	RCS	Upstream	2013 – 2019
Toe Drain at Road 22	RD22	Upstream	2013 – 2019
Toe Drain at I-80	I80	Upstream	2013 – 2019
Toe Drain at Lisbon Weir	LIS	Upstream	2013 – 2019
Toe Drain at Screw Trap	STTD	Upstream	2011 – 2019
Below Toe Drain in Prospect Slough	BL5	Downstream	2013 – 2019
Cache Slough at Liberty Island Near Rio Vista	LIB	Downstream	2013 – 2019
Cache Slough at River Island	RYI	Downstream	2013 – 2019
Sacramento River at Rio Vista Bridge	RVB	Downstream	2013 – 2019

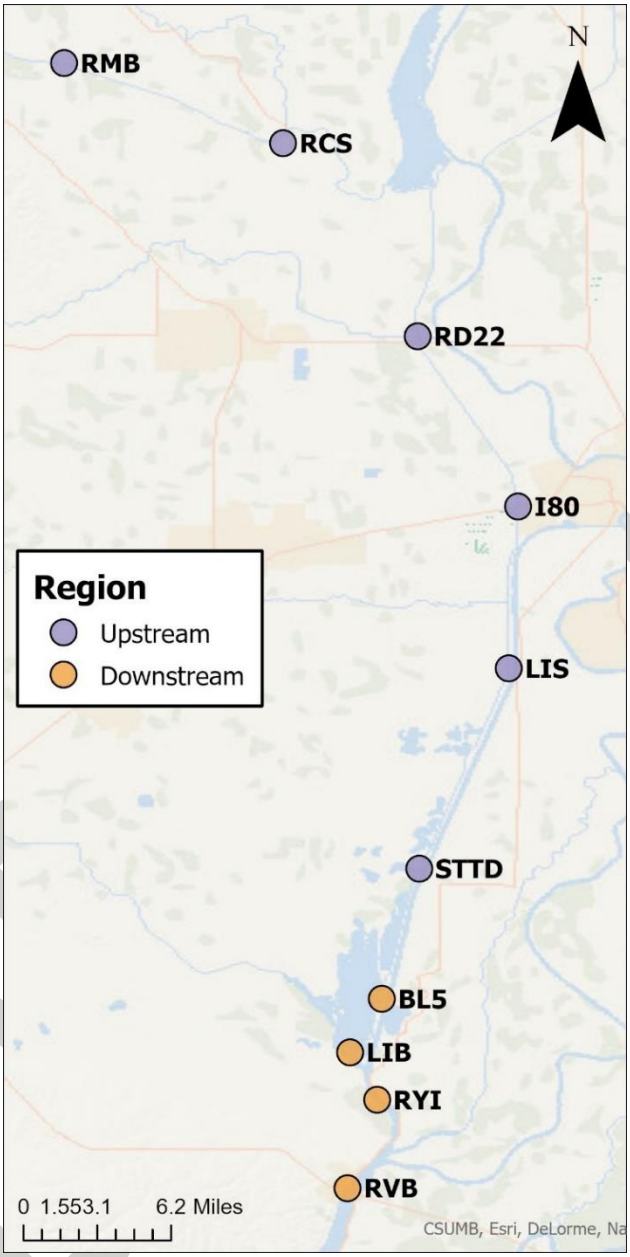

Figure 3-36. Map of discrete water quality stations.

To determine if the annual flow pulses led to evident changes in analyte concentrations, we qualitatively assessed each time series. We also assessed boxplots that were grouped by region (upstream and downstream) and flow pulse period (e.g., before, during, after); non-detect values (NDs) were not represented in these plots.

To determine which abiotic factors influenced discrete water quality analytes, we performed type-II ANOVAs using the 'car' package in R (R Core Team 2020, version 3.0-10) using models constructed via the 'lme4' package (version 1.1-26; Bates et al. 2021.).

We included year, flow pulse period, and region as fixed effects and station as a random effect to account for the autocorrelation within stations. We log-transformed our data and added lag terms to each model to meet ANOVA assumptions of normality, homoscedasticity, and independence, and we tested for residual autocorrelation using the Ljung-Box Test. We determined the number of lag terms for each model via exploratory analysis of partial autocorrelation (PCAF) and autocorrelation (ACF) diagrams. We did not include interaction terms or the Middle Sacramento River stations (Sacramento River at Hood, Sherwood Harbor) due to lack of data. We defined significant results as $p<0.05$ and marginally significant results as $0.05<p<0.10$. Due to insufficient data, 2011 and 2012 were excluded from these models.

Non-detect values (NDs) violate the parametric assumptions of ANOVA, but non-parametric methods were un-usable due to limitations in our data sets. Therefore, to use ANOVA, we had to ensure the results were robust to the ND values. To achieve this, for each analyte, we ran the type-II ANOVA three times where each substitute value for a ND was a randomly selected value from a uniform distribution between 0.01 and the reporting limit. If all three ANOVAs reached the same conclusions about significance, we assumed it was robust to the NDs and that it was the true result; if they did not, we declared the tests inconclusive.

After determining which fixed effects were statistically significant via ANOVA F-tests, we performed pairwise comparisons of estimated marginal means (EMM) using the 'emmeans' package in R (version 1.5.4; Length et al. 2021) to determine inter-group significance. P-values were adjusted using the Sidak correction.

3.4.2 Results

The significance of the explanatory variables for each analyte are summarized in Table 3-5. Due to data limitations, we could not formally decompose time series to account for seasonality in our regression analyses. While we added

a seasonal variable in the regression equations to account for this, some analytes still had residual autocorrelation as shown by the Ljung-Box test. ANOVA results are summarized in Appendix C.

Table 3-5. The significance of the explanatory variables for each discrete water quality analyte when no interaction terms are included. Significant: P < 0.05; Marginally significant: 0.05 < P < 0.1.

Water Quality Analyte	Flow Pulse Period	Region	Year	Residual Autocorrelation
Chlorophyll *a*	Not Significant	Significant	Marginally Significant	Yes
Pheophytin	Not Significant	Significant	Significant	Yes
Dissolved Ammonia	Not Significant	Significant	Marginally Significant	No
Dissolved Chloride	Not Significant	Significant	Significant	Yes
Dissolved Silica	Significant	Significant	Significant	Yes
Dissolved Nitrate Nitrite	Not Significant	Not Significant	Not Significant	Yes
Dissolved Calcium	Significant	Significant	Significant	Yes
Dissolved Organic Phosphorous	Significant	Not Significant	Significant	Yes
Dissolved Organic Nitrogen	Significant	Significant	Significant	Yes
Dissolved Organic Carbon	Not Significant	Not Significant	Marginally Significant	No
Total Organic Carbon	Not Significant	Significant	Significant	Yes
Total Organic Phosphorus	Not Significant	Not Significant	Not Significant	No
Total Kjeldahl Nitrogen	Not Significant	Significant	Significant	Yes
Total Dissolved Solids	Not Significant	Significant	Significant	Yes
Total Suspended Solids	Significant	Significant	Significant	Yes
Volatile Suspended Solids	Not Significant	Significant	Significant	Yes

Chlorophyll *a* and Pheophytin

Chlorophyll *a* and pheophytin values were, on average, higher upstream than downstream (Figure 3-37 - Figure 3-44). Across years, flow pulses did not lead to marked increases in chlorophyll or pheophytin concentrations that persisted past the end of the flow pulse. However, the flow pulses have some effects on analytes in given years and regions that were more prominent in high-flow pulse years compared low-pulses but varied (e.g., 2015, 2016, 2019) (Figure 3-39, Figure 3-40). In 2016, both analytes had higher variability post-flow action, especially downstream, compared to other years. Furthermore, there appeared to be downstream transport of chlorophyll from the upper to lower Yolo Bypass and other downstream stations in 2016 (consistent with continuous chlorophyll fluorescence results in section 3.3.2). Other observations include increased concentrations of chlorophyll at upstream sites in 2015, 2017, and 2019 immediately after the flow pulse. In multiple years, downstream concentrations increased during the flow pulse, and decreased again after, particularly at BL5.

Based on regression analyses, flow pulse period did not have a significant effect on chlorophyll *a*, while region had a significant effect and year a marginally significant effect (Table 3-5). Upstream values were significantly higher than downstream, which is supported by the time series graphs and boxplots (Figure 3-37 - Figure 3-44). Pheophytin showed similar patterns, although year significantly affected concentration, with higher values in 2017 than 2015 and 2018.

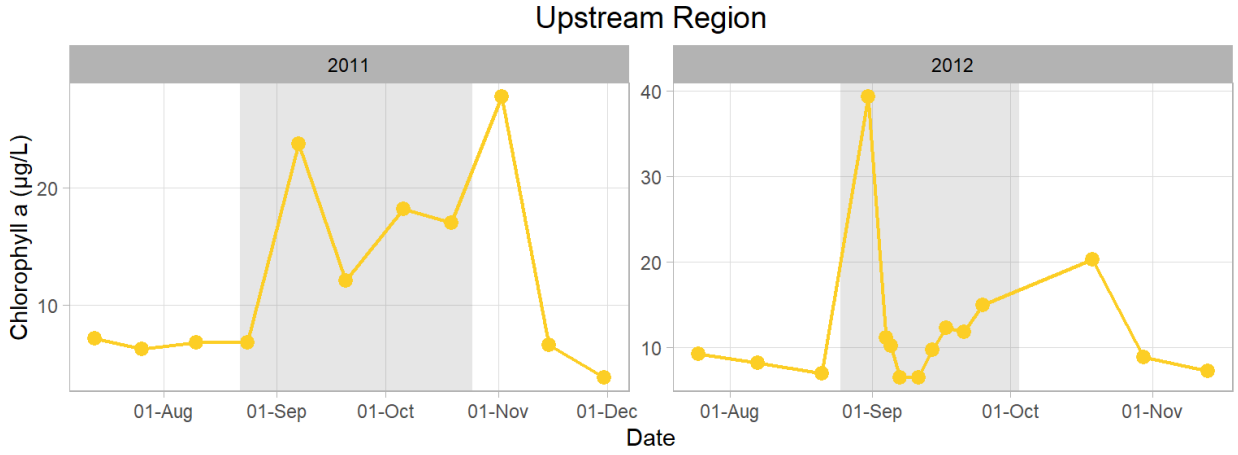

Figure 3-37. Chlorophyll *a* concentration at STTD for 2011 and 2012 (high-flow pulse years) across flow pulse periods. The light grey shaded box represents the "during" flow pulse period and each graph has a different y-axis scale. Connecting lines are imputed.

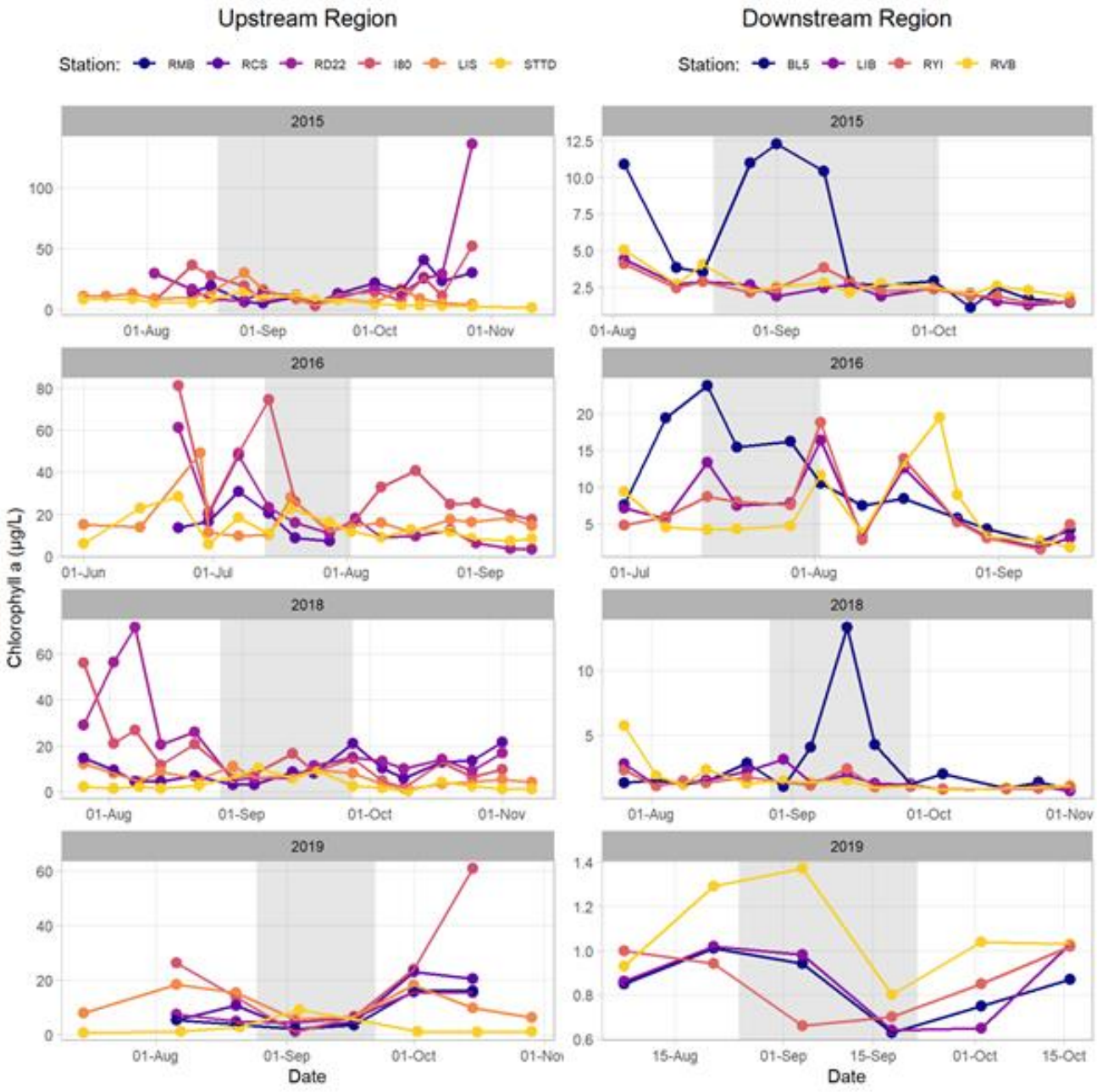

Figure 3-38. Chlorophyll *a* concentration in the upstream and downstream regions for high flow years (excl. 2011 and 2012) and all flow pulse periods. The light grey shaded box represents the "during" flow pulse period and each graph has a different y-axis scale. Connecting lines are imputed.

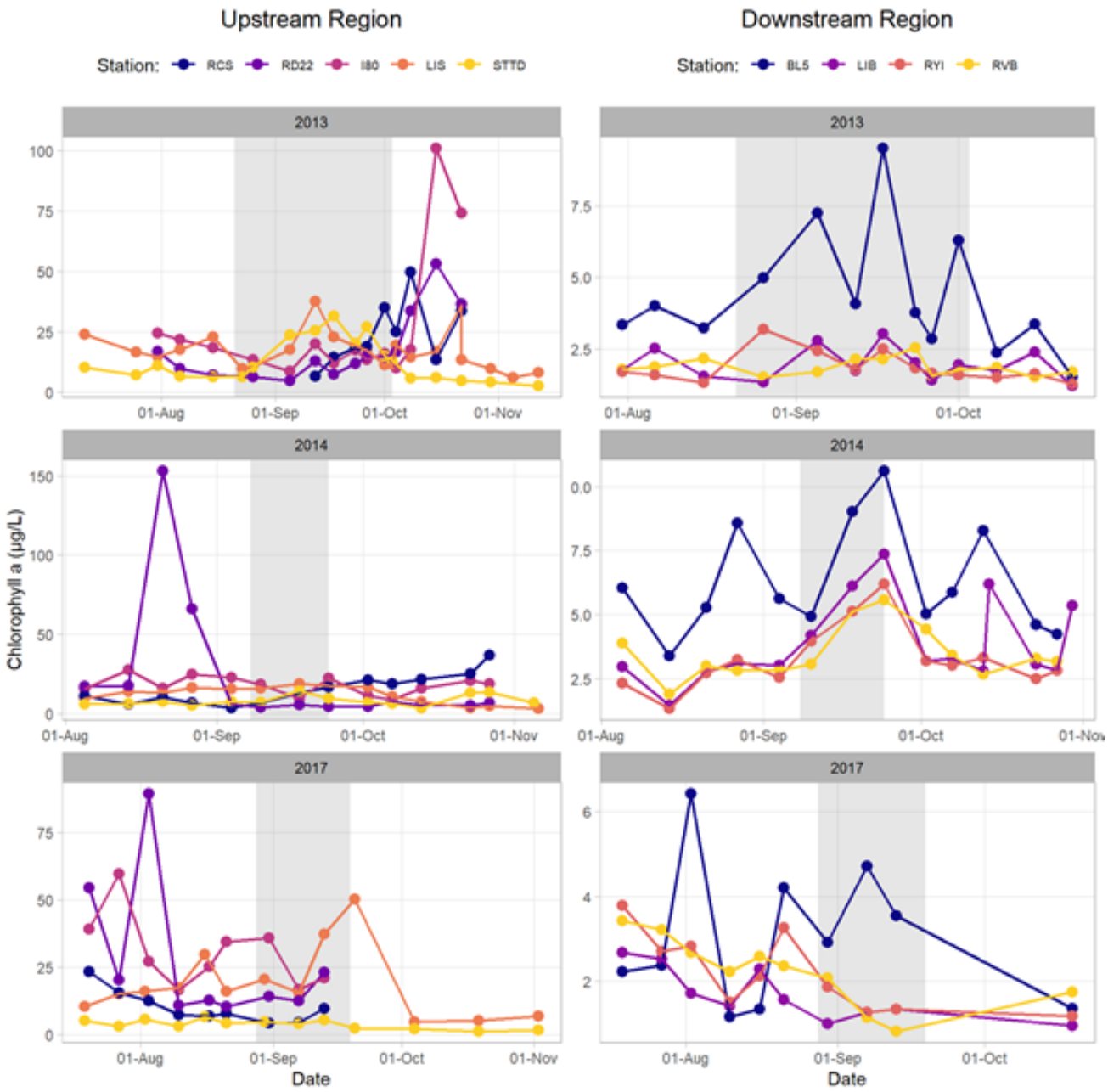

Figure 3-39. Chlorophyll *a* concentration in the upstream and downstream regions for low flow years and all flow pulse periods. The light grey shaded box represents the "during" flow pulse period and each graph has a different y-axis scale. Connecting lines are imputed.

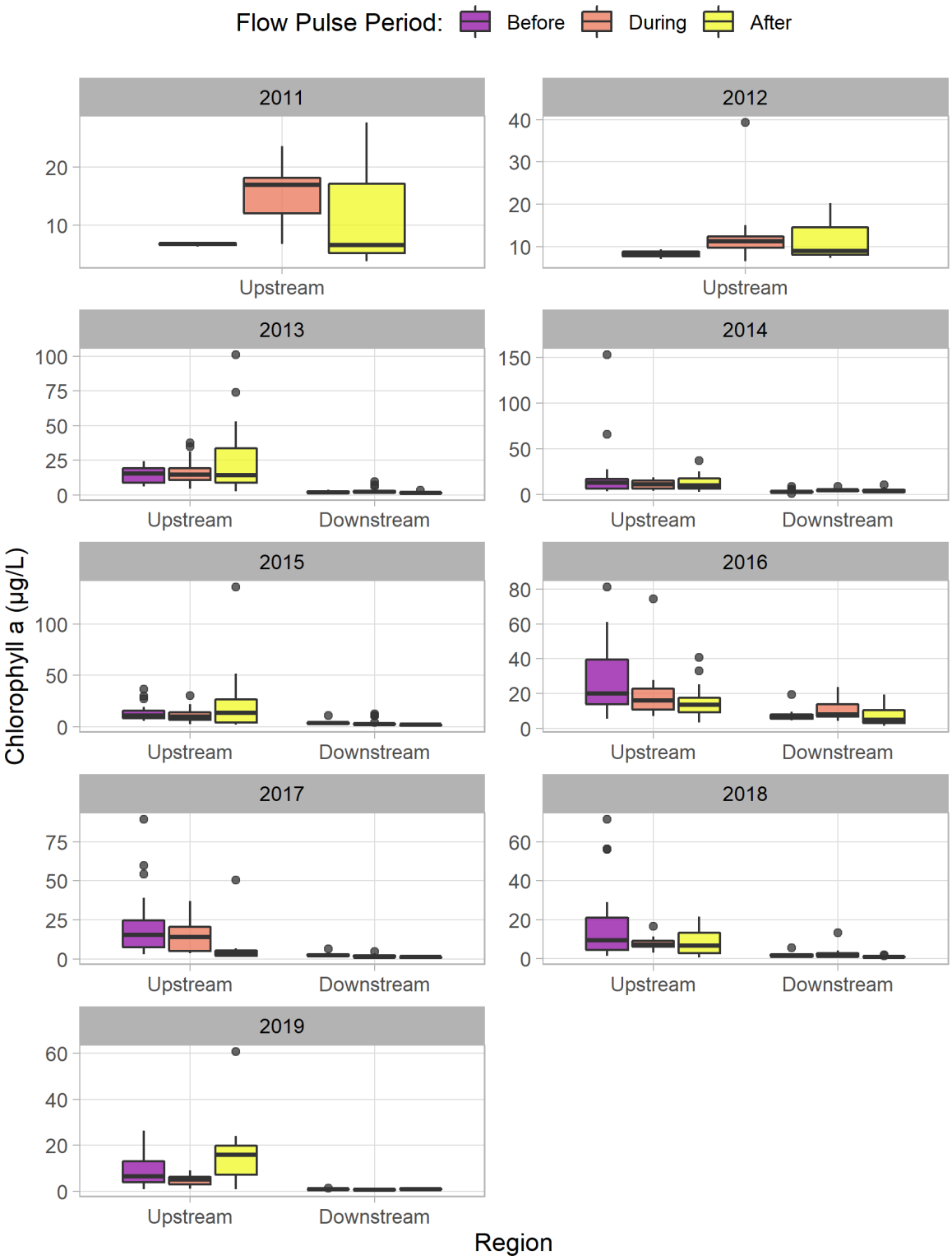

Figure 3-40. Chlorophyll *a* concentration in the upstream and downstream regions for all years and flow pulse periods. Each year has a different y-axis scale.

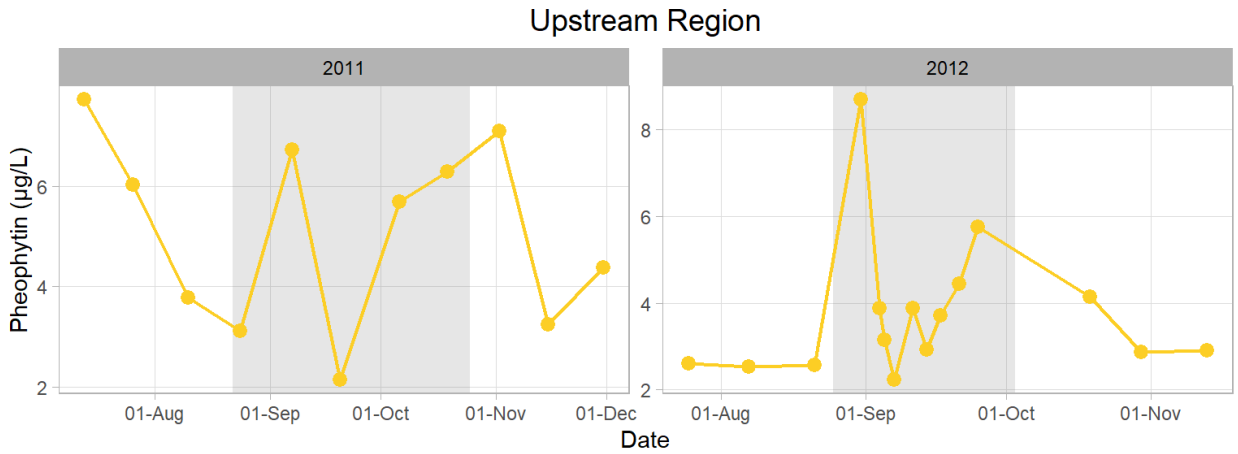

Figure 3-41. Pheophytin concentrations at STTD for 2011 and 2012 (high-flow pulse years) across flow pulse periods. The light grey shaded box represents the "during" flow pulse period and each graph has a different y-axis scale. Connecting lines are imputed.

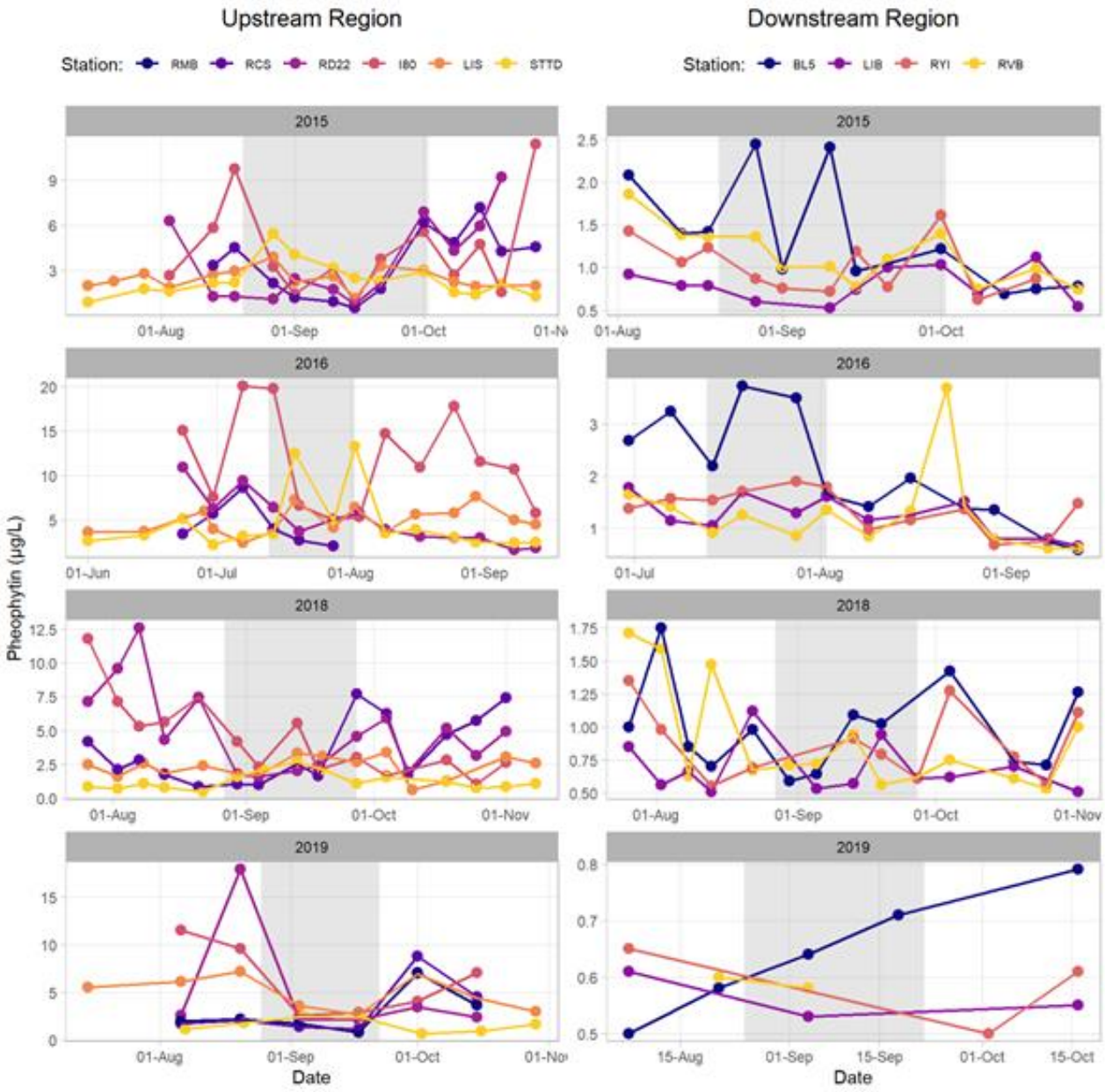

Figure 3-42. Pheophytin concentrations in the upstream and downstream regions for high-flow years (excluding 2011 and 2012) across flow pulse periods. The light grey shaded box represents the "during" flow pulse period and each graph has a different y-axis scale. Connecting lines are imputed.

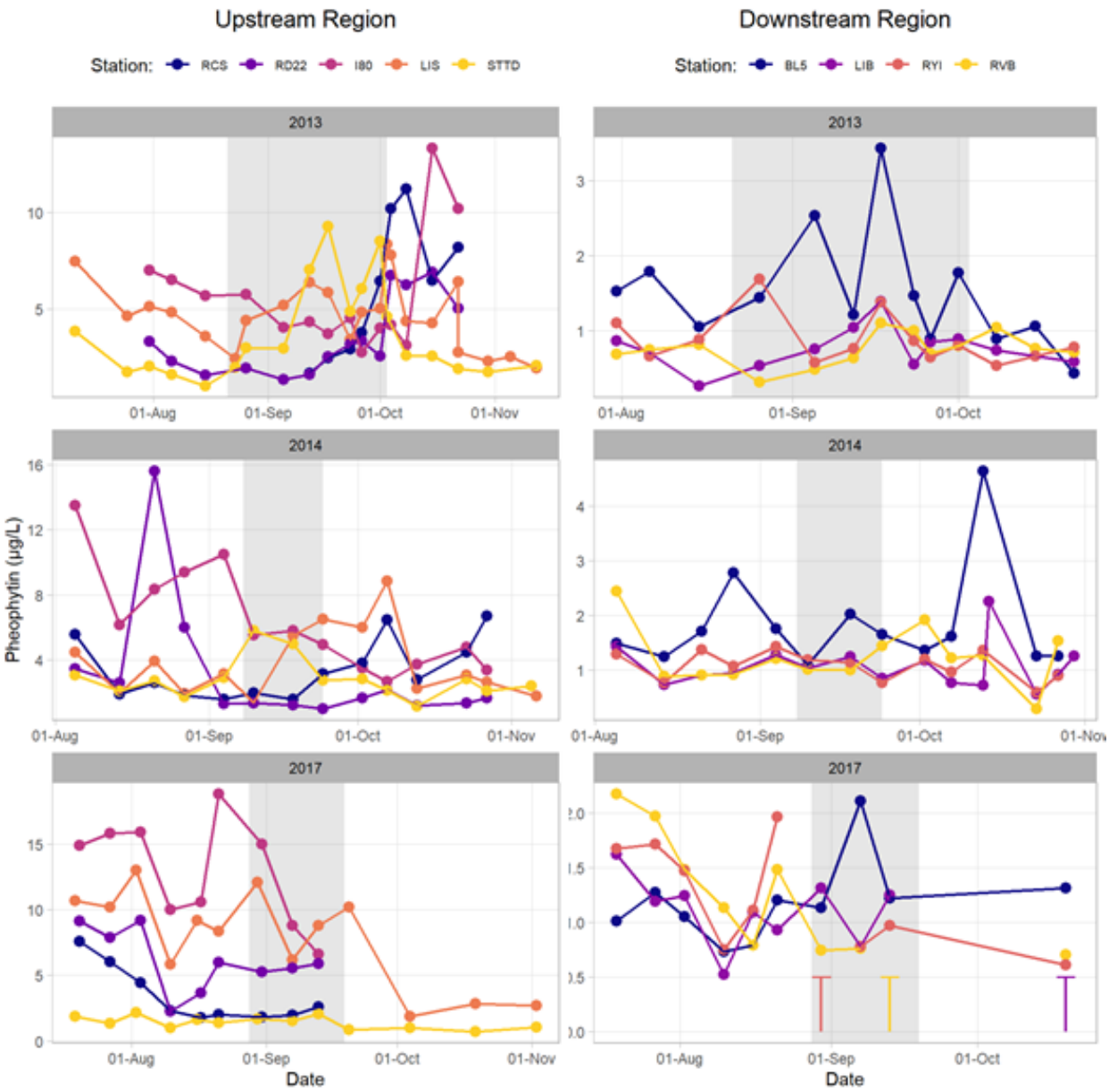

Figure 3-43. Pheophytin concentrations in the upstream and downstream regions for low-flow pulse years across flow pulse periods. The light grey shaded box represents the "during" flow pulse period and each graph has a different y-axis scale. Connecting lines are imputed.

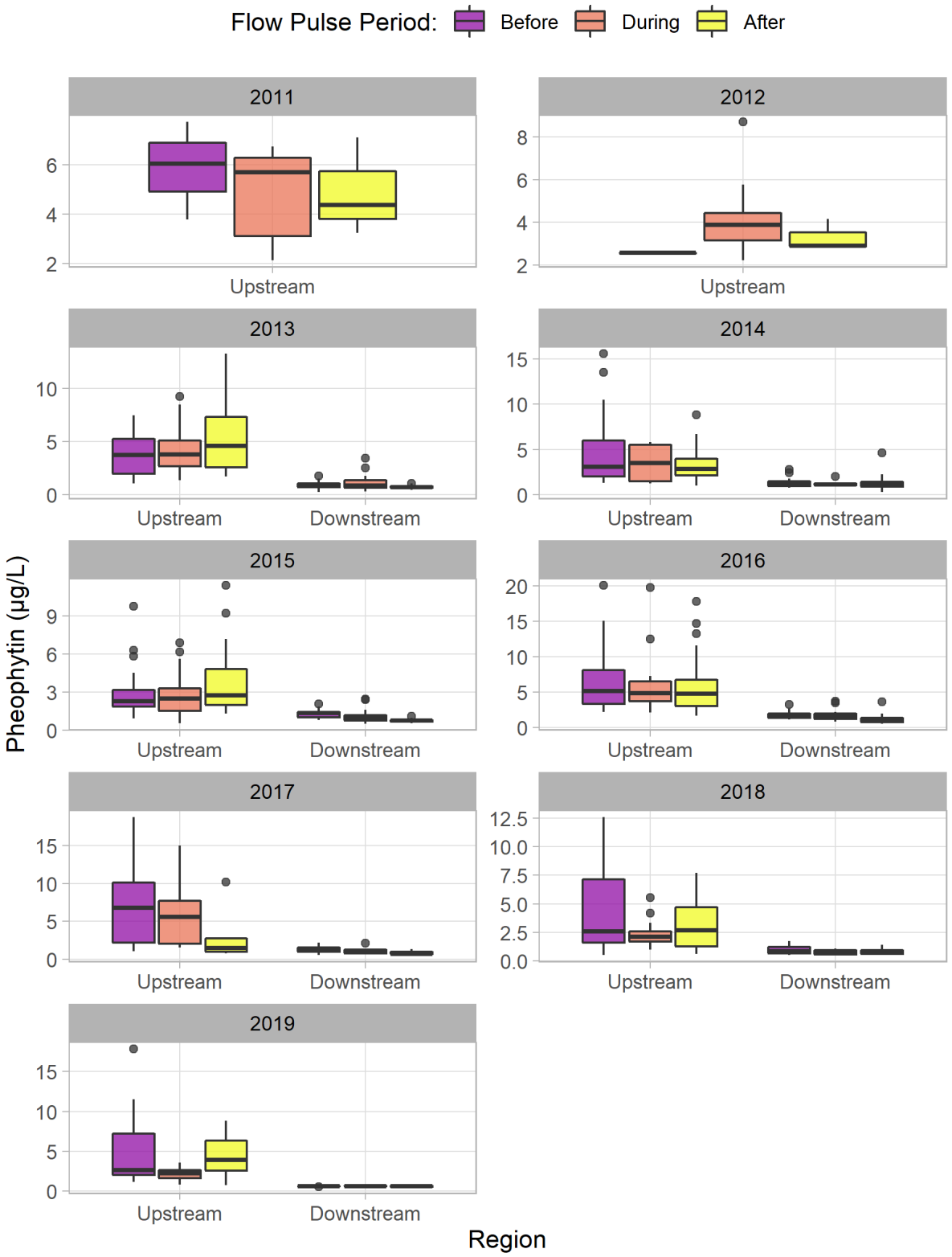

Figure 3-44. Pheophytin concentrations in the upstream and downstream regions for all years and flow pulse periods.

Nutrients

Dissolved ammonium values were, on average, higher downstream than upstream (Figure 3-46). Dissolved nitrate-nitrite, dissolved calcium, and dissolved silica concentrations, meanwhile, were higher upstream than downstream (Figure 3-45 - Figure 3-46). Mean DOP values were similar both upstream and downstream, and several high-flow years (2015, 2016, 2018) saw increases post-flow pulse in some stations for DOP (Figure 3-47 - Figure 3-49). Dissolved silica showed increased concentrations upstream at STTD during the flow pulse periods in 2013 and 2014, which were both low-flow pulse years; these reverted to pre-action concentrations afterward. The exception was downstream in 2016, where silica concentrations continued to rise (Figure 3-50 - Figure 3-52). Aside from an increase in 2016 and 2018 for dissolved phosphorus, the timeseries graphs and boxplots do not show obvious signs of changing analyte concentrations due to the flow pulses.

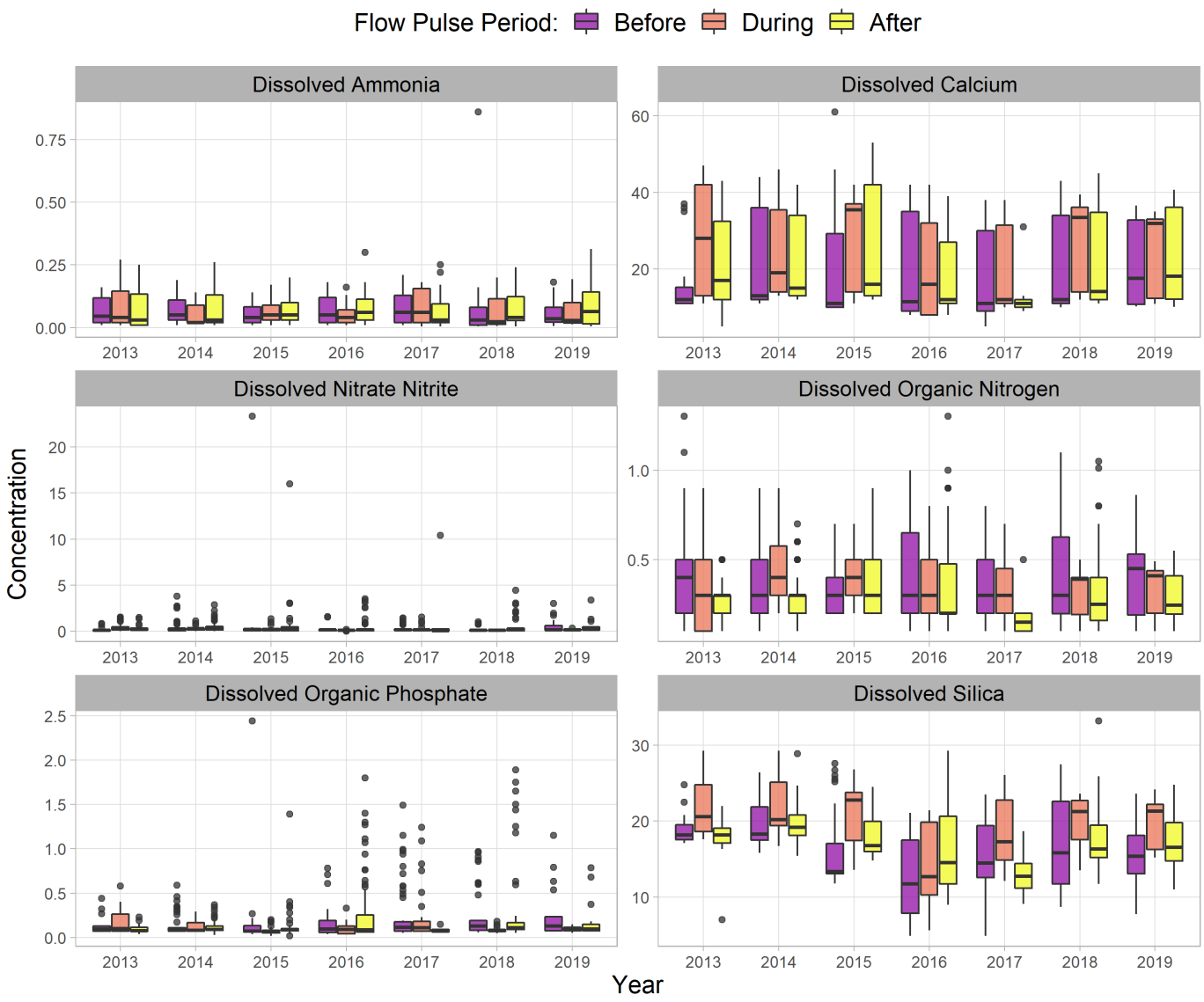

Figure 3-45. Nutrient concentrations (mg/L) for all years separated by flow pulse period. Each graph has a different y-axis scale.

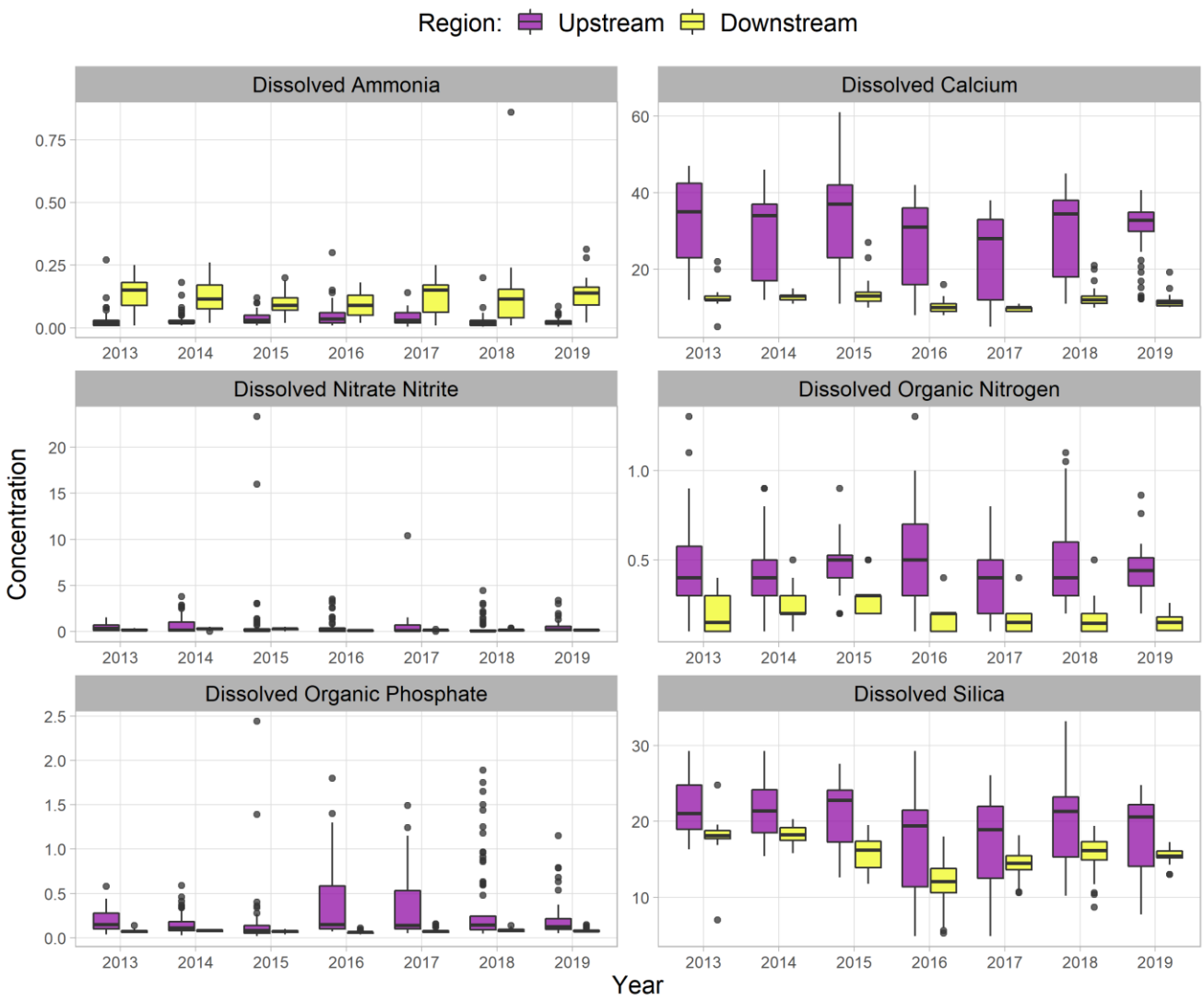

Figure 3-46. Nutrient concentrations (mg/L) for all years separated by region. Each graph has a different y-axis scale.

Based on regression analyses, flow pulse period had a significant effect on dissolved calcium, DOP, DON, and dissolved silica. It did not have a significant effect on dissolved ammonia or dissolved nitrate-nitrite (Table 3-6). During the flow pulses, calcium and dissolved silica concentrations were higher than before flow pulses, though they decreased after for silica and stayed the same for calcium. Concentration of DOP was higher after flow pulses than during. For DON, the concentration was higher before than during and after flow pulses.

Region had a significant effect on DON, dissolved calcium, dissolved silica, and dissolved ammonia but not on DOP and dissolved nitrate-nitrite. Of the

analytes for which region had a significant effect, upstream concentrations were higher than downstream for all but dissolved ammonia.

Table 3-6. The significance of the explanatory variables for the main nutrient analytes when no interaction terms are included. Significant: $P < 0.05$; Marginally significant: $0.05 < P < 0.1$.

Water Quality Analyte	Flow Pulse Period	Region	Year	Residual Autocorrelation
Dissolved Ammonia	Not Significant	Significant	Marginally Significant	No
Dissolved Silica	Significant	Significant	Significant	Yes
Dissolved Nitrate Nitrite	Not Significant	Not Significant	Not Significant	Yes
Dissolved Calcium	Significant	Significant	Significant	Yes
Dissolved Organic Phosphorous	Significant	Not Significant	Significant	Yes
Dissolved Organic Nitrogen	Significant	Significant	Significant	Yes

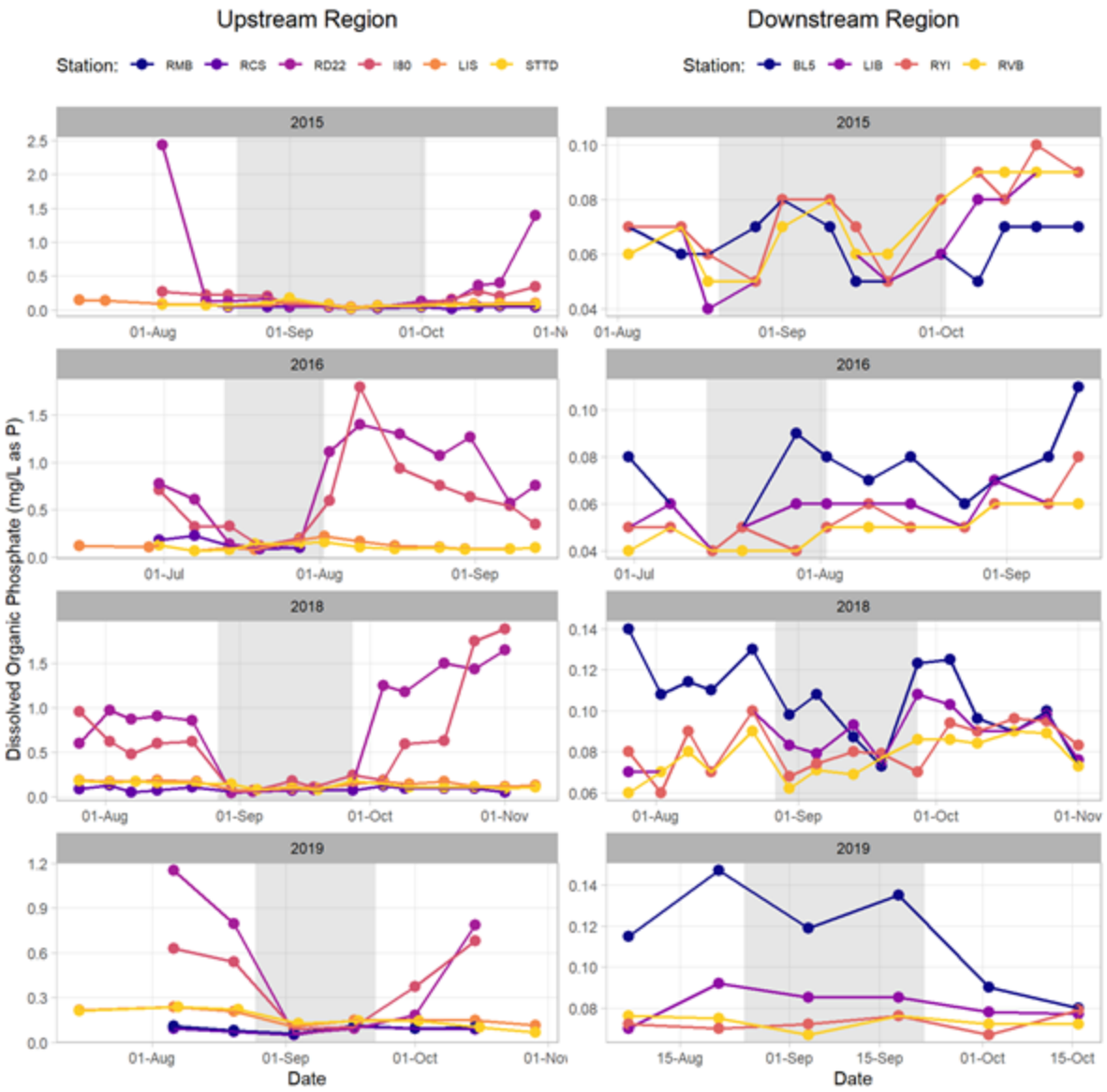

Figure 3-47. Dissolved organic phosphate concentrations in the upstream and downstream regions for high-flow pulse years across flow pulse periods. The light grey shaded box represents the "during" flow pulse period and each graph has a different y-axis scale. Connecting lines are imputed.

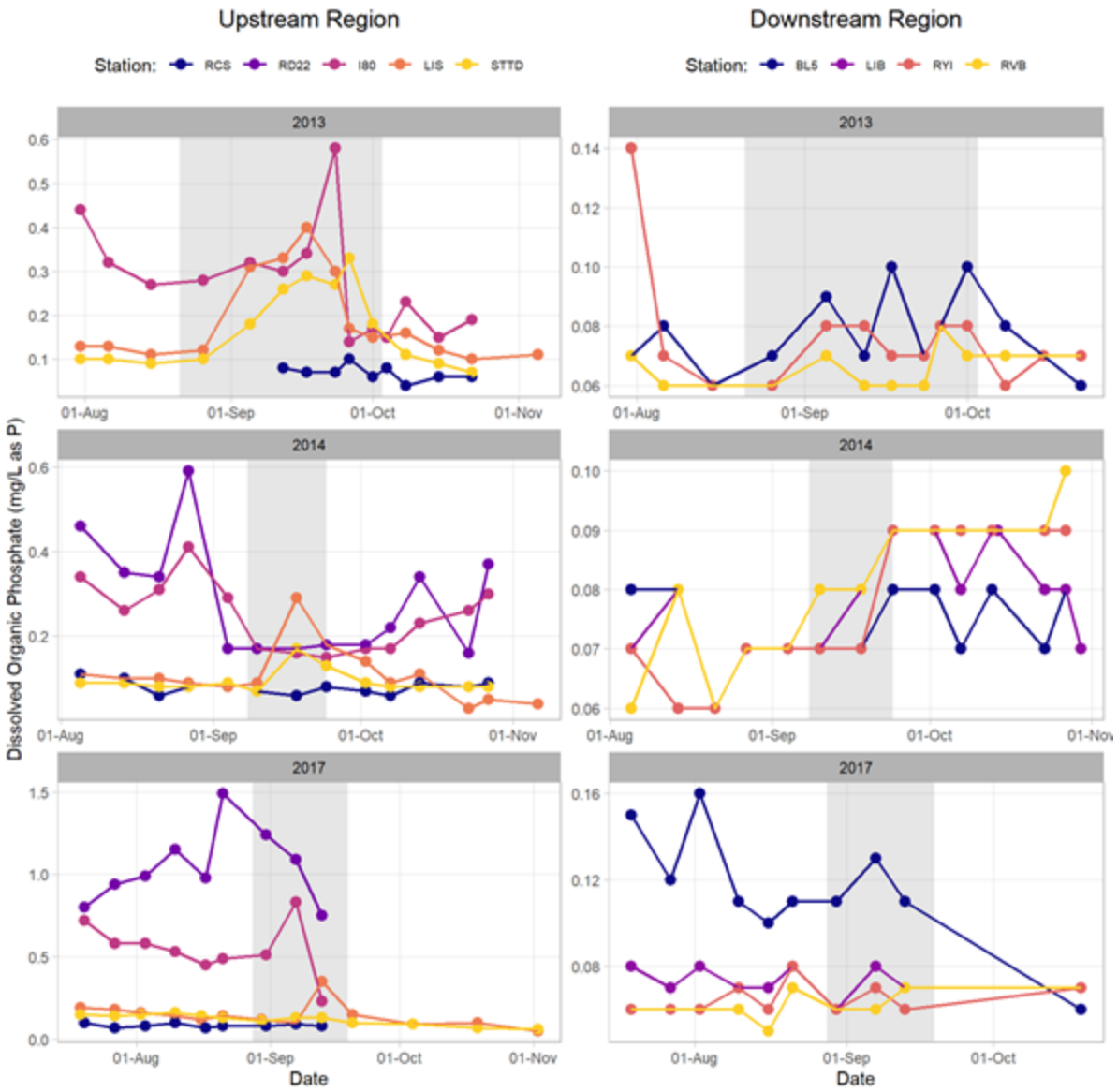

Figure 3-48. Dissolved organic phosphate concentrations in the upstream and downstream regions for low-flow pulse years across flow pulse periods. The light grey shaded box represents the "during" flow pulse period and each graph has a different y-axis scale. Connecting lines are imputed.

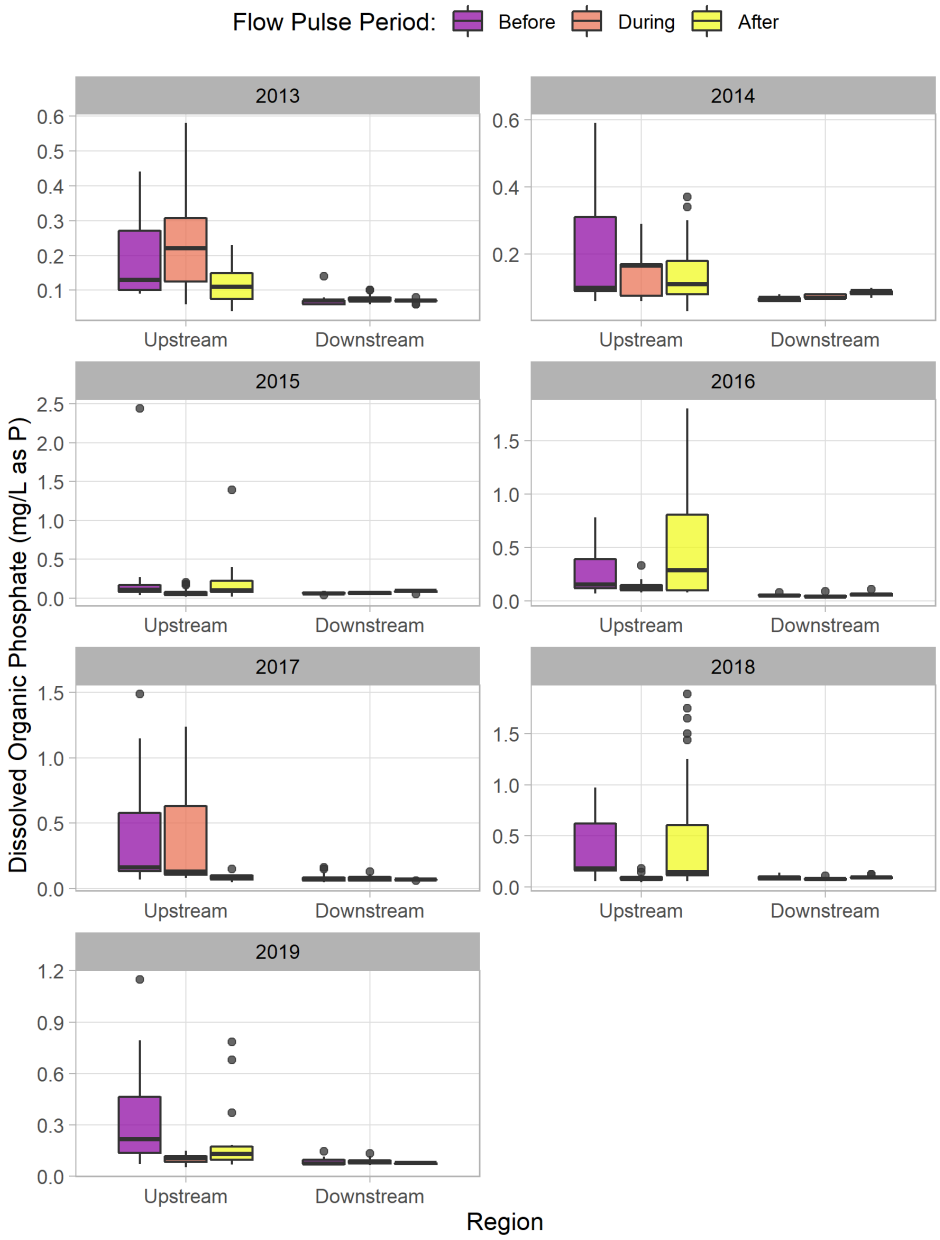

Figure 3-49. Dissolved organic phosphate concentrations in the upstream and downstream regions for all years and flow pulse periods. Connecting lines are imputed.

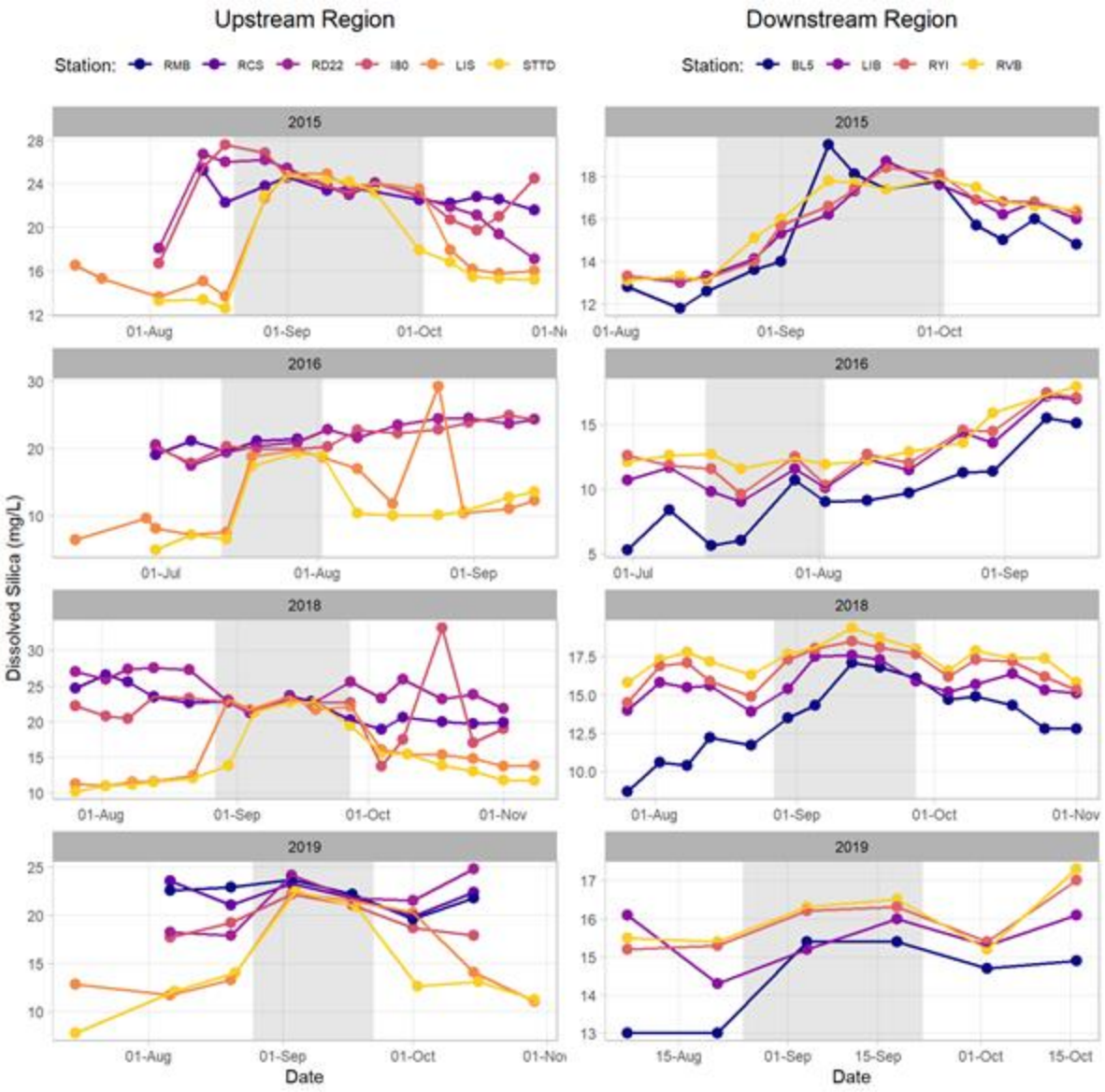

Figure 3-50. Dissolved silica concentrations in the upstream and downstream regions for high-flow pulse years across flow pulse periods. The light grey shaded box represents the "during" flow pulse period and each graph has its own y-axis scale. Connecting lines are imputed.

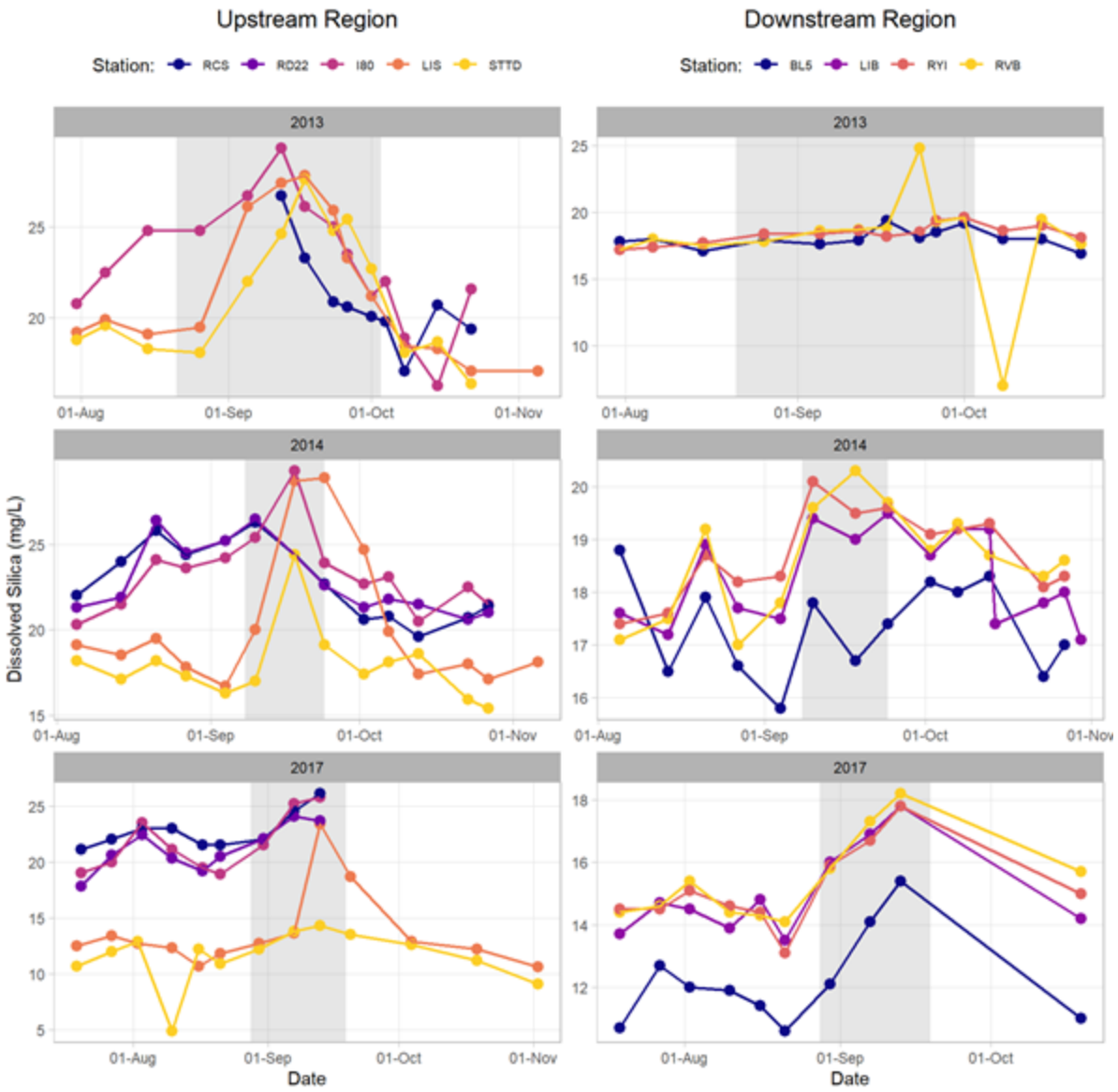

Figure 3-51. Dissolved silica concentrations in the upstream and downstream regions for low-flow pulse years across flow pulse periods. The light grey shaded box represents the "during" flow pulse period and each graph has its own y-axis scale. Connecting lines are imputed.

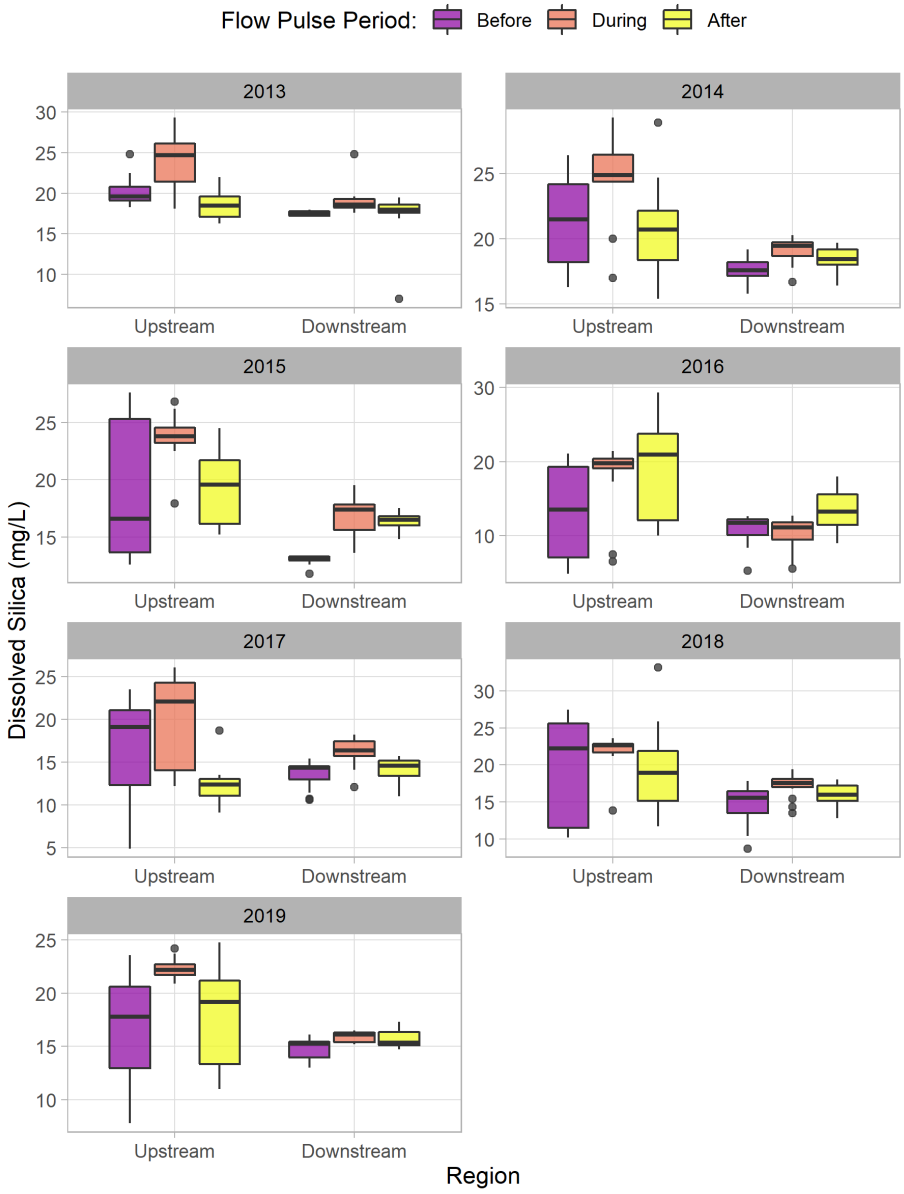

Figure 3-52. Dissolved silica concentrations in the upstream and downstream regions for all years and flow pulse periods.

Organic Carbon

DOC and TOC concentrations appeared higher upstream than downstream (Figure 3-53 - Figure 3-58). Across years, the flow pulses did not affect concentrations, except upstream in 2015 (a high-flow pulse year).

Based on regression analyses, flow pulse period did not have a significant effect on DOC or TOC concentrations. Year and region significantly affected TOC, with upstream concentrations higher overall than downstream and 2015

concentrations higher than 2014.

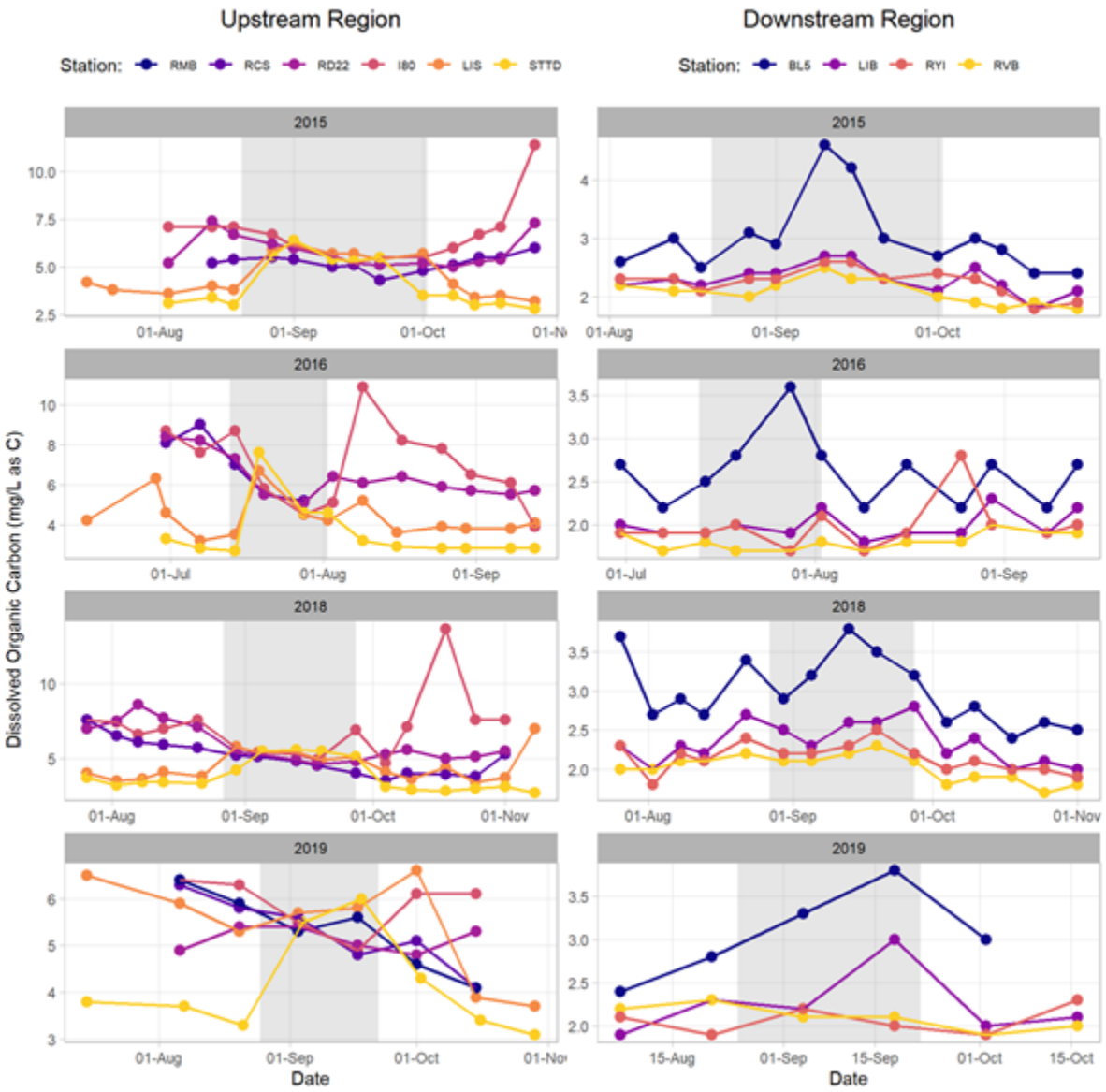

Figure 3-53. DOC concentrations in the upstream and downstream regions for high-flow pulse years across flow pulse periods. The light grey shaded box represents the "during" flow pulse period and each graph has a different y-axis scale. Connecting lines are imputed.

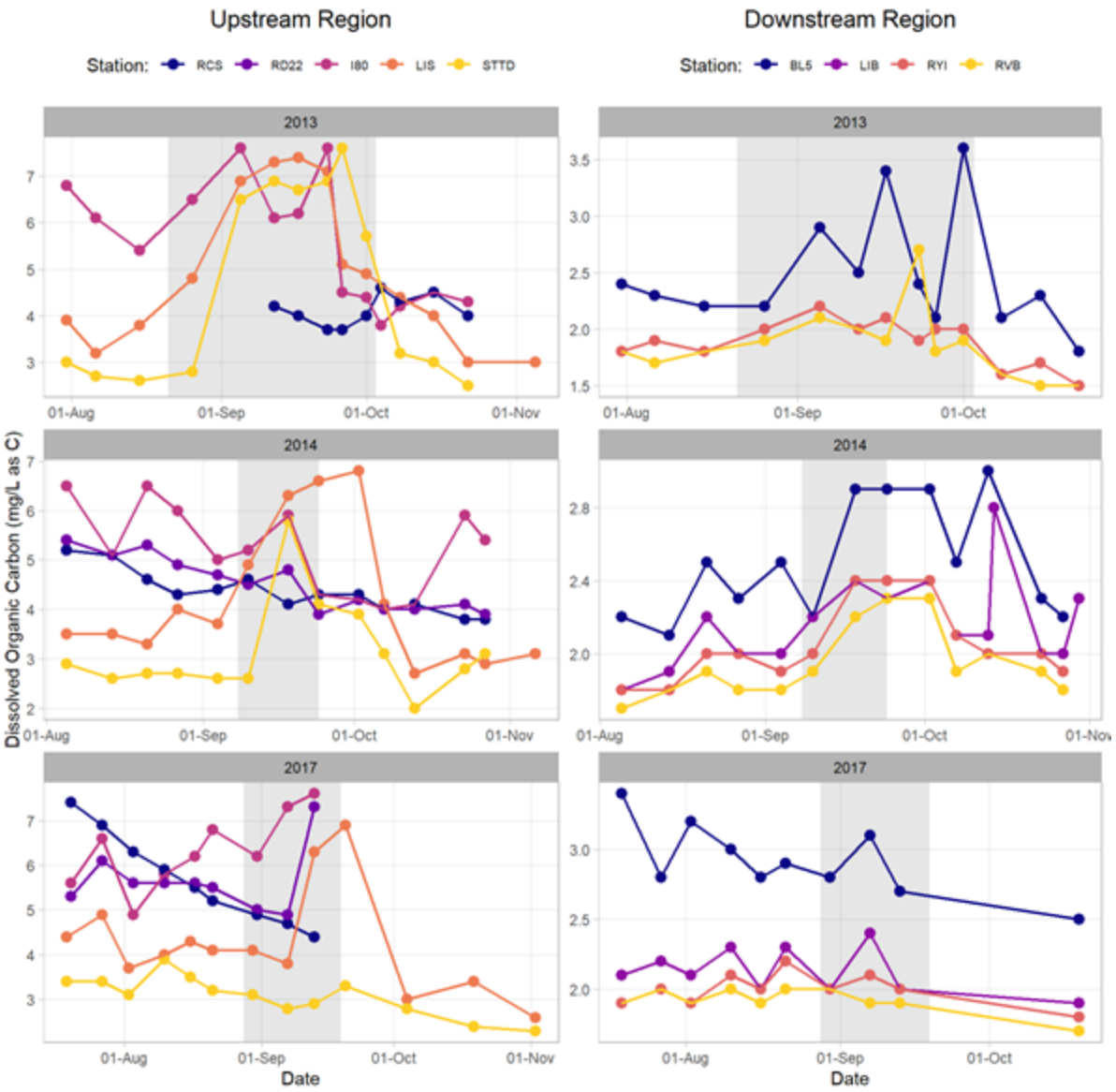

Figure 3-54. DOC concentrations in the upstream and downstream regions for low-flow pulse years across flow pulse periods. The light grey shaded box represents the "during" flow pulse period and each graph has a different y-axis scale. Connecting lines are imputed.

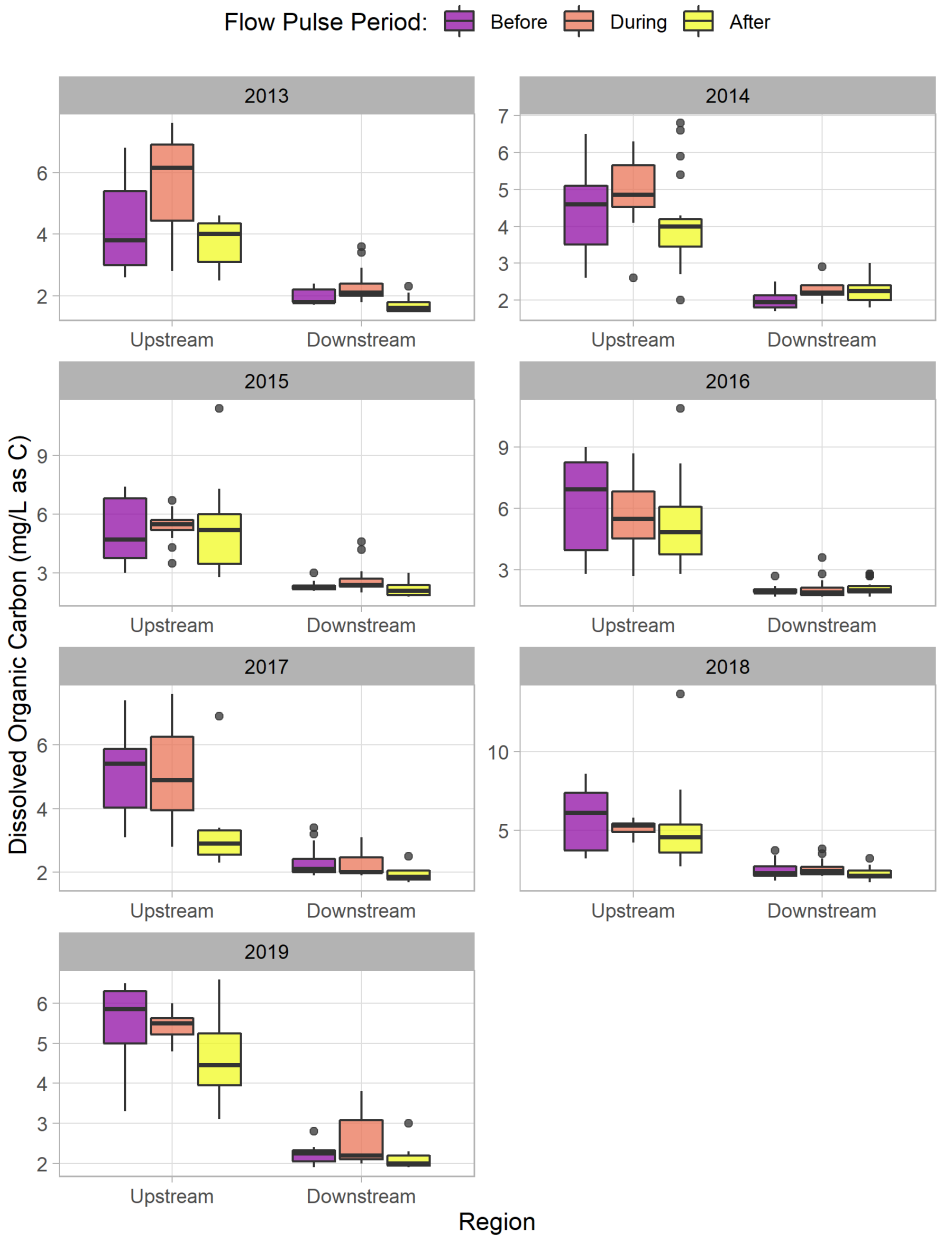

Figure 3-55. DOC concentrations in the upstream and downstream regions for all years and flow pulse periods.

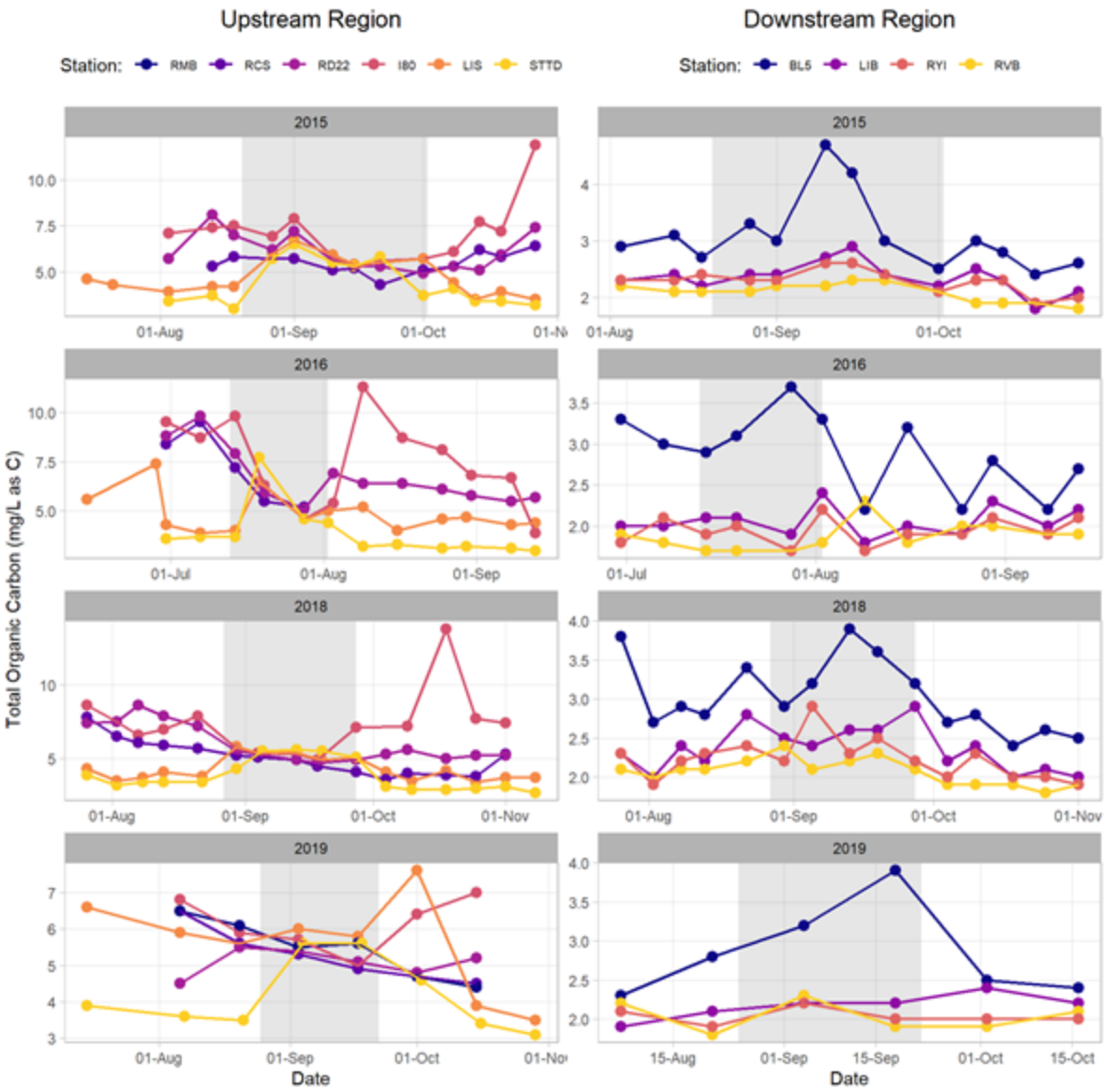

Figure 3-56. TOC concentrations in the upstream and downstream regions for high-flow pulse years across flow pulse periods. The light grey shaded box represents the "during" flow pulse period and each graph has a different y-axis scale.

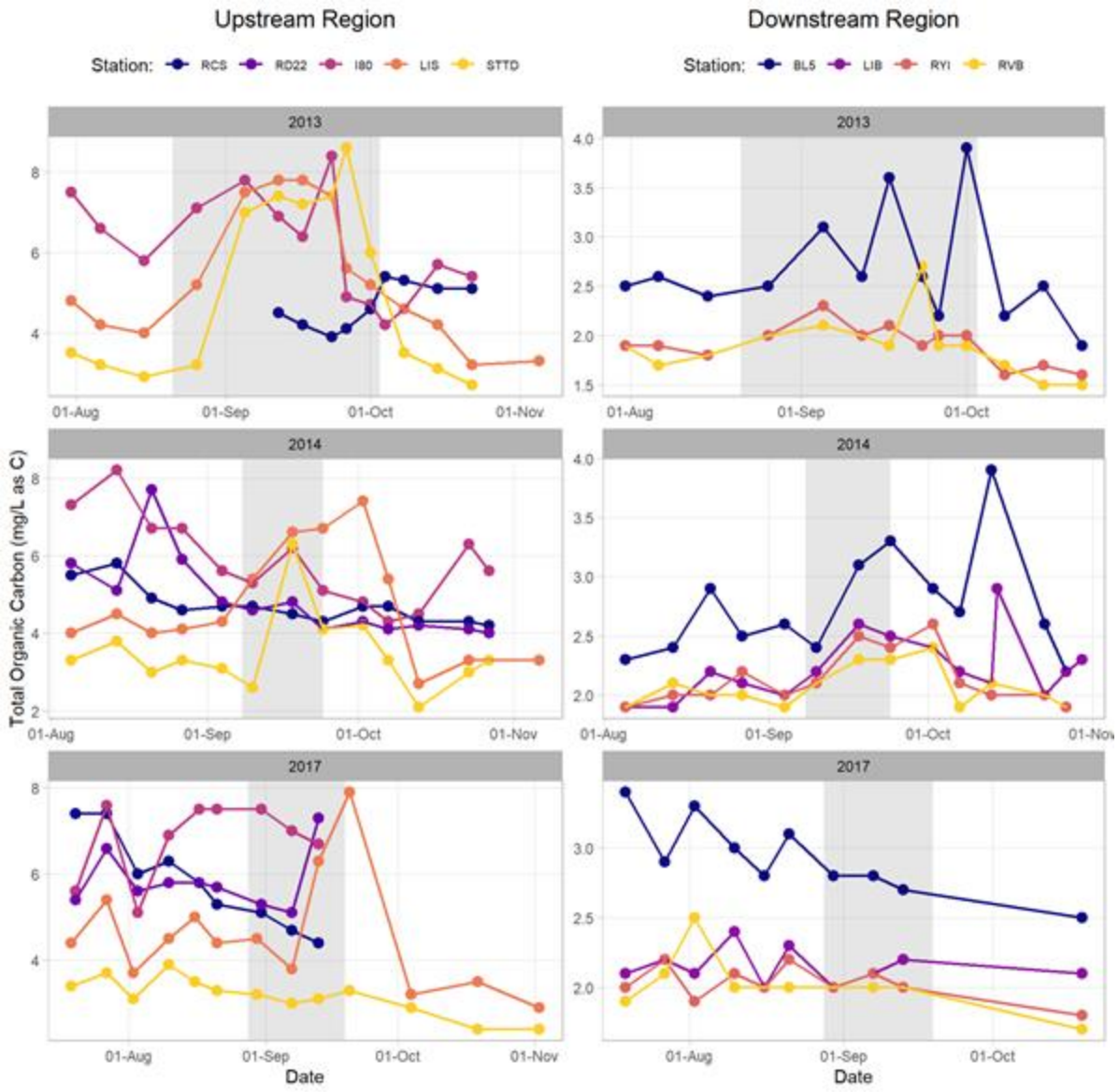

Figure 3-57. TOC concentrations in the upstream and downstream regions for low-flow pulse years across flow pulse periods. The light grey shaded box represents the "during" flow pulse period and each graph has a different y-axis scale.

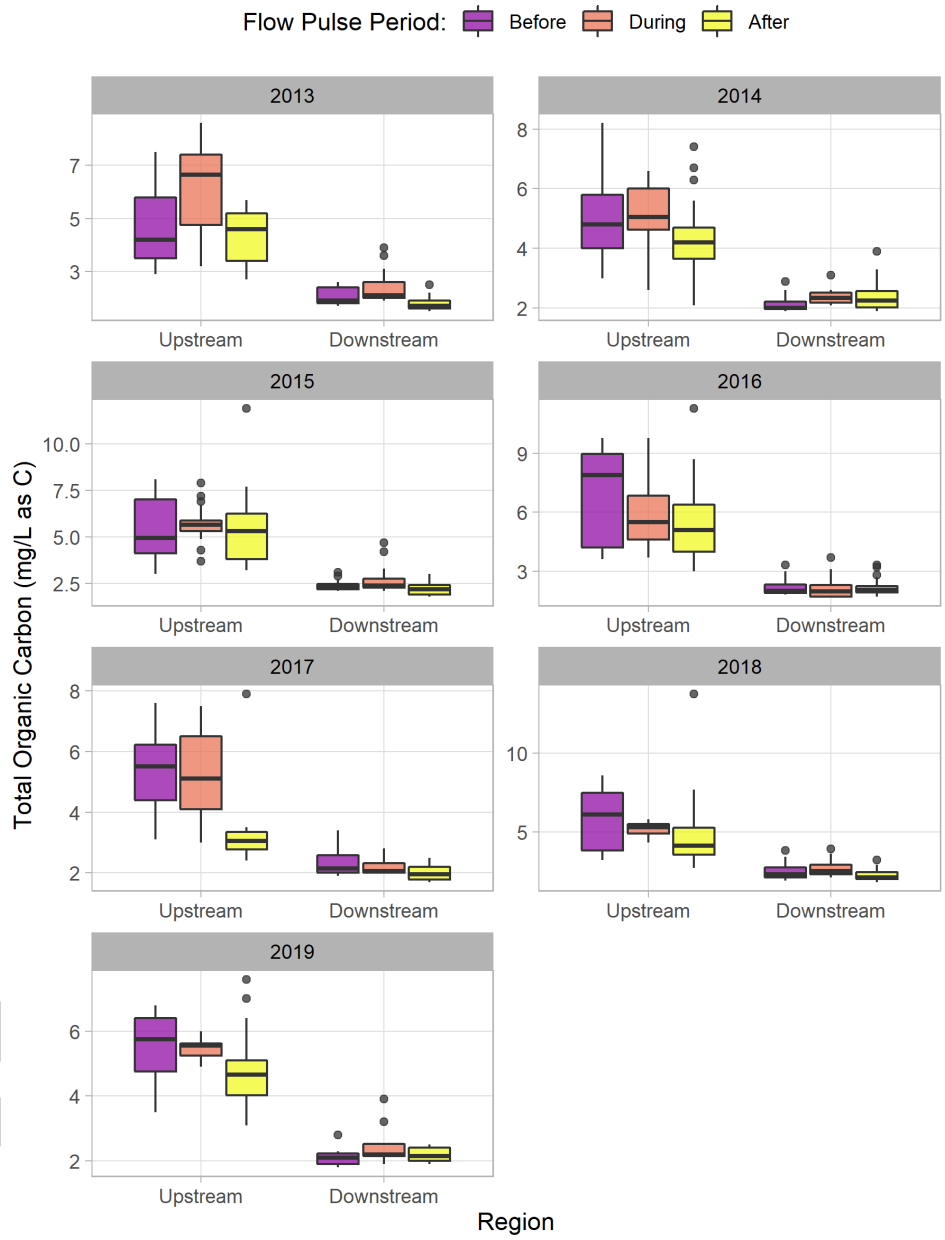

Figure 3-58. TOC concentrations in the upstream and downstream regions for all years and flow pulse periods.

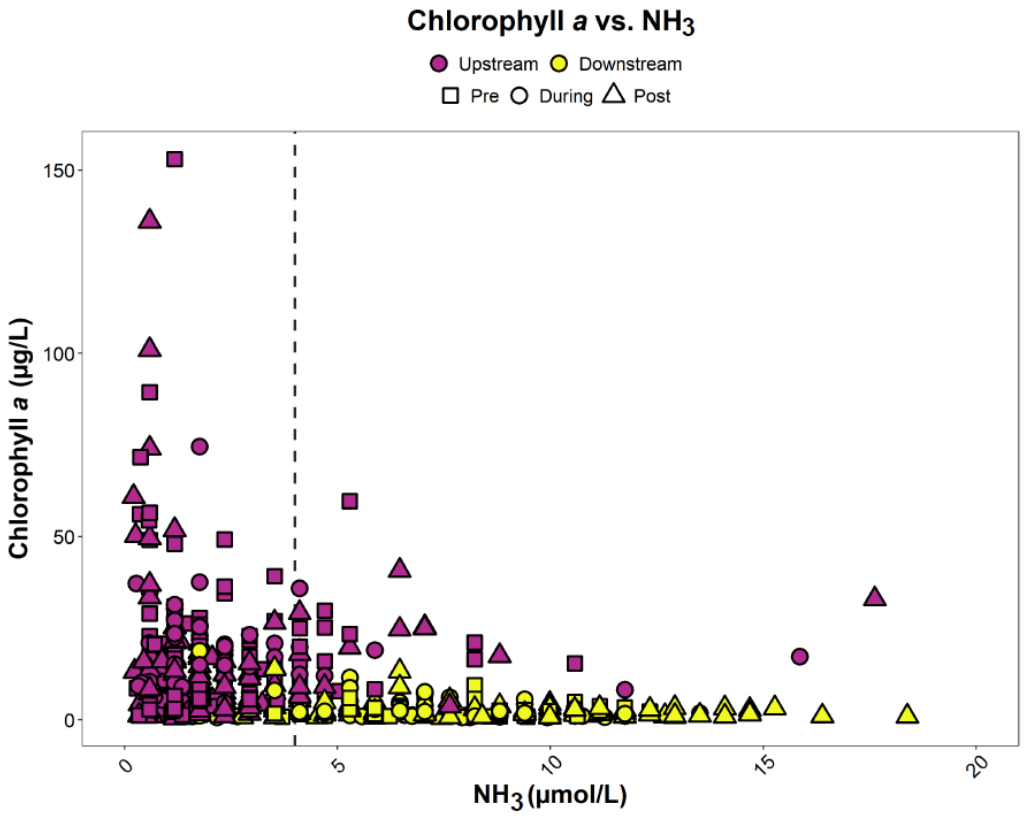

Figure 3-59. Ammonia (NH3) vs chlorophyll a concentration. Dotted line at NH3 = 4 µmol/L represents the concentration above which ammonia can suppress phytoplankton growth.

3.4.3 Discussion

Chlorophyll *a* is used by phytoplankton for photosynthesis and is therefore an important marker of productivity. While one of the goals of managed flow pulses (i.e. actions) is to increase chlorophyll *a* concentration in the downstream region, modeled results did not show any significant changes in discrete chlorophyll or pheophytin concentrations due to flow pulses. Instead, chlorophyll varied across years and regions, with higher concentrations consistently in the upstream region and correlation to high-flow years. Chlorophyll is extremely variable, and the high natural variability in chlorophyll may have masked any effect of the flow pulse. Although we could not test interactions between years, regions, and pulse periods, we did see some qualitative changes in chlorophyll with flow pulses that support increased transport of chlorophyll *a* downstream in 2016 marked with a 2-5-fold increase in chlorophyll (10-20 ug/L) at Liberty and Ryer Island (Figure 3-38) that were consistent with real-time continuous trends in chlorophyll fluorescence (Figure 3-4).

Dissolved calcium, an important constituent due to its importance in shell formation for phytoplankton and zooplankton, was the only parameter to increase during the flow pulse and stay elevated afterward to a statistically significant degree according to estimated marginal means (EMM) results. Dissolved silica, another biogenic constituent important for diatom growth, showed qualitatively similar results downstream in 2016; other years (2013 and 2014, both low-flow pulse years) saw a peak during the flow pulse followed by a decrease. Neither dissolved ammonia nor dissolved nitrate+nitrite, two important forms of nitrogen that are used for phytoplankton growth (Jassby et al. 2002, 2005), were influenced by the flow pulse to a statistically significant degree. Dissolved phosphorus, however, was affected by the flow pulses to a significant degree, with concentrations higher after flow pulses than during and several high-flow years (2015, 2016, 2018) seeing increases post-flow pulse in some stations. For both dissolved and total organic carbon, the flow pulses did not have a large effect on analyte concentrations, although upstream in 2013 showed brief increases during the flow pulse for both analytes. Overall, analyte concentrations were higher post-flow pulse in high-flow years.

It is important to note that our model results did not test the interactions between the flow pulse, region, and year variables due to limitations in statistical power. Therefore, it is possible that the flow pulses had different effects on the analytes across years and on the upstream and downstream regimes that our results do not reflect. Nutrients including Dissolved Calcium, Organic Nitrogen, Silica, Phosphate, Carbon, and total Carbon (Figure 3-46) were consistently higher in the upstream region across all years compared to downstream, but it is inconclusive if a portion of these nutrients were transported downstream as a result of flow pulses in given high- or low-flow years. In addition, because of residual autocorrelation, some explanatory variables may appear significant in our analyses when trends are in fact due to seasonality.

We found evidence of the ammonia paradox in our water quality data in the downstream region (Figure 3-59). The ammonia paradox states that dissolved ammonia values >4 µmol/L can prohibit some phytoplankton, especially diatoms, from accessing nitrate, leading to slower growth rates and lower chlorophyll values (Dugdale, 2007). High dissolved ammonium discharge from the Sacramento Regional Wastewater Treatment Plant is one of the largest sources of ammonium in the Delta and is hypothesized to be a leading factor

limiting phytoplankton, specifically nutritious diatoms from flourishing (Glibert 2011, Parker et al. 2012). This is a plausible explanation for why chlorophyll *a* values in the downstream region were, on average, lower than values in the upstream region while the reverse was true for ammonia concentrations (Figure 3-59). However, there are other factors – such as water temperature, irradiance, turbidity, depth, clam densities, downstream grazing, and residence time – that can also explain or contribute to these trends. Therefore, we cannot make any definitive conclusions.

The Sacramento Regional Wastewater Treatment Plant underwent an upgrade, completed in April 2021, that reduces dissolved inorganic nitrogen (DIN), including ammonia/ammonium, from its discharge (regionalsan.com/post/new-treatment-processes). Preliminary mapping of nutrients in the Delta by USGS has shown that the upgrade resulted in a reduction of ammonium concentration to near zero, a nearly ten-fold increase in nitrate, and a 60% decrease in DIN in the discharge (Tamara Kraus, USGS, email communication). This will likely reduce ammonium concentrations in the downstream region of our study area, potentially providing more favorable nutrient ratios for growth of diatoms and other beneficial algal taxa. Future years of the NDFS will assess changes in nutrient concentrations and how they interact with flow pulses to affect phytoplankton growth and community composition in the downstream region.

3.5 Contaminants

3.5.1 Methods

Field and laboratory methods

To determine contaminant concentrations in water and sediment samples, we collected near surface water samples in 1 L amber glass bottles between 2016 and 2019. We also collected samples to analyze pesticide concentrations in zooplankton between 2017 and 2019. See Table 3-7 below for a summary of sampling locations by year and region. The sampling frequency varied for each year of sample collection, and the total number of samples collected by year and flow pulse period ranged from 6 to 18 for water and sediment samples and 4 to 8 for zooplankton samples.

We sampled zooplankton using 5-minute surface tows with a 150 µm mesh zooplankton net, with 0.5 m diameter mouth opening, attached to a 150 µm mesh cod end (Sea-Gear Corporation, Melbourne, FL, USA). Zooplankton samples were kept on ice until analysis.

We measured concentrations of a suite of 163 current-use pesticides in water and zooplankton and 128 pesticides on suspended sediments (see Appendix B, Table 1 for pesticides analyzed) filtered from water samples at the USGS Organic Chemistry Research Laboratory (OCRL) within 24 hours of collection. Water samples were filtered through pre-weighed, baked 0.7 µm glass-fiber filters (Grade GF/F, Whatman, Piscataway, New Jersey) to remove suspended material, dried at room temperature overnight (in the dark), and then stored in a freezer at –20 °C until extraction. Following filtering, we extracted water samples and analyzed them using both liquid chromatography tandem mass spectrometry (LC/MS/MS) and gas chromatography/mass spectrometry (GC/MS). We analyzed water samples for 35 current-use pesticides by LC/MS/MS following the method described in detail in Hladik and Calhoun (2012), and an additional 127 current-use pesticides by GC/MS following the method described in Hladik et al. (2008, 2009). Suspended sediments were extracted and analyzed by GC/MS for 127 current-use pesticides following the method described in Hladik and McWayne (2012).

Table 3-7. Sampling sites by year and study region for pesticide concentrations in water/sediment and zooplankton. Empty cells indicate that no samples were taken for that year/region combination.

Year	Region	Water/Sediment Sites	Zooplankton Sites
2016	Upstream	RCS, RD22, LIS	
	Downstream	BL5	
	Middle Sac River		
2017	Upstream	RCS, RD22, LIS	STTD
	Downstream	BL5, RYI	
	Middle Sac River	SHR	SHR
2018	Upstream	RCS, RD22, LIS	STTD
	Downstream	BL5, RYI	
	Middle Sac River	SHR	SHR
2019	Upstream	RMB, RD22, LIS, STTD	STTD
	Downstream	BL5	
	Middle Sac River	SHR	SHR

To validate pesticide concentrations, we used a suite of performance-based quality-control samples, including trip blanks, field replicates, laboratory matrix spikes, and matrix-spike replicates, and surrogate recoveries. Field crews collected two trip blanks consisting of 1 L amber glass bottles of organic-free blank water that were open to the atmosphere during the time of water sample collection. Following sample collection, we transported, processed, and analyzed trip blanks at the OCRL in the same manner as all environmental samples. No pesticides were detected in either of the trip blanks. We also analyzed filter papers used in the processing of the trip blank by GC/MS and detected no pesticides.

We analyzed three sequential field-replicate sample pairs (two by LC/MS/MS and one by GC/MS) to test the reproducibility of results. In addition, we analyzed suspended sediments trapped on filter papers that were used in the processing of the one replicate sample analyzed by GC/MS. In all cases, we found that the relative standard deviation between the replicate and its complementary environmental sample concentration was less than the control limit of 25%. The correlation of pesticide detections between the paired environmental and replicate samples was 100%.

In addition to field-replicates, we validated analytical results using two laboratory water matrix spikes (one each by GC/MS and LC/MS/MS), and one

suspended-sediment matrix spike each paired with a matrix-spike-replicate, to assess pesticide recovery, degradation, sorption, and interferences caused by the sampling matrix. All samples met the data-quality objective of 70–130% matrix-spike recovery. The relative standard deviation between the matrix-spike samples and their complementary replicates was less than the 25% control limit in all cases. We also added surrogate compounds to each environmental and quality-control sample, as described in the method references listed earlier, to assess the efficiency of sample extraction for GC/MS and LC/MC/MS analytical methods. Recoveries of all surrogate compounds met the data-quality objective of 70–130% in every sample.

All data are available for public download via the U.S. Geological Survey National Water Information System database. For further details of methods, see Orlando et al. 2020.

Data analysis

Most analytes in sediment samples were below method detection limits, precluding statistical analyses. However, we ran statistical analyses (e.g., ANOVA) to assess the effects of year and flow pulse period at upstream and downstream sites on pesticides in water and zooplankton. In addition, we examined which analytes in water samples exceeded EPA benchmarks for toxicity to invertebrates and fish (EPA aquatic life benchmarks).

Effects of year and flow pulse period on total pesticide concentration

There was not enough replication to test the effect of region on pesticide concentrations in water or zooplankton samples. We also lacked the replication needed to examine interactions between year and flow period on total pesticide concentration in zooplankton when all sites were included (i.e. there was low replication for some sites across the year by flow period combinations), and there did not appear to be a significant interactive effect of year and flow period on total pesticide concentration in water (Figure 3-60). Therefore, we tested for main effects of year and flow pulse period on total pesticide concentrations in water and zooplankton using analysis of variance (ANOVA) with type 2 sums of squares for unbalanced sample designs. ANOVAs were run in R (version 4.0.2, R Core Team 2020) using the 'car' package (version 3.0-10, Fox et al. 2020). We removed data for the control site SHR, which is outside of our upstream/downstream study area, and data from 2015 for pesticides in water, when only the 'after' period was sampled. We then log-

transformed total pesticide concentrations for the remaining data to achieve normality and homoscedasticity in model residuals. We included year and flow pulse period as fixed effect predictors. Following ANOVA, we examined individual contrasts for significant model terms using post-hoc tests in the 'emmeans' package (version 1.5.1, Lenth et al. 2020) with the 'sidak' adjustment method. Significance levels were set to alpha = 0.05 for all tests here and in the following sections.

Interactions between year and flow period on pesticides in water at upstream and downstream sites

Our sampling design lacked replication within the downstream region. Therefore, we examined differences between representative upstream and downstream sites (upstream: RD22, downstream: BL5) and interactions between year and flow pulse period on pesticide concentration in water. We used ANOVA with type 3 sums of squares and included log-transformed total pesticide concentration in water as the response variable, site as a categorical predictor, and an interaction between year and flow pulse period. We tested the significance of individual contrasts as described above. We were unable to assess differences of pesticides in zooplankton at upstream and downstream sites, as there were no representative downstream sites (Table 3-7).

Comparisons among regions: Upstream, Downstream, Middle Sac River

To examine overall differences in pesticides in water among regions, we used one-way ANOVA with type 2 sums of squares, followed by post-hoc tests as above, with log-transformed total pesticide concentration in water as the response variable and site as the predictor. Representative sites for regions included: RD22 (upstream), BL5 (downstream), and SHR (control site in middle Sac River). In addition, we tested overall differences in log-transformed total pesticide concentration in zooplankton between STTD (upstream) and SHR (control site in middle Sac River) using Welch's two-sample t-test.

3.5.2 Results

Effects of year and flow pulse period on total pesticide concentration

There was a significant effect of flow period (ANOVA, $F_{2,125} = 12.45$, $p<0.01$) but not year ($F_{3,125} = 0.58$, $p=0.63$) on pesticide concentrations in water across all sites (Figure 3-60). Results of post-hoc tests are summarized in

figures, below. Overall, we detected greater pesticide concentrations in water during the flow pulse than before or after (Figure 3-60B). By contrast, both year ($F_{2,17}$ = 4.42, p=0.03) and flow period ($F_{2,17}$ = 4.56, p=0.03) significantly affected pesticide concentrations in zooplankton (Figure 3-62). Concentrations in zooplankton were higher in 2019, a high-flow pulse year, than 2017, a low-flow pulse year (Figure 3-62A), and higher during the flow pulse than before (Figure 3-62B).

Interactions between year and flow period on pesticides in water at upstream and downstream sites

When we used representative sites to test for differences between upstream and downstream regions on pesticide concentrations in water, we found a significant effect of site ($F_{1,41}$ = 212.20, p<0.01) and the interaction between year and flow pulse period ($F_{6,41}$ = 2.62, p<0.05) (Figure 3-61). Main effects of year ($F_{3,41}$ = 0.06, p=0.98) and flow period ($F_{2,41}$ = 1.43, p=0.25) were not significant, but patterns among years and flow periods were similar to the patterns including all sites (Figure 3-60). Overall, the total pesticide concentration in water was higher at RD22 (upstream) than BL5 (downstream), and concentrations were higher in 2018 during the pulse than 2016 during the pulse, or than 2016, 2017, and 2019 after the pulse.

Comparisons among regions: Upstream, Downstream, Middle Sac River

Overall, total pesticide concentration in water varied by site ($F_{2,73}$ = 85.65, p<0.01). Concentrations in water were highest at RD22 (upstream region), followed by BL5 (downstream region), and were lowest at SHR (control site in middle Sac River) (Figure 3-63). Fungicides, herbicides, and herbicide degradates comprised most pesticides at sites across the study area (Figure 3-63). Concentrations in zooplankton followed a different pattern, where concentrations were higher in zooplankton from SHR (control, middle sac River) than within the study region at STTD (upstream region) (t=2.09, p=0.05). The pesticide composition differed between zooplankton sampled from STTD and SHR, such that zooplankton at STTD had higher concentrations of fungicides, herbicides, and herbicide degradates, whereas there were higher concentrations of insecticides at SHR (Figure 3-64).

Analytes exceeding EPA benchmarks for toxicity

We detected pesticides exceeding EPA benchmarks for both acute and chronic

toxicity to invertebrates and fish across all years, flow periods, and regions (Figure 3-65). In addition, the number of analytes exceeding benchmarks increased over time. We found that all classes of pesticides included analytes exceeding benchmarks (Appendix B, Table 2).

The Strobin class was the most dominant group of Fungicides observed at all stations for most sampling events, followed by the Benzimidazole class. In particular, the Strobin Azoxystrobin and the Benzimidozole Carbendazim appeared in concentrations exceeding EPA benchmarks at many sites (Appendix B, Table 2). Among the herbicides, the Amine and Phenylpyridine classes were the most prevalent overall. In particular, the herbicide degradate 3-4 DCA was commonly detected across sites. However, Metolachlor, Propanil, Thiobencarb, Pendimethalin, Oxyfluorfen, and Clomazone were the most frequently detected herbicides exceeding EPA benchmarks. For the insecticides, Diacylhydrazines, Neonicotinoids, and Pyrethroids, such as Methoxyfenozide, Thiamethoxam, and Permethrin, respectively, were commonly detected at concentrations exceeding EPA benchmarks.

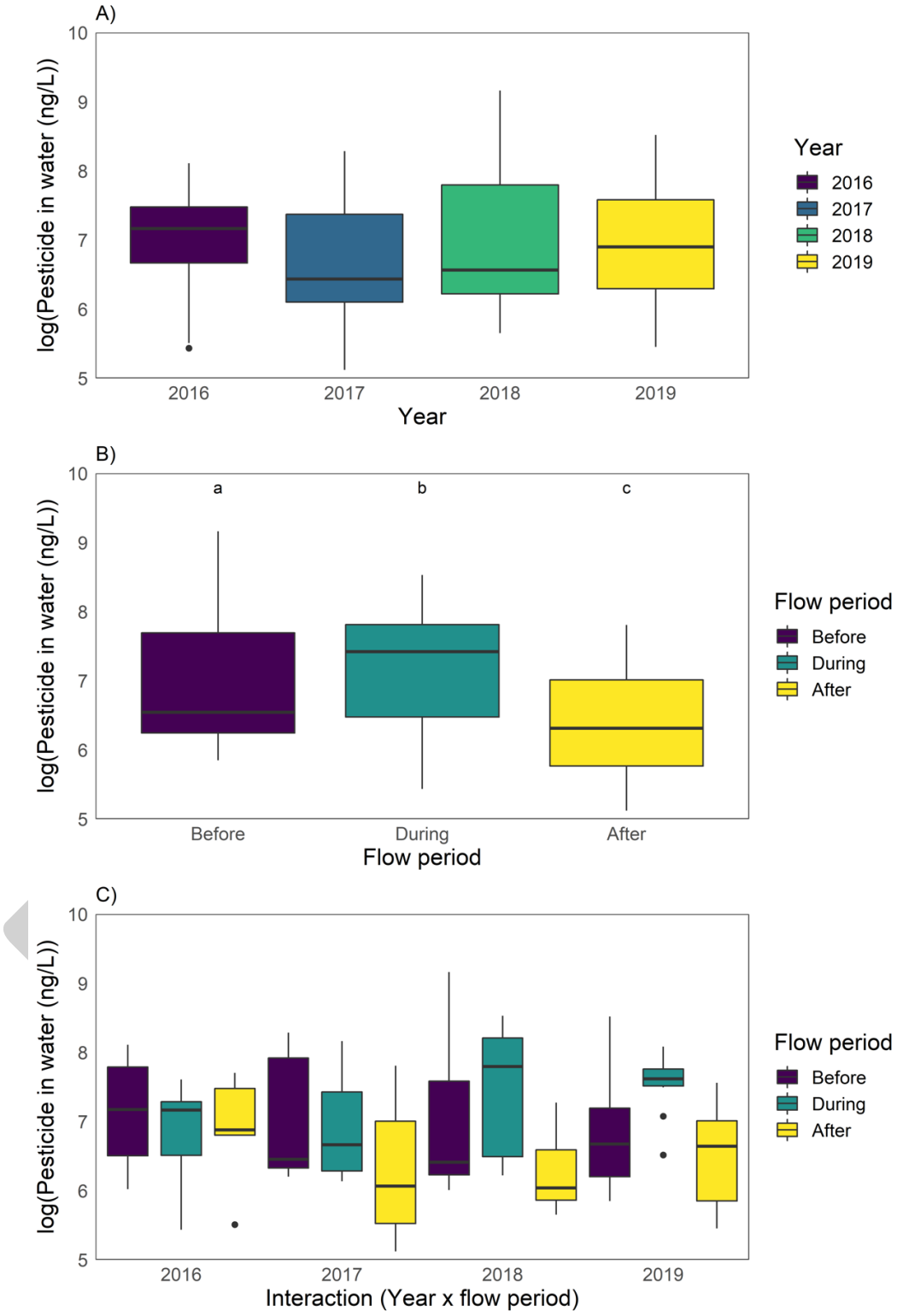

Figure 3-60. Boxplots of medians and quartiles of pesticide concentrations in water (ng/L) by A) year, B) flow period, and C) the interaction between year and flow period for all sites except SHR (Table 3-7). Different letters above boxes in B) indicate significant differences in contaminant concentrations among flow pulse periods according to post-hoc tests.

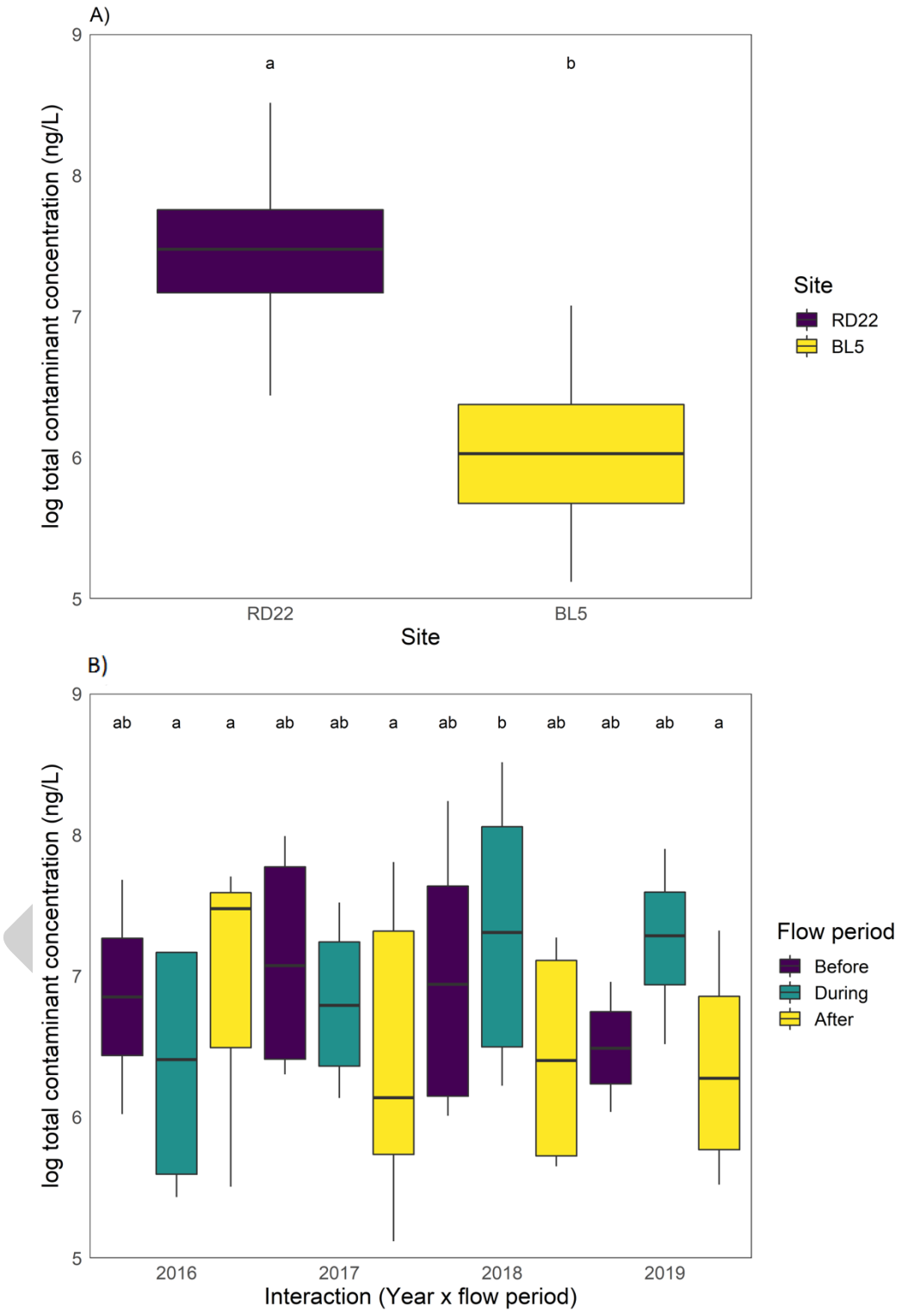

Figure 3-61. Boxplots of medians and quartiles of pesticide concentrations in water (ng/L) by A) upstream (RD22) vs. downstream (BL5) sites, and B) the interaction between year and flow period for RD22 and BL5. Different letters above boxes in indicate significant differences in contaminant concentrations among flow pulse periods according to post-hoc tests.

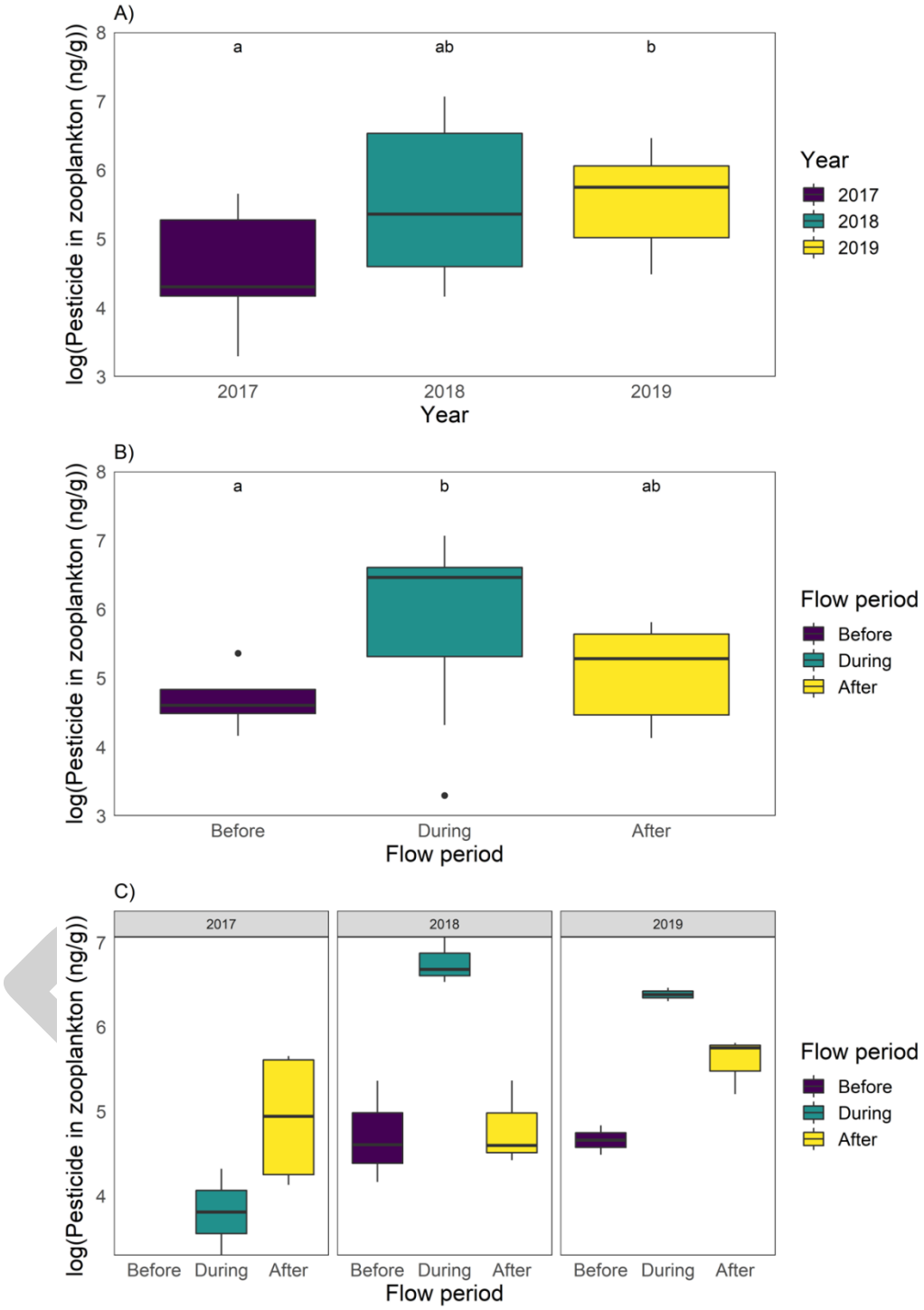

Figure 3-62. Boxplots of medians and quartiles for pesticide concentrations in zooplankton (ng/g) by A) year, B) flow period, and C) the interaction between year and flow period for STTD (Screw Trap at Toe Drain) in the lower Yolo Bypass (upstream region). Note that we had no data for 2017 in the "Before" period. Different letters above boxes in A) and B) indicate significant differences in contaminant concentrations among years and flow pulse periods, respectively, according to post-hoc tests.

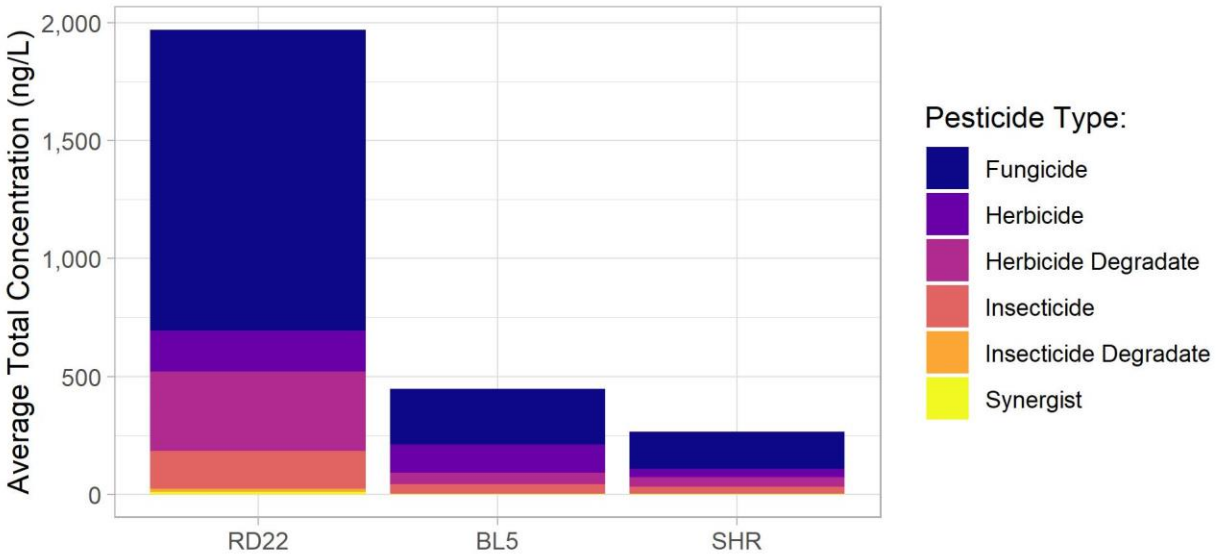

Figure 3-63. Contribution of fungicides, herbicides, herbicide degradates, insecticides, and insecticide degradates to total pesticide concentrations in water.

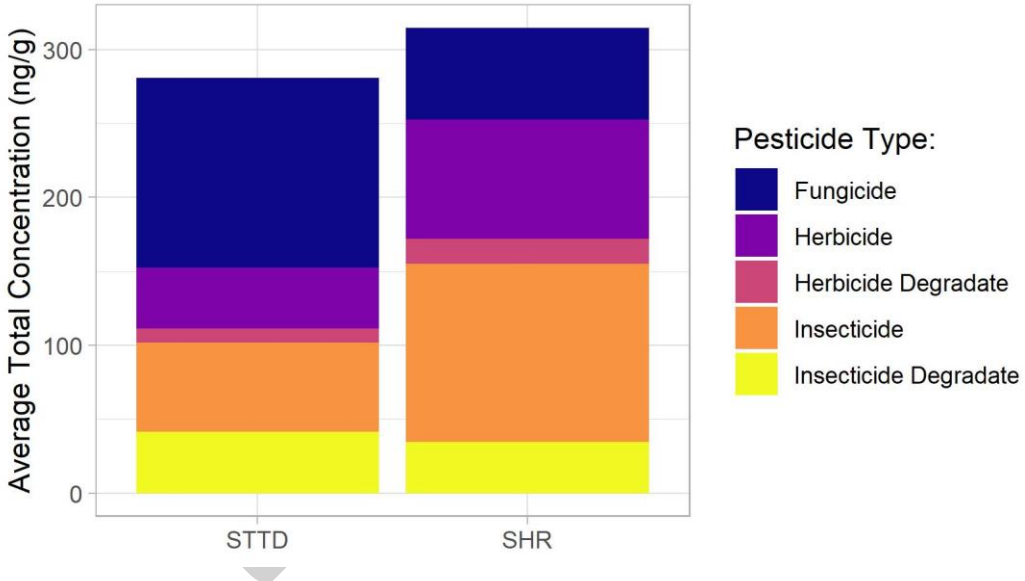

Figure 3-64. Contribution of fungicides, herbicides, herbicide degradates, insecticides, and insecticide degradates to total pesticide concentrations in zooplankton at STTD (Screw Trap at Toe Drain) in the lower Yolo Bypass (upstream region) and SHR (control site in middle Sac River).

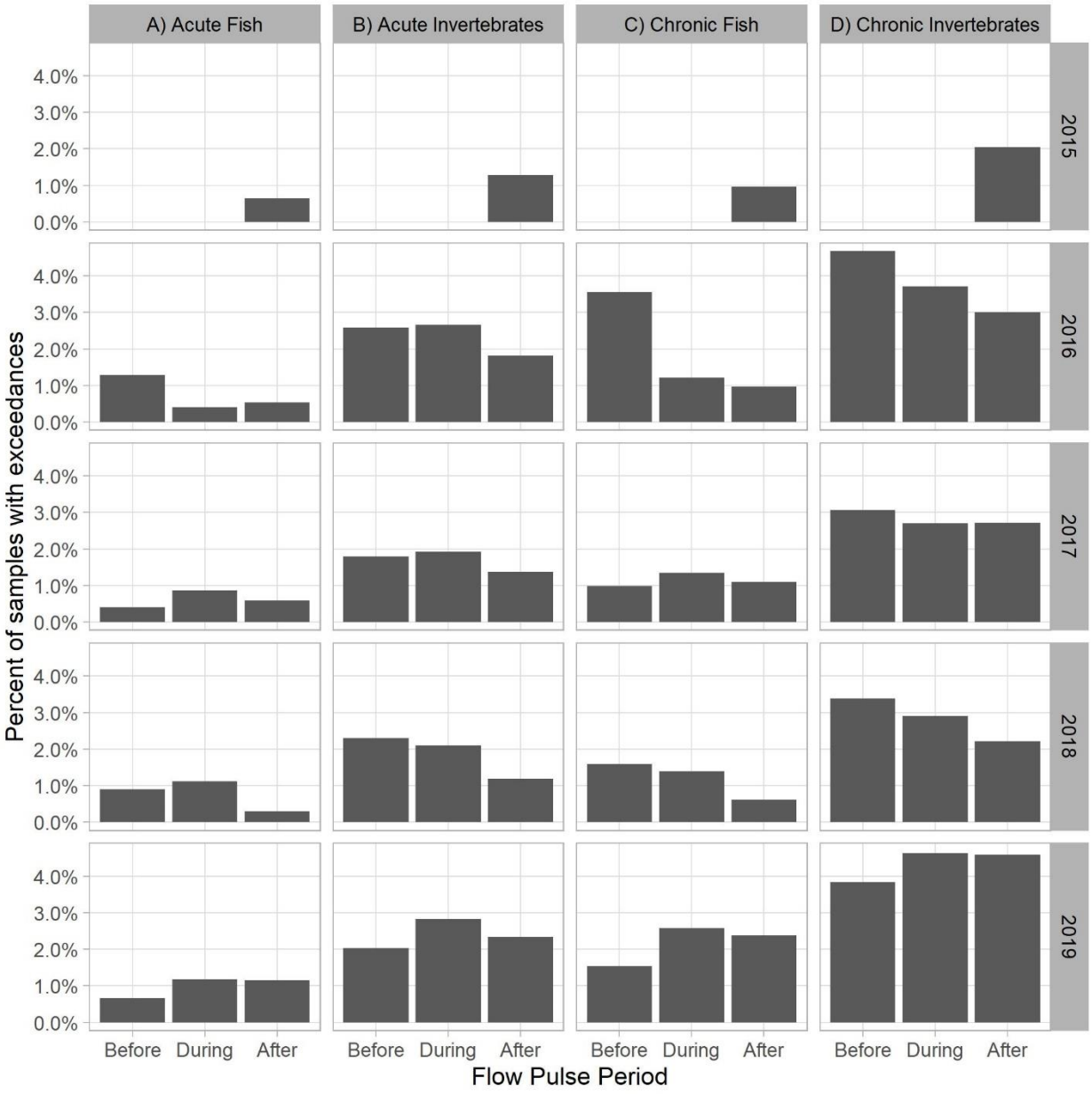

Figure 3-65. Percentage of samples exceeding EPA benchmarks for A) acute toxicity to fish, B) acute toxicity to invertebrates, C) chronic toxicity to fish, and D) chronic toxicity to invertebrates. Samples were not collected before and during the flow pulse in 2015.

3.5.3 Discussion

Overall, the total pesticide concentration in water was higher at the upstream site RD22 in the Yolo Bypass than at the downstream site BL5 in the Cache Slough Complex (Figure 3-61). Surprisingly, the total pesticide concentration in zooplankton was higher at the control site SHR in the middle Sacramento River than at STTD in the Yolo Bypass (Figure 3-64). In addition to differences between sites, we found that total pesticide concentrations in water and zooplankton were highest during the flow pulses (Figure 3-60 and Figure 3-62). Although pesticide concentrations increased during pulses, we found pesticides exceeding EPA benchmarks for toxicity to aquatic life across all flow pulse periods and years (Figure 3-65), suggesting that high pesticide concentrations are ubiquitous in our study area regardless of the NDFS management action.

Managed flow pulses using Sacramento River water may have different pesticide concentrations, including lower concentrations from agricultural sources and higher concentrations from urban sources. For example, SHR had relatively high insecticide concentrations, whereas sites in our upstream/downstream regions contained pesticides used in rice agriculture (e.g., azoxystrobin, clomazone, methoxyfenozide, penoxsulam, thiobencarb, and the propanil degradate 3,4-dichloroaniline) (Figure 3-63 and Figure 3-64), as expected based on previous contaminant research in the area (Smalling et al. 2007; Kuivila and Hladick, 2008). In addition, pesticide concentrations in water were higher during the flow pulse in high-flow years with agricultural source water (2018 and 2019) than during the high-flow year using Sacramento River water (2016) (Figure 3-61). Because Sacramento River water may have lower overall pesticide concentrations in water (Figure 3-63), future NDFS actions should repeat the 2016 flow action using diversions of Sacramento River to compare the effects of different water sources on contaminant concentrations in the study area.

More research is needed to understand what effects elevated pesticide concentrations during flow pulses have on the lower trophic food web. For example, pesticide levels appear relatively high in both high-flow pulse years with a managed flow action (e.g., 2018, 2019) and low-flow pulse years without a managed flow action (e.g., 2017). It is therefore challenging to determine the effects of the flow pulse on contaminants versus the responses to local agricultural inputs in the Yolo Bypass, especially as we had limited

availability of data to examine the effects of different types of flow pulses (e.g., low vs. high flow). More research is needed to distinguish differences among the flow pulse types and relative to events throughout the year that may increase contaminant loading (e.g., inundation during winter storms) (Orlando et al. unpublished data).

In addition, we need more information about potential negative effects of different pesticides on zooplankton populations and communities (van Wijngaarden et al. 2014). Studies suggest that zooplankton exposure to agricultural pesticides found in our study area (e.g., imidachloprid, azoxystrobin) can alter population dynamics, reduce biomass, and alter community structure (van Wijngaarden et al. 2014; Hébert et al. 2020). Across studies, copepods (calanoids, cyclopoids and nauplii) were most sensitive to pesticide exposures (van Wijngaarden et al. 2014; Hébert et al. 2020) including similar concentrations of azoxystrobin as measured throughout our study period (we found samples with azoxystrobin concentrations exceeding EPA benchmarks in all years of our study, Appendix B, Table 2). In addition, rotifers have found to be sensitive to imidachloprid found in our study area (Hébert et al. 2020) and cladocerans are sensitive to high levels of azoxystrobin (van Wijngaarden et al. 2014). These zooplankton taxa are important prey for fish in the downstream region of our study area, including Delta Smelt (IEP-MAST 2015, USBR 2019). Thus, pesticides may harm higher trophic levels directly through toxicity (Figure 3-65) or indirectly by reducing the abundance or nutritional value of zooplankton prey. Future years of NDFS could examine pesticide concentrations in zooplankton at more sites to evaluate the quality of food available for Delta Smelt and other native fishes. Further research, such as laboratory studies examining toxicity of pesticides found in our study area, could illuminate their consequences for the food web.

Chapter 4 Lower Trophic Levels

Technical Team: Theodore Flynn, Mallory Bedwell, Jesse Adams, Brittany Davis

4.1 Summary

Phytoplankton form the base of the food web in the San Francisco Estuary (SFE). These photosynthetic microorganisms are primary producers that convert sunlight into biomass and energy, providing an essential food source for zooplankton and the organisms that feed on them such as fish. The managed flow pulses used in this study target increased phytoplankton abundance in the Yolo Bypass and downstream in the Cache Slough Complex and lower Sacramento River. The increase in phytoplankton is expected to produce a corresponding increase in zooplankton – the primary source of Delta Smelt food.

Previous analyses of managed flow actions (e.g., high-flow pulses in 2016, 2018, and 2019) in the North Delta had shown variable responses in phytoplankton abundance after flow pulses, but no comprehensive and comparative analysis has yet been carried out to examine the effects of high- and low-flow pulses (with and without managed actions) on lower trophic communities since 2014.

4.2 Objectives

Our primary objective in this synthesis is to assess the effects of flow pulses on both the abundance and composition of phytoplankton and zooplankton communities in the upstream and downstream region of the North Delta over the study period where such samples were available (2014—2019). Our research questions are:

1. Was there a difference in phytoplankton and zooplankton abundance and composition at upstream sites compared to downstream sites?
2. Did the overall abundance of phytoplankton and zooplankton in these regions and at specific stations vary before, during, and after flow pulses?

3. Did the abundance of specific taxa of phytoplankton or zooplankton change in response to flow pulses?
4. Did the overall abundance and/or community composition of phytoplankton and zooplankton vary between years?
5. What is the distribution of benthic clams in 2014 and 2019 (a low- and high-flow pulse year), and could clam grazing affect plankton availability in the north Delta regions?

4.3 Phytoplankton

4.3.1 Methods

Concurrent with discrete water quality monitoring, we sampled the lower trophic food web at all sites (Table 3-4, Figure 3-36), except for wastewater treatment sites (DWT and WWT). We collected water for land sites (I80, LIS, RMB, RCS, RD22) at < 1 m from the surface using a Nasco Swing Sampler and homogenized samples in the field with a homogenization bucket. We sampled boat sites (STTD, BL5, RVB, LIB, RYI) using a 4L Van Dorn water sampler. We collected phytoplankton by subsampling (60 mL) of homogenized water, fixing it with Lugol's solution, and storing it in amber glass bottles. We sent phytoplankton samples to BSA Environmental Inc. (Beechwood, OH) for identification and quantification. There, phytoplankton were identified to at least the genus level using the Utermöhl method (Utermöhl 1958) and at least four hundred total algal units were counted in each sample, including one hundred units of the dominant taxa. Length (µm) was recorded for the first 25 units of major phytoplankton taxa and the first 5 units of minor taxa to calculate biovolume ($\mu m^3/mL$), a surrogate for biomass, from formulas given for different algal shapes by Kellar et al. (1980).

Phytoplankton data collected before, during, and after flow pulses during years 2013-2019 at the stations mentioned above were combined and analyzed in R. Because only three samples were taken during 2013, these were removed from comprehensive analyses. Samples from the furthest upstream station, Colusa Basin Drain at Rominger Bridge (RMB), were only taken in 2019 and are therefore only included in group analyses for that year.

Taxa were categorized into higher taxonomic groups based on the World

Register of Marine Species taxonomy (WoRMS Editorial Board, 2021). Due to changes in how phytoplankton were classified over the time frame of the study, we reclassified the species *Eucapsis microscopica*, which prior to Fall 2016 was classified as *Chroococcus microscopicus*. No other significant changes to phytoplankton taxonomy in the Delta were identified over this period (Tiffany Brown, personal communication).

The biovolumes for individual taxa were measured microscopically by BSA for up to 10 difference cells, and an average biovolume calculated. Biovolume per unit sample volume was calculated using this average and the density of cells per unit volume (μm^3 per mL). Biomass of specific phytoplankton groups (diatoms, cyanobacteria, green algae, cryptophytes, and dinoflagellates) was estimated from these biovolume calculations using empirical equations developed by Menden-Deuer and Lessard (2000). From these calculations, the biomass of long-chain essential fatty acids (LCEFA) per unit volume (µg per L) was estimated using the method of Galloway and Winder (2015).

Statistical analyses were performed on biovolume calculations using R (v. 4.0.4; R Core Team 2020) and Primer-7 (Primer-e, Ltd.) software. A three-way Analysis of Variance (ANOVA) was done to determine the effects of year, region (upstream and downstream), flow pulse period (before, during, after), and two-way interactions on phytoplankton biovolume. Normality tests were conducted using the Shapiro-Wilks test with the package 'rstatix' and variance was compared using the Levene test with the same package (Kassambara 2021). Station was included as the random effect term in the model. Post hoc contrasts of significant interactions were conducted using the 'emmeans' package in R (Length et al. 2021).

Comparisons of phytoplankton community composition (beta diversity) were done using the on the Bray-Curtis similarity coefficient (Bray and Curtis, 1951), calculated at the genus level using square-root transformed biovolume measurements to represent abundance and downweight highly abundance taxa. Differences in community composition were visualized using non-metric multidimensional scaling (NMDS), and similarity matrices were calculated separately for each year. The statistical significance of sample clustering in NMDS was calculated using the analysis of similarity (ANOSIM).

4.3.2 Results

Changes in Biovolume Over Time in Response to Flow Pulses

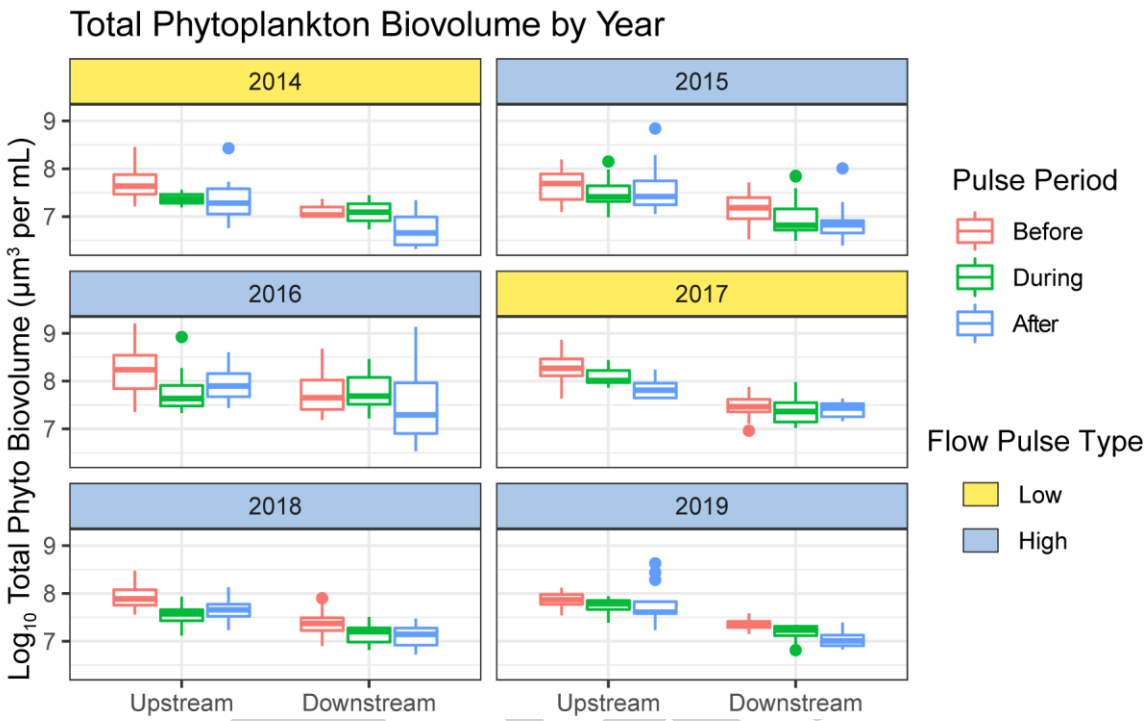

Figure 4-1. Box plot showing quartiles of total phytoplankton biovolume in the Upstream and Downstream regions of the study area before, during, and after the flow pulses.

Overall, the trend in total phytoplankton biovolume was consistent from year to year. As shown in Figure 4-1, the median biovolume was generally lower in downstream sites compared to upstream sites. Furthermore, most years saw generally lower median biovolumes in both upstream and downstream sites following the flow pulse. Some years, notably 2016, deviated somewhat from this trend as can be seen in the greater spread of quartiles in the box plots in Figure 4-1. Downstream stations LIB, RYI, and RVB, on average, saw an increase in phytoplankton biovolume following the flow pulse in that year (Figure 4-3). Other years, however, saw little to no change in the total overall biovolume downstream.

Our ANOVA test of log-transformed total phytoplankton biovolume found significant interactions by Year, Region, and Pulse Period. Overall, phytoplankton biovolume was significantly greater upstream compared to downstream (Table 4-1). Biovolume also varied significantly by year (Table 4-1), with 2017 having the greatest overall biovolume and 2014 the least.

Biovolume also varied significantly by pulse period, with the highest average amount in the Before phase and lower biovolume during and after the pulse. Biovolume during and after the pulse were not significantly different.

Table 4-1. Anova results of two-way interactive model of total phytoplankton biovolume by region, year, and flow pulse period.

Model Term	df (df res.)	F-statistic	p-value
Region	1 (545)	350.676	8.77e-61
Year	5 (545)	43.234	1.52e-37
Flow Pulse Period	2 (545)	31.825	8.47e-14
Region:Year	5 (545)	3.472	0.004
Year:Flow Pulse Period	10 (545)	0.631	0.788
Region:Flow Pulse Period	2 (545)	3.247	0.040

Pairwise comparisons using least-square means of two-way interactions found significant regional differences in phytoplankton biovolume at each phase of the flow pulse periods, with downstream biovolume being lower than upstream in each phase. This result matches the observations in Figure 4-1.

Table 4-2 shows the results of comparing estimated marginal means for phytoplankton biovolume (log base-10 transformed) before and after the flow pulse for each year of the study where this data was available. Four of the six years showed that the difference was not statistically significant, but 2016 and 2018 found a significant difference with each year having a lower biovolume after the flow action than before. This also matches the results seen in Figure 4-2.

Table 4-2. Table of estimated marginal means (least squares means) comparing log-transformed phytoplankton biovolume before and after flow pulses in a given year for the linear model.

Contrast	estimate	SE	df	t-ratio	p-value
Before – After (2014)	0.376670	0.1189	555	3.167	0.1340
Before – After (2015)	0.184966	0.0832	555	2.223	0.7375
Before – After (2016)	0.329157	0.0848	555	3.881	0.0138
Before – After (2017)	0.239659	0.0936	555	2.559	0.4859
Before – After (2018)	0.285513	0.0660	555	4.326	0.0024
Before – After (2019)	0.182401	0.0932	555	1.956	0.8883

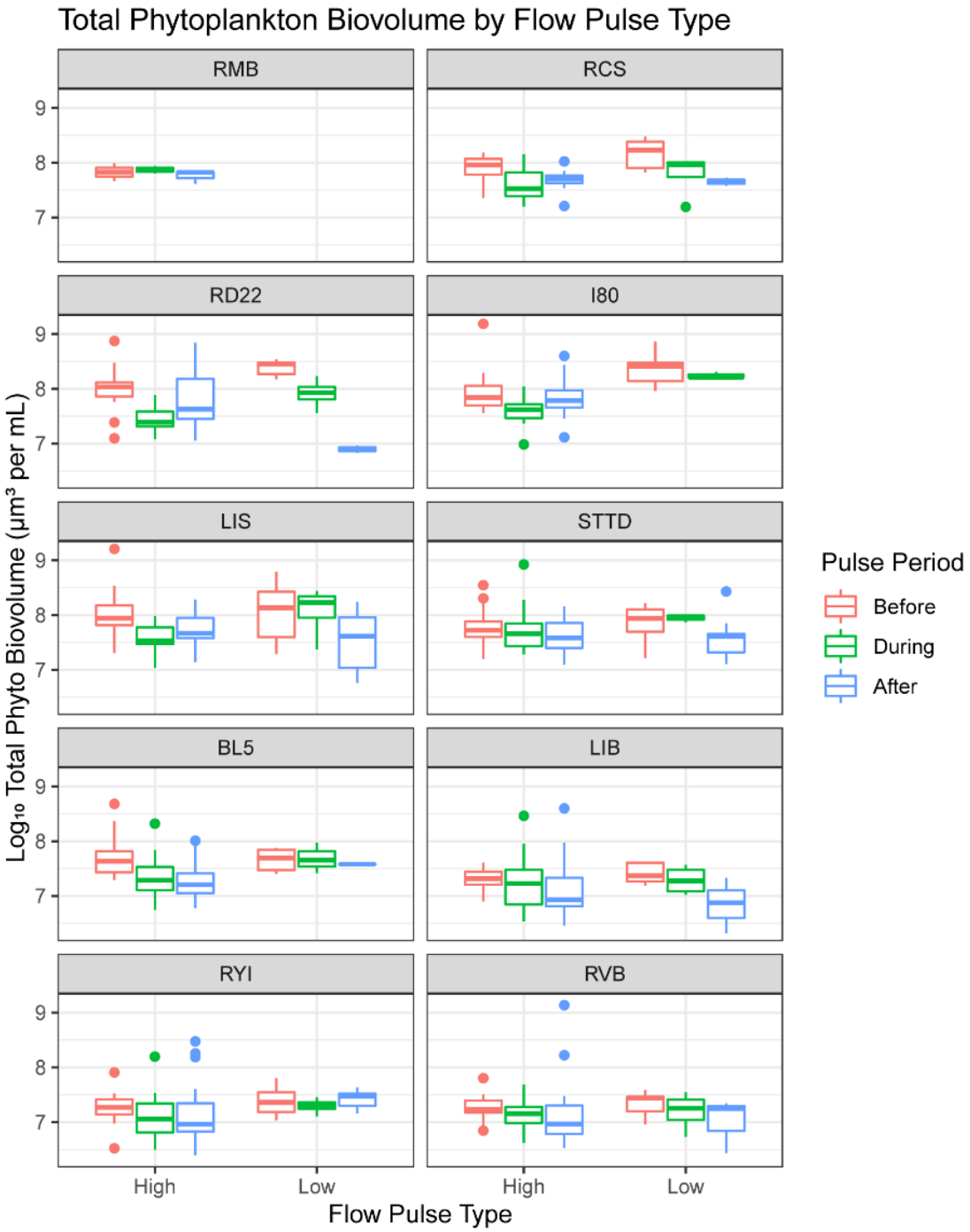

Figure 4-2. Box plot showing quartiles of total phytoplankton biovolume during high- and low-flow pulses at each station. No samples were collected at RMB during low pulse years.

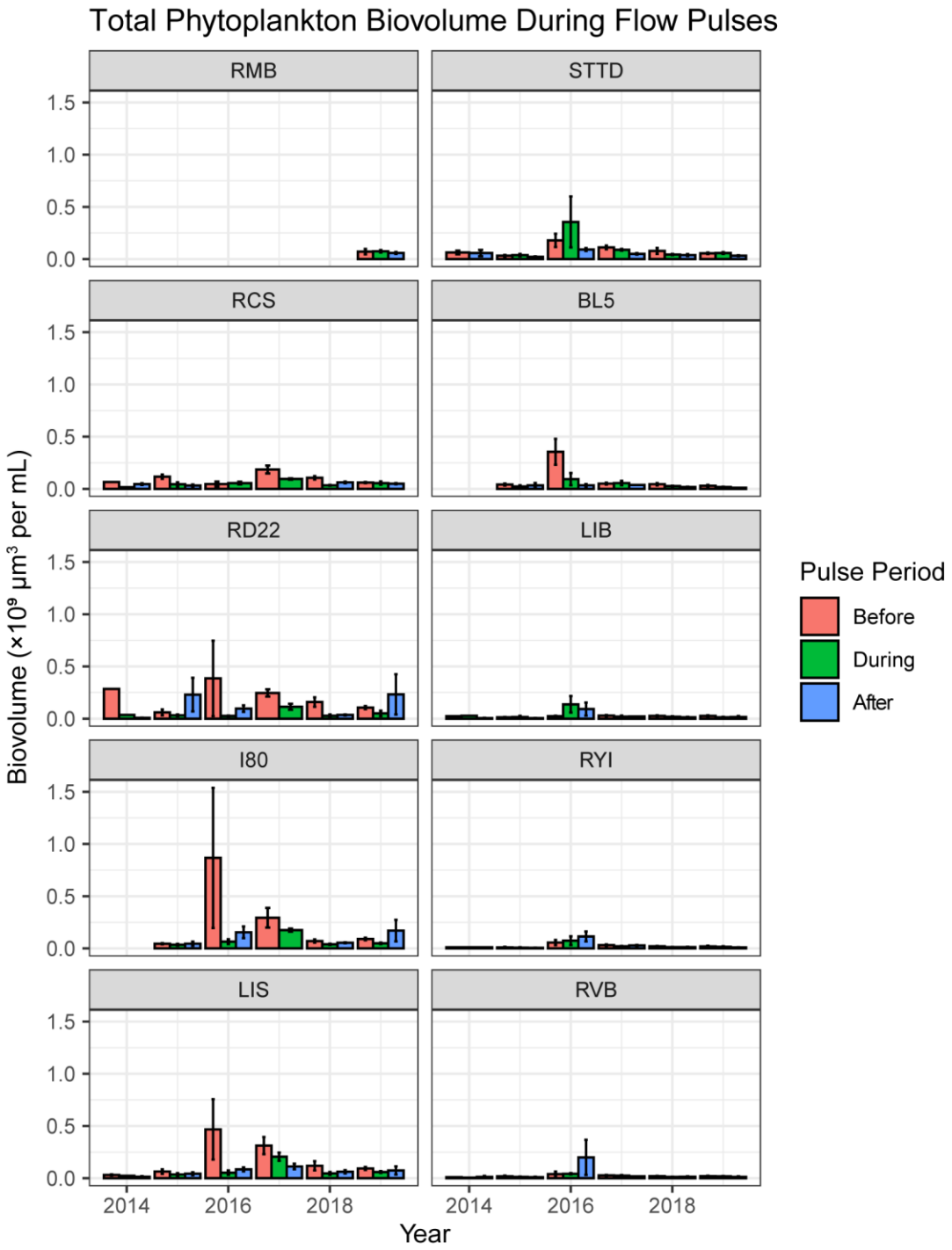

Figure 4-3. Mean phytoplankton biovolume at each station during each phase of the flow pulse (Before, during, after) over the years studied. Error bars represent standard error calculated for each group of samples.

Change in Taxonomic Composition in Response to Flow Actions Over Time

Figure 4-4 summarizes changes in the biovolume of specific functional groups (e.g., diatoms, blue-green algae, etc.) of phytoplankton in the North Delta. Figure 4-5 through Figure 4-10 show these trends in more detail for each year and station. Overall, blue-green algae were the most dominant functional group in both the upstream and downstream region for most years, representing 48—83% of the total biovolume upstream and 71—95% downstream for all years save 2016, when due to a bloom of the diatom *Aulacoseira* (Figure 4-11) they comprised only 20% of the downstream biovolume. Diatoms were the next most abundant group, although their abundance was more variable. Diatom biovolume comprised as little as 4-6% of the upstream biovolume in 2017 and 2018 and as much as 33% in 2014. Similarly, the biovolume of green algae, cryptophytes, and other functional groups varied from year to year and did not respond predictably to flow pulses.

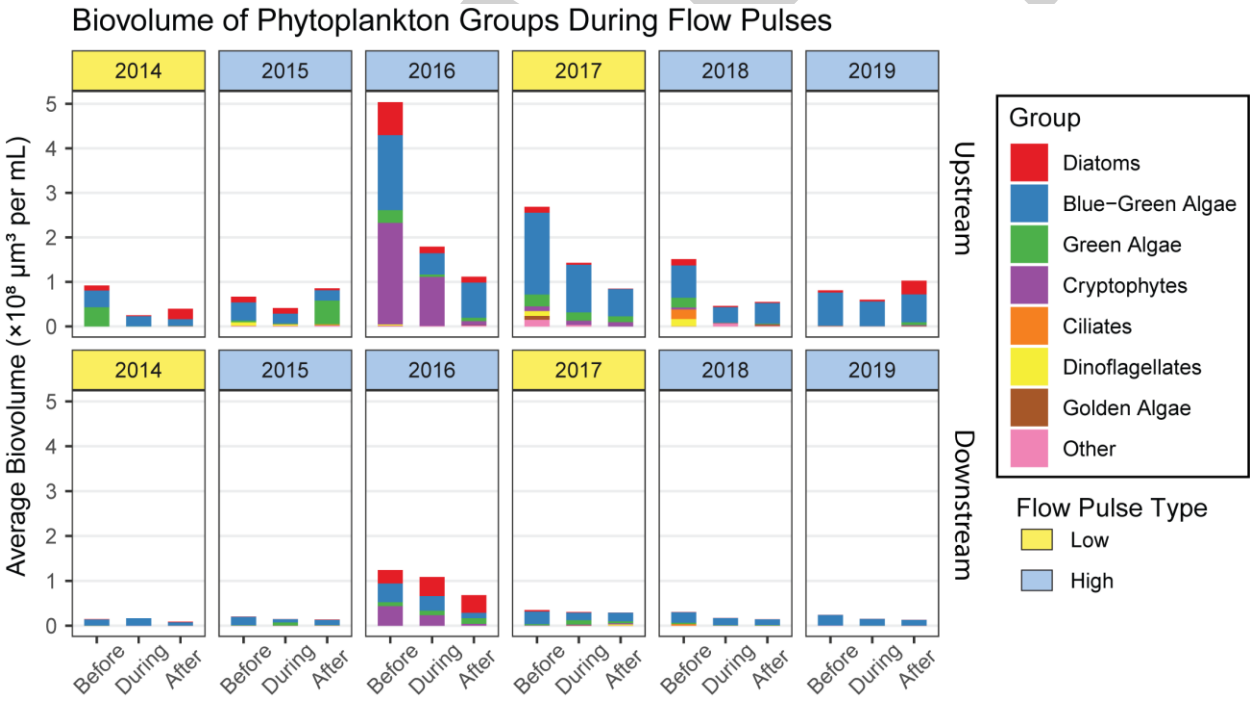

Figure 4-4. Average biovolume of phytoplankton functional groups detected before, during, and after flow pulses in the upstream and downstream regions for each year of the study.

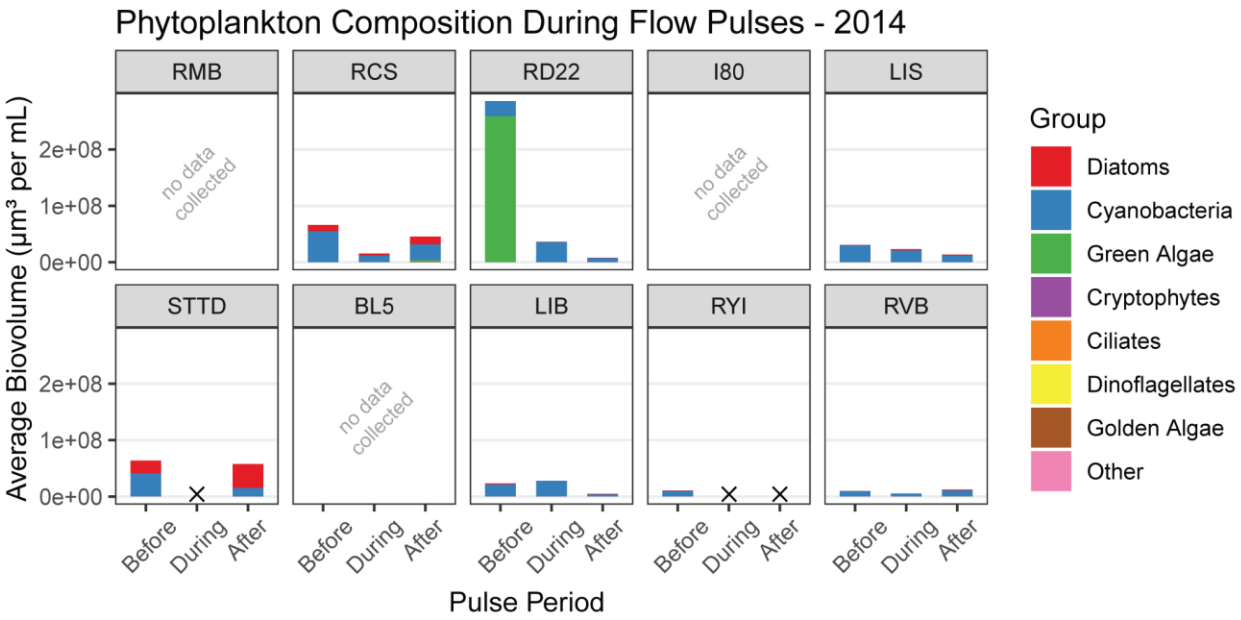

Figure 4-5. Average biovolume of phytoplankton functional groups detected at each station before, during, and after flow pulses in 2014. An x indicates that no samples were collected at that station during that period.

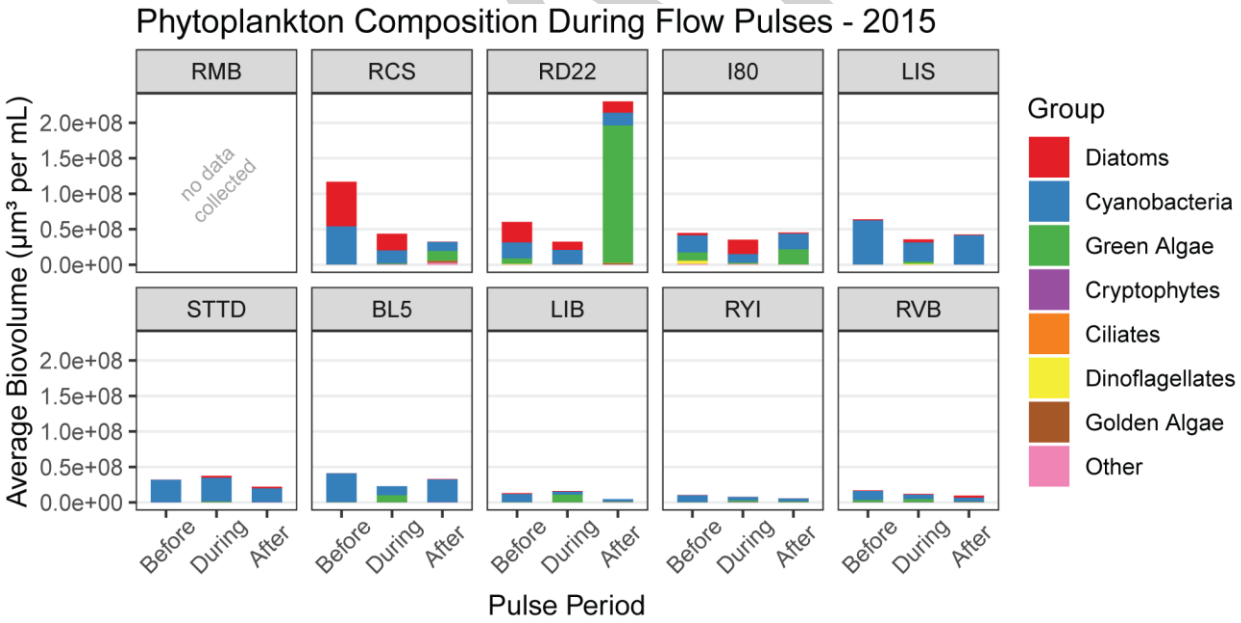

Figure 4-6. Average biovolume of phytoplankton functional groups detected at each station before, during, and after flow pulses in 2015.

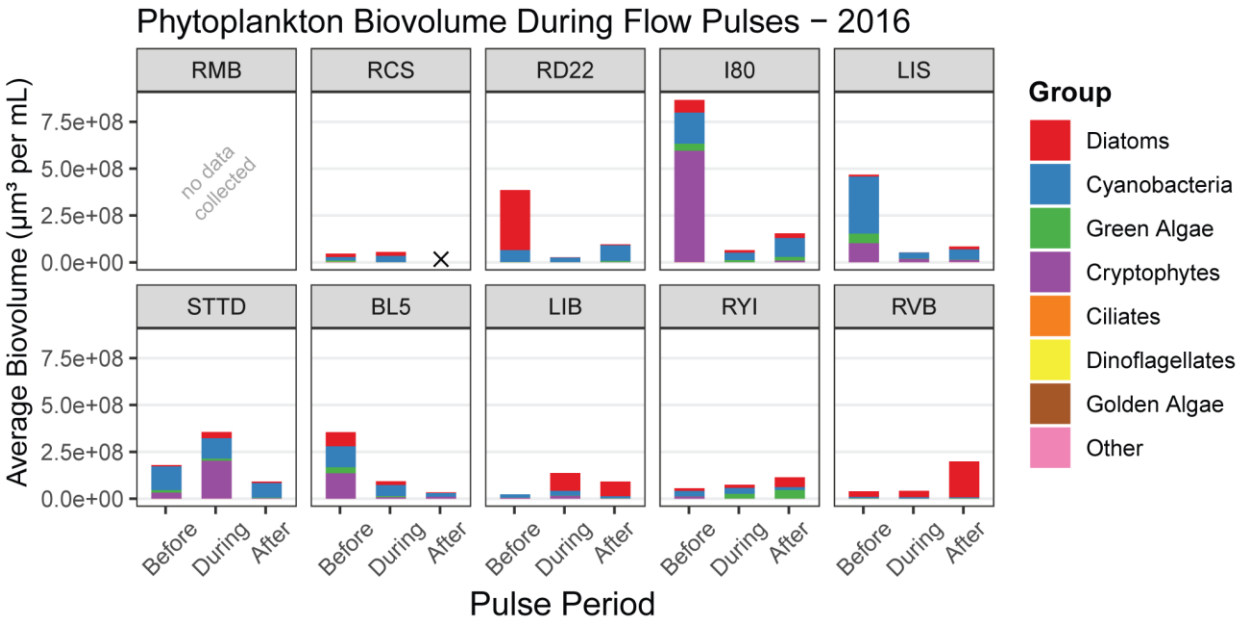

Figure 4-7. Average biovolume of phytoplankton functional groups detected at each station before, during, and after flow pulses in 2016. An x indicates that no samples were collected at that station during that period.

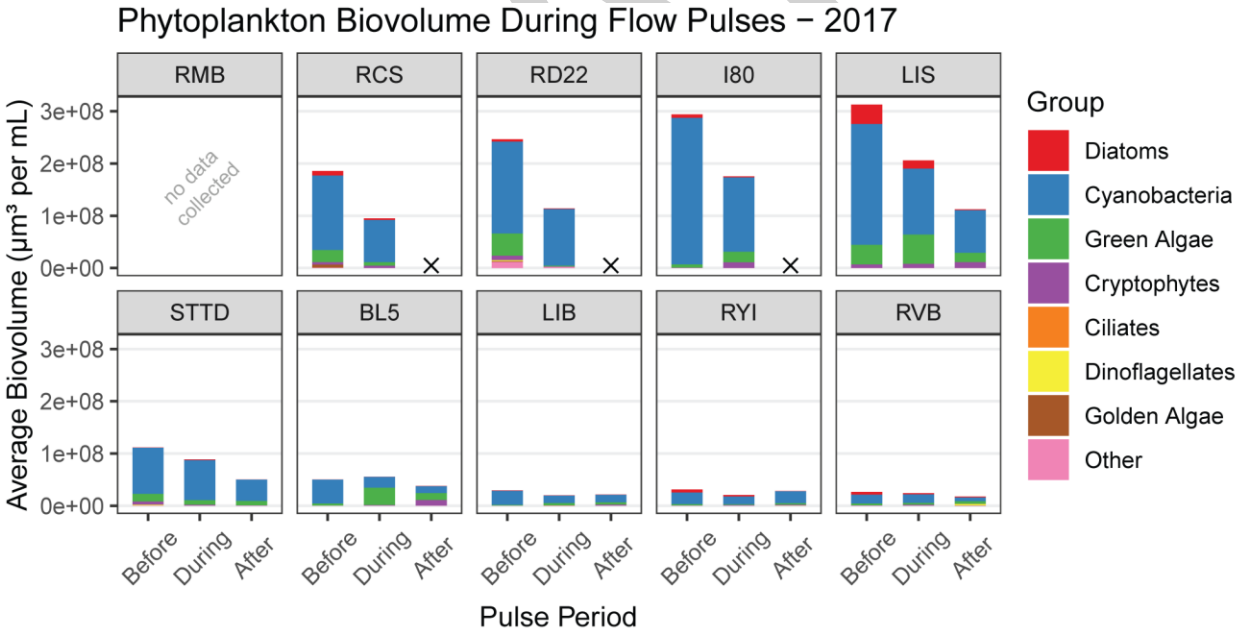

Figure 4-8. Average biovolume of phytoplankton functional groups detected at each station before, during, and after flow pulses in 2017. An x indicates that no samples were collected at that station during that period.

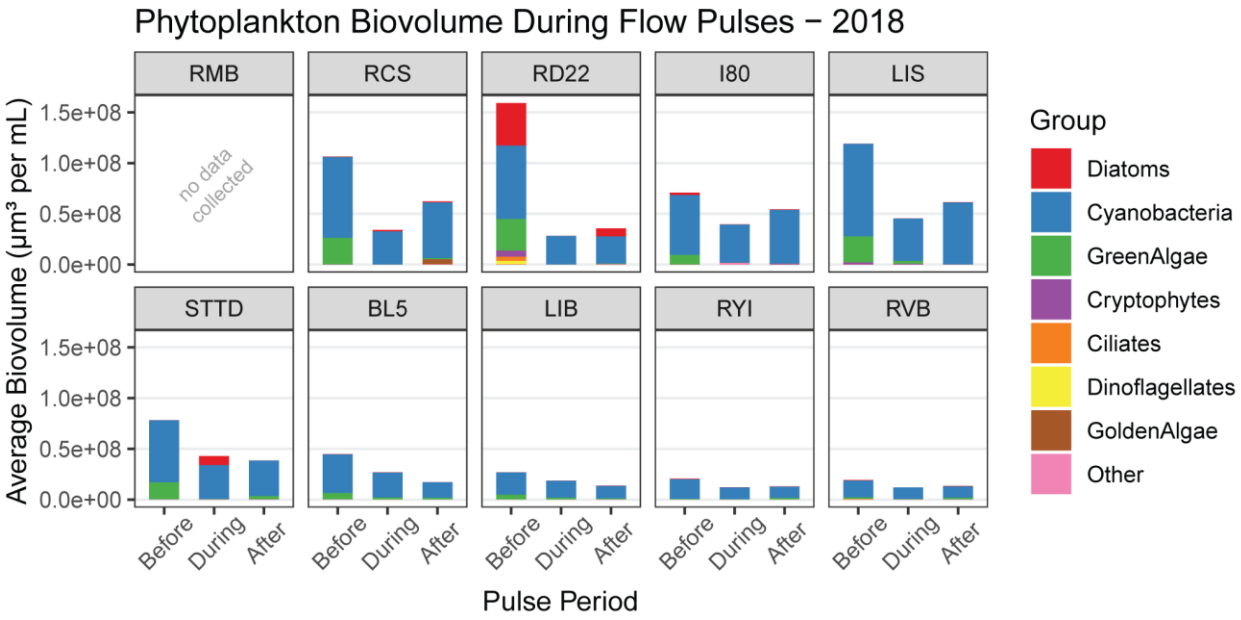

Figure 4-9. Average biovolume of phytoplankton functional groups detected at each station before, during, and after flow pulses in 2018.

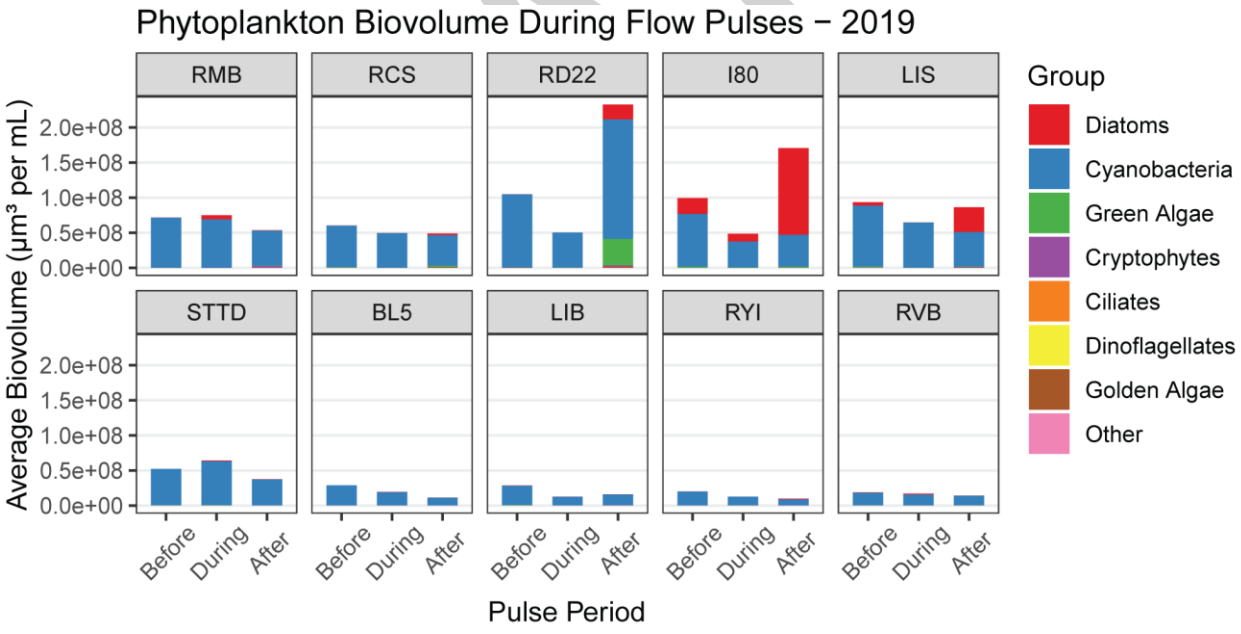

Figure 4-10. Average biovolume of phytoplankton functional groups detected at each station before, during, and after flow pulses in 2019.

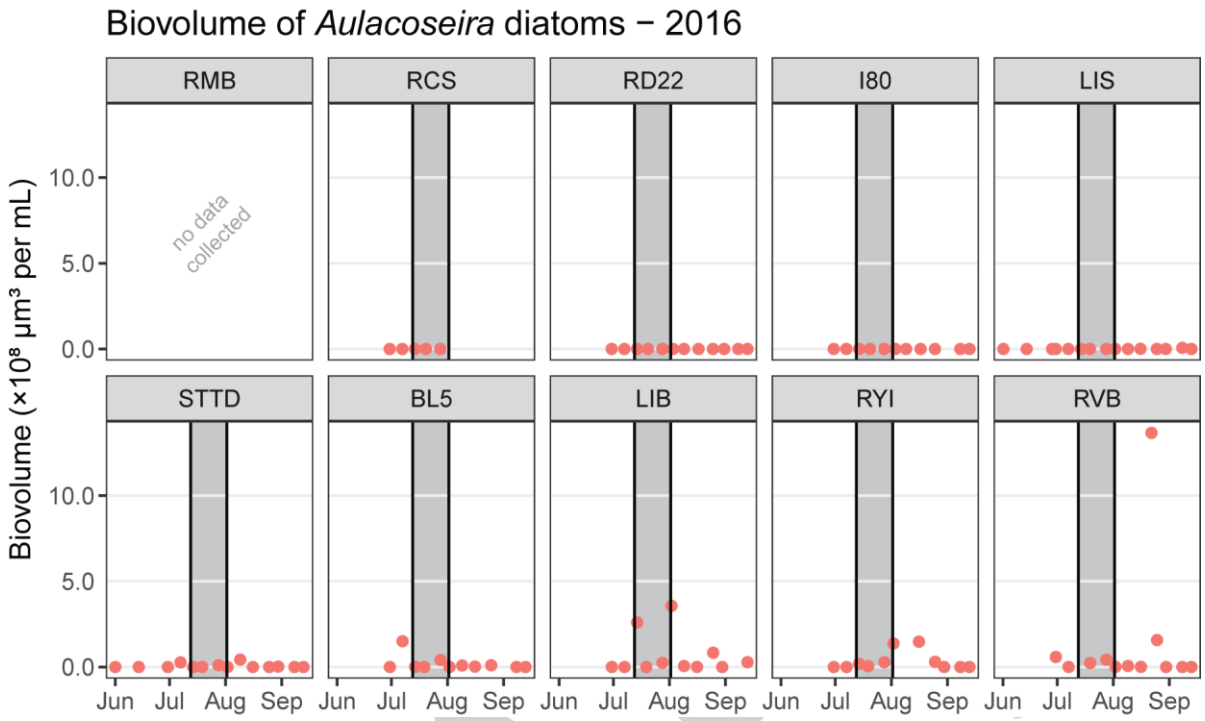

Figure 4-11. Total biovolume of the genus *Aulacoseira* at each station in the year 2016.

LCEFA Composition of Phytoplankton Communities

Compared to biovolume (Figure 4-5 – Figure 4-10, Figure 4-12), profiles of phytoplankton community composition based on LCEFA biomass are dominated by distinctly different groups of organisms (Figure 4-13). In most years, the total biovolume of both upstream and downstream sampling sites were dominated by cyanobacteria. When using estimates of LCEFA biomass for the five taxonomic groups listed in Figure 4-13 (diatoms, cyanobacteria, green algae, cryptophytes, and dinoflagellates), the profile of phytoplankton communities varies substantially. Instead of cyanobacteria, the phytoplankton community in the North Delta is dominated by diatoms, green algae, and cryptophytes.

The dominant group by LCEFA varied by both year and pulse phase, however apart from cyanobacteria the most dominant group by biovolume generally corresponded well with LCEFA biomass. Some taxa, dinoflagellates in particular, contribute a much greater share of total LCEFA biomass than biovolume (Figure 4-12, Figure 4-13). In 2015, for example, dinoflagellates contributed only 1.5% of the total biovolume, on average, in samples collected upstream before the flow pulse but represented an estimated 32.4% of the total LCEFA. Conversely, in 2019 cyanobacteria averaged 95-

97% of the total biovolume collected at downstream sites before, during and after the flow pulse but only 22-52% of the LCEFA.

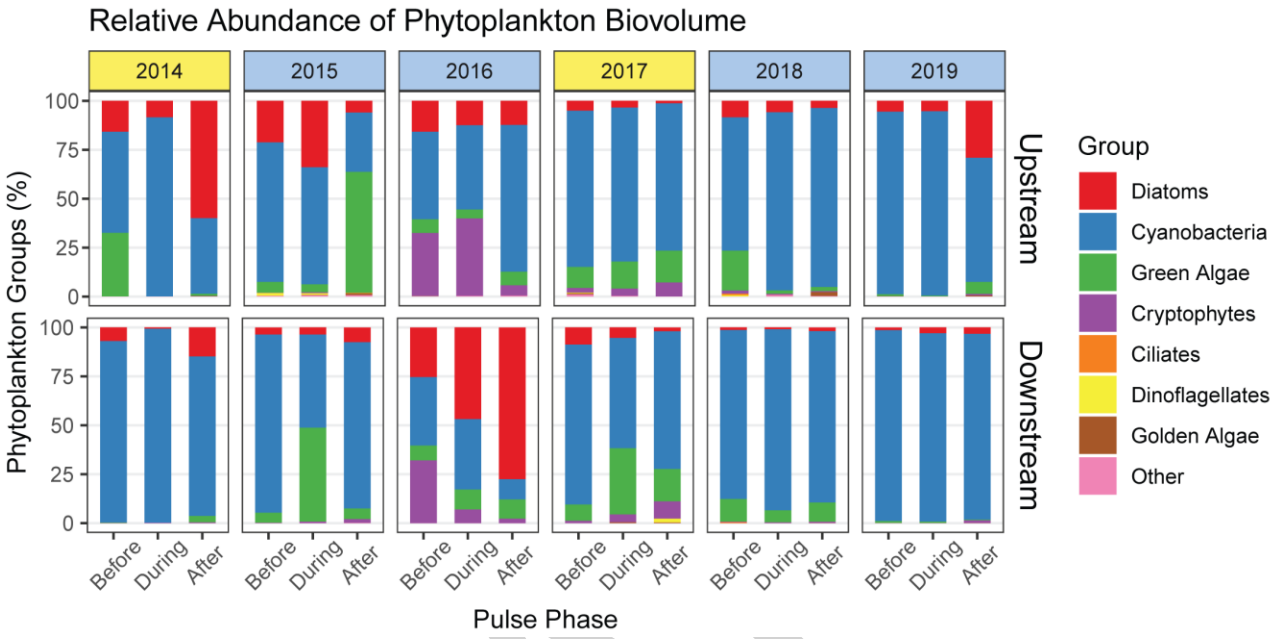

Figure 4-12. Relative abundance of phytoplankton group biovolume at Upstream and Downstream sites before, during, and after flow pulses.

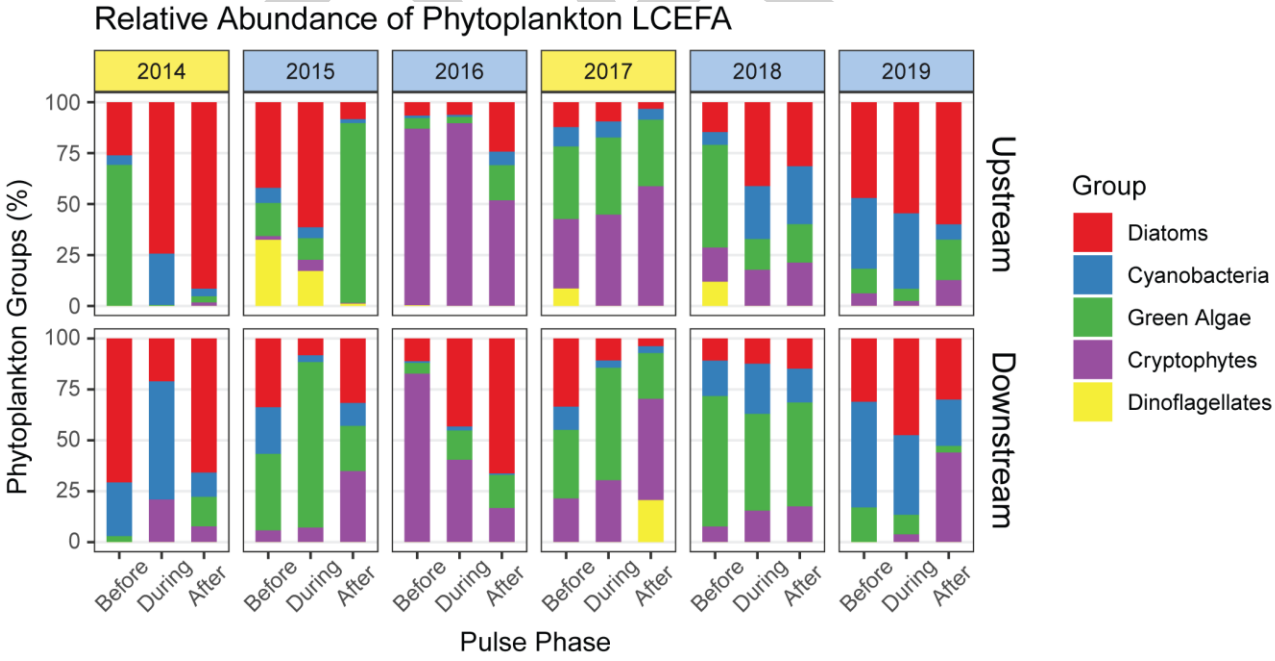

Figure 4-13. Relative contribution of long-chain essential fatty acids (LCEFA) to total biomass by phytoplankton group at upstream and downstream sites before, during, and after flow pulses.

Change in Phytoplankton Community Composition over Time

If phytoplankton in Yolo Bypass were transported downstream in the North Delta during flow pulses, we would expect the overall community composition in the downstream region to become more similar to the upstream region following the flow pulse. To test this, we plotted differences in community composition using non-metric multidimensional scaling based on the Bray-Curtis similarity coefficient.

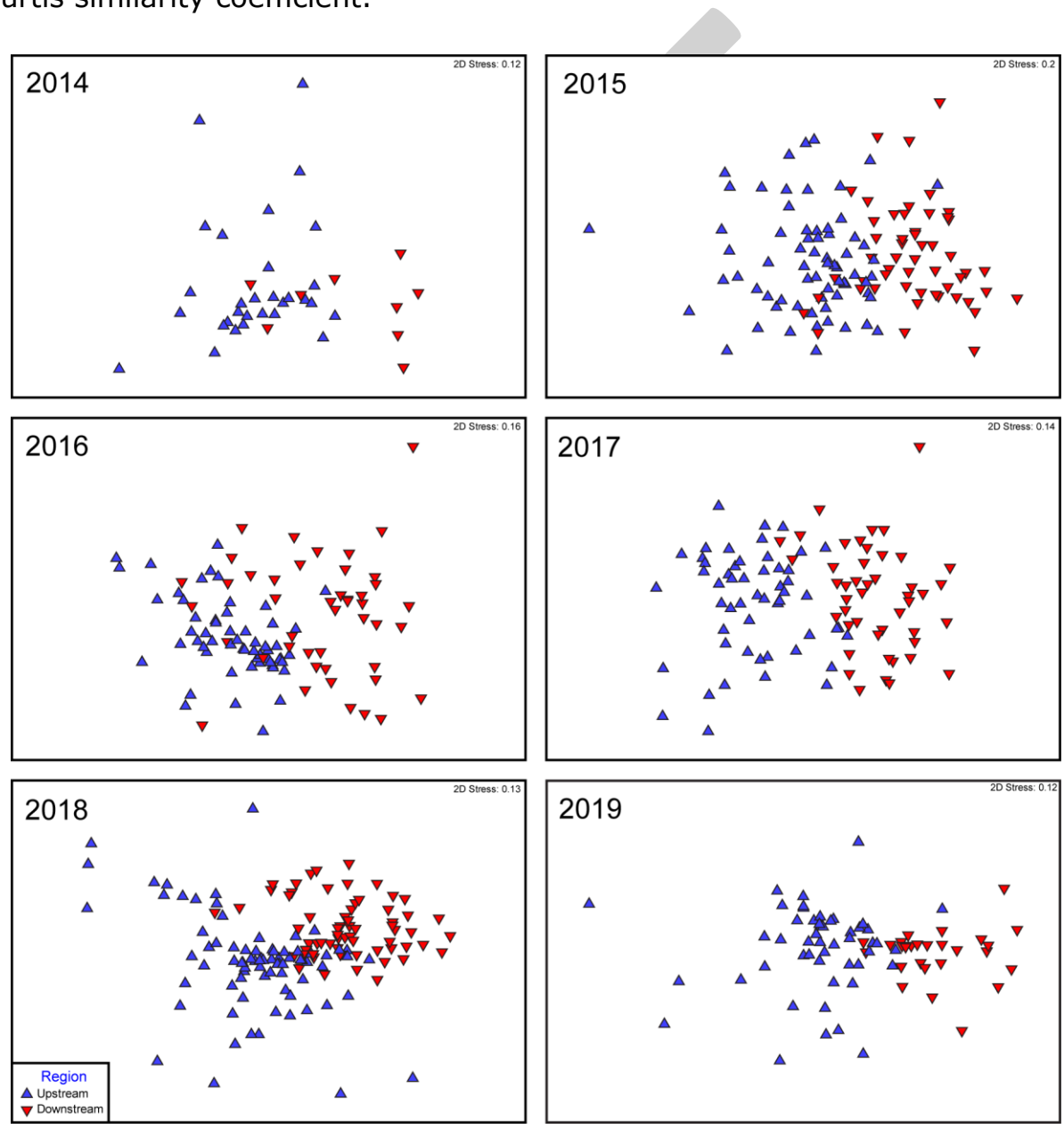

Figure 4-14. Non-metric multidimensional scaling plot of all phytoplankton samples colored by Region (Upstream, Downstream), faceted by year.

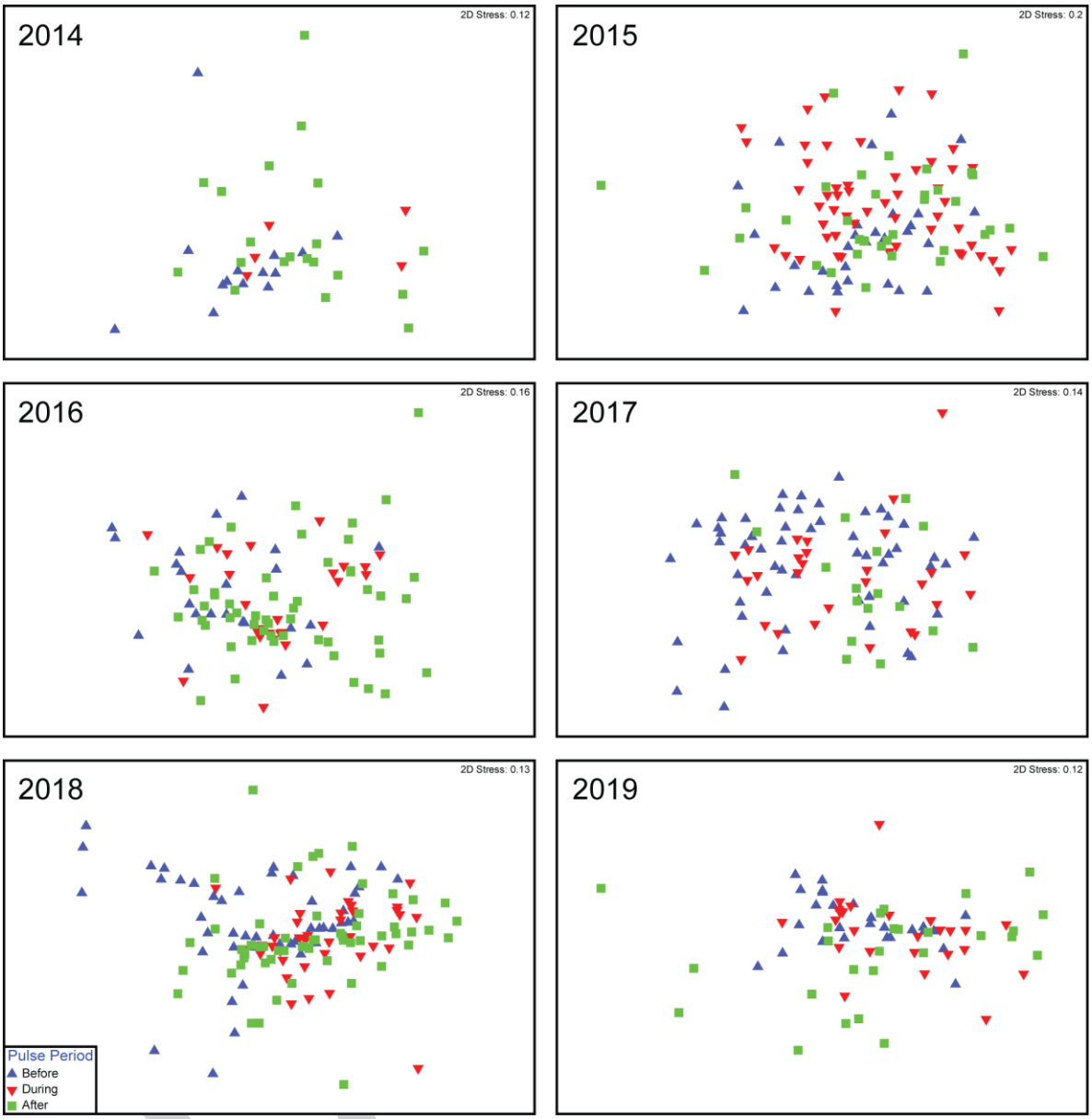

Figure 4-15. Non-metric multidimensional scaling plot of phytoplankton samples colored by flow pulse period (before, during, after), faceted by year.

Figure 4-15. shows that, taken as a whole, the community composition of phytoplankton in the North Delta is not significantly impacted by the flow pulse period (ANOSIM data not shown). Rather, as shown in Figure 4-14., differences in the overall community composition are primarily driven by region (upstream or downstream).

Table 4-3 below shows ANOSIM calculations indicating that differences between the upstream and downstream phytoplankton communities are

significantly different, although some years (e.g., 2014) show a less marked difference than others (2017, 2019).

Table 4-3. ANOSIM Results comparing upstream and downstream phytoplankton community composition for each year.

Year	Pulse	R	p-value
2014	Low	0.270	0.0160
2015	High	0.351	0.0001
2016	High	0.395	0.0001
2017	Low	0.534	0.0001
2018	High	0.354	0.0001
2019	High	0.466	0.0001

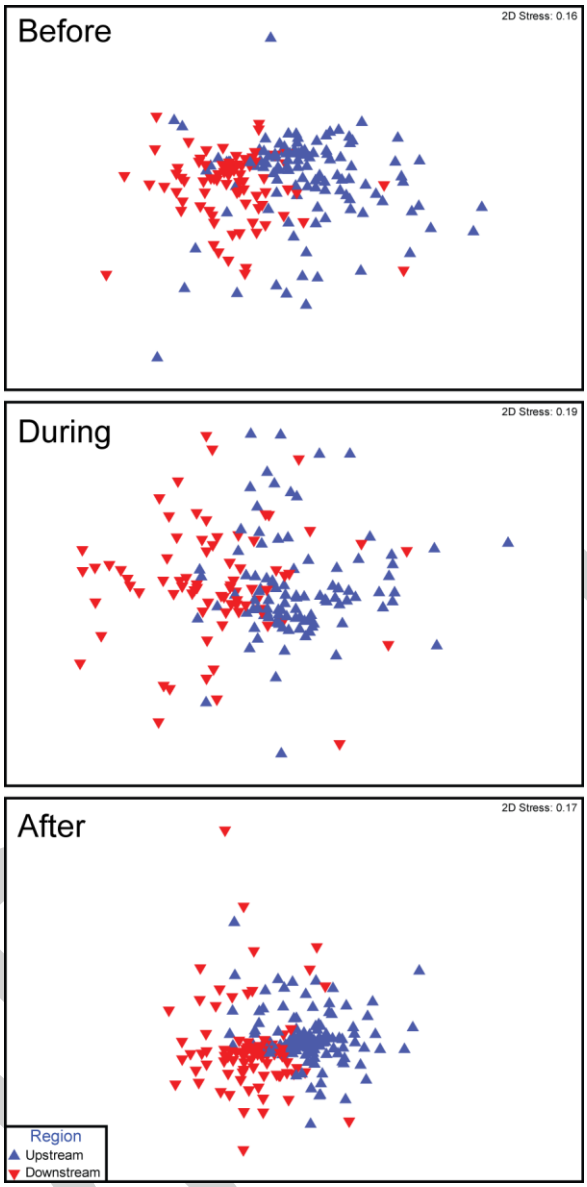

Figure 4-16. Non-metric multidimensional scaling plot of phytoplankton communities from all years (2014—2019) before, during, and after flow pulse, colored by region (upstream, downstream).

Figure 4-16 compares upstream and downstream samples of the phytoplankton community in the North Delta across all 10 sites before, during, and after the flow pulse. While the differences between the upstream and downstream sites remain subtle, this overall comparison shows that phytoplankton community composition diverges somewhat more (R_{ANOSIM} = 0.317) following flow pulses than before (R_{ANOSIM} = 0.246). Because the differences between region varied by year (

Table 4-3), however, we used ANOSIM to evaluate whether these differences were more significant within a specific year. Table 4-4 shows that this is indeed the case, although the magnitude of the difference and whether the upstream and downstream regions became more similar or more different varied by year. In the years 2014—2016, phytoplankton communities the two regions overlapped nearly entirely before the flow pulse (R_{ANOSIM} = 0.126—0.196) but diverged much more substantially afterwards (R_{ANOSIM} = 0.288—0.494). In 2018, the communities were distinct before the pulse (R_{ANOSIM} = 0.426) and remained so afterwards (R_{ANOSIM} = 0.552). Only in 2017 and 2019 were the upstream and downstream samples more similar following the flow pulse, and only in the former could they be said to be similar. Furthermore, few phytoplankton samples were collected upstream following the flow pulse in 2017 (Figure 4-8) so the statistical resolution of the ANOSIM comparison with downstream communities is limited.

Table 4-4. ANOSIM Results comparing upstream and downstream phytoplankton community composition for each year before, during, and after flow pulses.

		Before		During		After	
Year	**Pulse**	**R**	**p-value**	**R**	**p-value**	**R**	**p-value**
2014	Low	0.196	0.203	-	-	0.288	0.055
2015	High	0.126	0.033	0.539	0.0001	0.442	0.0001
2016	High	0.172	0.035	0.342	0.0005	0.494	0.0001
2017	Low	0.588	0.0001	0.723	0.0001	0.190	0.0014
2018	High	0.426	0.0001	0.359	0.0001	0.552	0.0001
2019	High	0.648	0.0001	0.691	0.0001	0.412	0.0007

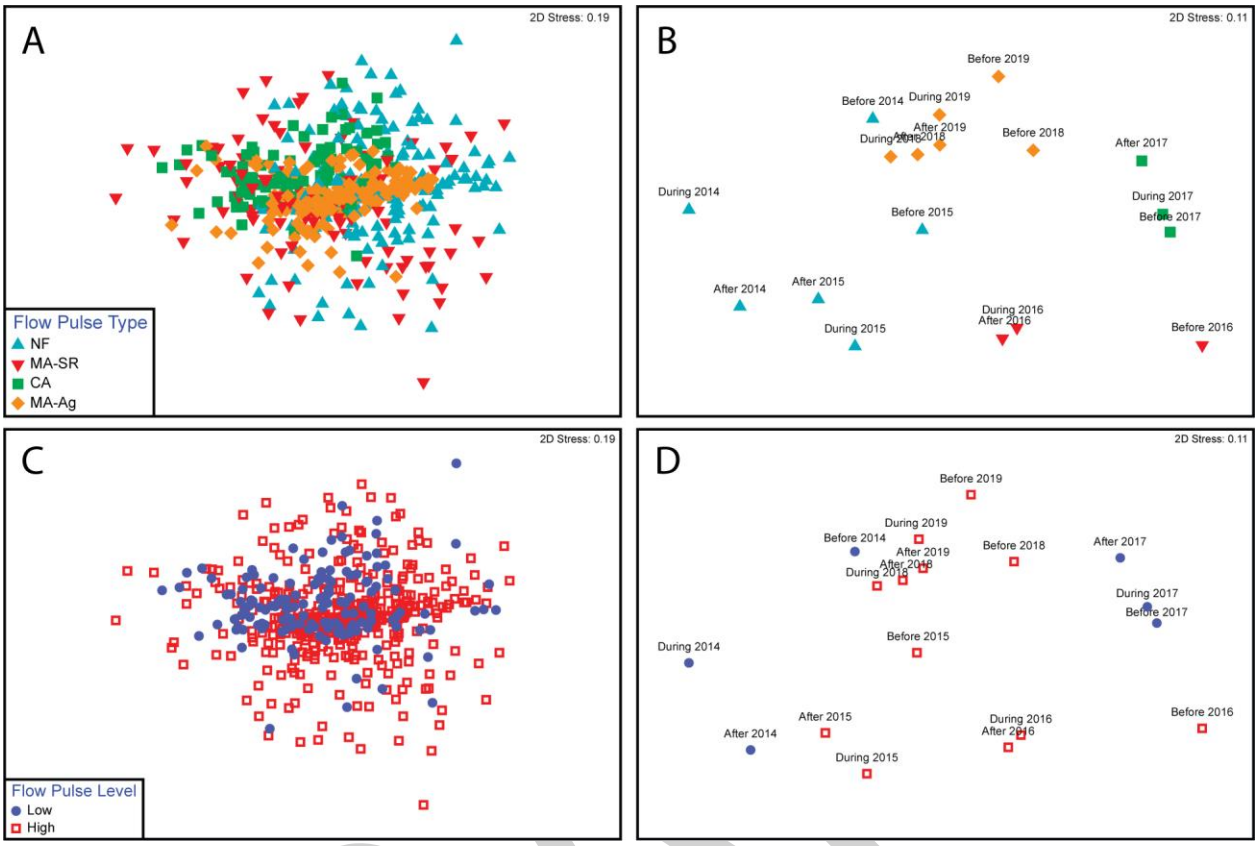

Figure 4-17. A) Non-metric multidimensional scaling plot showing differences between phytoplankton community samples for all years (2014—2019) and colored by flow pulse type (e.g., pulse events from non-managed flows (NF), construction actions (CA, also non-managed), or managed actions from the Sacramento River (MA-SR) or agriculture drainage (MA-Ag)) . B) Centroids of groups of phytoplankton communities (year × flow pulse type) calculated using PERMANOVA and colored by flow pulse type. C) Same plot as A, colored by flow pulse levels (high- or low-flow pulses). D) Same plot of as D, colored by flow pulse level (high or low).

Differences in Phytoplankton Community Composition by Flow Pulse Type

Calculating centroids for groups of phytoplankton samples shows how different flow pulse types can give rise to distinct communities. In the North Delta, these compositional differences are subtle: R_{ANOSIM} values for pairwise comparisons of samples based on flow pulse types are less than 0.250 for all comparisons save for the two types of managed pulses (Mg-Ag – MG-SR, R_{ANOSIM} = 0.384, p<0.0001) and the Mg-Ag pulse and non-managed (CA) (R_{ANOSIM} = 0.295, p<0.0001). While such values of R_{ANOSIM} indicate largely similar community compositions, this provides evidence that different types of flow pulse can influence the composition of phytoplankton communities in the North Delta. Comparison of high and low flow years, however, found no

significant compositional difference between low and high flow years (R_{ANOSIM} = 0.040, p-value = 0.06). Figure 4-17.D, however, based on the PERMANOVA centroids, shows that the two low-flow years are the most divergent communities from one another.

4.3.3 Discussion

Consistent with measures of chlorophyll (Chapter 3), the overall biovolume of phytoplankton was consistently higher in the upstream region of the North Delta compared to the downstream region over the study years 2014—2019. Phytoplankton biovolume was also significantly lower following the flow pulse than after, although seasonal effects may play a role in this trend (Jassby, 2008).

Changes in the downstream phytoplankton community brought about by flow pulses, however, were difficult to detect. Most years, the median biovolume downstream was in fact lower following the flow pulse than it had been previously (Figure 4-1). The one exception was the year 2016, when a bloom of diatoms from genus *Aulacoseira* were detected following the flow pulse at downstream stations LIB, RYI, and RVB (Figure 4-7). Whether or not this increase can be causally linked to the flow pulse, however, is difficult to say. As shown in Figure 4-11, *Aulacoseira* was present only at low levels in the upstream sampling stations at all three phases of that year's flow pulse.

The results also show that while recent trends are towards the numerical dominance of cyanobacteria in terms of biovolume, algal species like diatoms, cryptophytes, dinoflagellates, and other green algae still provide the bulk of key LCEFAs (Galloway and Winder, 2015). This shows that even small changes, such as the bloom of diatoms observed in 2016, can potentially have a significant impact on the nutrient quality of the base of the trophic pyramid.

Overall comparisons of phytoplankton communities in upstream and downstream regions show that, in 2016, differences in the composition of phytoplankton communities between these regions increased rather than decreased following the pulse (Table 4-4). Figure 4-17. further shows that the phytoplankton community in 2016, when Sacramento River water was used for the flow pulse, is generally distinct from other years of the study. Because phytoplankton data is only available for one year when Sacramento River

water was used for a managed action, it is difficult to ascertain whether this increase in diatom biovolume downstream is a direct result of the managed flow action.

4.4 Zooplankton

4.4.1 Methods

We sampled for zooplankton using a 150 µm mesh zooplankton net, with 0.5 m diameter mouth opening, attached to a 150 µm mesh cod end (Sea-Gear Corporation, Melbourne, FL, USA). A flow meter fitted with a low flow rotor (General Oceanics, Miami, FL, USA) was fastened to the net mouth opening. Zooplankton tows were conducted for 5 minutes along the surface either from a boat or kayak, depending on site. We fixed zooplankton samples in 10% formalin with rose Bengal. Zooplankton samples were then transferred to 8% Lugol's solution after a minimum of 2 weeks in fixative.

We sent zooplankton samples to BSA Environmental Inc., Beechwood, OH, for identification and quantification. Zooplankton samples were sub-sampled, and 200 to 250 individuals were counted per sample for mesozooplankton and then identified to at least the Order level, dependent on the taxon and life stage. Zooplankton count was calculated as follows: subsample count/[(subsample volume*number of subsamples)/total sample volume]. We then converted zooplankton counts to catch per unit effort (CPUE), a measure of density (Equation 4-1), by dividing zooplankton counts by the volume of water sampled (m3). Volume was determined by multiplying the net mouth area by the tow distance, where d is the net diameter and x = 57560, the low flow rotor meter constant.

$$\boldsymbol{CPUE = zooplankton\ count} / \left(\left(\boldsymbol{3.14 * (d)^2 / 4} \right) * \left(\frac{\boldsymbol{(EndMeter - StartMeter) * x}}{\boldsymbol{999999}} \right) \right)$$

Equation 4-1. Calculation of catch per unit effort (CPUE) for zooplankton. Zooplankton count is divided by the volume of water sampled (m3), which is calculated by multiplying the net mouth area by the distance, where d = diameter of the net and x=57560, the low flow rotor constant.

Data Analysis Methods

Statistical analyses were conducted in R (version 4.0.4; R Core Team 2020). To determine the effects of year, flow pulse period, and region on total zooplankton density we fit linear mixed-effects models using the 'lme4' package in R (Bates et al. 2021), selecting the best fit model using the 'AIC' (Akaike's Information Criterion) function from the 'stats' package in R. We then conducted a type 3 analysis of variance (ANOVA) using the 'Anova'

function from the car package in R (Fox et al. 2021), with the following model structure for total zooplankton density:

*log(total zooplankton cpue) ~ Region*Year + Year*FlowPulsePeriod + FlowPulsePeriod*Regions2 + (1|StationCode)*,

where year, flow pulse period and region are fixed effects and station a random effect. We subsequently ran post-hoc tests using the 'emmeans' package in R (Length et al. 2021), employing the 'Sidak' method for adjusted p-values. To evaluate responses in density of specific zooplankton functional groups, total zooplankton CPUE was subset for Calanoids, Cladocerans, Cyclopoids, and Microzooplankton and Nauplii. We then repeated the modeling procedures from above (ANOVA, post-hoc tests) separately for each functional group, using the same predictor variables, and density of each functional group as the response variable. Years 2011-2013 were removed from these analyses, as data for these years were incomplete either spatially, temporally, or both. In addition, we removed the stations SHR and RMB from these analyses, as they were either outside of the area of interest, or had too few samples, respectively, and removed macrozooplankton from our analyses, as our zooplankton sampling gear did not specifically target these taxa.

We also examined the effects of flow pulses on zooplankton community structure using non-metric multi-dimensional scaling (NMDS) and permutational multivariate analysis of variance (PERMANOVA). For NMDS, we summarized community similarity across sites using the Bray-Curtis similarity coefficient and then created NMDS plots using the 'vegan' package in R (Oksanen et al. 2020) to assess how community composition varied among flow pulse periods, high and low-flow pulses, years, and regions. We summarized zooplankton CPUE by functional group (Calanoids, Cladocerans, Cyclopoids, and Microzooplankton and Nauplii) for each site, subset the data by year, and then grouped the data by region and flow pulse period to create separate NMDS plots examining variation in community structure for each data grouping. The order Harpacticoid was removed from the data due to its overall rarity, likely due to inhabiting benthic and epibenthic habitats and not being targeted by our surface zooplankton tows, and because initial NMDS plots were skewed when this order was in the dataset. For PERMANOVA, we quantified CPUE for each functional group at each site: Calanoids, Cladocerans, Cyclopoids, and Microzooplankton and Nauplii and then summarized similarity in these CPUE values across sites using the Bray-Curtis similarity coefficient. The PERMANOVA model structure was as follows:

*Zooplankton community structure ~ Region*Year + Region*FlowPulsePeriod + Year*FlowPulsePeriod,*

where Region, Year, and FlowPulsePeriod, were fixed effect predictors and zooplankton community structure, measured as Bray-Curtis similarity, was the response variable. PERMANOVA was run using the 'ADONIS' package in R with 999 permutations of the model.

4.4.2 Results

Total Zooplankton

Type 3 ANOVA results of the AIC selected linear mixed-effects model showed that total zooplankton CPUE differed by year, and there was a significant interactive effect of region and year on CPUE (Table 4-5; Figure 4-18). However, the significant effects of the model terms Year and Year:Region were largely influenced by considerably higher CPUE in 2016 than in other years (Figure 4-18), and Sidak corrected post-hoc tests showed no significant effects of Region within a single year (Table 4-6). We also found no significant effect of flow pulse period or the interaction between Region and Flow Pulse Period or Year and Flow Pulse Period (Table 4-5).

Table 4-5. ANOVA results of two-way interactive mixed-effects model of total zooplankton CPUE ~ year, flow pulse period, and region.

Model Term	df (df res.)	F-statistic	p-value
Region	1 (24)	0.9724	0.3338
Year	5 (340)	10.9365	< 0.0001
Flow Pulse Period	2 (340)	0.4418	0.6432
Region:Year	5 (340)	6.6306	< 0.0001
Year:Flow Pulse Period	10 (340)	1.6791	0.0842
Region:Flow Pulse Period	2 (340)	2.6444	0.0725

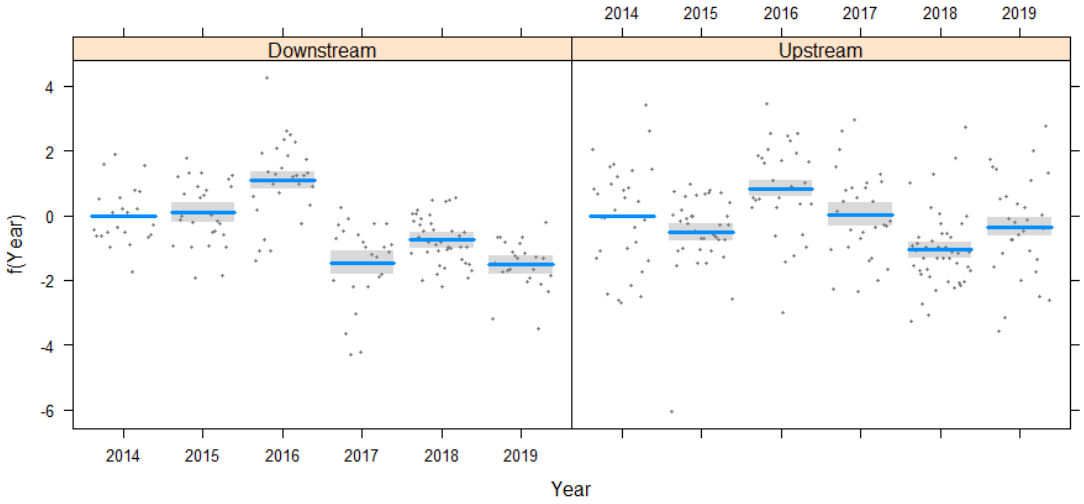

Figure 4-18. Median effect of Year by Region on total zooplankton CPUE (fitted line), partial residuals (points) and confidence intervals (shaded areas) relative to a reference point, median and variance of CPUE for Year 2014 (Visreg package in R).

Table 4-6. Post-hoc test of 'region' and 'year' interaction from two-way interactive mixed-effects model of total zooplankton CPUE ~ year, flow pulse period and region with the Sidak-Bonferroni method for adjusted p-values (non-significant contrasts omitted).

Contrast	estimate	SE	df	t-ratio	p-value
Downstream 2014 - Downstream 2016	-1.7916	0.3696	390	-4.847	0.0001
Downstream 2014 - Downstream 2019	1.5683	0.3708	390	4.229	0.0019
Upstream 2014 - Downstream 2016	-2.3640	0.5077	40	-4.656	0.0024
Upstream 2014 - Upstream 2016	-1.5276	0.3428	390	-4.456	0.0007
Downstream 2015 - Downstream 2016	-1.8844	0.3529	390	-5.340	< 0.0001
Downstream 2015 - Downstream 2019	1.4754	0.3494	390	4.223	0.0020
Upstream 2015 - Downstream 2016	-3.0534	0.4930	35	-6.194	< 0.0001
Upstream 2015 - Upstream 2016	-2.2170	0.3233	390	-6.857	< 0.0001
Upstream 2015 - Upstream 2017	-1.1173	0.3285	390	-3.401	0.0477
Downstream 2016 - Downstream 2017	2.8442	0.3752	390	7.581	< 0.0001
Downstream 2016 - Upstream 2017	1.9361	0.5131	41	3.773	0.0329
Downstream 2016 - Downstream 2018	2.1939	0.3212	391	6.830	< 0.0001
Downstream 2016 - Upstream 2018	3.0608	0.4864	33	6.292	< 0.0001
Downstream 2016 - Downstream 2019	3.3598	0.3629	390	9.259	< 0.0001
Downstream 2016 - Upstream 2019	2.7527	0.5014	38	5.490	0.0002
Upstream 2016 - Downstream 2017	2.0079	0.5166	43	3.887	0.0229
Upstream 2016 - Upstream 2018	2.2244	0.3133	390	7.100	< 0.0001
Upstream 2016 - Downstream 2019	2.5235	0.5105	40	4.943	0.0009
Upstream 2016 - Upstream 2019	1.9163	0.3389	390	5.655	< 0.0001
Upstream 2017 - Upstream 2018	1.1247	0.3162	390	3.557	0.0274
Downstream 2018 - Downstream 2019	1.1660	0.3196	391	3.648	0.0196

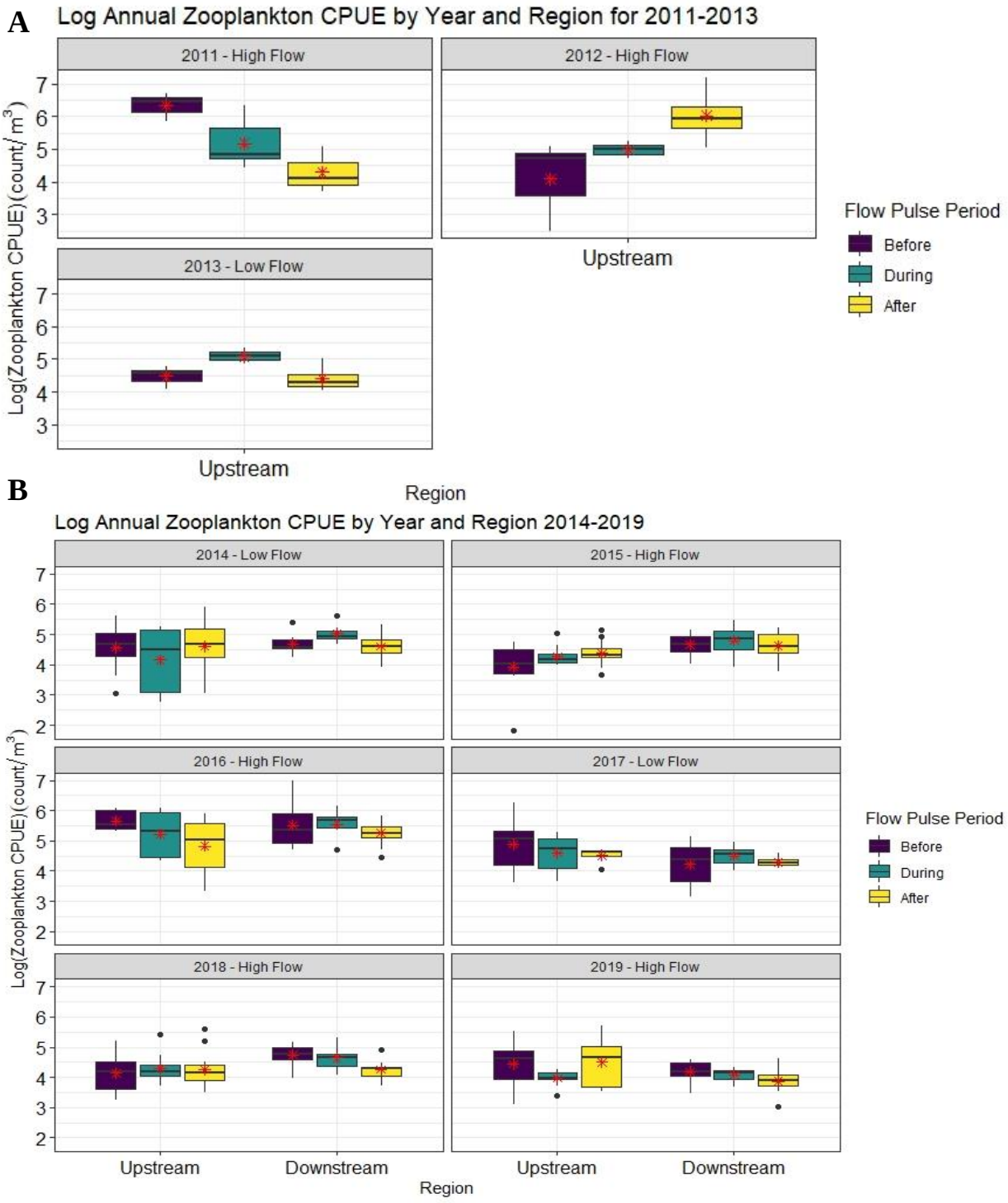

Figure 4-19. Boxplot quantiles of annual zooplankton CPUE for each year of flow pulses in the North Delta broken down by flow pulse period for A) early zooplankton data (2011-2013), which were only collected at STTD and at RCS (2012 only) in the upstream regions, and B) later zooplankton data (2014-2019) for which all sites were sampled in upstream and downstream regions. The red asterisks indicate average CPUE.

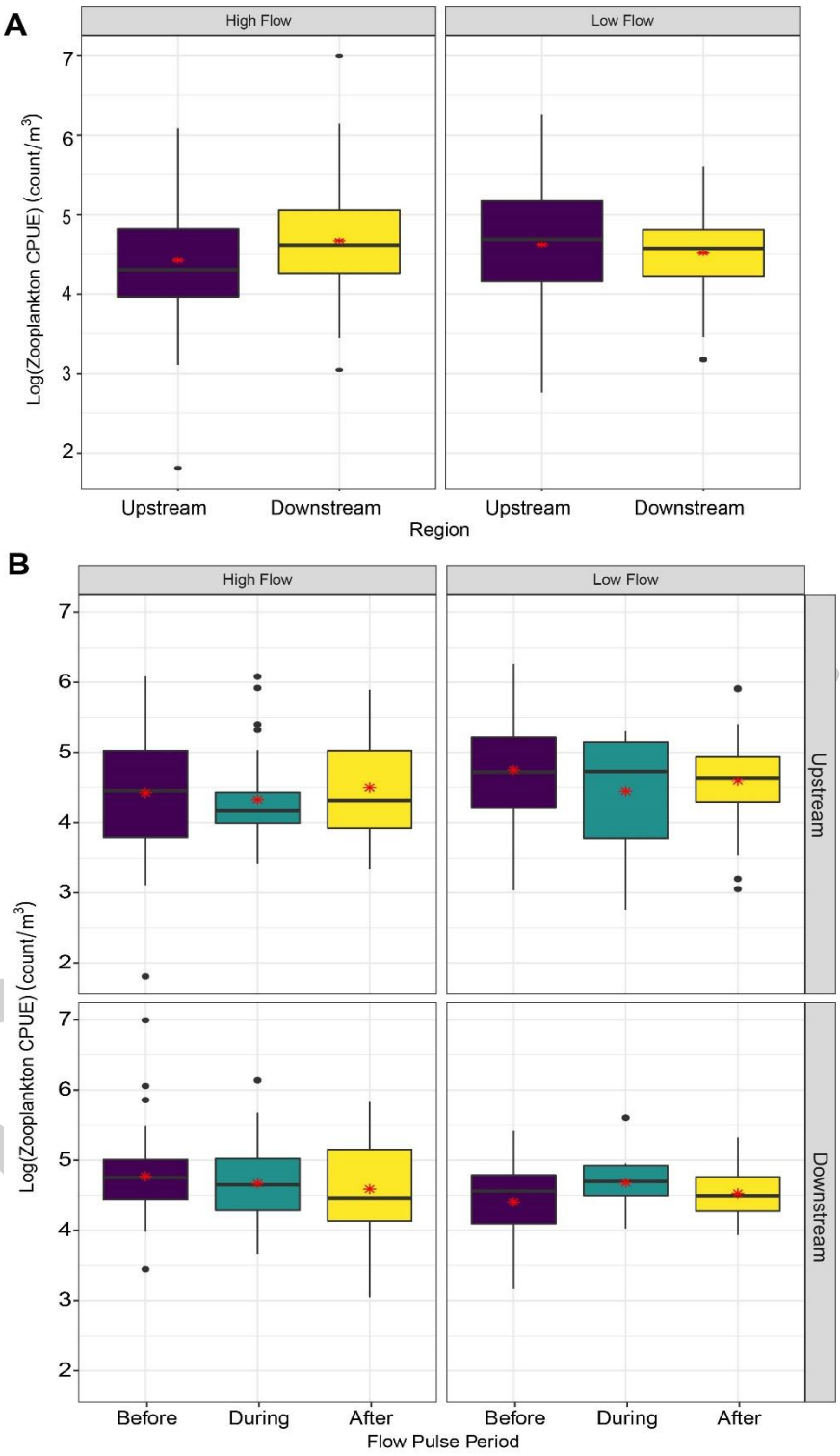

Figure 4-20. Boxplot quantiles of A) log annual zooplankton CPUE of high flow years (2015, 2016, 2018, and 2019) and low flow years (2014 and 2017) of flow pulses in the North Delta broken down by region and B) log annual zooplankton CPUE by flow pulse type and region further decomposed by flow pulse period. The red asterisks indicate average CPUE.

Individual Zooplankton Functional Groups

Cyclopoid copepods

Cyclopoid copepod CPUE differed by region and flow pulse period (p=0.0052 and p=0.0503, respectively), and there were significant interactive effects of region and year on CPUE (p=0.0066), and flow pulse period and year on CPUE (p=0.005; see Table 4-7). Post hoc analyses of significant main effects showed that overall, cyclopoid CPUE was higher in the upstream region (p=0.0022), and higher both during and after the flow pulse period than before (p=0.0003 and p=0.0024, respectively; see results of interaction effects below, and Appendices Tables 22-23). Post hoc analysis of the model interaction of region and year showed that cyclopoid CPUE was significantly higher upstream in 2017 (p=0.0107) and 2019 (p=0.0031), and marginally significant upstream in 2016 (p=0.0599; see Appendix E Table 24). Also, there were often significant differences in cyclopoid CPUE within a given region between years, but most of this was attributed to higher cyclopoid CPUE in 2016 (Appendix E Table 24). Post hoc analysis of the model interaction of flow pulse period and year showed that cyclopoid CPUE was significantly higher during than before the flow pulse period in 2015 (p=0.0100), but this was the only significant result supporting an effect of flow pulse period within the same year. Significant effects across years for a given flow pulse period were attributed to higher overall CPUE in 2016 (Appendix Table 25).

Calanoid copepods

Calanoid copepod CPUE differed by region, year, and flow pulse period (p=0.0222, p=0.0017, and p=0.0392, respectively), and there were significant interactive effects of region and year on CPUE (p=<0.0001), and flow pulse period and region on CPUE (p=0.0023; see Table 4-7). Post hoc analyses of significant main effects showed that overall, calanoid CPUE was higher in the downstream region (p=0.0316), that 2018 and 2019 generally had lower calanoid CPUE than other years, and that calanoid CPUE was higher before the flow pulse than after (p=0.0320; see Appendix E Tables 26-28). Post hoc analysis of the model interaction of flow pulse period and region showed that calanoid CPUE was significantly higher upstream before the flow pulse period than during the flow pulse period (p=0.0232; Appendix E Table 29). Post hoc analysis of the model interaction of region and year showed no significant differences within a single year between regions,

however, there were significant differences in calanoid CPUE within a given region across years (see Appendix E Table 30).

Cladocerans

Cladocera CPUE differed by region and year (p=0.0131, and p=<0.0001, respectively), and there were significant interactive effects of region and year on CPUE (p=0.0003), and flow pulse period and year (p=<0.0001; see Table 4-7). Post hoc analyses of significant main effects showed that overall, cladoceran CPUE was higher in the upstream region (p=0.0035), and cladoceran CPUE in 2016 was significantly higher than all of the other years (see Appendix E Tables 31-32, respectively). Post hoc analysis of the model interaction of year and region showed that cladoceran CPUE was significantly higher upstream in 2017 (p=0.0021) and 2019 (p=0.0044; see Appendix E Table 33). Also, there were significant differences in cladoceran CPUE within a given region across years, but again, most of this was attributed to higher cladoceran CPUE in 2016 (Appendix E Table 33). Post hoc analysis of the model interaction of flow pulse period and year showed significantly higher cladoceran CPUE before the flow pulse period than after in 2016 (p=<0.0001, Appendix E Table 34). Significant effects across years for a given flow pulse period were attributed to higher overall CPUE in 2016 (see Appendix E Table 34).

Microzooplankton and nauplii

Microzooplankton and nauplii CPUE differed by year (p=<0.0001), and there were significant interactive effects of region and year (p=<0.0001) and flow pulse period and year (p=0.0165; see Table 4-7) on CPUE. Post hoc analyses of significant main effects showed that overall, microzooplankton and nauplii CPUE was significantly higher in 2016 than all other years (p=<0.0001 (all years); Appendix E Table 35), whereas microzooplankton and nauplii CPUE in 2019 was significantly lower than most other years (see Appendix E Table 35). Model interactions of flow pulse period and year showed significant differences in microzooplankton and nauplii CPUE across years for a given flow pulse period, with most of these differences attributed to higher overall CPUE in 2016 (see Appendix E Table 36). Interactions between year and region showed that microzooplankton and nauplii CPUE was significantly higher upstream in 2019 (p=0.0382; Appendix E Table 37). There were also significant differences in microzooplankton and nauplii CPUE within a given region across years (Appendix E Table 37).

Table 4-7. ANOVA results of two-way interactive mixed-effects models for individual zooplankton functional group CPUE ~ year, flow pulse period, and region.

Taxa Group	Model Term	df (df res.)	F-statistic	p-value
Cyclopoid	Region	1 (32.9)	8.9729	0.0052
	Year	5 (317)	1.0725	0.3755
	Flow Pulse Period	2 (316)	3.0185	0.0503
	Region:Year	5 (317)	3.2838	0.0066
	Year:Flow Pulse Period	10 (317)	2.5860	0.0050
	Region:Flow Pulse Period	2 (317)	0.2313	0.7936
Calanoid	Region	1 (8.89)	7.6392	0.0222
	Year	5 (330)	3.9468	0.0017
	Flow Pulse Period	2 (330)	3.2706	0.0392
	Region:Year	5 (330)	6.2423	< 0.0001
	Year:Flow Pulse Period	10 (330)	1.7298	0.0730
	Region:Flow Pulse Period	2 (330)	6.1718	0.0023
Cladoceran	Region	1 (27.9)	7.0173	0.0131
	Year	5 (335)	8.1127	< 0.0001
	Flow Pulse Period	2 (334)	1.4408	0.2382
	Region:Year	5 (335)	4.8295	0.0003
	Year:Flow Pulse Period	10 (334)	5.3543	< 0.0001
	Region:Flow Pulse Period	2 (334)	0.2811	0.7552
Microzooplankton and nauplii	Region	1 (20.3)	3.3659	0.0813
	Year	5 (341)	19.707	< 0.0001
	Flow Pulse Period	2 (340)	0.1360	0.8729
	Region:Year	5 (340)	13.528	< 0.0001
	Year:Flow Pulse Period	10 (340)	2.2182	0.0165
	Region:Flow Pulse Period	2 (340)	0.8794	0.4160

Zooplankton Community Structure

PERMANOVA results showed that year explained the largest amount of variance (R^2 = 0.155) in the zooplankton community structure (Table 4-8). We also found region, flow pulse period, and interactions to be significant, though corresponding R^2 values were not as great as year.

Table 4-8. Summary of PERMANOVA results on zooplankton community structure (Bray-Curtis similarity).

Predictor	Df	F.Model	R^2	P-value
Region	1	36.2	0.0684	0.001
Year	5	16.5	0.155	0.001
Flow Pulse Period	2	4.21	0.0159	0.001
Region:Year	5	6.1	0.0576	0.001
Region:Flow Pulse Period	2	3.07	0.0116	0.001
Year: Flow Pulse Period	10	1.91	0.0361	0.001

Qualitative patterns show that average total zooplankton CPUE was greater downstream during high flow years vs. low flow years (Figure 4-20A), however, this seemed to be driven by first, greater zooplankton downstream before the pulses occurred in 2015 and 2018 compared to upstream (Figure 4-19), and second, higher overall calanoid abundance in the downstream region (Figure 4-20, calanoid CPUE ANOVA results Table 4-7). Certain taxonomic groups increased during and/or after flow pulses in some years at some upstream sites, including calanoids (in 2015), cyclopoids (in 2018), and microzooplankton and nauplii (in 2019) (Figure 4-21), but these patterns were not observed at downstream sites (Figure 4-21), and were not apparent in overall comparative assessments of low- and high-flow pulses across sites and years (Figure 4-23 and Figure 4-24). For example, on average, calanoids decreased downstream after high-flow pulses, while their average density appeared unaffected by low-flow pulses (Figure 4-23A). In contrast, cyclopoid density upstream showed positive trends during high-flow pulses but remained unaffected during low-flow pulses, whereas cyclopoid density subtly increased downstream in both high- and low-flow pulses, suggesting potential mediating effects of seasonality (Figure 4-23B). Cladocera and Microzooplankton and nauplii showed similar neutral trends to high- and low-flow pulses across regions and pulse periods (Figure 4-24).

Microzooplankton and nauplii comprised the greatest abundance of identified zooplankton most years, particularly at upstream sites, whereas calanoids comprised the greatest abundance downstream overall and upstream during dry years (2013, 2014, 2015) (Figure 4-21). Qualitative assessments of the composition of zooplankton taxa by percentage of the total community abundance also show rotifers comprised a large proportion of the total zooplankton CPUE upstream, while calanoid copepodids were often the dominant taxonomic group downstream (Figure 4-25). There were also subtle fluctuations in composition across flow pulse periods and years (Figure 4-26), but composition overall largely differed by region (Figure 4-27). For example, in 2016 downstream, during and after the high-flow pulse, copepod nauplii increased from roughly 15% to 25-40% of the total community abundance, and in 2019 copepod nauplii were only present after the managed flow pulse (Figure 4-25). Additionally, during high-flow pulses (managed flow actions) in 2018 and 2019, additional species were detected that were not present before or after the flow pulse (Figure 4-25), suggesting potential transport of these taxa from far upstream habitats or hatching of resting eggs.

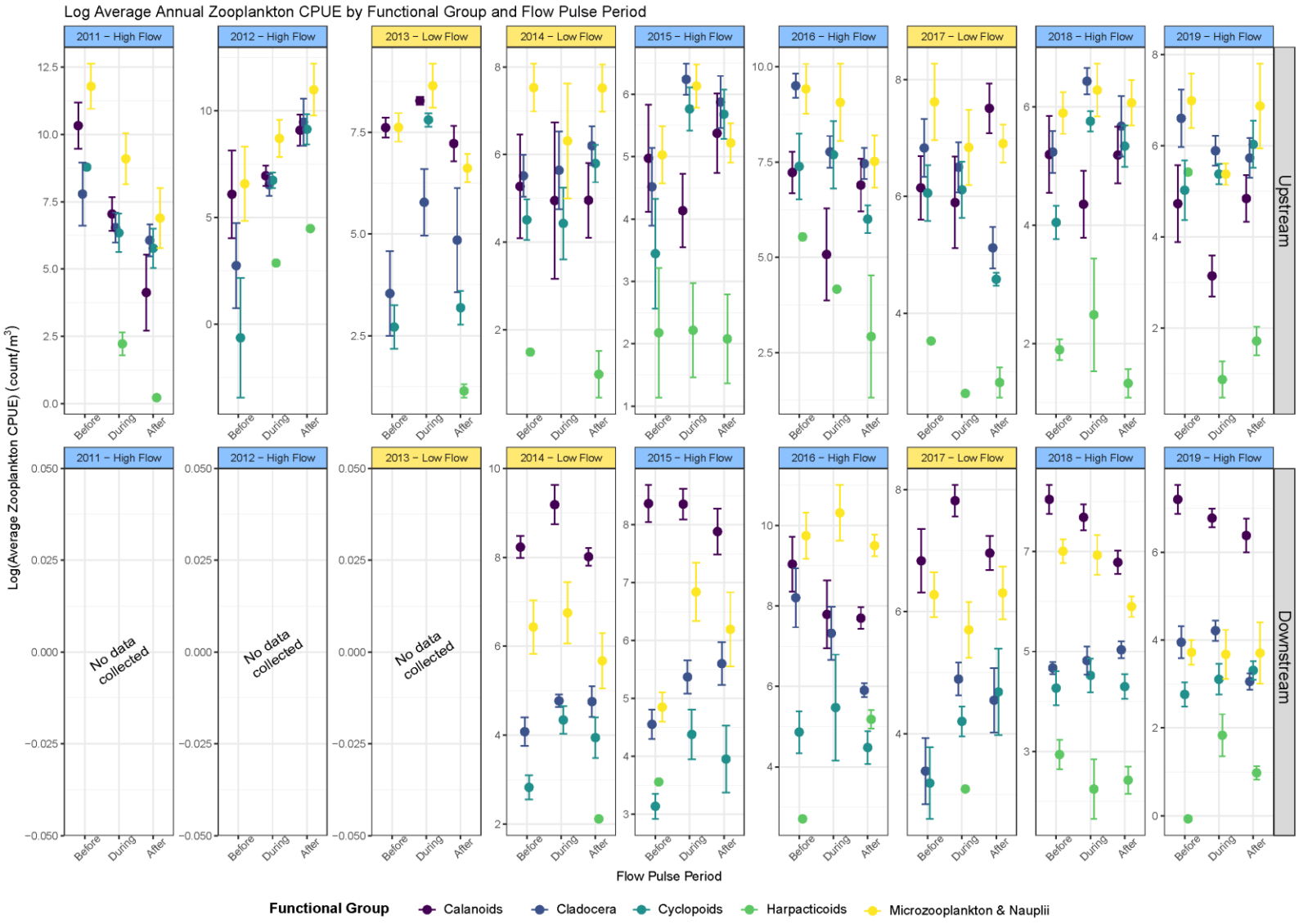

Figure 4-21. Average log zooplankton CPUE (±SE) by functional taxa group, region, and year (2014-2019). Early zooplankton data (2011-2013) were only collected at STTD and at RCS (2012 only). Flow pulse types are indicated by yellow (low) or blue panels (high).

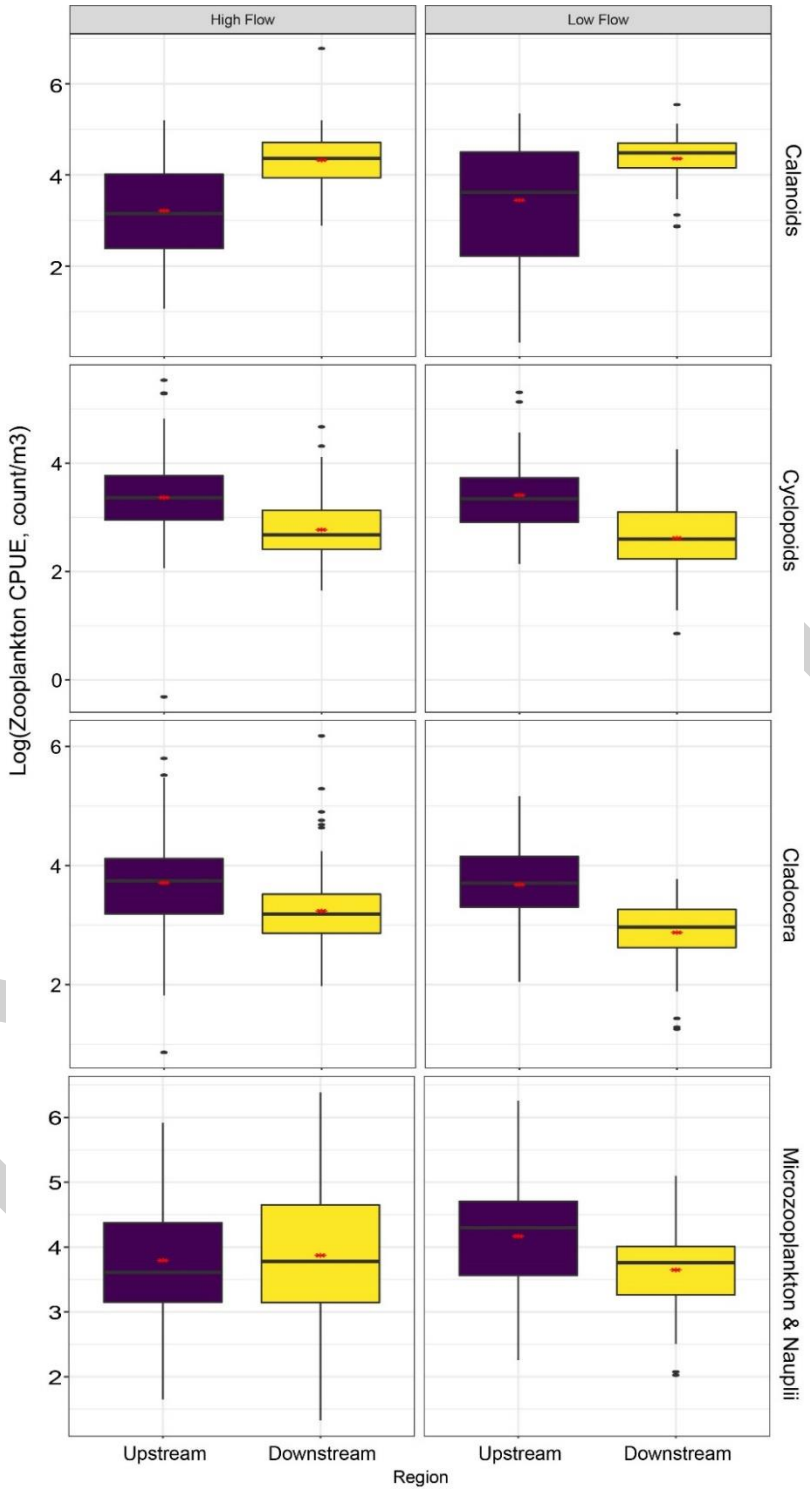

Figure 4-22. Boxplot quantiles of log annual zooplankton CPUE of high flow years (2015, 2016, 2018, and 2019) and low flow years (2014 and 2017) of flow pulses in the North Delta broken down by region and subset by zooplankton functional group. The red asterisk indicates average CPUE.

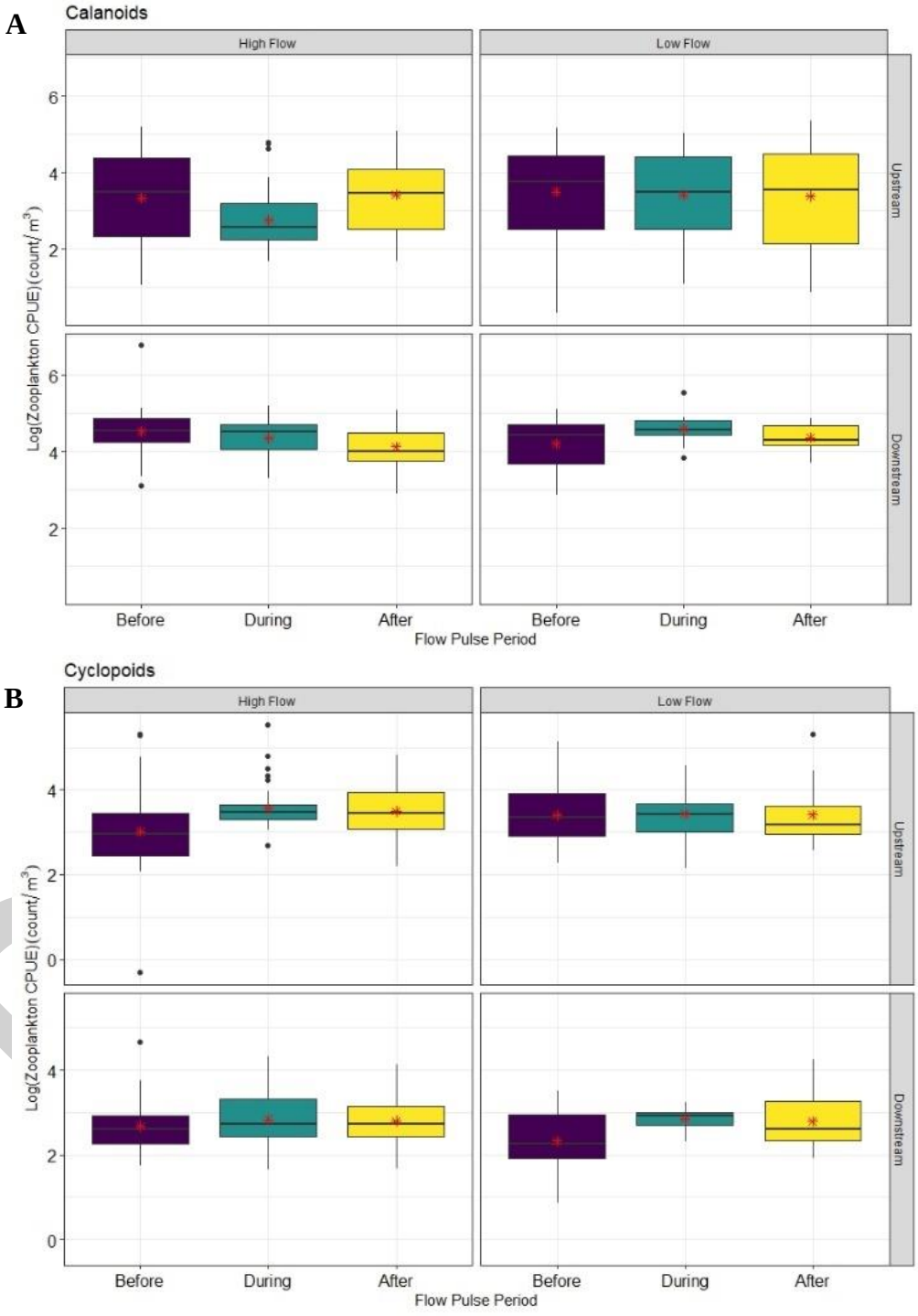

Figure 4-23. Boxplot quantiles of log annual A) Calanoid and B) Cyclopoid CPUE for high-flow pulses (2015, 2016, 2018, and 2019) and low-flow pulses (2014 and 2017) in the North Delta shown across regions (Upstream or Downstream) and flow pulse period. The black line indicated the median CPUE and red asterisks the average CPUE.

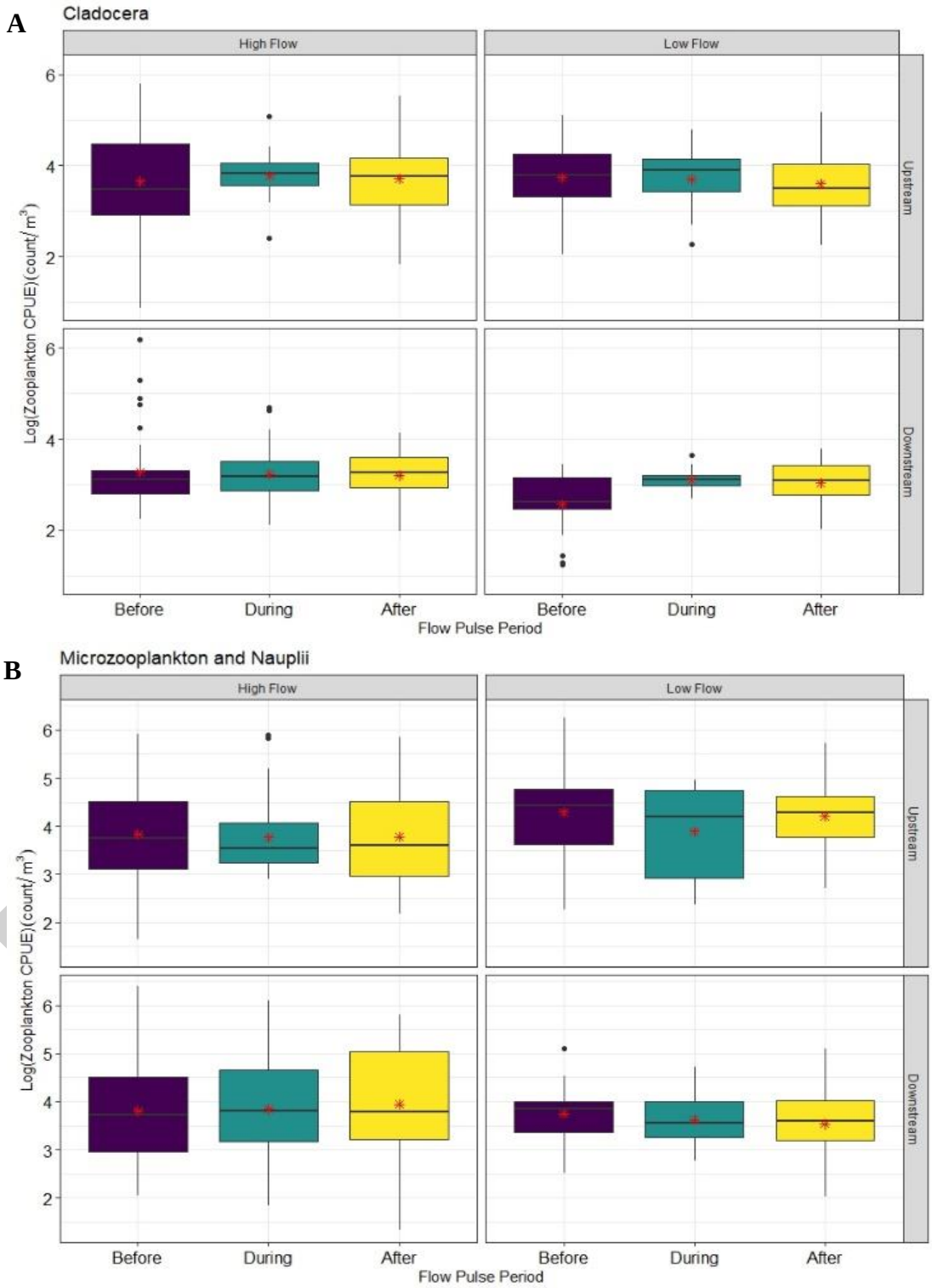

Figure 4-24. Boxplot quantiles of log annual A) Cladocerans and B) Microzooplankton and Nauplii CPUE for high-flow pulses (2015, 2016, 2018, and 2019) and low-flow pulses (2014 and 2017) in the North Delta shown across regions (Upstream or Downstream) and flow pulse period. The black line indicated the median CPUE and red asterisks the average CPUE.

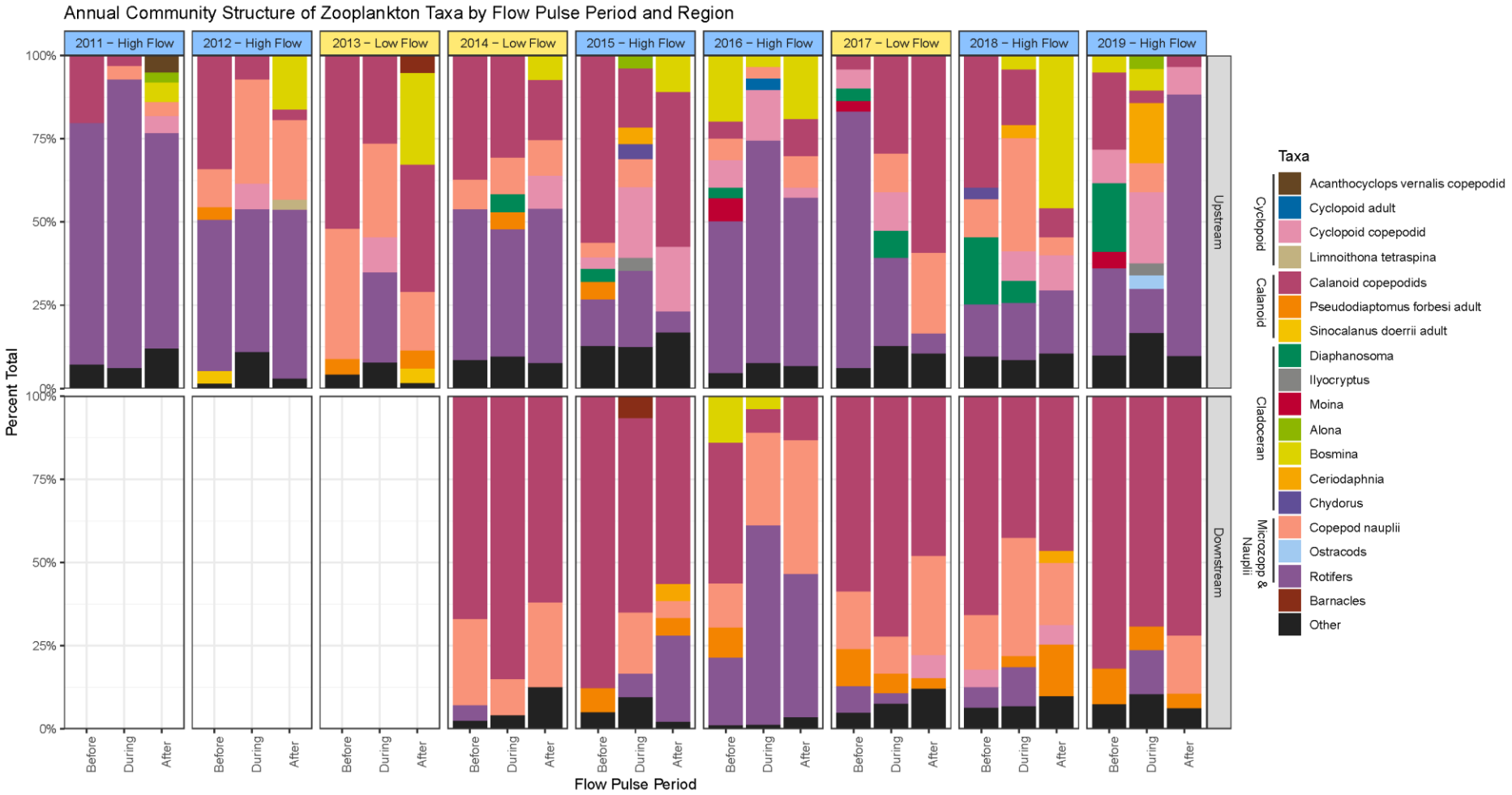

Figure 4-25. Composition of annual dominant zooplankton taxa as percentage of total community abundance (2011-2019) broken down by different flow pulse periods (before, during, or after) and region (upstream vs. downstream). Taxa comprising less than 3% of the total CPUE for that year and flow pulse phase were combined into the "Other" category. Early zooplankton data (2011-2013) were only collected at STTD and at RCS (2012 only). Flow pulse types are indicated by yellow (low) or blue panels (high).

Non-metric multi-dimensional scaling plots showed structure in subsets of data by year, region, and pulse period (Figure 4-26 and Figure 4-27). 2019, a high flow year, had the greatest amount of separation between regions (Figure 4-26). Year 2017, a high flow year, showed a change in community composition after the flow pulse (Figure 4-27), whereas other years demonstrate the lack of community difference across before, during, after flow pulse periods.

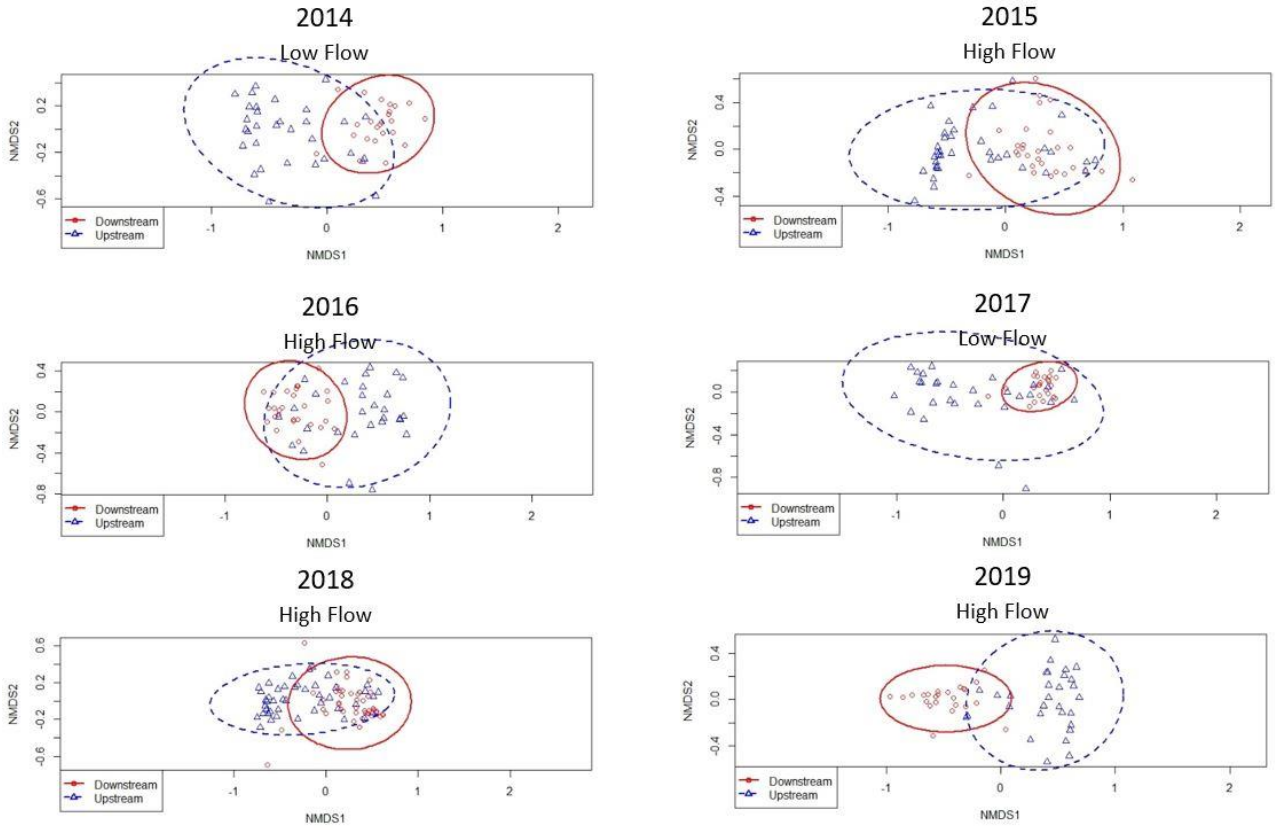

Figure 4-26. Non-metric multidimensional scaling plots highlighting annual differences in zooplankton community composition in the upstream and downstream regions over the flow pulse action years (2014-2019).

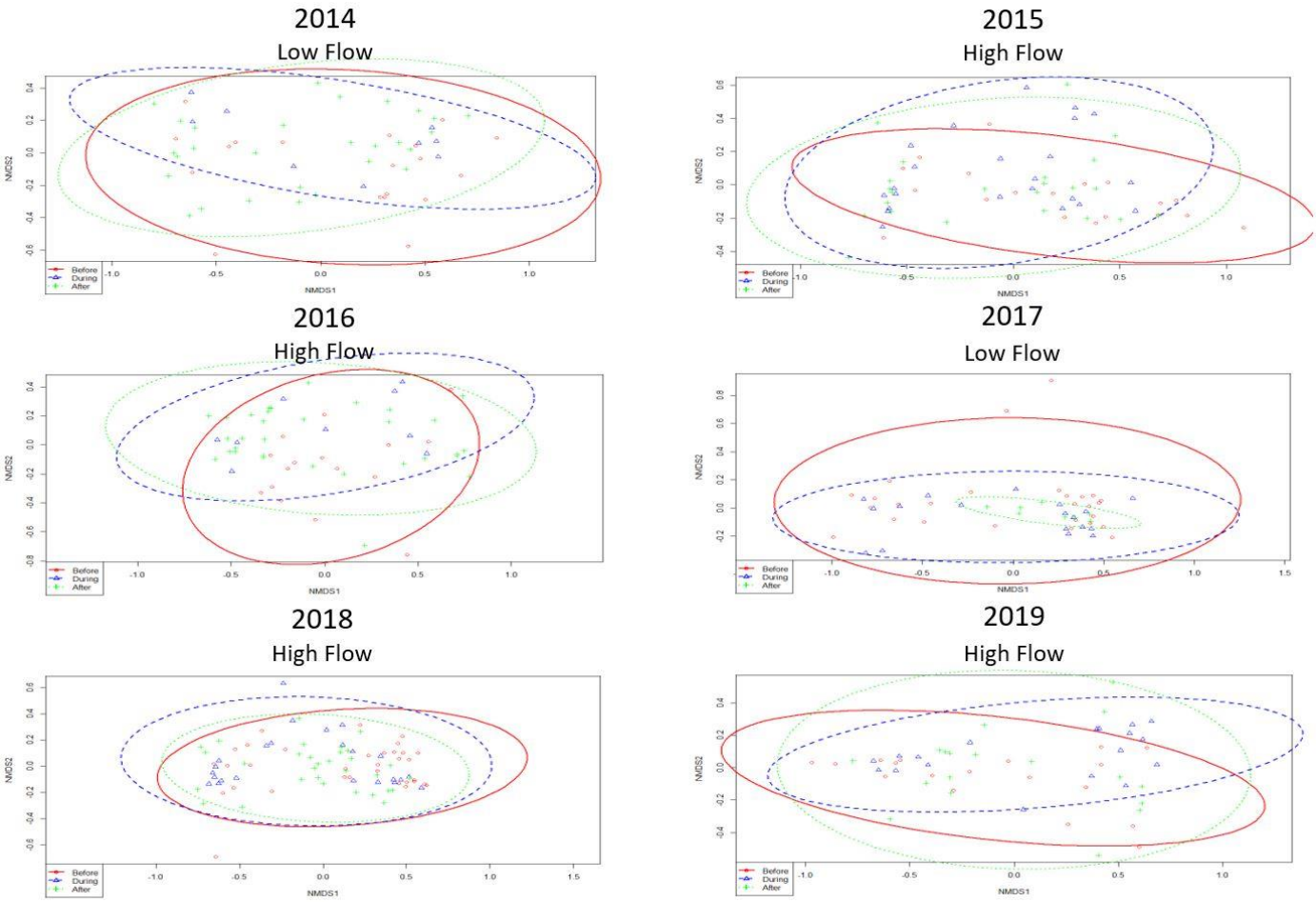

Figure 4-27. Non-metric multidimensional scaling plots highlighting annual differences in zooplankton community composition before (Pre), during, and after (Post) flow pulses for years 2014-2019.

4.4.3 Discussion

Total zooplankton CPUE in the North Delta varies significantly from year to year (Table 4-5), and between some upstream and downstream regions in different years (Table 4-6; Figure 4-18). However, within any single year, there were no significant differences in average total zooplankton abundance in upper and lower regions of the North Delta. Furthermore, zooplankton abundance in 2016, the only year with a Sacramento River flow action, was significantly higher than in any other year (Figure 4-18, Figure 4-19). However, there were no statistically significant effects of flow pulse period in any year, which suggests that 2016 may have been a particularly productive year for zooplankton, independent of flow pulse period, but replication of a similar 2016 action is required to confirm. There was a delta-wide phytoplankton bloom preceding the flow action that year (Frantzich et al. 2021), which may have benefited zooplankton production through increased food availability.

Quantitative results also suggest that flow pulses might not increase average zooplankton abundance downstream as expected. Increased transport of chlorophyll from the bypass due to the flow action may not have benefited zooplankton if the chlorophyll was not in the right form. A high percentage of phytoplankton produced from the flow pulse was cyanobacteria (see Figure 4-4 through Figure 4-10), which have low food quality (though see Kimmerer et al. 2018) and the large *Aulacoseira* bloom in 2016 may not have provided accessible food either (Jungbluth et al. 2020). While zooplankton in the Cache Slough Complex tend to have higher growth and reproductive rates than open-water habitats (Kimmerer et al. 2018; Gearty et al. 2021), there may be other factors controlling zooplankton abundance downstream, such as increased predation by fish or clam grazing (Kimmerer and Lougee 2015, see also next section 4.5), or higher concentrations of pesticides in zooplankton during certain flow pulses (e.g., flow pulses using agricultural water, Figure 3-62) potentially leading to higher overall zooplankton mortality rates in the lower Yolo Bypass. While zooplankton mortality rates were not investigated in this study, they may be an important component to understanding how flows affect food web dynamics in Yolo Bypass and the Cache Slough Complex.

While total zooplankton density was similar across flow pulses, qualitative evaluations of compositional changes demonstrate that there may be species-specific responses to flow pulses that require further investigation. For

example, copepod nauplii increased as a percentage of the total zooplankton community downstream during and after the 2016 managed flow pulse using Sacramento River water (Figure 4-25), and community composition in 2016 during and after the action deviated from before the action and other years (Figure 4-25). It is unknown whether these differences were due to the delta-wide phytoplankton bloom in 2016 (Frantzich et al. 2021), the flow action, or other factors; however, this warrants further investigation of the effects of flow actions using Sacramento River water (2016) vs. agricultural water (all other years) on zooplankton community composition.

Regional differences (upstream vs. downstream) in composition were also evident across years (Figure 4-21, Figure 4-25, Figure 4-26). For instance, calanoid copepods, especially of the species *Pseudodiaptomus forbesi*, an important part of the diet of Delta Smelt (*Hypomesus transpacificus*), were found in greater abundance in downstream regions (Figure 4-25). The Cache Slough Complex, the uppermost portion of the downstream sampling region, is a source of this important prey (Kimmerer 2018, 2019). Hydrologic differences between the regions could affect zooplankton community composition and distributions (Dickerson et al. 2009). The higher total zooplankton CPUE in the upstream region could also be due to a dilution effect caused by the Yolo Bypass merging with the larger Sacramento River at the terminus of the Toe Drain in the northern end of the downstream region.

Our sampling methodology and confounding seasonality may have influenced our evaluations of zooplankton responses to flow pulses. For example, some zooplankton taxa, such as calanoid copepods and cladocerans, significantly decreased upstream during flow pulses (Appendix E Table 29) and qualitatively decreased in density downstream during and after flow pulses in both high- and low-flow years (Figure 4-21), suggesting that these taxa may be transported downstream during pulses, decreasing residence time, an important factor influencing densities (Kimmerer 2018). The duration of our sampling after the flow pulse may need to be extended to provide zooplankton time to recover their densities after being transported during the pulse. This could provide a more accurate assessment of longer-term flow pulse effects. In addition, there may be seasonal effects on calanoid and cladoceran populations. There has been limited research examining the effects of seasonality on zooplankton in the north delta, but Kimmerer et al. (2019) did not detect strong declines in calanoid abundances in the fall in Cache Slough Complex. However, the upstream habitat of the Yolo Bypass is defined by its

shallow, channelized habitat and a lack of tidal influence, such that food limitation, temperature or other variables may have a larger impact on calanoid copepod populations in this region later in the season.

Our sampling methodology could also have influenced our finding that calanoid copepod adults decreased, yet calanoid copepodids increased after some flow pulses downstream (Figure 4-25). Turbidity decreased downstream during and after flow pulses, which can cause adult calanoid copepods and copepodites to remain near the bottom of the water column (Kimmerer and Slaughter 2016), potentially decreasing their catch. Conducting oblique tows rather than surface tows could resolve the effects of the flow pulse on the zooplankton community, as oblique tows have been found to catch more calanoid copepod adults and copepodites than surface tows (Kimmerer et al. 2019).

Antecedent conditions, such as food availability and water year type, may also influence zooplankton responses to flow pulses. Overall, 2016 was a good year for zooplankton, possibly due to a Delta-wide phytoplankton bloom providing abundant food resources (Frantzich et al. 2021). Cyclopoid copepod and Cladocera CPUE were higher upstream during wet water years (2017 and 2019), possibly due to increased wetted areas in the bypass providing more habitat for zooplankton, higher DO, and resting eggs hatching, possibly coupled with higher levels of carbon sources transported from upstream (Figure 3-53 - Figure 3-58). In 2015, a critically dry water year, cyclopoids were more abundant during the flow pulse than before. During critically dry years cyclopoids may be transported from epibenthic and edge habitat (e.g., SAV) into the water column during the flow pulse, or the onset of more favorable conditions from the flow pulse (e.g., higher DO, increasing carbon sources, etc.) could spur more rapid population growth.

4.5 Benthic Invertebrates

Invasive clams in the San Francisco Estuary, CA consume plankton and organic particulates, reducing food availability for zooplankton, a key prey for critical fish species including Delta Smelt (Winder and Jassby 2010, Kimmerer and Lougee 2015). The invasive clam, *Corbicula fluminea,* is common in low salinity habitat within the estuary, and may have the potential to deplete phytoplankton in the Delta by filtering the water column, particularly in shallow habitats (Jassby et al. 2002, Lopez et al. 2006, Lucas et al. 2016, Lucas and Thompson 2012). With adaptive management actions, such as NDFS, that use augmented flows to improve primary productivity and food availability in the Cache Slough Complex (CSC) and lower Sacramento River, it is important to understand the impact of these clams on lower trophic food webs.

Benthic measurements were conducted in 2014 and 2019 in the North Delta as they were expected to be a critical part of future biological modeling and understanding food web interactions. While effects of flow pulses on the benthic clam community were predicted to be neutral (Table 1-2), it is important to estimate densities and filtration rates by clams that might reduce flow pulse benefits of potential increases and transport of phytoplankton downstream. Filtration rates represent the theoretical maximum volume of water pumped by clams at a given temperature, assuming phytoplankton concentrations near the benthos do not become depleted (Lucas et al. 2002). While grazing rate calculations account for such resource depletion and refiltration, we felt that filtration rates relied on fewer assumptions given the limitations in our data. However, it should be noted that filtration rates may overestimate actual grazing by neglecting boundary layer depletion of phytoplankton, refiltration, and periods of valve closure due to disturbances (e.g., predator presence, flow). Nonetheless, we feel that the filtration rates calculated here provide a useful approximation of the spatial variability and maximum potential grazing by clams throughout the North Delta and help to better understand possible impacts by benthic consumers to plankton resources during and after flow pulses. The following is based on collections during the 2019 NDFS (a high-flow year) and additional benthic data from 2014 (a low-flow year) in collaboration with USGS.

4.5.1 Methods

Clams were sampled in August 2019 prior to the high-flow pulse (managed action) across six locations throughout the North Delta from Lisbon Weir in the Yolo Bypass Toe Drain to the Sacramento River at Rio Vista. Triplicate ponar grabs with a standard 9 in x 9 in sampler were conducted by boat at 5 sites including 1) LIS, 2) STTD, 3) BL5, 4) LIB, and 5) RYI. Benthic grabs at RVB were conducted by EMP (DWR) in August and used in the dataset. For consistency with the five triplicate ponar grabs collected in the Yolo Bypass and Cache Slough Complex, three of the five grabs that EMP conducts were randomly selected and used in these analyses. Ponar grabs were conducted near the softer edges of Toe Drain sites due to the hard clay pans in the center channel. Following each grab, the sample was rinsed of excess organic sediment in a fine mesh bag and transferred to a collection bottle and preserved in 10% ethanol with Rose Bengal for later analyses at the DWR laboratory.

In the laboratory, clams were then rinsed over several sieves to further remove sediment, identified to species if possible (otherwise, to genus), sorted by size (>1 mm and larger), and counted. Ash-free dry mass (AFDM) per unit area ($g \cdot m^{-2}$) was estimated using length to mass regression generated from log-transformed clam size-class data (from EMP) at select north Delta sites, fitted using the equation: $y = 10^{(3.1661*(\log(x+0.5))-5.0812)}$, $R^2 = 0.9874$ (Hartman et al. 2021); with x = clam size-class rounded to the nearest 1mm. Maximum filtration rates by *C. fluminea* ($L \cdot m^{-2} \cdot day^{-1}$) were estimated based on temperature-dependent filtration rates (expressed in $L \cdot g^{-1}$ AFDM $\cdot day^{-1}$) for *C. fluminea* in the Delta (Foe and Knight 1986) using measured average water temperatures at sampling locations (rounded to the nearest degree Celsius) and clam biomass (g^{-1} AFDM $\cdot m^{-2}$). We estimated filtration rates as a percent of the water column in Cache Slough Complex (CSC) by dividing the mean filtration volume (converted to m^3) by the mean depth in meters for each site. These values were then used to calculate the mean percent of the water column filtered using sites that overlap spatially with the core NDFS sites in the CSC (Prospect Slough, Cache Slough and Liberty Island, see Table 3-4 and Figure 3-36) and that are within the tidally 'sloshing' area of CSC (i.e. net flows near zero).

Clam data from October 2014 were collected by USGS and EMP (RVB). Data collections were not correlated with a flow pulse but included sampling sites within the spatial scope of NDFS and supplementary to understanding 2019 data. Methodologies for field sampling, laboratory analyses, and data calculations were similar to 2019 as described above. One noted difference in sampling was that 2014 replicate grabs were taken across a channel, whereas in 2019 replicate grabs were taken more randomly at locations within a site. Overlapping sites in 2014 and 2019 included Prospect Slough (BL5), Cache Slough (LIB), Toe Drain (STTD) and Rio Vista (RVB). Sites exclusive to 2014 were the Deep-Water Shipping Channel (DWS), Lindsey Slough (LS), and Stair Step (SS). Additional sites sampled in 2019 included Ryer Island (RYI) and Lisbon Weir (LIS) in the Toe Drain. LIS was not included in the current analysis due to anomalous catch (e.g., hardly any clams, but several of unusually large size) and the site's physical structure; the site is located behind a weir, creating a large, channel-wide eddy with highly variable substrate atypical of the region.

Statistical analyses were conducted in R (version 4.0.4; R Core Team 2020). Data were first tested for normality using the Shapiro-Wilk normality test (from the 'stats' package) on log-transformed clam AFDM and density. To determine if 2014 and 2019 data could be pooled (due to limited sampling effort in 2019) and to provide descriptive statistics and visualization of clam density and filtration rates, we used paired t-tests to compare overlapping sites from 2019 to data collected in October of 2014 by USGS and DWR.

4.5.2 Results

There was no difference in mean clam density for the North Delta ($t = 0.0443$; $df = 3$; $p = 0.967$) and AFDM ($t = 0.176$; $df = 3$; $p = 0.871$) between 2014 and 2019 (Figure 4-28). However, density and biomass between sites within the region was highly variable ($\mu_{density}$ = 947 clams·m^{-2}, $\sigma^2_{density}$ = 1019 clams·m^{-2}; $\mu_{biomass}$ = 21.6 g·m^{-2}, $\sigma^2_{biomass}$ = 30.3 g·m^{-2}) The clam community in the North Delta is dominated by the invasive *Corbicula fluminea* in both density (80.4%) and biomass (99.8%). Mean clam biomass in the North Delta during late summer/fall suggests a median filtration rate for *C. fluminea* of 647 L·m^{-2}·day^{-1}, with a range from 16 L·m^{-2}·day^{-1} to 9903 L·m^{-2}·day^{-1} depending on the location (Figure 4-29). Using

estimated filtration rates and mean depths for selected sites within Cache Slough Complex, and assuming zero net flow, we estimate that *C. fluminea* may filter on average approximately 22.5% of the water column each day in the CSC (Table 4-9).

Table 4-9. Estimated *C. fluminea* filtration rates and percent daily water column filtered within sites in the Cache Slough Complex.

CSC Site	Depth (m)	Filtration Rate ($m^3 \cdot m^{-2} \cdot day^{-1}$)	Water Column Filtered (% daily)
Cache Slough (CS)	5.41	0.65	11.95
Liberty Island (LIB)	1.50	0.41	27.38
Prospect Slough (PS)	6.78	1.91	28.16

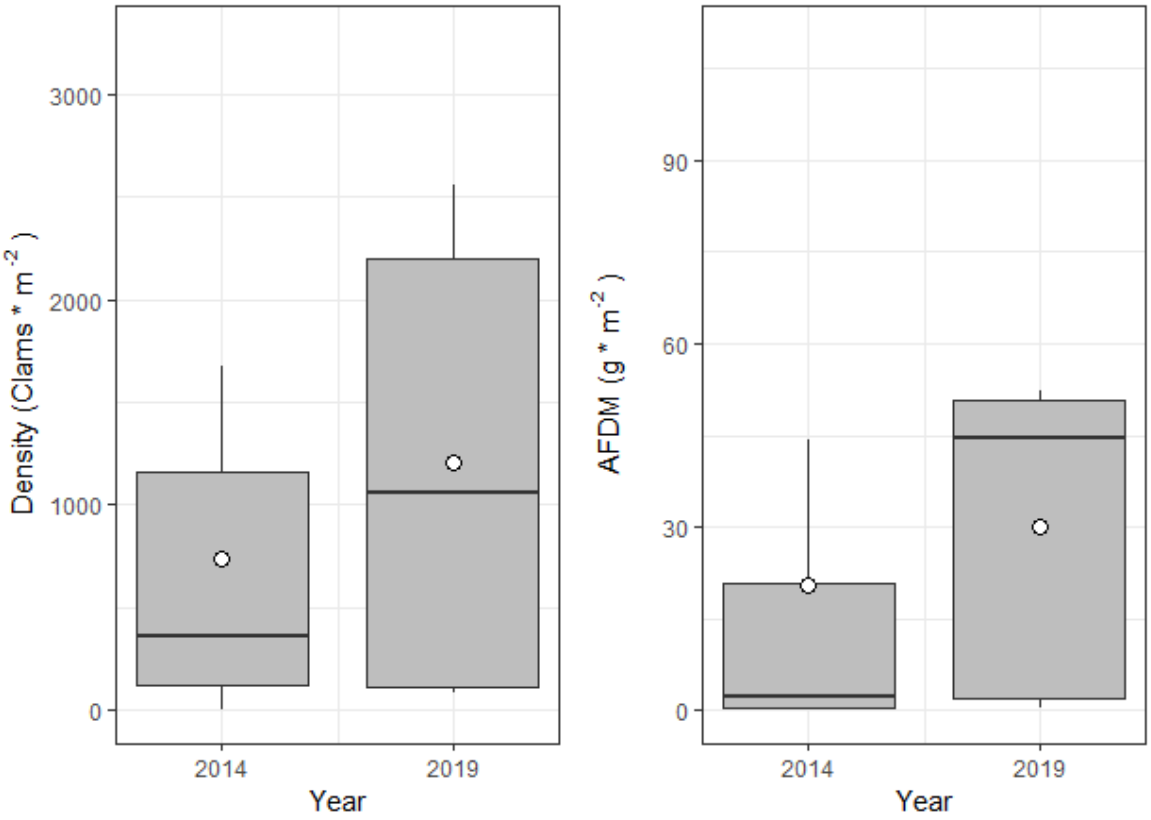

Figure 4-28. Boxplots of density and biomass from select sites in 2014 and 2019; the solid line indicates the median value and open circle the group mean.

A)

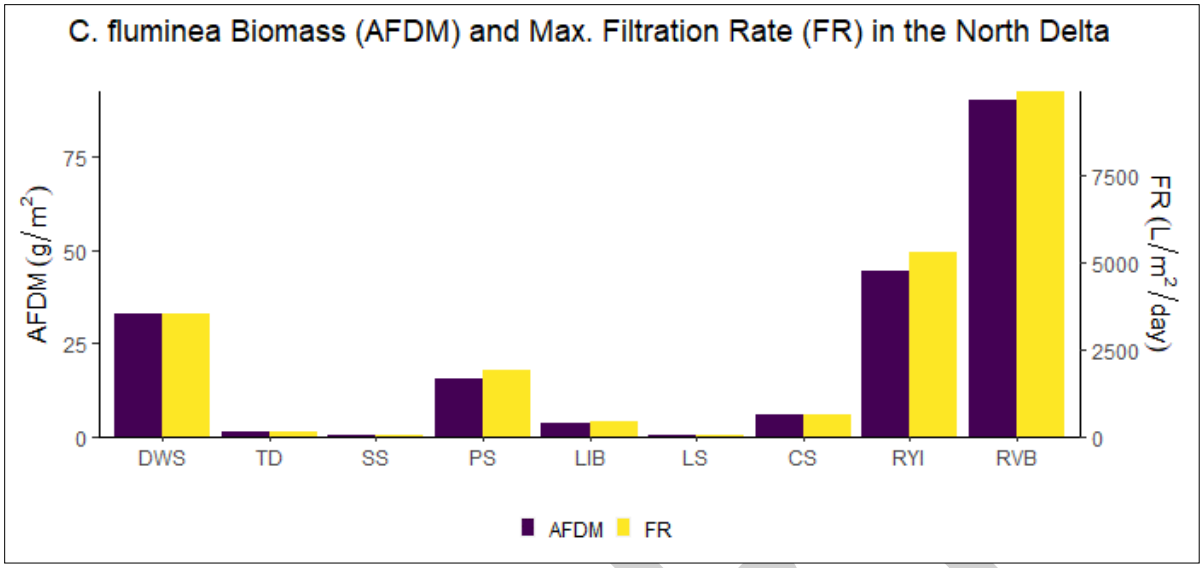

B)

Figure 4-29. (A) *Corbicula fluminea* biomass as Ash-Free Dry Mass (AFDM) and maximum potential filtration rates (FR) in the North Delta. DWS=Deep Water Ship Channel, TD=Toe Drain, SS=Stair Step, PS=Prospect Slough, LIB=Liberty Island, LS=Lindsey Slough, RYI= Ryer Island, RVB=Rio Vista. (B) A map of the North Delta benthic sampling sites with correlated clam biomass (grey vertical bars, $g \cdot m^{-2}$), and density (colored discs, $clams \cdot m^{-2}$).

4.5.3 Discussion

Our preliminary findings suggest the potential for clams to filter a large volume of water in the lower reaches of the North Delta from lower Prospect Slough to Cache Slough and the lower Sacramento River (Figure 4-29); *C. fluminea* may filter between 12-28% of the water column per day in different areas of the CSC (based on clam biomass, site depth, and temperature, see Table 4-6), though more data are needed for a clearer picture of the impacts of invasive clams in the North Delta. While we were limited in our ability to sample clam communities, both temporally and spatially, there were some general observations that warrant consideration. In particular, clam biomass in Yolo Bypass seems to decrease from south to north, suggesting that clam grazing may be a more important factor in the regions of the lower Sacramento River and Cache Slough complex, and less so in the upper bypass where channels are narrower and more subjected to scouring from high flows, higher temperatures, and dewatering during dry periods (Sommer et al. 2004). Clams generally have a patchy distribution in the Delta (Lopez et al. 2016), both on a broader regional scale, as noted by variable clam density estimates for different sites throughout the region (σ^2 = 1019 clams·m^{-2}; see also Fig. 4-29), and on a more localized scale with high variation in bivalve densities found within individual grabs at sampling sites.

Other research in the North Delta has found that *Corbicula* biomass followed mostly seasonal patterns, with peak clam sizes in late spring to early summer, and a peak in some years in late fall (Crauder et al. 2016). Thus, interpretations of our results, given the limited sampling (only once during the summer) should also take seasonality into consideration along with high inter- and intra-regional variability. As our estimates of filtration rates for clams were taken during summer and early fall when water temperatures are near their peak and optimal for clam growth, they may overestimate filtration for cooler parts of the year, when the ability for clams to pump water declines (Foe and Knight 1985). Furthermore, climate change may warm waters in the upper reaches of Yolo Bypass to temperatures that are less hospitable to clams during the peak of summer, while conversely, milder winter temperatures may increase clam growth (Weitere et al. 2009). Nonetheless, clam distributions, and their potential for grazing a significant proportion of the water column, may be important when considering plankton exports from the upper bypass, in-situ production in Cache Slough Complex, and overall exports of plankton from the North Delta.

Chapter 5 Fish

Technical Team: Nicole Kwan, Cat Pien, Jeff Jenkins, Hailey Wright, Rosemary Hartman

5.1 Summary

This chapter marks the first effort to fully analyze connections between flow pulses and fish communities in the North Delta region. Monitoring for the North Delta Food Subsidy (NDFS) action primarily focuses on hydrodynamics, water quality and lower trophic productivity. However, one of the overarching goals of the action is boosting food resources for Delta fishes, namely the endangered Delta Smelt. Since flow action monitoring does not specifically include fish monitoring, we compiled various Interagency Ecological Program fisheries data from locations that could potentially be impacted by the NDFS action.

Fish abundance data were collected from the upper San Francisco Estuary, including the Sacramento River from Decker Island to Sherwood Harbor, the Cache Slough Complex, Yolo Bypass, and Wallace Weir Fish Rescue Facility between 2011-2019. We also obtained data from the 2019 Delta Smelt Enclosure Study at Yolo Bypass and Rio Vista locations. Data for Chinook Salmon and Central Valley Steelhead (collectively referred to as salmonids) were compiled from monitoring programs, the Wallace Weir Fish Rescue Facility, and various adult and juvenile release and returns databases for the Sacramento River watershed. Data were synthesized and analyzed to help better understand the connections between the flow pulses in the North Delta and fish communities of interest. For each species or community of interest, our main methods of analysis were comparisons by region (upstream, downstream, and middle Sacramento River), water year, and time (before-during-after the flow pulse).

5.2 Objectives

The objective of this chapter is to better understand the relationship between flow pulses (high- and low-flow, managed and non-managed) and the local fish community. We looked at overall fish assemblage, Delta Smelt health, survival, and diet, and adult salmonid straying and health. Our detailed questions were as follows:

1. Do flow pulses influence fish assemblage?
    a. What is the relationship between total catch of all fish species, flow pulse period, region, and year?
    b. What is the relationship between total catch of native fish species, flow pulse period, region, and year?
    c. What is the relationship between Delta Smelt-similar fish species, flow pulse period, region, and year?
2. Is there a notable correlation between zooplankton, fish abundance, and flow pulses?
3. Do flow pulses benefit Delta Smelt?
    a. What were the effects on Delta Smelt growth and survival during the 2019 enclosure study?
    b. Did Delta Smelt diets from the enclosure study resemble the food resources present in the environment?
4. Do flow pulses negatively impact adult salmonids?
    a. Do flow pulses cause more salmonids to stray into the Yolo Bypass than would if no pulse occurred and is there a relationship between flow and salmonid catch?
    b. Do flow pulses lead to exceedance of salmonid temperature and dissolved oxygen (DO) tolerance thresholds when fish are present?

5.3 Fish Assemblage

5.3.1 Methods

Data Compilation

To assess overall changes in fish community, we used data from several different long-term monitoring surveys (Table 5-1; Figure 5-1), which were combined into one integrated dataset for analysis. Data were downloaded from public repositories, or, in the case of the Yolo Bypass Fish Monitoring

Program (YBFMP), from the Department of Water Resources (DWR) internal database. Data tables were re-formatted so that each table had a single row containing the catch of a single species from a single sampling event and all related environmental information. Column headings were renamed where necessary and converted to the same units across surveys. All files were integrated into a master table of all relevant fish data (see ND-FASTR Fish Metadata for details). Data were then subset so that only data from regions that may be impacted by the NDFS action from 2011-2019 were included. Data were also subset to include only data from 45 days before the flow pulse through 45 days after the flow pulse from each year.

Table 5-1. Datasets used for fish community analyses. FMWT = Fall Midwater Trawl. STN = Summer Townet. DJFMP = Delta Juvenile Fish Monitoring Program. EDSM = Enhanced Delta Smelt Monitoring, YBFMP = Yolo Bypass Fish Monitoring Program.

Survey	Agency	Gear type	Regions covered	Months sampled	Years sampled	Data access
FMWT	CDFW	Midwater Trawl	All	Sep-Dec	1964-present	FTP site
STN	CDFW	Tow Net	Upstream, Downstream	Jun-Aug	1959-present	FTP site
DJFMP	USFWS	Beach Seine	Downstream, Middle Sac	Year-round	1976-present	EDI
EDSM	USFWS	Kodiak Trawl	All	Year-round	2016-present	EDI
YBFMP	DWR	Beach Seine	Upstream	Year-round	1998-present	EDI/internal database

Sites were grouped into three regions (Figure 5-1). The 'Upstream' and 'Downstream' sites were analogous to the regions used in the water quality and lower trophic analyses. Sites in the Yolo Bypass and Sacramento River Deep Water Ship Channel north of the intersection of the Stairstep and the Toe Drain were categorized as 'Upstream'. This includes beach seine data collected by the YBFMP, as well as some data from FMWT, STN, and EDSM (Ship Channel only). Sites in Liberty Island, the Cache Slough Complex, and the Sacramento River south of the intersection with Cache Slough were categorized as 'Downstream'. This included most of the FMWT data, STN data, EDSM, and the Liberty Island beach seines of DJFMP. Sites in Steamboat Slough and the Sacramento River north of the intersection with Cache Slough and south of Fremont were categorized as the "Middle Sacramento River". These were mostly DJFMP trawl and beach seine sites, with a few FMWT sites.

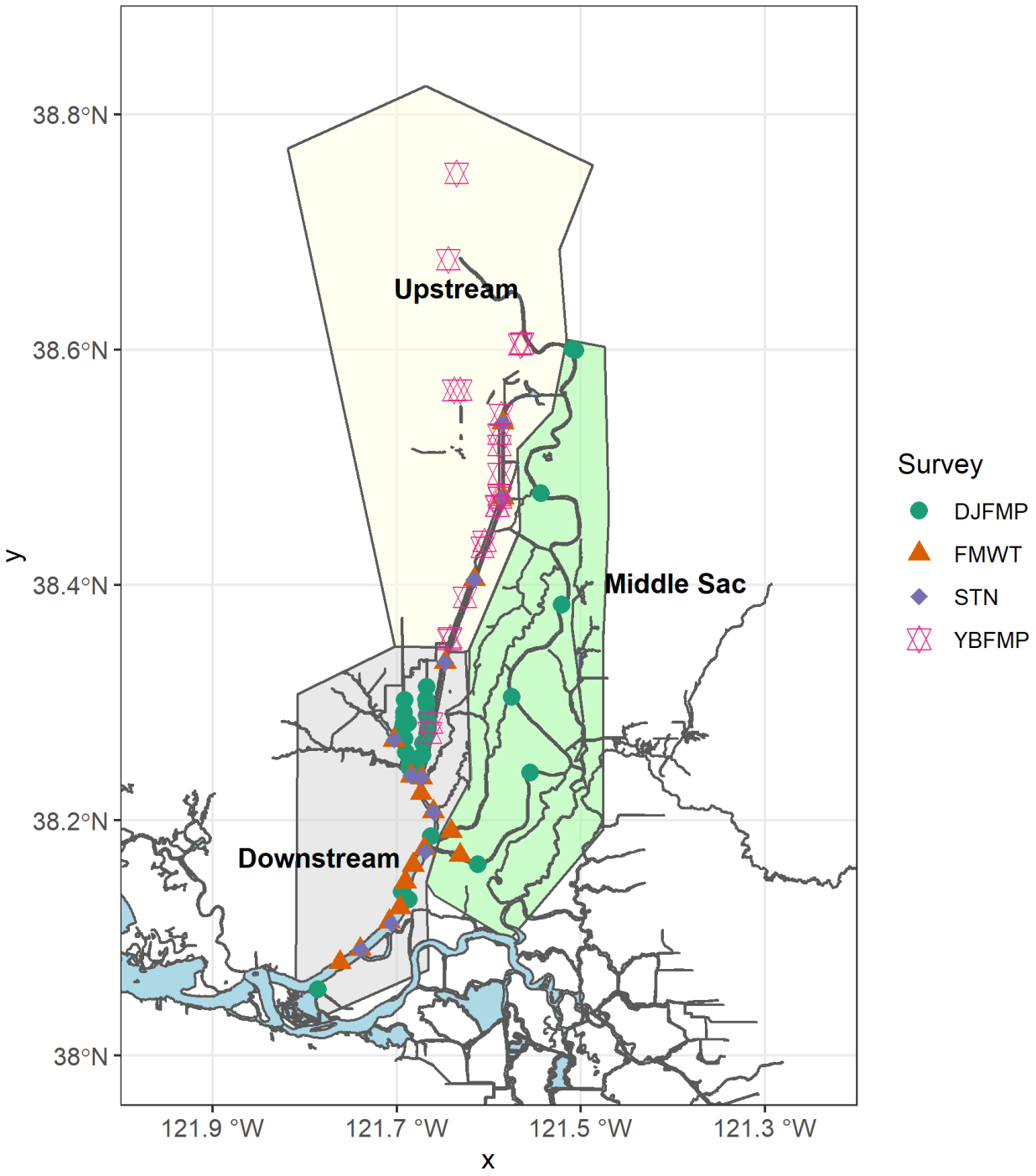

Figure 5-1. Map of fish sampling stations. EDSM samples are randomly selected, so not shown on the map as they would overwhelm the other sites.

In brief, component data sets were:

Summer Townet (STN)

The California Department of Fish and Wildlife operates the Summer Townet Survey (SNT; survey website), which collects juvenile fish samples at all stations shown in Figure 5-1, twice per month in June, July, and August. The townet consists of a fixed D-frame sled on runners with a 5.5 m net. The main net body is 3.5 m long with 1.3 cm stretch, knotted, nylon, mesh tapering down to a 2.1 m cod-end with a section of woven mesh with approximately 16 holes per 5 cm. Two 10 minute stepped oblique tows are performed at each station. A third tow is conducted if any fish are captured during the first two tows. All fishes and several invertebrate species are counted and measured.

Fall Mid-Water Trawl (FMWT)

In September, the SNT is replaced by the Fall Midwater Trawl (FMT; survey website) which operates on a monthly basis and targets larger fish than the STN. The midwater trawl net has mouth dimensions of 3.7 x 3.7 m. Net mesh sizes graduate in nine sections from 2.4 cm stretch-mesh at the mouth to 1.3 cm stretch-mesh at the cod-end. All four corners of the net mouth are connected to planing doors that hold the net mouth open when being towed through the water. At each station a 12-minute stepped-oblique tow is conducted. All fishes and several invertebrate species are counted and measured.

Enhanced Delta Smelt Monitoring (EDSM)

The Enhanced Delta Smelt Monitoring (EDSM) program was initiated by the U.S. Fish and Wildlife Service in 2016 to provide estimates of Delta Smelt distribution and abundance (survey website). EDSM conducts stratified random sampling via Kodiak trawls (July-March) and larval gear (May-June). Over the course of a week, field crews sample between 18 and 37 random sites, with at least two samples in the North Delta (sites are randomly selected, so not shown on sampling figure). A minimum of two tows are

conducted at each site. All fish collected are identified (in the field when possible, in the lab for early life stages), measured, enumerated, and recorded. In addition to fish information, environmental data are collected for each sampling event. Full details on methods and data are available on their Environmental Data Initiative data package (USFWS et al. 2019).

Delta Juvenile Fish Monitoring Program (DJFMP)

The U.S. Fish and Wildlife Service Delta Juvenile Fish Monitoring Program (DJFMP) has monitored juvenile Chinook Salmon and other fish species since 1976 using a combination of surface trawls and beach seines. Since 2000, three trawl sites and 58 beach seine sites have been sampled weekly or twice per month within the Estuary, the lower Sacramento and San Joaquin Rivers, and Liberty Island. The beach seine net used by the DJFMP is a 15.2 m x 1.3 m seine net with 15.9 kg Delta 0.3 cm^2 mesh and a 1.3 m x 1.3 m bag. Each net has a float line and lead line attached to 1.8 m long wooden poles at each end. For more information, see the project website and data publication (IEP et al. 2020).

Yolo Bypass Fish Monitoring Program (YBFMP)

California Department of Water Resources has operated a fisheries monitoring program in the Yolo Bypass, a seasonal floodplain and tidal slough, since 1998. The Yolo Bypass Fish Monitoring Program (YBFMP) operates a rotary screw trap, which targets outmigrating juvenile fish, a fyke trap, which targets upmigrating adult fish, and conducts beach seines twice per month to sample near-shore juvenile and small bodied adult fishes. Currently, beach seine sites are sampled every-other week with a single haul from a 7.6 m by 1.2 m pole seine (3.2 mm sq. mesh). These are modified beach seine hauls; because the levee banks are generally steep, the seine is towed parallel to the shoreline as opposed to netting straight toward the shoreline. For more information, see the project website and data publication (IEP et al. 2018).

Data Analysis

Fish data were analyzed separately for seine (DJFMP, YBFMP) and tow (FMWT, STN, EDSM) data, since each method targets a different habitat and species

assemblage. Seines target shallow, littoral habitats, while tows target deeper, more pelagic habitats. Statistical analysis included only data from 2013-2019, though species composition plots display data from 2011-2019.

For each dataset, fish catch per unit effort (CPUE) was calculated by dividing catch/volume and, for each sampling event, zeroes were filled in for fish species that existed in the dataset but were not caught in the sampling event. Models were run on several subsets of the fish data, based on our interest in different types of fish assemblages. These assemblages included:

1) **"Smeltish"** fishes, an assemblage that was both a proxy for Delta Smelt and for potential competitors for Delta Smelt (Mississippi Silversides, Delta Smelt, Wakasagi).
2) **Native fishes** (Sacramento Pikeminnow, Splittail, Hitch, Hardhead, Sacramento Sucker, Sacramento Blackfish), and
3) **All fish**

Fish in each assemblage were summed for total CPUE per sampling event. Data were visually inspected, and outliers were removed. Fixed explanatory variables in the models included year, region, and pulse phase (PulsePhase; before-during-after the action phase), all specified as factors, as well as interactions between combinations of the variables. The interactions included differed for each model and station was included as a random effect in some of the models. Station was included as a random effect where possible.

For smeltish and native fishes datasets, we encountered model convergence errors when running mixed models that included station as a random effect. This was likely due to the large number of stations, and relatively smaller number of samples compared with the full dataset. Therefore, for these datasets, we ran a generalized linear model on mean CPUE, grouped by year, pulse phase and region. For the datasets containing all fish, data were overdispersed. Thus, we ran a negative binomial mixed model using the glmmTMB package (Brooks et al. 2017). For negative binomial models, the response variable has to be specified as an integer, so the model included total count as a response variable, with an offset of volume included in the model to account for effort.

For the tow data, random stations were reassigned to fixed stations by using nearest neighbor analysis with the nngeo package prior to models being run (Dorman 2021). Post-hoc tests were done on all models for all factors using

the sidak correction with the emmeans package (Lenth 2020). All analyses were run in R Version 4.0.2 (R Core Team 2021).

5.3.2 Results

Total annual CPUE for beach seined fish ranged from 607.4 fish*m-^{3} in 2014 to 1583.1 fish*m-^{3} in 2015. Species composition was dominated by non-native species, especially the Mississippi Silverside, which contributed to greater than 60% of catch across all years, and greater than 80% of catch across most years (Figure 5-1). Western Mosquitofish and Threadfin Shad were also common across years.

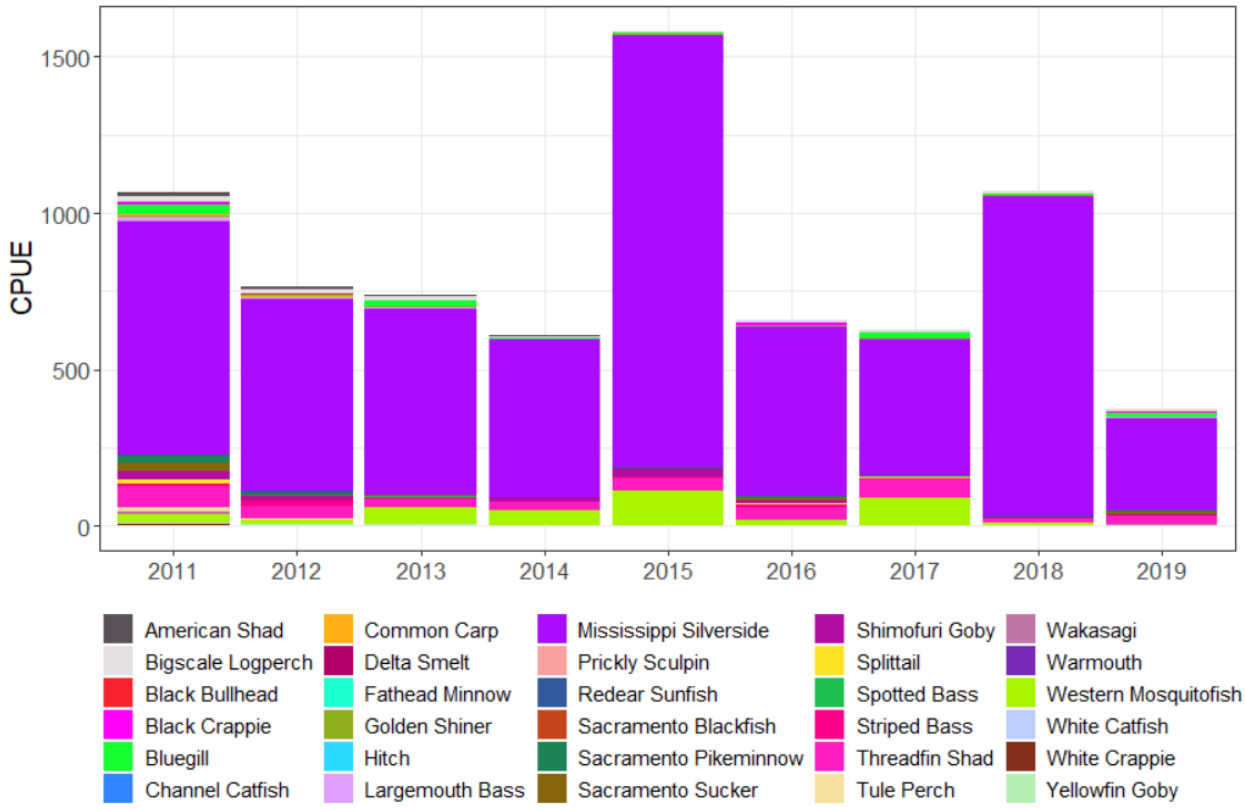

Figure 5-2. Beach Seine Fish Total Catch Per Unit Effort. Data include fishes caught between 2013-2019 by the Delta Juvenile Fish Monitoring Program and the Yolo Bypass Fish Monitoring Program. Only species that were caught in more than 1% of samples were included.

Total annual CPUE of tow surveys ranged from 0.5 fish*m-^{3} in 2014 to 19.6 fish*m-^{3} in 2017. Species composition was dominated by non-native species,

especially the Threadfin Shad between 2017-2019 (Figure 5-3). American Shad and Mississippi Silversides were also commonly caught between 2017-2019, and *Tridentiger spp.* (gobies too small to identify to species) were especially prevalent in 2015-2016. Notably higher CPUE between 2017-2019 is largely attributed to the addition of data collected by the Enhanced Delta Smelt Monitoring Program, which began in 2017.

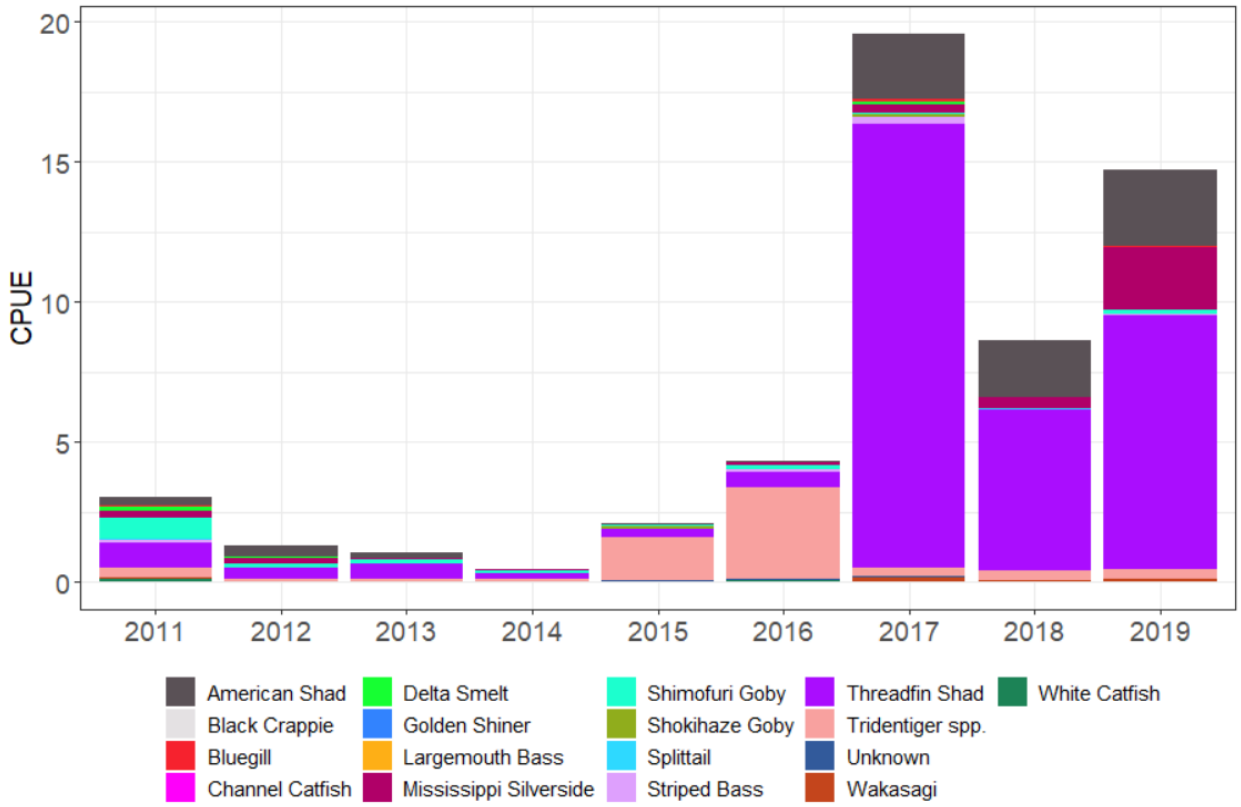

Figure 5-3. Tow Fish Total Catch Per Unit Effort. Data include fishes caught between 2013-2019 by the Summer Townet Survey, Fall Midwater Trawl Survey, and the Enhanced Delta Smelt Monitoring Program.

Overall, there was a large amount of variability in fish CPUE across tows and seine data. While there were generally higher CPUEs downstream in the seines, and upstream in the tows, there was variation depending on the year, pulse phase, and fish assemblage, and there was no clear preference for any particular pulse phase or year.

Result tables for fish models are reported in the Appendix D due to complexity of tables.

Smeltish Fishes

For smeltish fishes, there were more fish downstream in the seines, and upstream in the tows (Figure 5-4). There were no large differences between flow pulse phases (i.e., before, during, after), though there were slightly less fish after the flow pulse in the seines. These fish were largely composed of Mississippi Silversides for both data types, though there were more smelt caught in the tows compared to the seines.

The model selected for seine smeltish data was: *meanCPUE~ Region * Year + PulsePhase* (R^2 = 0.72, df =24). Region, pulse phase, and the interaction between region and year were significant (Appendix D, Table 1). There was a significant effect of region, with significantly more smeltish downstream in most years, then in MiddleSacRiver, then upstream (Appendix D, Table 2; Figure 5-4). There were more smeltish after the pulse compared with before the pulse (Appendix D, Table 3; Figure A). The significance of the interaction term was primarily due to the low smeltish CPUE downstream in 2019 compared with 2013, 2015, and 2017, and the high smeltish CPUE in MiddleSacRiver in 2015 compared with 2013, 2014, and 2016 (Appendix D, Table 4; Figure A).

The model selected for tow smeltish fish was: *meanCPUE~Region + Year + PulsePhase* (R^2 = 0.56, df = 12). Region and year were significant, with more fish upstream compared with downstream and MiddleSacRiver (Appendix D, Table 11 & 13; Figure C), and significantly higher smeltish CPUE in 2019 compared with all years but 2017 (Appendix D, Table 12; Figure C).

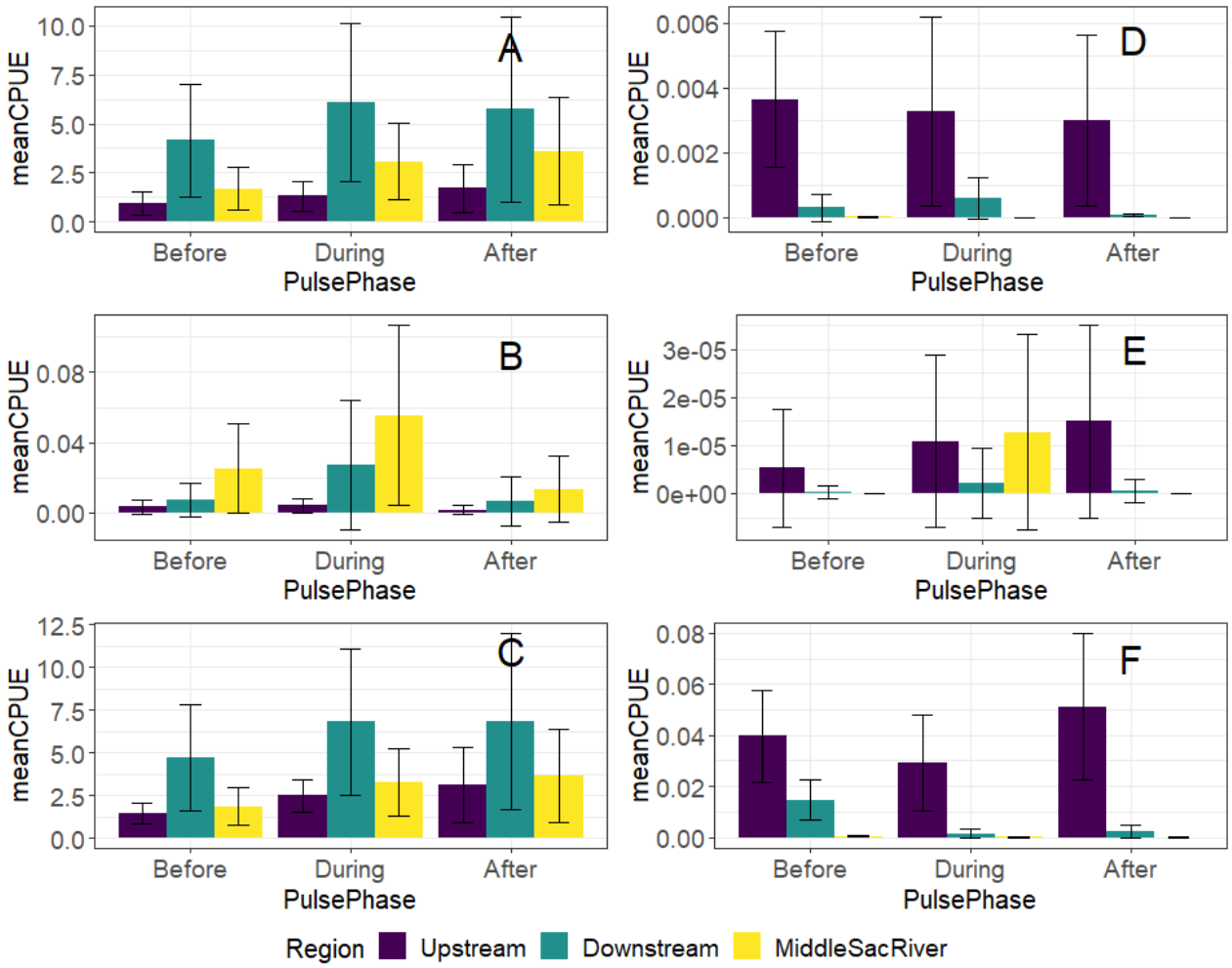

Figure 5-4. Mean Fish CPUE and Standard Error by Pulse Phase and Region. A, B, and C represent beach seine data, whereas D, E, F are tow data. Community assemblages include A and D as Smeltish, B and E as Natives, C and F as All fish.

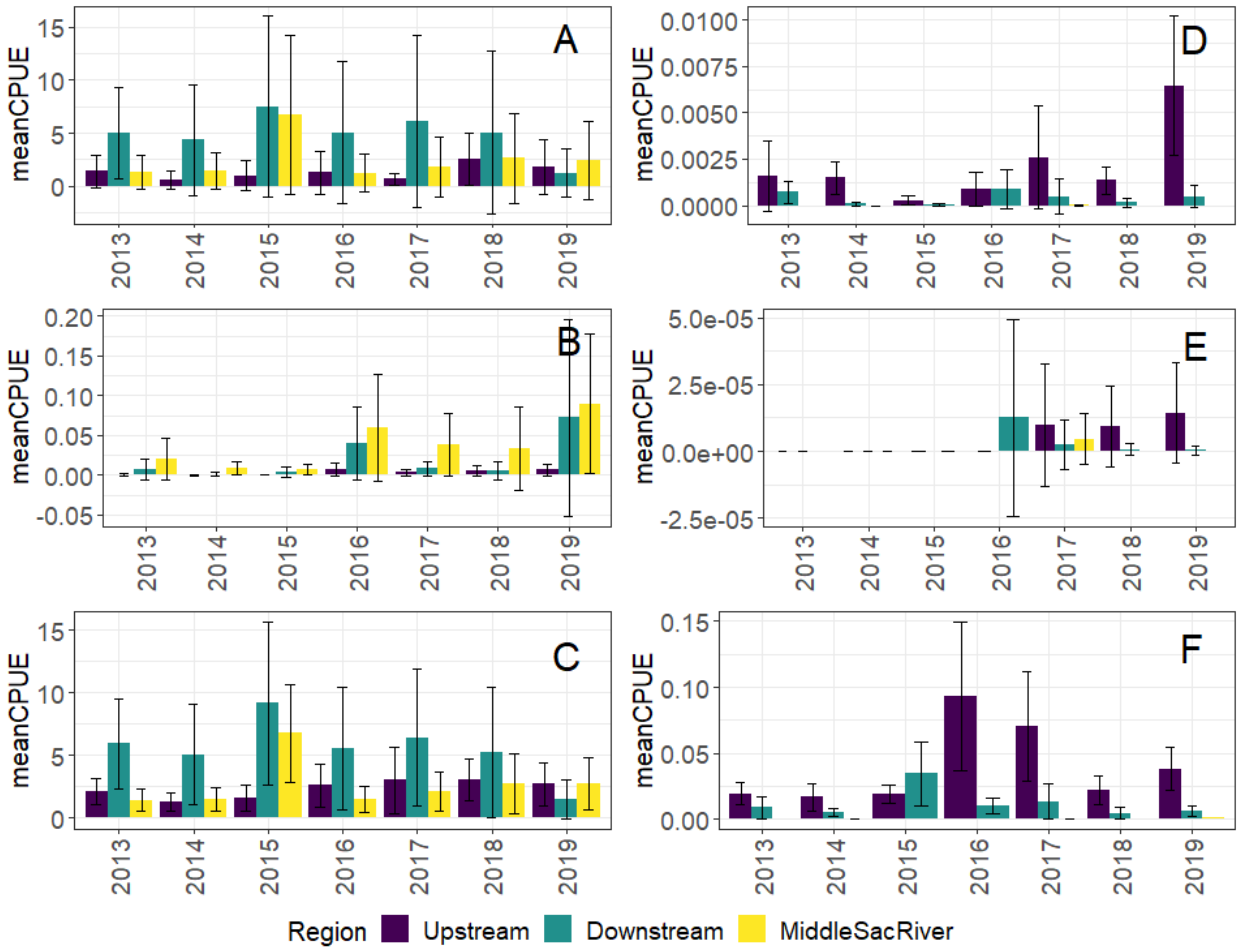

Figure 5-5. Mean Fish CPUE and Standard Error by Year and Region. A-C = Beach Seine/ D-F = Tow. A and D = Smeltish, B and E = Natives, C and F = All fish

Native Fishes

For native fishes, there were generally more fish in MiddleSacRiver for seines, and more fish upstream in the tows (Figure B, D). There were generally more fish before the pulse for both seines and tows. These fish were largely composed of Sacramento Suckers and Sacramento Pikeminnow for seines, and Splittail for the tows.

The model selected for seine native fish data was: *meanCPUE~Region * PulsePhase + Year (*R^2 = 0.59, df = 16*).* Year and the interaction between region and pulse phase were significant. Overall, there were more natives during the pulse and in MiddleSacRiver (Appendix D, Table 8). There was particularly high CPUE in 2019, significantly more than in 2013, 2014, and

2015 (Appendix D, Table 9; Figure B). There were significantly more native fishes during the pulse compared with before and after the pulse in MiddleSacRiver and downstream (Appendix D, Table 10; Figure 5-4B) and there were significantly more native fishes in MiddleSacRiver and downstream compared with upstream before the pulse (Appendix D, Table 11; Figure 5-4B).

Due to the low numbers of native fish caught in the tows, a model was not run for these data (only 29 catch events of 3144 tows).

All fish

For combined fish species, there were more fish downstream in the seines, and more fish upstream in the tows (Appendix D, Figure C,F). There were not any large differences by pulse phase. Higher CPUE was observed in the tows in 2016 and 2017 (Appendix D, Figure F).

The model selected for all fish was: *sumCount~ Region + PulsePhase + Year + Region:Year + PulsePhase:Year + offset(Effort) + error(1|StationCode).* Pulse phase, year, the interaction between region and year, and the interaction between pulse phase and year were significant (Appendix D, Table 13). Generally, there were more fish before the pulse, and there was no difference by region. Significant interactions are attributed to fluctuations in MiddleSacRiver CPUE between 2014-2017, with especially high CPUE in 2015 before the pulse followed by lower CPUE in 2016 before and during the pulse.

The final model for all fish in the tows was: *sumCount~ Region + PulsePhase + Year + Region:PulsePhase + PulsePhase:Year + offset(Effort) + error(1|StationCode)*. All included parameters and interactions were significant in the model (Appendix D, Table 14). There were generally more fish upstream, before the pulse, and in 2016, 2017, and 2019. Significant interactions can be attributed to low CPUE in 2013-2014 overall, and especially low CPUE 2013-2016 downstream and in MiddleSacRiver, as well as high CPUE in 2019 after the pulse.

5.3.3 Discussion

The predictions of this analysis were that high-flow pulses (several with managed actions) would alter fish CPUE as compared to low-flow pulses, potentially increasing CPUE with increased food availability in the upstream and downstream regions. While there were differences in CPUE observed over the course of the pulse phase in high-flow years, the expected increase from before-pulse to after-pulse was not observed; conversely, the highest CPUE was found before or during the pulses for the majority of analyses. While there is large variability in the magnitude of flow pulses that can affect fishes, it seems that flow pulse measures (and magnitude) in the present study may fall within the noise of tidal influences that would likely result in changes in CPUE.

Region and year were also considered as explanatory variables for fish CPUE. For tow data, CPUE was high in the upstream regions and in 2019, and for seine data, there was higher CPUE downstream and in 2015 for the smeltish and all fish assemblages (with were both composed of mostly Mississippi Silversides), and in Middle Sacramento River and 2019 for the native fish assemblage. While it was thought that perhaps water year type or flow pulse type (high- and low-flow) might influence catch in certain years, there is no evidence that there was higher catch during certain types of water years or flow pulse types.

High variability was exhibited in all the fish datasets. While fish catch is inherently variable, the variability of the dataset also indicates that there are many factors outside of region, year, and flow pulse phase that are influencing observed CPUE. Some of these factors are related to the natural environmental and biology of the organisms, while others are related to how the data were collected.

While fish movement may be influenced by the flow pulse, fish absence/presence is also strongly influenced by environmental conditions that were not used in these analyses (e.g., flow, tides, water temperature, turbidity, dissolved oxygen), as well as by fish biology and life history. While we did not have enough replicate years to explicitly detect the impact of water year type on the fish community, spring flows are known to control the abundances of many fishes and invertebrates in the region (Feyrer et al. 2017; Kimmerer et al. 2002), so a flow pulse during a wet year may impact the fish community differently than a flow pulse during a dry year. Previous studies of fish ecology in this region have found that water temperature is also a key

factor in determining winter fish migration through the region (Sommer et al. 2014), and Delta Smelt abundance (Brown et al. 2016).

The drought of 2012-2016, encompassing most of the years of our study, may have caused other changes that impact our ability to see the effects of the flow action. Evidence for a shift in the littoral fish community, with an increase in silversides, has been linked to the drought (Mahardja et al. 2017). Increases in the toxic cyanobacteria *Microcystis* and aquatic weeds seen during the drought may also have caused changes in the fish community in our study region (Lehman et al. 2017; Kimmerer et al. 2019).

The lack of a clear fish response to the flow pulse may also be partially due to the lack of clear zooplankton response to the flow pulse (See Chapter 4.4). Our hypothesized mechanism for increased fish catch was based on the premise that there would be increased zooplankton. Without a clear increase in zooplankton biomass, it is less clear that the flow pulse provided food benefits for pelagic fishes such as Delta Smelt. However, as described previously, the NDFS pulse signal may remain within the noise of tidal influences that affect fish as compared to other high magnitude pulses or outflow actions conducted in the Delta.

The before, during, after pulse phases overlap with certain months of the year in which fish may naturally move in or out of a given region. For example, many fishes, such as native minnows, spawn in late spring- early summer and then may move to deeper waters, while non-native species may spawn later in the summer (Moyle 2002). Thus, their movement may be due to natural patterns of movement rather than a relationship to the flow pulse. Similarly, high catches before the flow pulse may be picking up high abundance of young-of-the-year fish, many of which will not reach adulthood even under ideal conditions, so decreases in catch over the season is not surprising. Splittail, in particular, are consistently more abundant in the spring than in the fall due to their spawning pattern (McKenzie and Mahardja 2021).

It is important to note that this study was not designed to influence the fish analyzed from these surveys, and that the surveys were not designed to measure the effects of the flow pulses. The fish dataset composed of fish catch from several different surveys and survey types, each with their own set of stations, methods, and objectives that are independent of the flow pulse. Thus, some surveys may only have covered certain regions, or may have only

sampled during certain months or years. For example, EDSM is a high-frequency monitoring program that started in 2017, so total CPUE was higher 2017-2019 compared with 2013-2016. The two seine surveys (DJFMP and YBFMP) sampled in different regions, and have slightly different methods, which causes the comparison in regions to be confounded by survey.

The objective of the North Delta Food Subsidy action is to benefit certain fish species, such as Delta Smelt, through increased food subsidies. Thus in the future, if we want to monitor fishes more directly, it might be more useful to use more targeted experiments (such as described in section 5.5) and balanced surveys around the locations and dates of the flow pulses, or to specifically track Delta Smelt or congeners before/during/after the flow pulse to get a better idea of how flow pulses influences these species. Additionally, as described in this chapter, experimental enclosures can be a tool for assessing the impact of flow action on Delta Smelt health. With planned supplementation of the species, and/or experimental releases, there is potential to coordinate better tracking of managed flow pulse effects on supplemented fish.

5.4 Fish and Zooplankton Interactions

5.4.1 Methods

To see if zooplankton abundance correlated with fish abundance, we merged the zooplankton data synthesized in Chapter 4 (Lower Trophic Food Web) with the general fish data described above in section 5.3. Next, we filtered the data to dates within before, during, and after flow pulse periods and summed fish count and zooplankton CPUE by flow pulse phase and year. The data were separated by fishing method type: Fall midwater trawl, townet, and Kodiak trawl were defined as 'tow' methods and beach seines from the YBFMP and DJFMP were defined as the 'seine' method. We then analyzed the data using a generalized linear model with a negative binomial distribution in R (version 4.0.4; R Core Team 2021) using the MASS package (Ripley et al. 2021). We used the summed fish count as the response variable and a combination of zooplankton CPUE, year, pulse phase, and an offset of log sampling effort as coefficients. We then compared models using Akaike Information Criterion adjusted for small sample size (AICc).

5.4.2 Results

The model which incorporated zooplankton CPUE and flow pulse phase ranked highest for both the tow and seine sampling methods (Table 5-2; Table 5-4). Zooplankton CPUE was negatively correlated with beach seine fish count and was not significantly correlated with the tow fish count.

AICc results for comparing generalized linear models of summed fish catch data from tow methods are summarized in Table 5-2. Fish_Count_sum = the summed fish count data by year, flow pulse phase, and method. Zoop_CPUE_sum = the summed zooplankton CPUE summed by year and flow pulse phase. PulsePhase = the flow pulse phase during which the sample was taken (Before, During, or After). Year = the year the sample was taken (2014, 2015, 2016, 2017, 2018, or 2019). Offset(SampleEffort) = an offset of the log of the sample effort (volume sampled) by year and flow pulse phase.

Table 5-2. Fish Count Models Using Tow Methods.

Rank	Model	AICc	dAICc	Df	weight
1	Fish_Count_sum ~ Zoop_CPUE_sum + PulsePhase + offset(SampleEffort)	341.6	0	5	0.9930
2	Zoop_CPUE_sum + Year + offset(SampleEffort))	353.2	11.7	8	0.0029
3	Year + PulsePhase + offset(SampleEffort))	353.4	11.8	9	0.0027
4	Zoop_CPUE_sum + Year + PulsePhase + offset(SampleEffort))	354.7	13.1	10	0.0014

A summary of coefficients from the top-ranking model using tow data are reported in Table 5-3. Zoop_CPUE_sum = the summed zooplankton CPUE summed by year and flow pulse phase. PulsePhase = the flow pulse phase during which the sample was taken (Before, During, or After). None of the factors had a statistically significant effect on fish count.

Table 5-3. Summary of Top-Ranking Tow Model.

Coefficient	Estimate	Standard Error	Z-Value	P-Value
Intercept	-5.007	3.122×10^{-1}	-16.039	$<2 \times 10^{-16}$***
Zoop_CPUE_sum	6.379×10^{-7}	4.496×10^{-7}	1.419	0.156
PulsePhaseBefore	4.265×10^{-1}	4.231×10^{-1}	1.008	0.313
PulsePhaseDuring	1.559×10^{-1}	4.149×10^{-1}	0.376	0.707

AICc results for comparing generalized linear models of summed fish catch data from seine methods are reported in Table 5-4. Fish_Count_sum = the summed fish count data by year, flow pulse phase, and method. Zoop_CPUE_sum = the summed zooplankton CPUE summed by year and flow pulse phase. PulsePhase = the flow pulse phase during which the sample was taken (Before, During, or After). Year = the year the sample was taken (2014, 2015, 2016, 2017, 2018, or 2019). Offset(SampleEffort) = an offset of the log of the sample effort (volume sampled) by year and flow pulse phase.

Table 5-4. Fish Count Models Using Seine Methods.

Rank	Model	AICc	dAICc	Df	weight
1	Fish_Count_sum ~ Zoop_CPUE_sum + PulsePhase + offset(SampleEffort)	346.9	0	5	0.9982
2	Zoop_CPUE_sum + Year + offset(SampleEffort))	359.6	12.7	8	0.0018
3	Year + PulsePhase + offset(SampleEffort))	367.2	20.3	9	<0.001
4	Zoop_CPUE_sum + Year + PulsePhase + offset(SampleEffort))	376.4	29.5	10	<0.001

Summary of coefficients from the top-ranking model using seine data are reported in Table 5-5. Zoop_CPUE_sum = the summed zooplankton CPUE summed by year and flow pulse phase. PulsePhase = the flow pulse phase during which the sample was taken (Before, During, or After). Zooplankton CPUE displayed a weak negative correlation with fish count (p = 0.033).

Table 5-5. Summary of Top-Ranking Seine Model.

Coefficient	Estimate	Standard Error	Z-Value	P-Value
Intercept	-7.512 x 10-1	1.370×10^{-1}	-5.481	4.22×10^{-8}***
Zoop_CPUE_sum	-4.204×10^{-7}	1.974×10^{-7}	-2.129	0.0332*
PulsePhaseBefore	2.907×10^{-1}	1.858×10^{-1}	1.565	0.1176
PulsePhaseDuring	2.197×10^{-1}	1.821×10^{-1}	1.207	0.2276

5.4.3 Discussion

Our analyses found little correlation between fish count with zooplankton CPUE, year, and pulse phase. However, the datasets available were not ideal matches. The fish data came from a variety of sampling programs targeting various fish species, of which zooplankton is not always a top prey item. Additionally, the main location we would expect to see an effect on planktivorous fish is in the Yolo Bypass Toe Drain and upper Cache Slough Complex. The only fish data collected in this location during the flow pulse phases is the YBFMP's bi-weekly beach seines, which may be an insufficient sampling frequency to detect changes in fish abundance for these purposes. Furthermore, fish abundance in the region is complicated by season, life history, and environmental conditions, as discussed in section 5.3.3.

More data is needed to understand if flow pulse-related zooplankton abundance directly impacts fish abundance through the increase of food resources. Other studies have found a positive relationship between zooplankton abundance and pelagic fish abundance in the system (Feyrer et al. 2014; Hammock et al. 2017; Hammock et al. 2019) and a more targeted data collection might allow us to better evaluate the effect of the flow pulse action. This data could come in the form of increased fish sampling before, during, and after the flow pulse periods and more years of flow pulse data, especially form years in which a phytoplankton bloom occurs. However, collecting this additional data may be infeasible or not occur soon enough to help inform adaptive management. It may be timelier and more effective to focus on smaller studies targeting key fish species of interest.

5.5 Delta Smelt

5.5.1 Methods

Delta Smelt Enclosure Study

To evaluate the potential for flow pulses to benefit Delta Smelt directly, smelt from the Fish Conservation and Culture Facility (FCCL; Byron, CA) were individually marked with visible implant alpha (VIA) tags and placed in experimental enclosures within the Yolo Bypass Toe Drain and in the Sacramento River near the city of Rio Vista (Figure 5-6). This targeted study occurred only during the 2019 flow action period and included two separate deployments of cultured smelt.

1. The first deployment took place at Rio Vista from July 30th – August 28th and at the Yolo Bypass from July 30th – August 19th. The Yolo Bypass cage was pulled early due to increasing temperatures in the Toe Drain. Due to a limited number of cages available, three were placed at Rio Vista and only one at the Yolo Bypass. The three at Rio Vista were strung between two anchoring points and the one in the Yolo Bypass Toe Drain was attached to the DWR screw trap, which was not being operated at the time.

2. The second deployment took place at Rio Vista from October 8th – November 6th and at the Yolo Bypass from October 9th – November 7th. This included three cages strung between anchoring points at both the Rio Vista and Yolo Bypass location. While overall cage design, size, and mesh opening was the same, the cages used in this deployment were made from aluminum, rather than steel as was the case in the first deployment. These new cages were used as they allowed for more replication and were easier to transport.

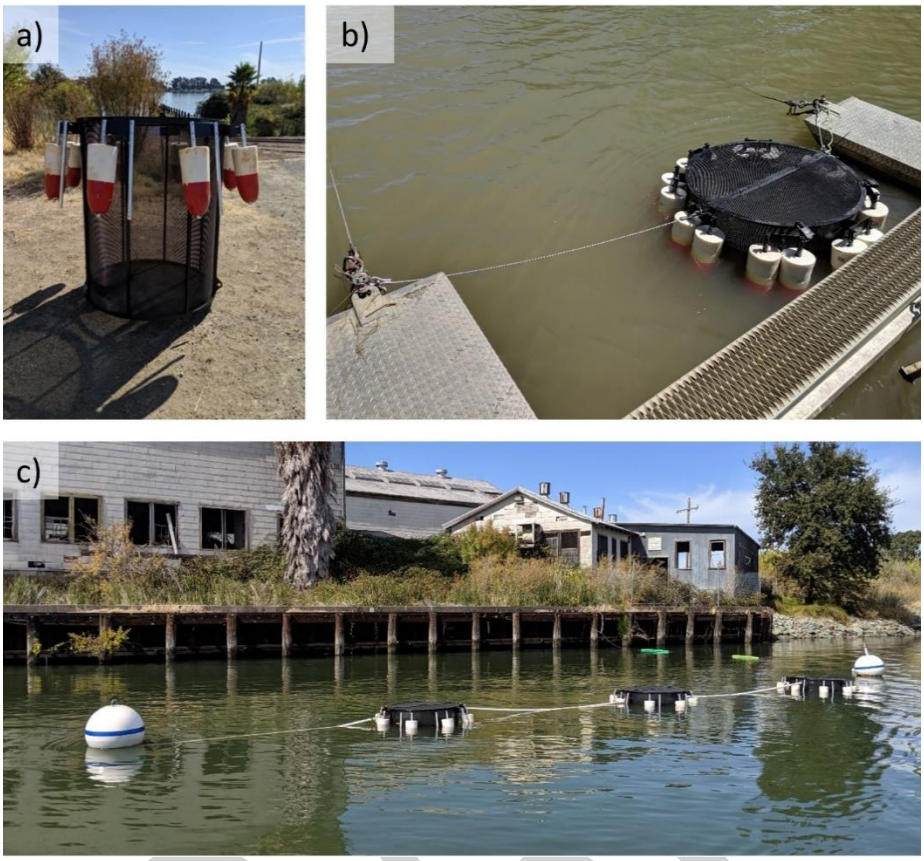

Figure 5-6. a) Design of the Delta Smelt enclosures; b) A smelt cage in the Yolo Bypass, tethered to the DWR screw trap; c) Three cages anchored in the Sacramento River in Rio Vista.

At the conclusion of each experimental period, all remaining fish were collected from each enclosure. They were subsequently euthanized, weighed (g), and measured (mm fork length). Following this, the preserved bodies of 10 fish per enclosure were subsequently dissected and the stomach was removed for diet analysis at the Wetland Ecosystem Team laboratory (Seattle, Washington USA). The total contents of each stomach were weighed and identified. A subset of fish was also kept at the FCCL to serve as a control population and were similarly weighed and measured following the conclusion of the field deployment. Since the fish were too small to individually tag for the study, a batch measurement was taken of a subset of fish pre-deployment to serve as a comparison for weight and length prior to the study.

Data Analysis

Statistical analyses were conducted for all deployments besides the summer Yolo Bypass deployment, in which all fish perished due to high water

temperatures. The health of the fish was measured by calculating condition factor: Weight / Fork Length^3, where weight is in grams and fork length is in centimeters. Delta condition factor was subsequently calculated to determine whether the health of the fish increased or decreased over the deployment:

Condition Factor [post-deployment] – Condition Factor [pre-deployment].

While VIA tags were used to keep track of individual fish, a small proportion of fish shed their tags, or may have been misread. Thus, delta condition factor was calculated only for fish with matching pre- and post- VIA tags.

Due to violations of normality and homogeneity of variance for parametric analyses, non-parametric tests were used for statistical analyses. The Kruskal Wallis test (R, stats package) was used to assess differences in delta condition factor between caged fish, batch fish, and control fish within each deployment period. If results were significant at alpha = 0.05, the post-hoc Dunn test (R FSA package; Ogle et al. 2021) with a Bonferroni correction was used to assess which groups were significantly different from each other.

Non-metric multidimensional scaling (nmds) and permutational multivariate analysis of variance (PERMANOVA) were used to evaluate whether zooplankton present during the flow action were similar to those present in the diet contents of caged Delta Smelt (R, vegan package; Oksanen et al. 2021). Zooplankton data was obtained from the present Lower Trophic technical team (Chapter 4) and filtered to only include data from the YBFMP screw trap (STTD) and RVB station, which were respectively located adjacent to the Yolo Bypass and Rio Vista smelt cage locations. The zooplankton STTD and diet Yolo Bypass site were collectively referred to as "YB" while the RVB and Rio Vista sites were called "RV." Next, available data was filtered to months in which the caged smelt were present and categorized by season: August (summer) and October (fall). Finally, taxa were standardized across diet and zooplankton samples. As zooplankton taxa were commonly identified in greater detail, these taxa were merged where necessary to match the higher taxonomic levels reported in the diet data. Unique taxa that did not have matches across zooplankton and diet samples were kept in the analysis. For each zooplankton or diet sample, each prey abundance was converted into overall proportion of the sample, to account for the large difference in total count between zooplankton ("ambient") and diet samples. Zooplankton were analyzed by type (diet or ambient), season (summer or fall), and site (YB or

RV).

5.5.2 Results

Health and Survival

With high water temperatures during the summer deployment, Delta Smelt survival was lower, ranging from 0% in the Yolo Bypass to 67% at Rio Vista (Table 5-6). While Yolo Bypass fish did not survive the duration of the deployment, several live fish were observed in the Yolo Bypass cage via underwater video camera three days before cage removal, indicating that fish were able to survive in high temperatures (mean 24.8ºC, up to 27ºC) for moderate periods of time (Figure 5-7). Smelt survival during the fall deployment was much higher (Table 5-6).

Table 5-6. Proportion of Delta Smelt Survival during Summer and Fall Deployments. For July-August in Yolo, n = 60; for all other sites and deployments, n = 180.

Period	Site	Survival
July-August	Rio Vista	67%
July-August	Yolo Bypass	0%
October-November	Rio Vista	89%
October-November	Yolo Bypass	92%

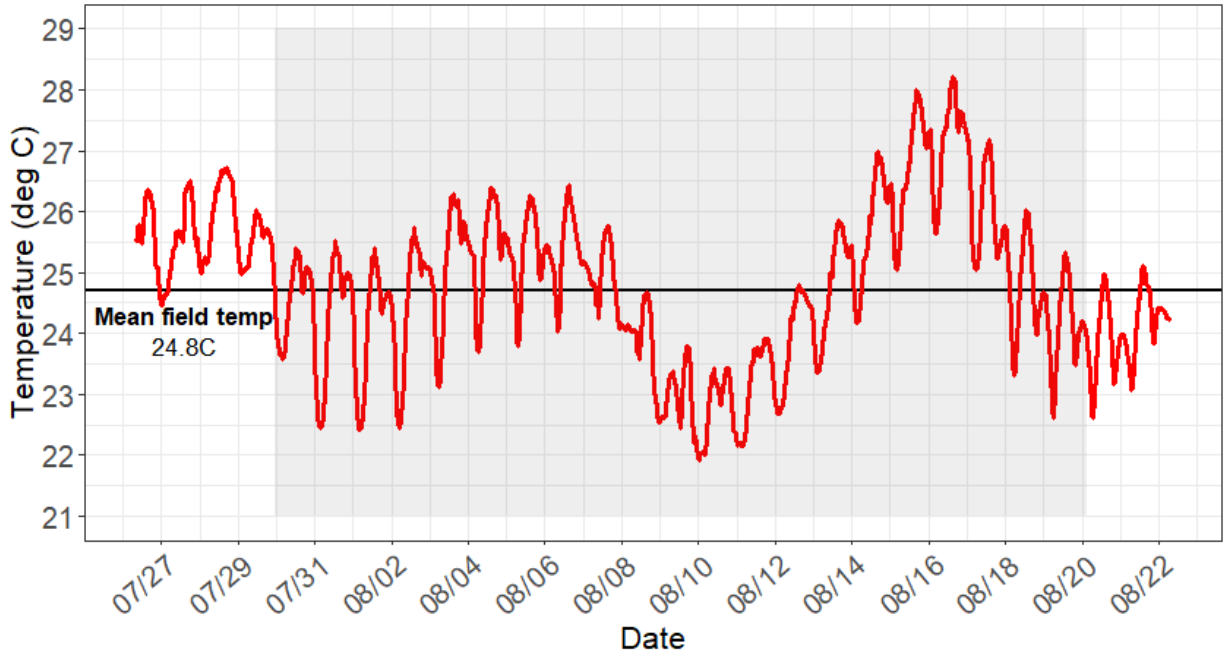

Figure 5-7. Temperature Profile at Yolo Bypass during August Cage Deployment. Continuous temperature data plotted from Lisbon sensor in the Yolo Bypass. Gray box outlines the dates of Delta Smelt deployment in the Yolo Bypass.

Delta Smelt condition factor decreased between pre-deployment ("batch") fish and post-deployment field fish in the fall but not the summer (Table 5-7; Figure 5-8). In the summer, the delta condition factor was -0.039 in RV, which was higher than delta condition factor for control FCCL fish. In the fall, delta condition factors were not significantly different, ranging from -0.130 in the Yolo Bypass to -0.150 at Rio Vista. All delta condition factors for fall deployments were lower than delta condition factor for FCCL control fish.

Table 5-7. Average Delta Condition Factor for Delta Smelt during Summer and Fall Deployments. Because fish were not individually tagged and tracked, condition factors were averaged for each site, and for pre-deployment.

Period	Site	Delta Condition Factor	n
July-August	Rio Vista	-0.039	121
July-August	Control	-0.048	60
October-November	Rio Vista	-0.150	161
October-November	Yolo Bypass	-0.130	161
October-November	Control	-0.064	60

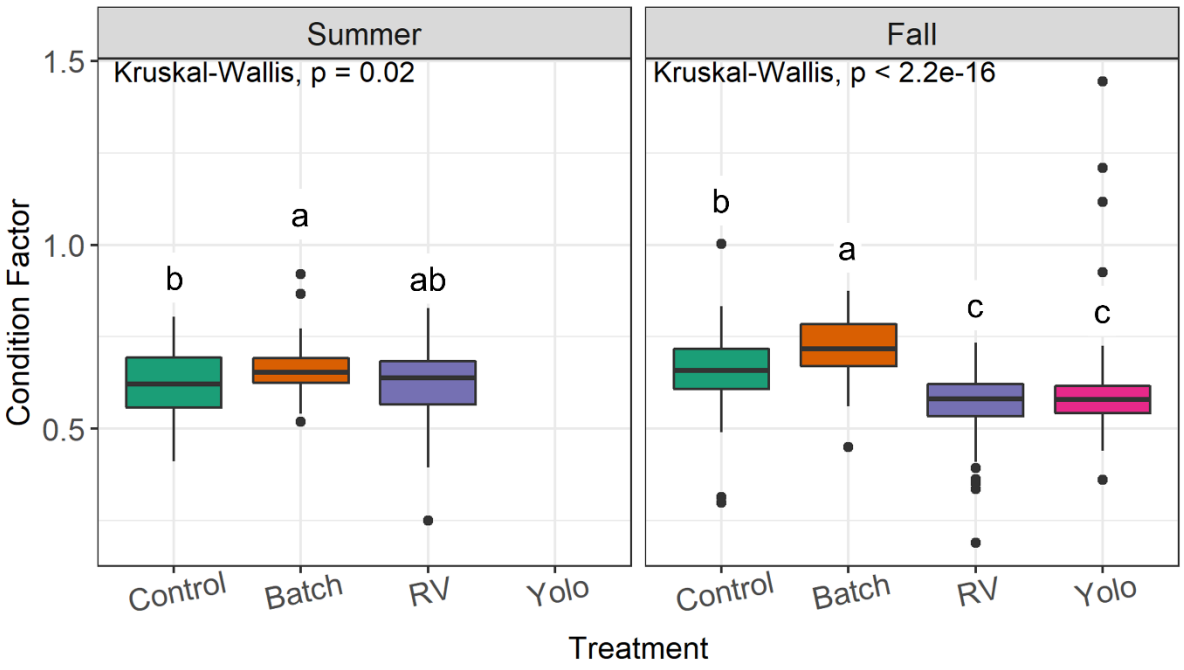

Figure 5-8. Condition factor boxplots of caged Delta Smelt during the summer and fall deployments. Batch = FCCL fish measured at the beginning of the study period, Control = FCCL fish measured at the end of the study period.

Diet vs. Ambient Zooplankton

Proportional species catch based on the type of sample (diet vs. ambient) was somewhat different but also contained a fair amount of overlap. There was more overlap of catch between sites, though the two sites still contained some differences. There were also differences by season, though this only explained 7% of the variance. (Table 5-8).

Table 5-8. PERMANOVA results of Delta Smelt diet and ambient zooplankton.

Factor	Df	SS	MS	F	R2	P
Type	1	4.0482	4.048	21.251	0.166	0.001
Site	1	4.9208	4.920	25.832	0.202	0.001
Season	1	1.7359	1.7359	9.113	0.071	0.001

A non-metric multidimensional scaling (NMDS) plot of proportional species catch highlights the difference in catch between diet and ambient samples (Figure 5-9). There was some selectivity at play, as Delta Smelt often did not eat smaller zooplankton such as nauplii or rotifers and also consumed macroinvertebrate species, such as *Gammarus sp.* and *Hyalella sp.* that are not designed to be captured by zooplankton tows.

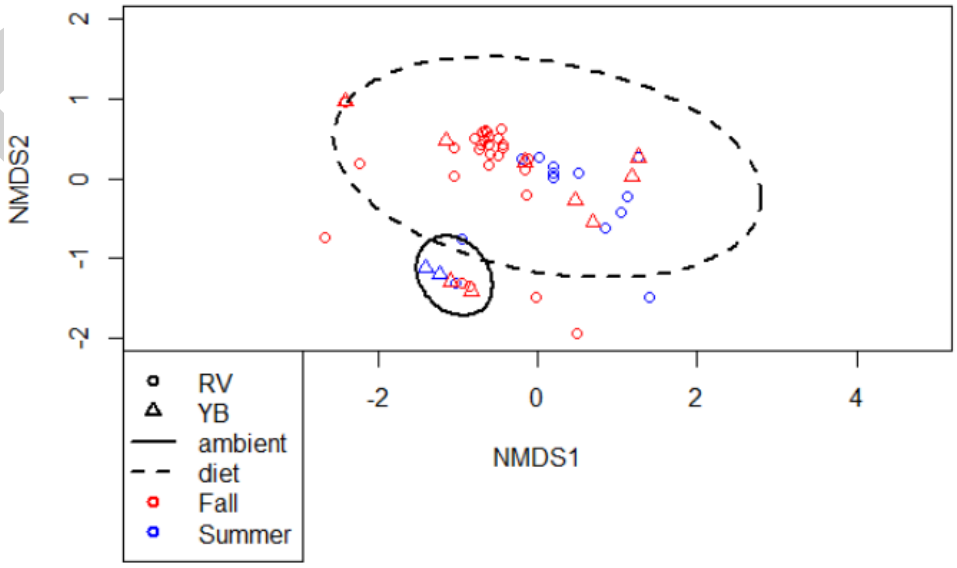

Figure 5-9. NMDS plot showing the relationship between zooplankton taxa as categorized by type, site, and season.

5.5.3 Discussion

Our limited data suggest that Delta Smelt could survive and benefit from any food resources exported by the flow action. The Delta Smelt enclosure studies of 2019 found that fish were able to survive and forage in both the Yolo Bypass and at Rio Vista during time periods in which the flow actions occur. While the caged Delta Smelt in the Yolo Bypass experienced high mortality during the extreme mid-August heat wave, wild fish would likely have been able to escape to cooler water during such a period and return when temperatures decreased. Additional years of data and tailored studies are needed to draw meaningful conclusions about the effect the managed North Delta Food Subsidy (NDFS) action on Delta Smelt health, survival, and diet.

Analysis of zooplankton tow and smelt diet data showed differences between the two sample types and between sites, but there was also a fair amount of overlap. Some of the key drivers of these differences were due to prey selectivity for larger species and the presence of macroinvertebrates on the cages. Previous studies of Delta Smelt diets have found that smelt do select for certain copepod species over others, and regularly consume amphipods and insects not sampled by zooplankton tows (Slater and Baxter 2014; Whitley and Bollens 2014). The presence of amphipods in our Delta Smelt diet data highlights the fact that by comparing diet to zooplankton abundance this analysis does not necessarily encapsulate all food resources that may be in the system and/or produced as a result of flow actions. The fair amount of overlap, however, suggests that Delta Smelt caged in the field were able to forage on many of the zooplankton species present in the environment. Generally, this analysis suggests that Delta Smelt could take advantage desirable food resources, if produced or exported by NDFS.

5.6 Chinook Salmon and Central Valley Steelhead

5.6.1 Methods

Salmon Straying

Data Compilation

We obtained Chinook Salmon and Central Valley Steelhead (steelhead) catch data from DWR's Yolo Bypass Fish Monitoring Program (YBFMP), which has been monitoring adult fish composition in the Yolo Bypass through fyke trap sampling since 2000. The YBFMP operates this sampling from October - June in the Toe Drain utilizing a 3 m diameter, 7.3 m long fyke trap (Figure 5-10). DWR sets the fyke trap every Monday morning and leaves the trap in the Toe Drain through Friday, checking for fish catch every 24 hours or less. We used flow data from the Lisbon Weir flow gauge in the Yolo Bypass, which is located just upstream of the YBFMP fyke trap. Data from 2011-2019 were obtained from the Water Quality technical team (Chapter 3) and additional data from 2003-2010 was downloaded from the California Data Exchange website.

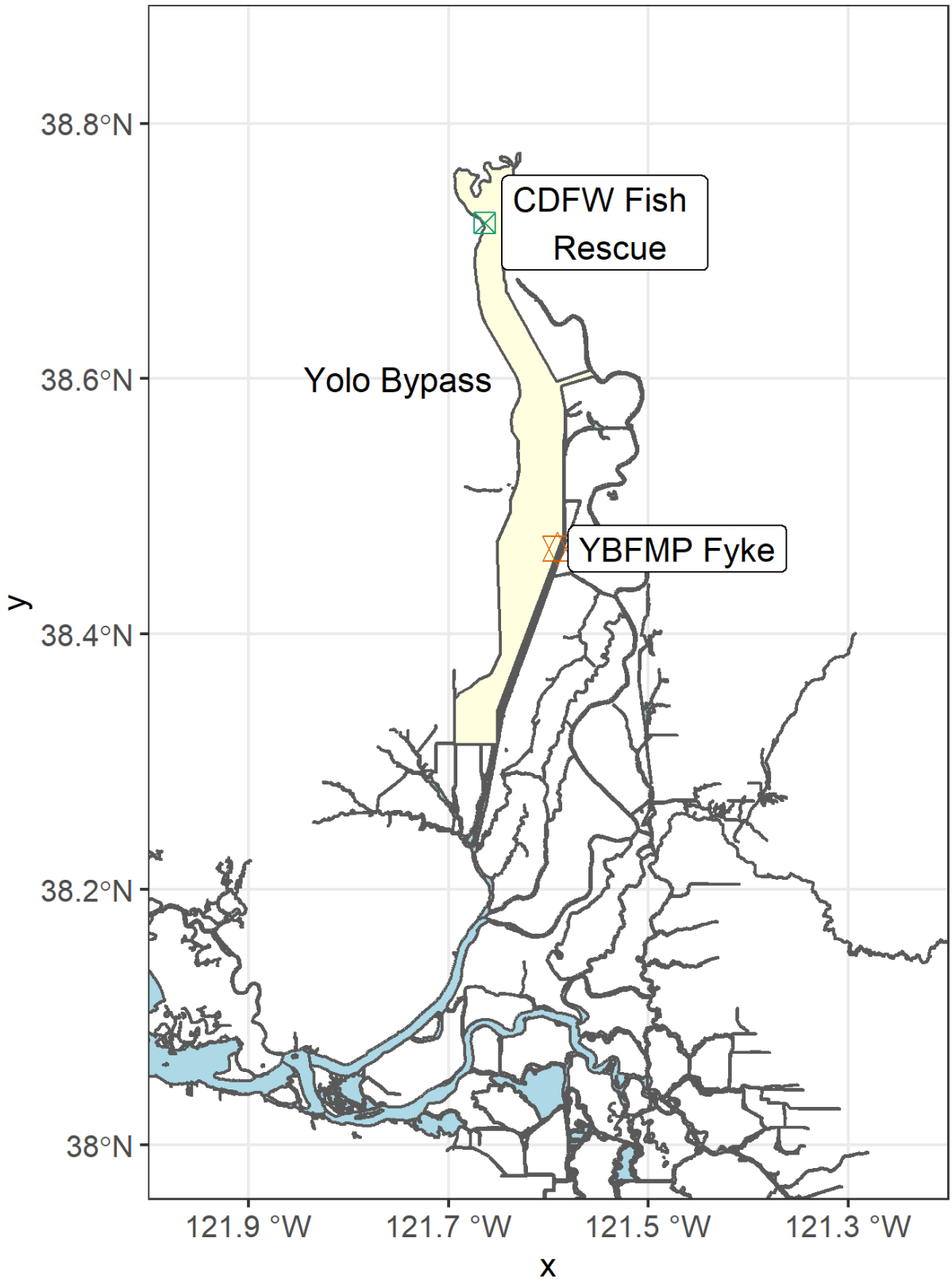

Figure 5-10. Sites of adult Chinook Salmon sampling in the Yolo Bypass.

To understand how catch in the Yolo Bypass related to overall regional salmon abundance, we obtained data on Sacramento River watershed overall salmon returns for all runs and origin types (CDFW 2000-2018). This data was provided by the CDFW GrandTab Adult Escapement's California Central Valley Chinook Population Database Report (Columbia Basin Research 2020). This data describes adult returns on an annual basis. To better describe how the timing of catch in the Yolo Bypass aligns with salmon migration, we obtained data on the historical timing of fall-run Chinook Salmon adults entering the Sacramento River in average percent per week from 1970-1988 from Doug Killam of CDFW (pers. comm.). Only 18 steelhead were caught in the fyke trap during the years of interest, so were excluded from further analysis.

Previous studies have found that an increase in transport distance (downstream of the hatchery) of juvenile Chinook hatchery fish results in higher straying rates when salmon return as adults (Lasko et al. 2014; Sturrock et al. 2019). To understand how this might apply to the Yolo Bypass system, we synthesized juvenile Fall-run Chinook Salmon hatchery trucking data downloaded from the Bay Delta Live website.

It is possible for salmon that migrate into the Yolo Bypass to find suitable spawning habitat in Putah Creek, a tributary to the Toe Drain. Thanks to restoration efforts and better management of fish barriers, this small creek has seen a rebound in salmon population beginning in 2014. Since this time, the Solano County Water Agency and University of California, Davis have been tracking adult return estimates through carcass and redd surveys (Miner et al. 2020; Willmes et al. 2021). However, data from acoustically tagged Fall-run Chinook, a subset of all salmonids entering the Bypass, suggest that most straying fish successfully exit the Yolo Bypass (Johnston et al. 2020).

Finally, to get a sense of annual stray rates of Central Valley Chinook Salmon, we obtained coded-wire tag (CWT) recoveries annual stray estimates from the California Department of Fish and Wildlife (CDFW) coded-wire tag recovery reports.

Data Analysis

We examined Chinook Salmon catch data from the YBFMP fyke trap from 45 days before the start of the NDFS action (or from the date the YBFMP fyke trap was deployed for the season, whichever came fist) extending 45 days beyond the end of the NDFS action each season (to determine if the flow pulses might attract migrating adult Chinook into the Bypass). This time period encompasses the time we would expect migrating Fall-run adult salmon, potentially influenced by the flow pulses, to be in the system. Additionally, we examined genetic identification (2015-2019) of YBFMP Chinook catch for the presence of state-and federally threatened spring-run or state- and federally endangered winter-run. Overall, there were too many zeros in the catch data to effectively model count, thus we converted the data into weekly presence/absence of salmon. We then used the R stats package (version 3.6.3) to perform a logistic regression on the presence/absence data, weekly average flow, week, and year to determine if there was a relationship between flow and salmon presence, week, or year (R Core Team 2020).

Analysis of the relationship between flow and Chinook catch showed a negative relationship; higher flow resulted in lower catch rates and vice versa (see 5.6.2 Results). However, given the complexity of Chinook Salmon migration and straying influences, we explored further by collating the other synthesized datasets into a multi-plot comparing YBFMP Chinook salmon catch, both as total annual catch and annual monthly catch per hour, to:

1. Yolo Bypass average flow at Lisbon Weir between the months of July – October. We subset the flows to this period to better isolate pulse flows from other, unrelated periods of flow such as late winter/early spring storm events.
2. Annual Sacramento River adult returns of all Chinook Salmon runs and origin types.
3. The average miles juvenile hatchery fish were transported 2-, 3-, and 4-years prior. Most adult salmon return to spawn between the ages of 2-4, so this average would encapsulate the period in which they were juveniles.
4. The annual estimated number of adult returns to Putah Creek, a tributary to the Toe Drain canal.
5. The annual estimated stray rate of Central Valley Chinook Salmon

returns based on CWT recovery data.

We also assessed how the timing and type of flow pulses correlate to Chinook salmon. We visually compared the timing of flow pulses with the timing of historic fall-run Chinook migration and catch in the Yolo fyke trap. To see the impact of flow pulse types on Chinook Salmon catch, we calculated the total Yolo fyke catch of adult Chinook Salmon in the 45 days before the flow pulse, during the flow pulse, and 45 days after the flow pulse for each year. We then used two generalized linear models with a negative binomial distribution to model the total catch of salmon in each period versus flow pulse size (high versus low pulse or managed versus non-managed) and flow pulse period.

2019 Wallace Weir Rescues

Data Compilation

Salmonid rescues at Wallace Weir are carried out by the California Department of Fish and Wildlife (CDFW; Figure 5-10, Figure 5-10). More information on this program and the associated fish rescue and environmental data can be found at the CalFish website. Although CDFW has been conducting and recording data on fish rescues at this site since 2014, the only year with substantial salmonid catch overlapping with NDFA operations was 2019, due in part to the completion of the Wallace Weir Fish Rescue Facility (WWFRF; Figure 5-11). Because of the difference in methods and magnitude of total catch between years, only the "Wallace Weir Catch Data 2019-2020" file (CalFish website) was used for this analysis. During the timeframe of this analysis, CDFW used both WWFRF operation and beach seining to rescue fish. Method of operations of the WWFRF varied over the course of this analysis, as this was the first season of operation, but generally involved passing approximately 50 cfs of flow through the fish rescue facility entrance (Figure 5-11) for one to 25 hours, and checking the trap for fish once or twice per day. Beach seine methods were used when the WWFRF was not operational in the "After" period, and safely rescuing the salmonids was the top priority during these activities. The methods are adapted from Hahn et al. (2007). Generally, CDFW staff hauled a 29-meter-wide beach seine approximately 90 meters once or more per day to corral all salmonids present in the area for rescue. Both methods conclude by hauling the rescued salmonids in a

transport tank to the Sacramento River for release. The WWFRF method was used more often, operating most of the days between 8/26 and 10/11, while the beach seine method was used for only four days (10/18, 10/24, 10/28, and 11/4). Because these methods were irregular, total daily catch was used in this analysis instead of catch per unit effort (CPUE). CDFW records the species and adipose fin presence/absence of each individual captured during sampling. For fall-run Chinook Salmon, if the adipose fin is clipped, it means the fish is most likely of hatchery origin. If the adipose fin is present, it indicates the fish could be of wild or hatchery origin.

Figure 5-11. Wallace Weir.

The flow data used in this portion of the analysis is from the DWR Lisbon Weir water quality gauge (CDEC gauge: LIS; 38.474781°, -121.588226°). This data was compiled and QA/QC'd by the water quality sub-team, and further information about this process can be found in section 3.3.1 Continuous Water Quality.

Data Analysis

This analysis was primarily visual and qualitative in nature, with the following data manipulation, analysis, and graphing carried out using R statistical software (R Core Team 2021). The data from the above sources were filtered to only include 2019 NDFS dates (During phase) as well as 45 days before the flow pulse began (Before) and 45 days after the flow pulse ended (After). The 15-minute flow readings were averaged to generate a daily average flow, with any missing values in a day resulting in an NA value for daily average flow. The salmonid catch data was broken out by species and adipose fin presence/absence, with values representing total daily catch.

Salmonid Health

Data Compilation

The temperature and dissolved oxygen (DO) data used in this portion of the analysis are from the DWR Lisbon Weir water quality gauge (CDEC gauge: LIS; 38.474781°, -121.588226°). This data was compiled and QA/QC'd by the water quality sub-team, and further information about this process can be found in section 3.3.1, Continuous Water Quality. Continuous water quality data collection began at this site in 2013, therefore there is no continuous temperature or dissolved oxygen (DO) data for 2011 or 2012. The conservative temperature maximum (degrees Celsius) and DO minimum (mg/L) thresholds for salmonids were agreed upon based on review of relevant literature (Richter and Kolmes 2005; NMFS 2008).

Data Analysis

The following data manipulation, analysis, and graphing was carried out using R statistical software (R Core Team 2021). The data from the above source was filtered to only include relevant flow pulse dates (Before, During, and After). The 15-minute temperature and DO readings were averaged to generate a daily average temperature and daily average DO, with any missing values in a day resulting in an NA value for daily average temperature/DO.

5.6.2 Results

Salmon Straying

YBFMP sampling found zero genetically confirmed (>80% genetic probability) winter-run or spring-run Chinook Salmon catch. There were two inconclusive spring-run captured and released on November 10, 2015, and October 5, 2016. The genetic probabilities for these fish were 0.604 and 0.614, respectively. A run identity is only confirmed when the genetic probability exceeds a 0.8 probability. Examining the data for federally threatened Central Valley steelhead caught in the YBFMP fyke revealed four individuals were captured and released. All were captured in November and December (one in 2017, two in 2018, and one in 2019.

To evaluate whether flow (cfs) had any notable impact on adult salmon catch, we plotted average weekly salmon catch in the YBFMP fyke trap compared to average weekly flows at the Lisbon Weir (

Figure 5-12). This visual analysis shows the most salmon presence during periods of low flows. A logistic regression using salmon presence/absence data and Lisbon flow data supported the visual analysis, finding a negative relationship between catch and increasing flows (p=0.006;Figure 5-9; Table 5-12).

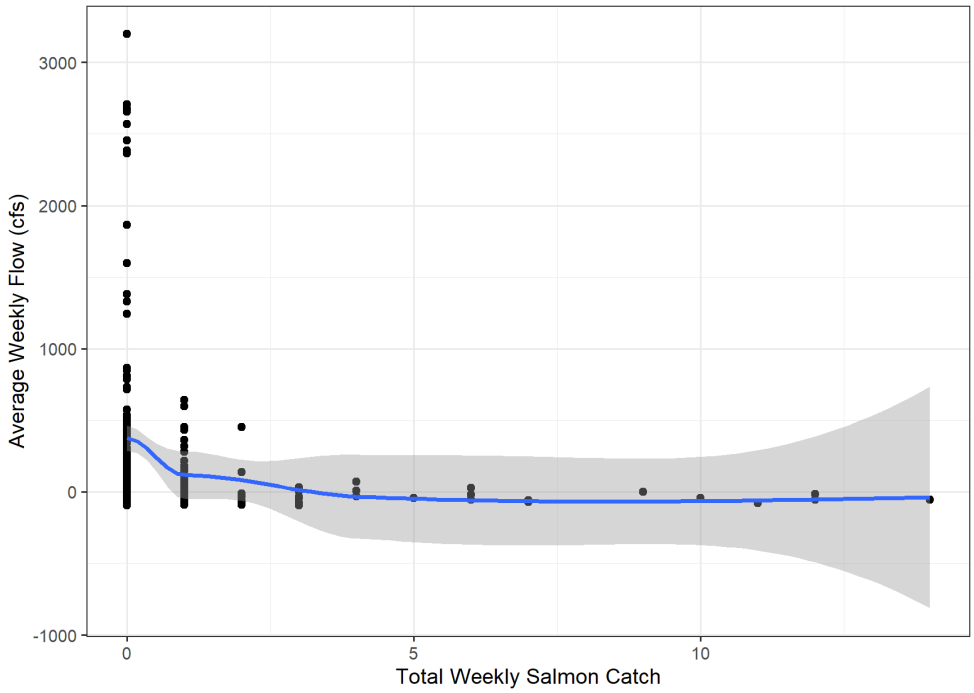

Figure 5-12. Weekly average salmon catch in the YBFMP fyke trap vs average weekly flow at Lisbon Weir between September-December with a LOESS regression line in blue.

Table 5-9. Results of logistic regression of salmon presence/absence and average weekly flow.

	Estimate	**Standard Error**	***p value***
intercept	4.737e+00	2.340e+00	0.0429 *
Average flow	-3.524e-03	1.277e-03	0.0058 **
week	-7.220e-02	4.642e-02	0.1199
2004	-2.872e+00	1.481e+00	0.0524
2005	-1.275e+00	1.234e+00	0.3012
2006	-4.726e-01	1.301e+00	0.7164
2007	-2.024e+00	1.242e+00	0.1032
2008	-1.877e+01	1.010e+03	0.9852
2009	-2.118e+00	1.237e+00	0.0870
2010	-2.400e+00	1.323e+00	0.0696
2011	-2.383e+00	1.293e+00	0.0653
2012	-1.289e+00	1.259e+00	0.3060
2013	-1.397e+00	1.194e+00	0.2422
2014	-1.630e+00	1.312e+00	0.2143
2015	-1.465e+00	1.166e+00	0.2091
2016	-1.908e+00	1.287e+00	0.1383
2017	-8.395e-01	1.211e+00	0.4882
2018	-1.368e+00	1.219e+00	0.2618
2019	-1.042e+00	1.185e+00	0.3792

A faceted plot of potential influences for adult salmon presence in the Yolo Bypass highlight the complex suite of straying factors which make it difficult to disentangle the impact of flow pulses on salmon (Figure 5-13). There is a notable uptick in adult salmon catch in the Yolo Bypass fyke trap beginning in 2012 with large peaks in 2015 and 2017. We see that around the same time salmon catch increases, overall Sacramento River watershed salmon returns decrease, juvenile transportation miles and watershed-wide straying rates increase, and more adults return to Putah Creek. Further confounding these data are the environmental conditions faced by all outmigrating juveniles in the Sacramento watershed which may influence future homing ability, prevailing ocean conditions, sampling frequency and trap efficiency of the YBFMP fyke trap, and water temperature.

Examining the timing of flow pulses and fyke trap catch in relation to historic migration timing shows that the flow pulses typically coincide with the time of

year adult fall-run Chinook are beginning their upstream migration (Figure 5-14). There is no regular monitoring of adult salmon on the lower Sacramento, so we cannot be sure this timing is accurate for the years used in this analysis. However, the fall time period when the flow pulse occurs is likely the time period when Chinook Salmon abundance in the system is increasing. Therefore, an increase in Chinook catch during or after the flow pulse may be due to the pulse or may be due to increase in the number of fish in the system.

Analysis of catch of salmon in the Yolo fyke found there were significantly more adult salmon caught after the flow pulse (Figure 5-15, Figure 5-16, Table 5-10, Table 5-11), and significantly more salmon caught in years with low-flow pulses than high-flow pulses (Table 5-10), but no significant difference between years with managed versus non-managed pulses (Table 5-11).

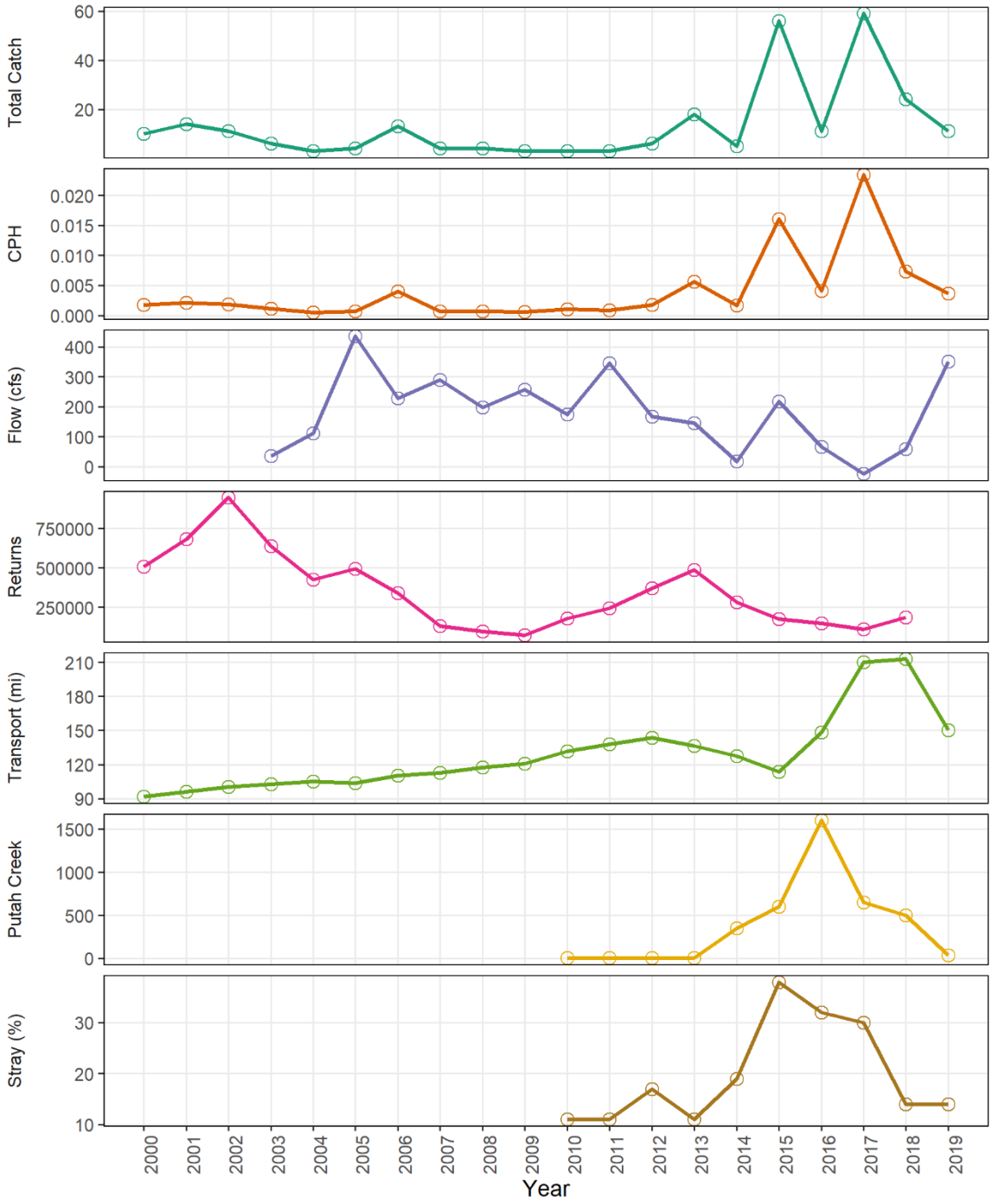

Figure 5-13. Chinook Salmon catch relative to other straying influences. In descending order: YBFMP Chinook Salmon total catch, YBFMP Chinook Salmon catch per hour (CPH), flow at Lisbon Weir (July-Oct average), Sacramento River watershed adult salmon returns, trucking miles of hatchery fish as juveniles 2-4 years prior, Putah Creek salmon returns, and Central Valley estimated stray rates.

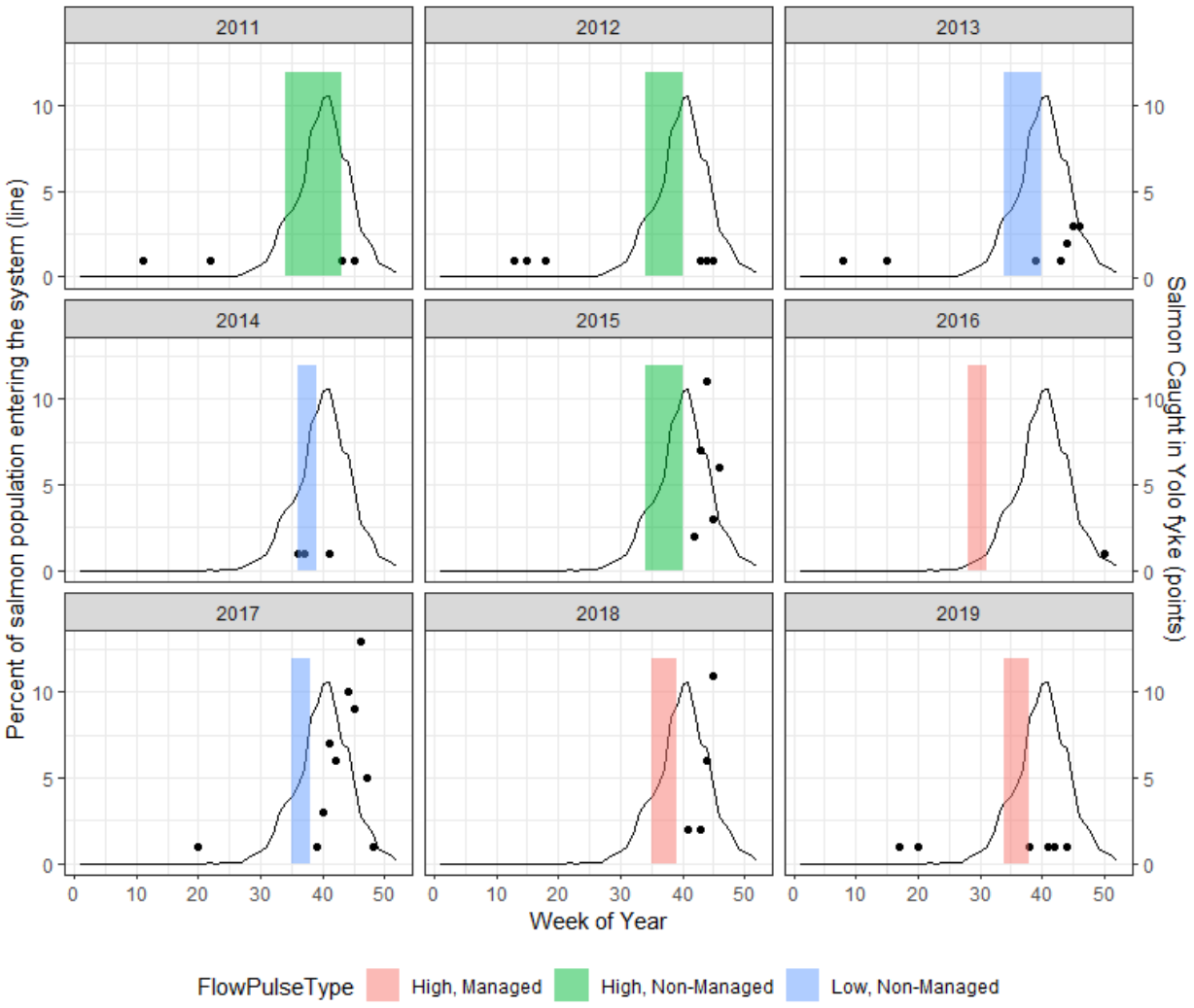

Figure 5-14. Timing of flow pulses in relation to historic Fall Run Chinook migration timing and Yolo Bypass Fish Monitoring Program fyke trap catch.

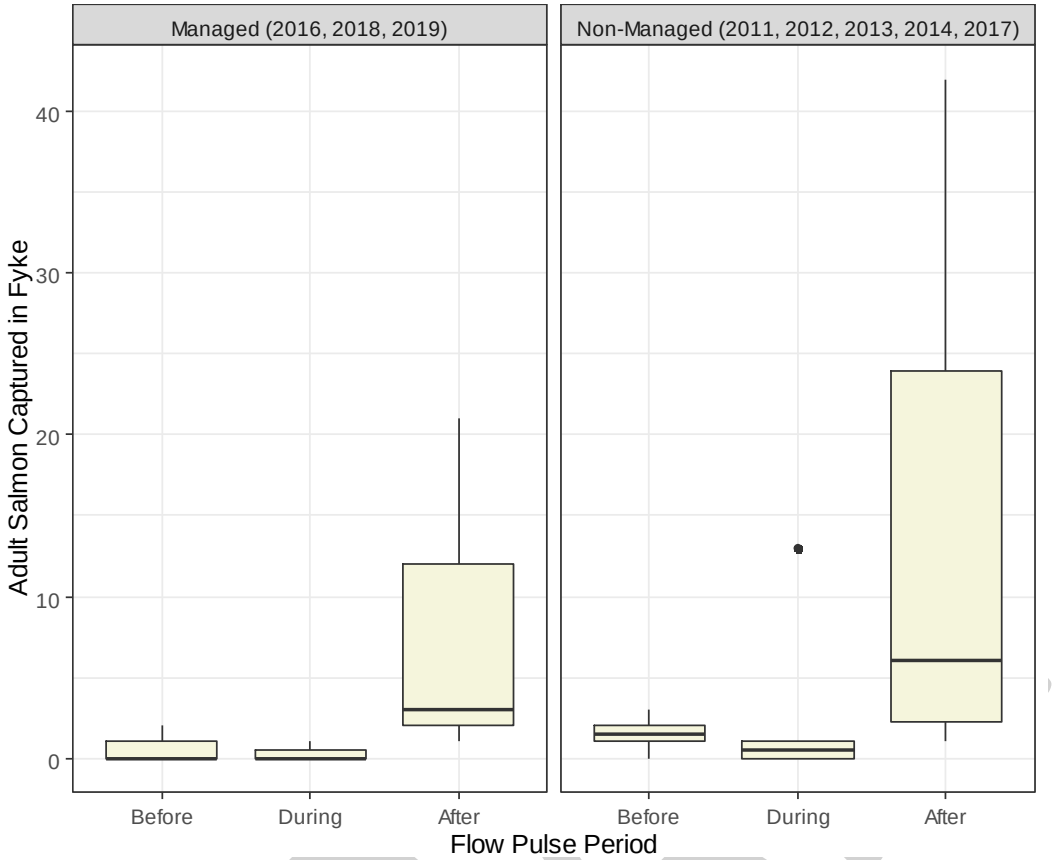

Figure 5-15. Number of adult salmon captured in the Yolo Bypass Fish Monitoring Program fyke trap during the 45 days before the flow pulse, during the flow pulse, and 45 days after the flow pulse by year for managed and non-managed flow pulse types.

Table 5-10. Results of generalized linear model of salmon catch in the Yolo Bypass Fish Monitoring Program fyke trap in the periods before, during, and after the flow pulse testing the impact of managed versus non-managed pulses.

	Estimate	Std. Error	z-value	Pr(>|z|)	
(Intercept) - Before, Managed	-0.503	0.663	-0.759	0.448	
During	0.288	0.689	0.418	0.676	
After	2.369	0.641	3.697	<0.0001	**
Non-Managed	0.942	0.580	1.624	0.104	

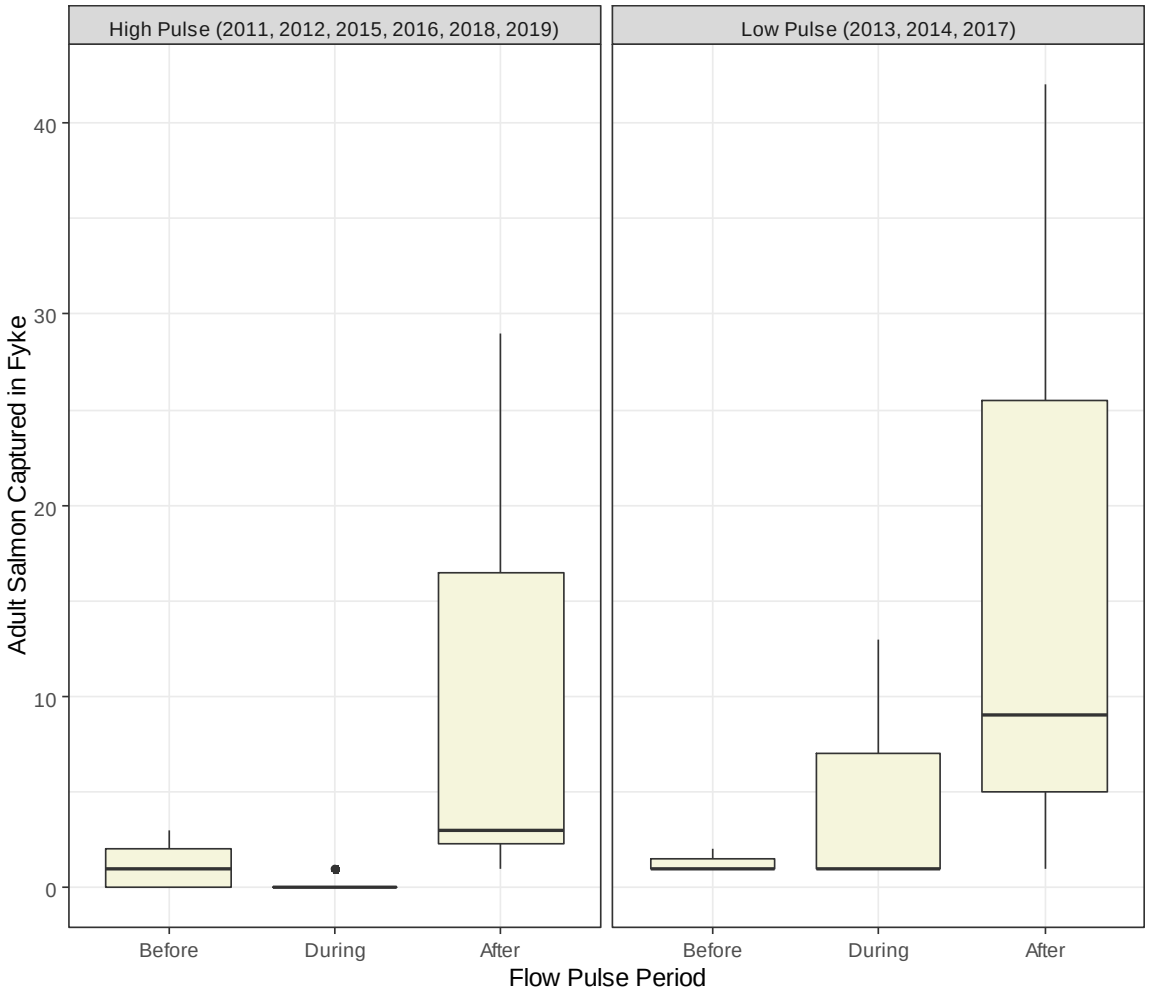

Figure 5-16. Number of adult salmon captured in the Yolo Bypass Fish Monitoring Program fyke trap during the 45 days before the flow pulse, during the flow pulse, and 45 days after the flow pulse by year for low and high flow pulse types.

Table 5-11. Results of generalized linear model of salmon catch in the Yolo Bypass Fish Monitoring Program fyke trap in the periods before, during, and after the flow pulse testing the impact of low pulse versus high pulse.

	Estimate	Std. Error	z-value	Pr(>|z|)	
(Intercept) – Before, High pulse	-0.178	0.532	-0.335	0.738	
During	-0.102	0.687	-0.148	0.882	
After	2.286	0.618	3.702	<0.001	**
Low Pulse	1.197	0.526	2.275	0.023	*

2019 Wallace Weir Rescues

The 2019 flow pulse began on 8/26 and continued through 9/21 (Figure 5-17). CDFW began operation of the Wallace Weir Fish Rescue Facility (WWFRF) at the start of the flow pulse, so no salmonids were caught in the Before phase. The first salmonid caught at Wallace Weir was on 9/6, approximately two weeks after the start of the flow pulse. Seventy-six Chinook Salmon and three Central-Valley steelhead were captured in the During phase with most individuals from both species having their adipose fin intact (62% and 67% respectively). Two hundred and ninety-three Chinook Salmon and nine Central Valley steelhead were captured in the After phase with adipose fin presence differing by species; 91% of Chinook Salmon had adipose fins while 89% of Central Valley steelhead were adipose fin-clipped. Due to the hatchery constant fractional marking of 25% for Fall-run Chinook Salmon, when the percentage of adipose-intact fish in a sample exceeds 87.5%, there are likely more natural-origin fish than hatchery fish in that sample. Since the hatcheries mark 100% of Central Valley steelhead, the presence of an adipose fin implies that the individual is most likely of natural origin.

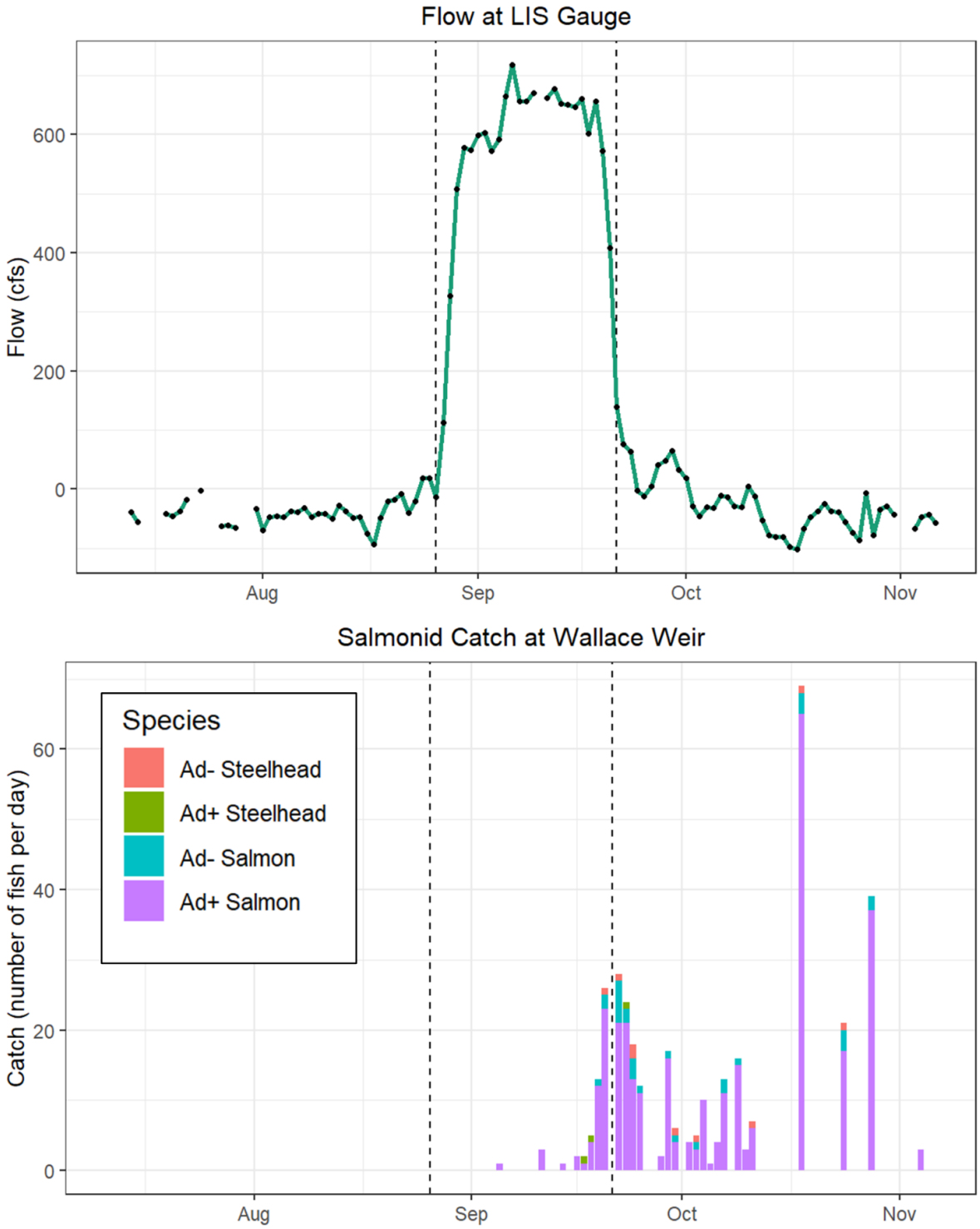

Figure 5-17. Flow at Lisbon Weir and salmonid catch at Wallace Weir in the Before, During, and After phase dates of the 2019 flow pulse. Vertical dashed lines represent the start and end of the flow pulse. In the salmonid catch graph, the last four bars in late October and early November represent the four beach seine rescue days.

Adult Salmonid Health

Salmonid Temperature Threshold Analysis

Daily average water temperature values in the Before, During, and After phases within the seven years on record ranged from 12.04°C to 27.97°C, with a mean of 21.42°C (Figure 5-18). The mean daily average temperatures for the Before, During, and After phases were 24.26, 22.16, and 18.29°C, respectively. Considering all seven years on record, daily average temperatures exceeded the 21°C salmonid benchmark in at least one day of each pulse phase, specifically 99% of days in the Before phase, 70% in the During phase, and 22% in the After phase. The breakdown of percent day exceedances by year is shown in (Table 5-12) During each year on record, the last calendar day that exceeded the 21°C salmonid threshold fell between 9/20 and 10/16, with the non-statistical relationship of wetter years having an earlier date, and drier years having a later date (Table 5-13). The timing of this date does not appear to correlate with flow pulse type.

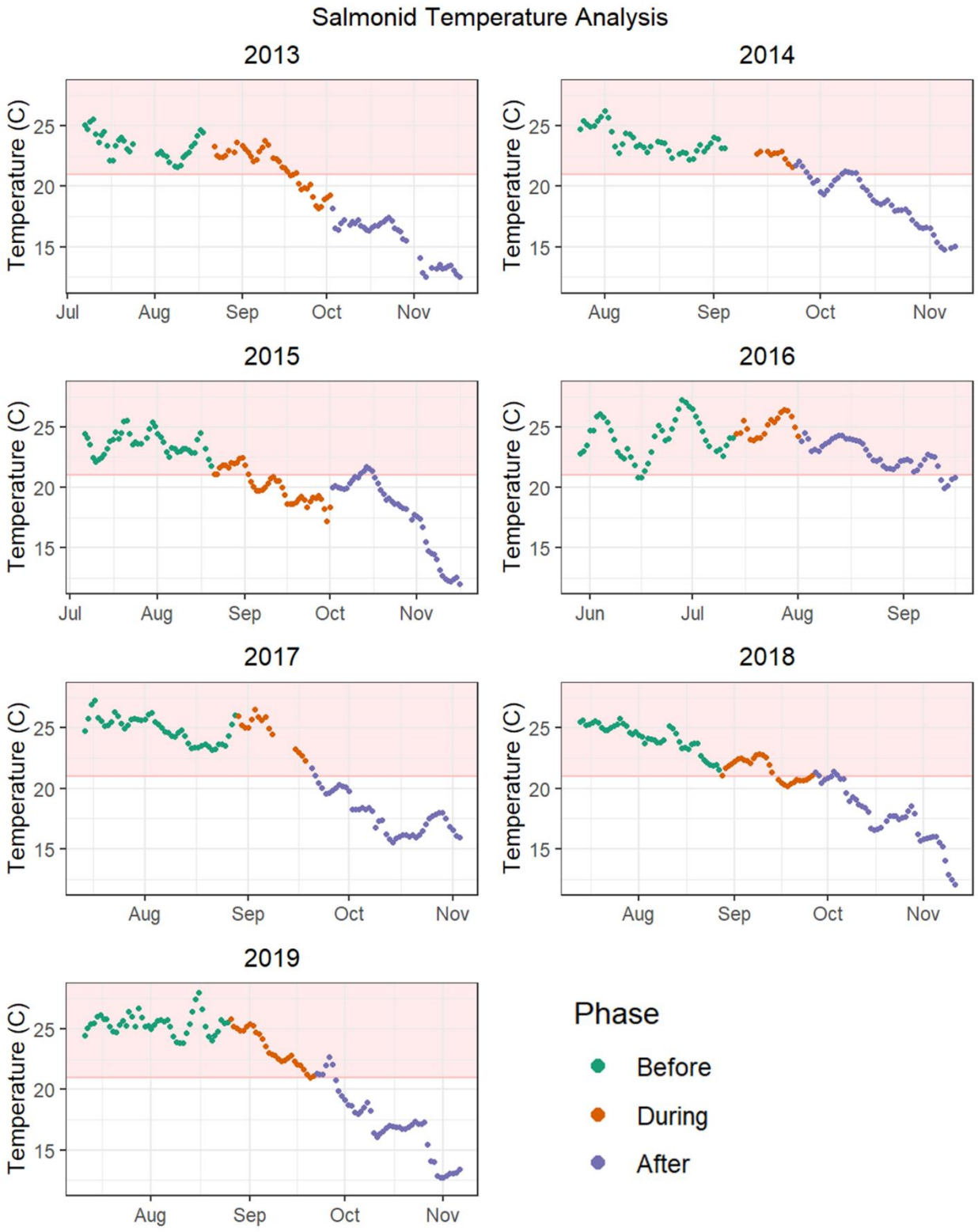

Figure 5-18. Comparison of daily average water temperature at Lisbon Weir in the Before, During, and After phases for each year on record in relation to the adult salmonid temperature maximum threshold of 21°C. Each point represents one day.

Table 5-12. Percentage of days in the Before, During, and After phases when daily average recorded temperature levels at Lisbon Weir fell above the adult salmonid maximum threshold of 21°C.

Year	2013	2014	2015	2016	2017	2018	2019	Total
Pulse Type	Low	Low	High	High	Low	High	High	
Phase								
Before	100.0	100.0	100.0	95.6	100.0	100.0	100.0	99.3
During	64.1	100.0	31.0	100.0	100.0	62.1	96.3	69.6
After	0.0	20.0	11.1	89.1	4.4	11.1	13.0	21.9

Table 5-13. Details of each year on record including the latest calendar day with an average temperature above the adult salmonid maximum threshold of 21°C, the water year type designation, and the flow pulse type.

Year	Last Day Above 21°C	Water Year Type	Flow Pulse Type
2013	2013-09-20	Dry	Low
2014	2014-10-11	Critical	Low
2015	2015-10-16	Critical	High
2016	2016-09-28	Below Normal	High
2017	2017-09-21	Wet	Low
2018	2018-10-04	Below Normal	High
2019	2019-09-27	Wet	High

Adult Salmonid Dissolved Oxygen Threshold Analysis

Daily average dissolved oxygen (DO) values in the Before, During, and After dates within the seven years on record ranged from 3.80 to 9.35 mg/L, with a mean of 6.52 mg/L (Figure 5-19). The mean daily average DO values for the Before, During, and After phases were 6.76, 5.40, and 6.93 mg/L, respectively. Considering all seven years on record, daily average DO values fell below the 6.0 mg/L adult salmonid benchmark in at least one day of each phase, specifically 18% of days in the Before phase, 67% in the During phase, and 16% in the After phase (Table 5-14). The breakdown of percent day exceedances by year is shown in Table 5-14.

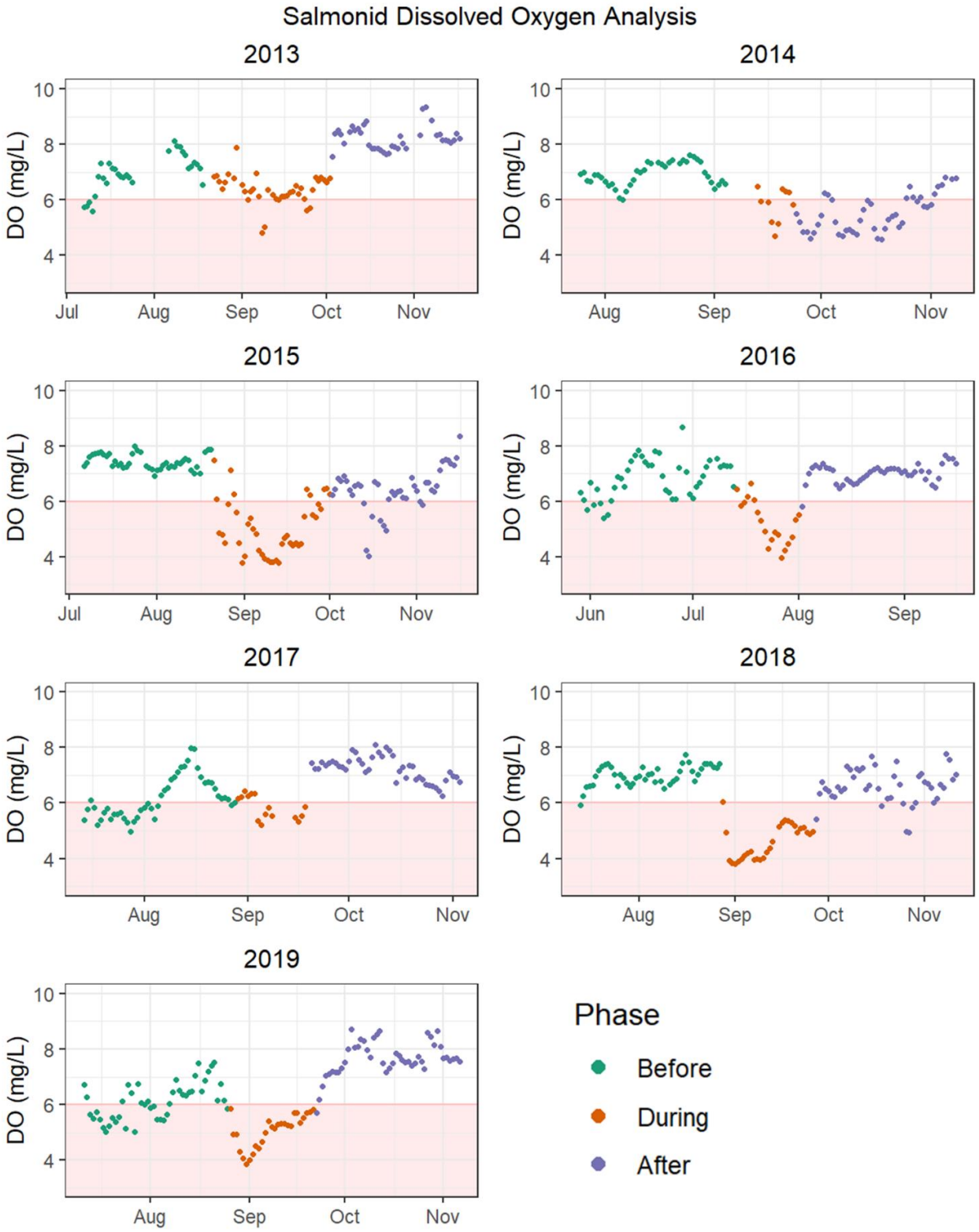

Figure 5-19. Comparison of daily average dissolved oxygen levels at Lisbon Weir in the Before, During, and After phases for each year on record in relation to the adult salmonid dissolved oxygen minimum threshold of 6 mg/L. Each point represents one day.

Table 5-14. Percentage of days in the Before, During, and After flow pulse phases when daily average recorded dissolved oxygen levels at Lisbon Weir fell below the adult salmonid minimum threshold of 6 mg/L.

Year	2013	2014	2015	2016	2017	2018	2019	Total
Pulse Type	Low	Low	High	High	Low	High	High	
Phase								
Before	13.3	0.0	0.0	11.1	50.0	2.2	41.3	17.6
During	10.3	60.0	78.6	78.9	60.0	96.6	100.0	67.4
After	0.0	73.3	17.8	2.2	0.0	13.3	2.2	15.8

5.6.3 Discussion

Salmon Straying

Our results are largely inconclusive on whether flow pulses influence Chinook Salmon catch in the Yolo Bypass. We found a negative relationship between Lisbon weir flow and YBFMP fyke trap salmon catch, and we found that low flow pulses were accompanied by higher salmon catch than high flow pulses (Figure 5-16). However, it is important to note that the flow pulse period generally occurs prior to peak salmon returns (Figure 5-14). Timing of NDFS actions and fyke trap operations do not fully coincide, creating data deficiencies for this analysis, thereby making interpretations and conclusions on the influence of NDFS flows on salmon presence in the Yolo Bypass difficult. Aside from flow, there are several other key factors influencing salmon migration timing and straying which could be confounding this simple catch-versus-flow analysis. Inspection of other factors that may influence salmon straying highlights the complexity of making any meaningful conclusions. For example, salmon return rates for the Sacramento River have decreased over time, which may make the increase in catch in the Yolo Bypass appear alarming. However, the distance hatcheries transport juvenile Chinook Salmon for release has been increasing, potentially impacting rates of straying. This is consistent with research that shows increased trucking of juvenile hatchery salmon reduces their ability to navigate back to their natal stream as adults (Lakso et al. 2014; Sturrock et al. 2019). Additionally, CWT recoveries show a rising trend in Central Valley Chinook Salmon stray rates, tracking with Yolo Bypass Chinook Salmon catch trends. Lastly, aside from Putah Creek inputs, the majority of Yolo Bypass drain water originates as Sacramento River water, although diverted miles upstream for anthropogenic uses. The Yolo Bypass water may still exhibit chemical

signatures providing homing olfactory cues for salmonids, though potentially reduced, and likely contains increased contaminant loads (see Chapter 3).

Ultimately, limitations in the available data make it difficult to determine the effect of flow on salmonid presence in the Yolo Bypass. First, the YBFMP usually deploys the fyke trap around the beginning of October each fall. The NDFS flow pulses in most years had concluded by this time and Chinook Salmon may already be in the system but unaccounted for. Accordingly, we have limited data for salmonid presence immediately preceding and during flow pulse events. Additionally, the ten-foot-wide YBFMP fyke trap is deployed in the Toe Drain where the channel is approximately 120 feet wide. The fyke trap, when deployed, sits in the deep part of the channel and fish may swim around the fyke, reducing the trap's catch efficiency. Importantly, during NDFS flows, water is still confined to the channel and does not overtop its banks, so catch efficiency during NDFS flows may not significantly change compared to lower flow periods. Second, Chinook Salmon catch in the YBFMP fyke trap, even in years that appear to have high numbers (2015, 2017), still have too many weeks with no-catch for the statistical models to be effective. Third, other data sources we examined may be too broad scale to account for Chinook Salmon behavior. For example, we were unable to incorporate the influence of water year type as the months of September to December may not relate to the entire year classification. These fall months may experience plentiful rainfall in an otherwise dry year or be relatively dry in an overall wet year. Additional years of stray rate data may help determine if Yolo Bypass catch can be related to overall straying of Chinook salmon in the Central Valley.

As one of the elements funded by the current project, Johnston et al. (2020) conducted telemetry studies on adult salmon and sturgeon in the Yolo Bypass between 2012-2018. They found approximately 74% of tagged salmon were successfully able to exit the Yolo Bypass. This was less than exit rates for White Sturgeon (99%), but still indicates that straying into the Bypass does not represent complete loss of spawning fish.

Future data collection that would help this study objective include determining Chinook Salmon presence in the Sacramento River near the base of the Toe Drain and in the lower Yolo Bypass before and during flow pulse events. This could help determine if the NDFS is affecting straying of Chinook Salmon into

the Bypass. The distance that hatcheries transport juvenile Chinook Salmon for release and relation of Yolo Bypass catch to overall reported salmon straying in the Sacramento watershed should continue to be monitored.

Overall, the variables examined were inconclusive for determining causes of Chinook Salmon catch in the Yolo Bypass. We were unable to determine if flow manipulations associated with NDFS independently influenced salmon presence in the Yolo Bypass. Likely, many of these factors play a role in Chinook Salmon straying, as well as other variables we did not examine. Our results were skewed due to some outlier years, but additional years of NDFS and the above-mentioned data sources could help determine which factors, including elevated NDFS flows, may influence Chinook Salmon presence in the Yolo Bypass.

2019 Wallace Weir Rescues

Although CDFW has carried out fish rescue efforts at Wallace Weir since early 2014, there was very little catch in the Before, During, and After phases of the flow pulses in the years prior to 2019. Before DWR constructed the Wallace Weir Fish Rescue Facility (WWFRF), CDFW could only rescue using a temporary fyke trap and/or beach seines. These methods could not be carried out at if flows were too low, temperatures were too high, or during high flow events such as flow pulses. The WWFRF became operational in the fall of 2019, contributing to the high salmonid catch at the facility in the During and After phases of the 2019 flow pulse. Due to the variability in the time it takes for adult salmonids to travel from the southern extent of the Yolo Bypass to Wallace Weir, we do not know the exact date that each individual strayed into the Yolo Bypass, so this analysis uses the date they were captured at Wallace Weir. There is not enough Wallace Weir salmonid catch data to determine how flow pulses generally affect salmonids, but continued operation of the WWFRF during flow pulses will build a more consistent database to analyze in future years. In addition to being a valuable data source, the WWFRF will continue to guarantee safe and timely passage for adult salmonids if they are attracted up the Toe Drain by a flow pulse.

Adult Salmonid Health

During the seven years on record for this analysis, temperature appears to be correlated with time of year, with values dropping consistently during early fall of each year (consistent with Chapter 3). Despite this drop, daily average temperatures at Lisbon Weir are regularly above the maximum salmonid threshold of 21°C during most of the flow pulse phase dates. From the seven years on record, virtually all the Before days exceed the threshold, more than two out of three days of the During phase do, and nearly one out of four days in the After phase also fall above the threshold. Dissolved oxygen (DO) does not appear to follow a seasonal trend, with daily average values regularly below the 6 mg/L minimum salmonid threshold in all three phases, most commonly in the During phase (Figure 5-19).

Due to the low Wallace Weir salmonid catch in and around managed flow actions in most years, we did not compare salmonid timing to temperature or DO levels as part of this analysis. However, fall-run Chinook Salmon can return from the ocean and enter the Sacramento River system as early as June or July (Yoshiyama et al. 1998; CalFish), so salmon could have been present in the Yolo Bypass during the majority of the Before, During, and After dates of most years and present during short-term exposures to low DO. With two phenotypes ("summer-run" and "winter-run"), Central Valley steelhead had the potential to be migrating upriver during the entire flow pulse date range of each year on record (CalFish). Although it has been shown that salmonid presence in the Yolo Bypass is more closely correlated to fall season than increased flow (CFSM 2019), higher flow in the Toe Drain creates passable channels out of previously impassable barriers, allowing salmonids to move further up the system than they could otherwise. As salmonids move further up the system, they are less likely to backtrack course and exit at the base of the Toe Drain where they could reconnect with the Sacramento River and continue their upstream migration (CFSM 2019).

Salmonids' bodies begin to break down as soon as they enter freshwater, and this process is expedited when exposed to high temperatures due to the higher energetic cost. It is vital that fish traveling up the Yolo Bypass Toe Drain during and after flow pulses are quickly rescued and returned to the Sacramento River to complete their migration. This need for timely rescues validates the importance of CDFW operating the Wallace Weir Fish Rescue Facility.

Continued support of this work and this facility are essential for the long-term success of the NDFS project.

Chapter 6 Synthesis Summary

6.1 Summary

The goal of the current study was to synthesize and evaluate the ecological benefits and consequences of flow pulses in the North Delta and assess if the benefits of high-flow pulses (with and without managed actions) exceed those of low-flow pulses. Since 2011, there have been three general types of flow pulses observed in the North Delta: 1) low- and high-flow pulses (non-managed or no action) due to local agriculture activities, 2) high-flow pulses with a managed flow action using agricultural return water, and 3) a high-flow pulse with a managed action using diversions of Sacramento River water. Non-managed pulses were observed in 2011-2015, and 2017, whereas managed NDFS flow pulses were conducted in 2016 (Sacramento River action), 2018 and 2019 (agricultural action). It should be noted that 2012 (high-flow pulse) and 2017 (low-flow pulse) had similar management intervention as NDFS actions due to construction activities at the Knights Landing Outfall Gates or Wallace Weir that led to redirection of agriculture pulse water, but we classified them as non-managed because these pulses were not intended to produce ecological responses.

The goal of managed flow pulses (actions) is to reverse negative summer-fall flows and improve the food web via transport of food resources and trigger a phytoplankton bloom in downstream habitats of Delta Smelt. We found all flow pulses (managed and non-managed) resulted in a moderate period of positive net flow in the upstream region, and larger-than normal (managed) flows created positive net flow downstream. These flow increases contrast with normal conditions during summer-fall, when net flows are negative (in the upstream direction) because of water diversions in the Cache Slough and Yolo Bypass regions. Hence, flow increases help generate more natural transport conditions. Moreover, years in which we intentionally augmented flows (2016, 2018, 2019) resulted in better flows (i.e. net positive flow downstream) than would otherwise have been seasonally present. There is a large body of scientific literature indicating that more natural hydrographs have multiple ecological benefits (e.g., Richter 1997; Poff et al. 1997; 2010).

We found evidence of chlorophyll and plankton transport in upstream regions with high-flow, managed pulses by assessing real-time monitoring and

plankton densities. In contrast, we found limited indications that the average plankton abundance downstream increased; however, plankton responses downstream varied based on regional versus station-based assessments. When examining individual stations, we found evidence for moderate increases in abundance of certain beneficial plankton, such as diatoms, and changes in community composition in some managed pulse years. Our results demonstrate that a complexity of other factors such as nutrient ratios (Chapter 3) or clam grazing (Chapter 4) downstream may limit the benefits of upstream transport on downstream plankton.

The following sections summarize our synthesis findings of flow pulse effects on hydrodynamics and habitat complexity, water quality, lower trophic food web ecology, and fishes in the North Delta. We provide a conceptual figure summarizing quantitative and qualitative findings of parameter responses to low- and high-flow pulses to facilitate understanding of ecological benefits and consequences of flow-pulses (Figure 6-1). Lastly, we evaluate remaining uncertainties, as well as recommendations for future adaptive management of the North Delta Food Subsidy action and pulses in the North Delta given this large synthesis effort and findings.

Figure 6-1. Conceptual heat map of ecological responses to low- and high-flow pulses in the North Delta. Color assignments of abiotic and biotic responses are indicated for upstream and downstream regions. Overall quantitative (statistic) or qualitative results (trend) for the general effects of flow pulses (with focus on managed flow actions) are provided. The response scale ranges from acute, moderate and significant negative (-) or positive (+) responses. Details for assignments are provided in Appendix F.

6.2 Hydrodynamics

Hydrodynamic modeling demonstrated managed actions in 2018 and 2019 resulted in larger than normal high-flow pulses in the North Delta and were most similar to a non-managed high-flow pulse in 2012. However, 2012 was indeed a larger than normal pulse due to construction on infrastructure and redirection of flow through the bypass. We found benefits of both high- and low-flow pulses in the upstream region but relatively greater benefits of high-flow-pulses in the downstream region, such that all flow pulses (managed and non-managed) restored positive net flow upstream in the Yolo bypass (as measured at Lisbon Weir; Figure 2-1), but only high-flow pulses restored positive net flow downstream (Figure 2-4) where hydrodynamics are dominated by tides. Thus, we met flow objectives and goals of the NDFS managed action of restoring positive net flow downstream and more natural flow patterns.

We found that the magnitude and duration of flow pulses affect the hydrodynamics of the CSC and the transport of flow pulse water and CSC water out of the CSC and downstream. Larger-magnitude high-flow pulses (managed actions), with longer duration of net positive flow southward out of the CSC, resulted in more transport of both flow pulse water and CSC water downstream past Lower Liberty Island and Rio Vista in the lower Sacramento River. Further, our modeling demonstrated that managed flow pulses in 2016 and 2019 affected the hydrodynamics in the CSC such that there was increased net flow out of the CSC in the southward direction relative to conditions that would have been present if the flow pulses had not occurred (Table 2-6; Figure 2-9 and Figure 2-11).

Restoring net positive flow and downstream transport during summer-fall when conditions are typically net negative (because of substantial water diversions) is an ecologically important goal (e.g., Poff et al. 1997; Kiernan et al. 2011), particularly in the context of major habitat restoration efforts in the North Delta, which are designed to improve food production in the region. Hence, summer-fall flows will help maximize the regional benefit of this productivity by transporting it to downstream habitats.

6.3 Water Quality

Consistent with variation in hydrodynamics and habitat complexity across North Delta regions, water quality also differed by regions across years. The upstream Yolo Bypass during summer-fall was more turbid and saline and had higher average water temperatures, higher and more variable pH values, higher chlorophyll fluorescence values, and lower and more variable dissolved oxygen concentrations as compared to CSC and lower Sacramento River downstream. In addition, the upstream region had higher concentrations of nutrients (e.g., calcium, dissolved organic nitrogen and phosphate, dissolved nitrate-nitrite, and silica), organic carbon, chlorophyll *a* and pheophytin (markers of phytoplankton). The downstream region had greater ammonia concentrations.

As predicted, we found upstream water quality was more responsive to low- and high-flow pulses compared to downstream, and only high-flow pulses (with and without managed actions) altered a few downstream parameters in given years. During or after flow pulses in the bypass we observed changes in specific conductivity and DO consistent with most pulse water from agriculture activities, but we also found increased fDOM (in 2018 and 2019), phosphorus, and chlorophyll. Only during and after high-pulse events, and inconsistently across years, did we detect either quantitative or qualitative changes in downstream water quality such as increased specific conductivity (all high-flow years), fDOM (2018 and 2019), nutrients (e.g., Silica in 2015 and 2016), organic carbon (all high-flow years), and chlorophyll (2011, 2012, 2016). These changes in water quality downstream, compatible with hydrodynamic modeling results, demonstrate transport and mixing of upstream pulse water and other parcels of water to downstream habitats of CSC; however, our results were not consistent across all high-flow pulses and varied by years.

Concentrations of nutrients (DOP, DIN, and silica) were generally above levels limiting to phytoplankton growth upstream and downstream in all years and flow pulse periods (Jassby et al. 2002, Jassby 2005). Although DIN was not limiting, ammonia concentrations were much higher downstream than nitrate and nitrite (Figure 3-45,Figure 3-46), which could have contributed to the ammonia paradox (Figure 3-59) (Wilkerson et al. 2006, Dugdale et al. 2007) and suppressed growth of phytoplankton transported to downstream habitats by flow pulses. Effluent from the Sacramento Regional Wastewater Treatment Plant contributed much of this ammonia to the downstream habitat (Glibert

2011, Parker et al. 2012). However, recent upgrades to wastewater discharge may result in more favorable nutrient ratios for growth of nutritious diatoms, improving the efficacy of future flow actions.

We found similar spatial and temporal patterns in discrete and real-time continuous chlorophyll data; however, as noted above, differences in quantitative and qualitative assessments suggest the need for increased monitoring and replication across the summer-fall to increase statistical power required to adequately determine responses by testing interactions. For example, in both discrete and continuous models we did not find low-or high-flow pulses to significantly alter chlorophyll across flow pulse periods (before, during, after), but chlorophyll values differed across years and regions (as mentioned above). Unfortunately, we could not test for interactions due to limited replication (discrete) and/or lack of model fit, but we suspect interactions are likely to be present. Qualitative trends in real-time and discrete chlorophyll demonstrate increased transport of chlorophyll *a* downstream in 2011 (Figure 3-4), 2012 (Figure 3-4; similar to a managed flow pulse), and 2016 (Figure 3-3 and Figure 3-38; a managed, high-flow pulse). During these years, chlorophyll increased by roughly 2 to 5-fold (10-20 µg/L) at lower Liberty Island and Ryer Island in the CSC, and the increases coincided with elevated DO and pH values (Figure 3-9, Figure 3-10, Figure 3-16, and Figure 3-17) suggesting new algal growth and increased primary production. Overall, 2018 and 2019 were generally lower productivity years than the remaining years in the study period.

In recent years there has been concern whether managed flow pulses, particularly agricultural actions, increase contaminants in the North Delta. Consistent with most of the other water quality parameters, total pesticide concentrations in water were higher upstream in the Yolo Bypass than downstream in the CSC. Total pesticide concentrations in both water and zooplankton were highest during flow pulses in all years, although concentrations in water were somewhat lower during the flow pulse in 2016. The managed flow pulse in 2016 was conducted using Sacramento River water, while the other high-flow pulse years (2018 and 2019) consisted of agricultural water. This suggests that managed flow pulses using Sacramento River water may have fewer unintended consequences for the food web and provides justification for repeating the Sacramento River flow action in future years. Moreover, although pesticide concentrations increased during pulses, pesticides exceeded EPA benchmarks for toxicity to aquatic life across all flow

pulse periods and years, suggesting that high pesticide concentrations are ubiquitous in the study area regardless of managed flow actions.

6.4 Lower Trophic Food Web

Measuring the response of the lower trophic community (phytoplankton, zooplankton, and benthic invertebrates) to flow pulses is essential to understanding the impact of these pulses on the food web ecology of the North Delta. Phytoplankton, as primary producers, form the base of the food web in the Delta and are essential food sources for zooplankton, which in turn are fed on by larval fish and juvenile fishes such as Delta Smelt, and larger invertebrates.

Consistent with predictions and measures of chlorophyll, overall biovolume of phytoplankton was consistently higher in the upstream region of the North Delta compared to the downstream region over the years of study 2014-2019. Given correlations of chlorophyll and phytoplankton, we suspect similar trends of phytoplankton biovolume were present in 2011-2013 demonstrated by continuous chlorophyll fluorescence data, but we did not have adequate phytoplankton biovolume data to include those years in our evaluations. In general, we detected changes in the downstream phytoplankton community brought about by high-flow pulses; however, in most years, the biovolume downstream was lower following the flow pulse than before (Figure 4-1) and these findings may be influenced by seasonality (Jassby 2008). One exception was 2016, when a bloom of diatoms was detected following the high-flow pulse at downstream stations (Figure 4-7, Figure 4-11), but whether or not this increase can be causally linked to the flow pulse, antecedent, or seasonal conditions is uncertain.

Though total phytoplankton biovolume did not respond strongly to flow pulses (or decreased due to seasonal influences), comparative profiles of phytoplankton nutritional quality, measured as biomass of long-chain essential fatty acids (LCEFA), demonstrated that even small changes in the biomass of specific taxa in response to flow pulses improved food quality indices. For example, most years cyanobacteria dominated phytoplankton biovolume across regions in the North Delta (Figure 4-12), but algal species such as diatoms, cryptophytes, dinoflagellates, and other green algae still provided the bulk of key LCEFAs (Figure 4-13; Galloway and Winder, 2015). During high-flow pulse years the relative percent of diatom LCEFA increased

during or after pulses upstream (2015, 2016, 2018, and 2019), and increased in 2016 and 2019 (both managed flow actions) downstream. These increases in LCEFAs may have a significant impact on the nutrient quality of the base of the trophic food web and provide important ecological benefits of high-flow pulses.

Overall, the phytoplankton community structure in the upstream Yolo Bypass differed from downstream habitats of CSC and Sacramento River (Figure 4-14) but neither region was strongly influenced by flow pulses (Figure 4-15, Figure 4-16). Instead, we found evidence to suggest that specific flow pulse types (and potentially water sources) may influence community structure. For example, community structure was most distinct among managed, high-flow pulses using Sacramento river water (2016) and agricultural return water (2018, 2019; Figure 4-17). In 2016, differences in the composition of phytoplankton communities between regions increased following the pulse (Table 4-4), counter to our predictions, which may be an artifact of the water source (Sacramento River) used for the managed flow pulse. Because phytoplankton data is only available for one year when Sacramento River water was used for a managed action, it is difficult to determine whether the community structure changes (specifically increases in diatom biovolume downstream) is a direct result of the action and flow pulse or other factors influencing habitat that year. Antecedent conditions and a spring phytoplankton bloom in 2016 may have provided a good year for phytoplankton composition independent of pulse effects. Nevertheless, future adaptive management of this action may be improved by repeating the Sacramento River action and evaluating which phytoplankton taxa are most responsive to specific types of flow pulses and/or managed actions (e.g., Sacramento River, Agriculture drainage, etc.) and their nutritional profile.

Zooplankton responses did not follow the same trends as phytoplankton. Total zooplankton density was similar across regions, which was surprising given our expectation that zooplankton abundance would correlate with greater phytoplankton biovolume and higher nutritional quality (LCEFAs) after flow pulses upstream. In addition, while phytoplankton community structure was more similar across regions, zooplankton communities varied regionally across years. For example, calanoid copepods were generally more abundant downstream, whereas cyclopoid copepods, cladocerans, and microzooplankton and nauplii were more abundant upstream. Together, these mismatched responses in primary and secondary trophic levels indicate that

food webs in floodplain, wetland, and deep channel habitats of the North Delta are complex, possibly with non-linear topologies, as described by Brown et al. (2016). For example, Kimmerer et al. (2019) found evidence that calanoid copepods may consume and derive some of their nutrition from cyanobacteria or ciliates in the CSC, which suggests that sources of phytoplankton other than nutritious diatoms and green algae, and even some small animals, may support zooplankton growth in this region. Our focus on sampling pelagic plankton as food sources may overlook other important prey that contribute to a more reticulate food web.

In contrast to our prediction that high-flow pulses may increase zooplankton in the North Delta, many taxa tended to have higher abundance before the flow pulses than after. Some taxa such as calanoid copepods even decreased even during pulses upstream, suggesting that they were transported downstream; however, we did not find correlated increases of the same taxa downstream. Consistent with other ecological responses (water quality and phytoplankton) to the 2016 flow pulse, zooplankton taxa such as copepod nauplii increased during and after the high-flow pulse (Sacramento River managed action), and community composition also deviated more following the pulse than in other years. Mediating factors other than the flow action could have contributed to these differences across years, including seasonal effects and pulse timing (summer vs. fall), and source water with different contaminant concentrations. In addition, the overall lack of zooplankton responses downstream could be attributed to several factors identified in our synthesis aside from flow pulse efficacy, such as sampling methodology (i.e., our surface tows may have omitted taxa that undergo diurnal vertical migrations, or predation by other species on zooplankton that are transported downstream (e.g., larger zooplankton, clams, and fishes). Without a clear increase in zooplankton biomass, it is less clear that the flow pulse provided food benefits for pelagic fishes such as Delta Smelt.

Overall regional differences in chlorophyll, phytoplankton, and zooplankton upstream and downstream are likely due to a complexity of physical, chemical, and biological factors that make it difficult to understand flow pulse effects on the lower trophic food web in downstream habitats. For example, downstream is strongly influenced by tidal dynamics, higher levels of ammonia (Figure 3-46), suboptimal nutrient ratios to support growth of nutritious phytoplankton taxa such as diatoms (Figure 3-45, Figure 3-49, Figure 3-56), and higher biomass and grazing rates of *C. fluminea*. We found that *C.*

fluminea could filter 11-28% of the water column in downstream Prospect Slough and Cache Slough habitats with the potential to negatively affect phytoplankton directly and zooplankton indirectly. In addition, small fishes such as invasive Mississippi Silversides, caught in high abundances and comprising 80% of littoral fish composition in the North Delta (Figure 5-2), likely serve as secondary consumers of plankton. Together, these findings may underly why downstream habitats are somewhat less productive, but other differences such as residence time, light availability, and temperature among the regions may also contribute to these differences (Sommer et al. 2004; Frantzich et al. 2018). Furthermore, linear food web models described for marine and freshwater environments may not be accurate in estuaries and in the current North Delta study area (Brown et al. 2016), making interpretations of plankton responses to flow pulses particularly challenging. In addition to the complexity of wetland and floodplain trophic responses described above, introductions of invasive species have further impacted the food web in the North Delta. While this study evaluated biomass and grazing rates of benthic clams and non-native fish abundance, other invasive invertebrates that we did not sample including the Siberian prawn *Exopalaemon modestus* (Brown and Hieb 2014) or cladoceran *Daphnia lumholtzi* (Mueller-Solger 2001) impact the food web by consumption of phytoplankton and/or zooplankton and could affect the efficacy of flow pulses in the downstream region of the North Delta (Brown et al. 2016).

Lastly, it is important to note that our synthesis may provide different interpretations of lower trophic organism responses to flow pulses than previous studies (Franzich et al. 2018, Twardochleb et al. 2021, Frantzich et al. 2021), but findings appear dependent on the evaluation approach and scale of statistical power. For example, previous evaluations focused on a single year and flow pulse and assessed the spatial and temporal data at a finer scale. For example, in Frantzich et al. (2020, 2021) and Twardochleb et al. (2021) changes in phytoplankton or zooplankton before, during, and after the flow pulse were determined at the following smaller regional scales separately: Ridge Cut Slough, the Upper or Lower Yolo Bypass, Cache Clough Complex, and Lower Sacramento River, which increased their ability to detect local responses to flow pulses. In the current synthesis, the temporal scale of data before and after pulses was greater, we defined regions as upstream or downstream to balance the statistical design, which resulted in reduced ability to evaluate specific habitat responses to pulses (as observed in station-specific assessments). In addition, we compared 6-9 years of data, taking a broader

approach to determine overall effects of flow-pulses on lower trophic ecology in the North Delta. In general, both the current and previous studies found similar trends in plankton responses in 2016 and some similarities in 2019, highlighting potential benefits of high-flow managed actions.

6.5 Fish

Understanding fish responses to NDFS action is important, as one of the overarching goals of the action is to increase food resources for the benefit of fish, namely endangered species such as Delta Smelt. This synthesis was the first concerted effort to understand fish community composition and abundance as it relates to flow pulses and the NDFS action in the North Delta. Consistent with our predictions, our analysis of synthesized fish datasets did not show any increase in fish catch per unit effort (CPUE) during flow pulses. Fish CPUE was consistently higher before flow pulses. There was no evidence that water year or flow pulse type (e.g., high-flow or low-flow pulses) influenced CPUE. Additionally, we found little correlation between fish count and zooplankton CPUE, year, and pulse period. This conclusion is not surprising as there are not any simple relationships in the estuary between food availability and fish counts. In addition, the NDFS study was not designed to directly influence fish abundance and the fish monitoring surveys used were not designed to measure the effect of flow pulses. As such, the data were quite variable, indicating that there are many confounding factors outside of those we explored that are likely influencing CPUE, such as how the data were collected across different monitoring programs, and seasonal life history patterns of the various fish species.

In 2019, cultured Delta Smelt were held in enclosures in the Yolo Bypass and at Rio Vista to see if we could detect an impact of the NDFS action on their health or diet. While complications in the study design prevent us from making any definite conclusions, the limited data suggest that Delta Smelt could survive in areas influenced by managed flow pulses. We saw differences between zooplankton in the environment and in the diets of the study fish, but also a fair amount of overlap driven by certain prey species, signifying that Delta Smelt can forage on species present in the Yolo Bypass when influenced by a managed flow pulse.

As noted previously, Yolo Bypass seasonally has high straying rates of adult salmon because strong tidal flows at the base of the system (+/- 80,000 cfs)

help guide fish into Cache Slough Complex and the floodplain (Sommer et al. 2013; Johnston et al. 2020). One of the early questions for the NDFS was whether increased flows in fall could attract more fish into the Yolo Bypass. We still do not have all the data necessary to fully answer that question. Overall, the range of fall flow increases were quite low, representing less than 1% of the typical tidal flows through Cache Slough Complex. The flow actions in 2018 and 2019 represent an increase in peak flows (e.g., 200-300 cfs) that would have been present in fall without a targeted management action but may play an important role in passage through migratory barriers. Hence, there is a high "signal to noise" challenge with any analysis of whether salmon straying increases during flow actions.

Some of the most comprehensive data regarding adult salmon movements through Yolo Bypass was summarized by Johnston et al. (2020), who conducted telemetry studies on fish that strayed into the system during 2012-2018. This study found that around 74% of salmon that enter Yolo Bypass are successfully exited the system. This number is lower than White Sturgeon during the same period (99%), but still represents a reasonable majority of fish. However, their survival and spawning success after exiting remains unknown. As an additional source of information about straying, we compiled data on multiple factors that may cause salmon to stray and compared them with salmon catch at a fyke trap in the Yolo Bypass. Looking at this broad picture, we were unable to conclude whether the flow action has an impact on salmon straying given the absence of salmon sampling for all of the before and most of the during phases, the seasonality of salmon migration, and the complexity of various factors influencing salmon straying. Salmon straying into the bypass is likely a byproduct of many factors (as described in Figure 5-13), including some variables we may not have examined.

We also sought to understand if the flow action could negatively impact salmonid health when in the bypass due to high temperatures or low dissolved oxygen levels. We were unable to disentangle temperature from seasonal trends, but we did see an influence of flow pulses on dissolved oxygen levels. These low dissolved oxygen events appeared to occur across different flow pulse types (low- and high-flow pulses with and without managed actions; Table 5-12, Table 5-14) but oxygen levels generally returned to levels within the healthy range for adult salmonids prior to peak migration periods. Continued operation of the new Wallace Weir Fish Rescue Facility during flow pulses hopefully will build a more consistent salmon catch database to analyze

while continuing to mitigate straying by providing safe and timely passage for adult salmonids that stray into the bypass. Moreover, a long-term objective for Yolo Bypass is to construct a better fish passage structure at Fremont Weir to allow adult fish to successfully migrate upstream in a broader range of flow conditions.

6.6 Management Implications

In this synthesis study we examined hydrodynamic, habitat, and ecological responses to flow pulses in the North Delta since 2011. Assessing the ecological benefits of flow pulses, we found high-flow pulses (with and without management actions) reverse summer-fall net flow downstream restoring the North Delta to more historical hydrologic conditions. The management value of restoring more natural flow regimes is supported by a large body of literature from other areas (though pulse volumes may be much larger, Poff et al. 1997; 2010). In a particularly relevant local example, Kieranan et al. (2012) showed how restoring flows to Putah Creek over multiple years had a positive effect on the fish community. This is also consistent with Yolo Bypass research during winter and spring, which shows multiple ecological benefits of higher flow events (Sommer et al. 2001a,b; Opperman et al. 2009).

The Cache Slough Complex represents an example of an altered flow regime since substantial water diversions in the region result in net negative (upstream) flows during summer-fall. Our modeling and monitoring indicated that seasonal flow pulses, including years when we conducted management actions, resulted in increased downstream transport of water masses, a clear characteristic of more natural flow regimes. The ecological consequences of these changes are summarized below, and the more natural flow patterns are clearly an improvement over baseline conditions.

6.6.1 Adaptive Management

While adaptive management is commonly stated as a goal for resource management in the Bay-Delta (e.g., CDFW 2020), examples of major adaptive management efforts are surprisingly rare in the system (Delta ISB 2016). There are multiple reasons for this including regulatory constraints, resource availability, and a relatively low tolerance for risk given sensitive natural resources (Nagarkar and Raulund-Rasmussen 2016). The NDFS represents an

example of a large-scale adaptive management effort. Part of the appeal of the system is that it is a regionally defined area, has clear comparisons (e.g., Cache Slough Complex/Sacramento River vs. Yolo; upstream vs. downstream), and the water cost of actions are modest. The project included a range of water years, specific interventions, detailed monitoring, and synthesis. In addition, there was coordination with landowners and partners, and public outreach (e.g., media, CAMT). Our hope, therefore, is that the project helps inspire other similar focused evaluations of large-scale management actions. At the very least, the past decade of work has helped motivate future work in the North Delta. The NDFS has showed sufficient promise that it has been included in two of the recent major regulatory efforts (USFWS 2019; NMFS 2020; CDFW 2020). In future years, these adaptive management activities will be guided by the Delta Coordination Group, a team created by the recent state and federal permits. In addition, other planning efforts such as the Voluntary Agreements and Sites Reservoir design have also discussed the possibility of allocating new resources to augment Yolo Bypass flow during summer-fall.

6.6.2 Ecological Effects

A primary goal of our evaluation was to determine whether flow pulses improve downstream transport and production of lower trophic level resources. We found higher phytoplankton biomass upstream in the Yolo Bypass compared to downstream in the Cache Slough Complex and Lower Sacramento River, indicating that the Yolo Bypass contains a substantial "reservoir" of plankton biomass (Chapters 3 and 4). We found evidence that high-flow pulse events transport upstream water to downstream habitats demonstrated by changes in physical and chemical water quality metrics (Chapters 2 and 3). Data from multiple years show that flow pulses help transport phytoplankton downstream; however, the geographic extent of the influence varied substantially across years (see Chapters 3 and 4 on chlorophyll and phytoplankton). In general, there is very little downstream transport of plankton during low-flow years (e.g., 2013, 2014, 2017) compared to years when flow pulses were substantial (e.g., 2012, 2016, 2018). In the highest flow years, the degree of downstream influence was highly variable. For three of the years (2011, 2012 and 2016), there was evidence that the flow pulse led to increases in phytoplankton abundance as far downstream as Rio Vista (Frantzich et al. 2018). One of these years (2016) was a summer event when infrastructure was manipulated to generate a

managed flow pulse. Nutritious diatoms increased in biomass downstream after the 2016 managed Sacramento River flow action (Figure 4-7, Figure 4-11 to Figure 4-13), there was evidence for new copepod growth downstream (Figure 4-25), and some zooplankton taxa increased in density in the Yolo Bypass after the flow pulse (Figure 4-21, Figure 4-23B). However, these results from the 2016 high-flow event were not replicated during the fall 2018 and 2019 pulses generated by redirecting agricultural drainage water. These pulses had much lower levels of phytoplankton and did not result in detectable changes in the food web downstream of the base of Yolo Bypass. Overall, the lack of consistent findings and correlations between phytoplankton metrics and zooplankton abundance (i.e., Delta Smelt prey) suggest a mechanism model approach to evaluating the effects of flow-pulses on lower trophic responses is warranted.

As is typical for flow events in the system, pulses can have negative consequences. For example, we found that contaminant concentrations are higher in water and zooplankton during flow pulses (Chapter 3.5); however, these observations during summer and fall are consistent with contaminant measurements during winter and spring in Yolo Bypass and other parts of the system (Smalling et al. 2007; Brooks et al. 2011). Flow pulses can also result in acute periods of low dissolved oxygen (Chapter 3.3 and 5.6) in the Yolo Bypass, but levels return to baseline or increase following the pulse. An additional potential concern was whether flow pulses might result in increased straying of adult Chinook Salmon into Yolo Bypass (Johnson et al. 2020). We did not find evidence that managed flow pulses (i.e. actions) increase salmon straying (Chapter 5.6) as compared to non-managed pulses, though we acknowledge that other factors may influence straying, obscuring any effects of flow pulses. For example, large numbers of fish have historically strayed into Yolo Bypass because of exceptionally strong tidal flows at its base. A fish rescue facility at Wallace Weir was recently constructed to help address this issue, thereby reducing stranding and returning strays to the Sacramento River.

6.6.3 Recommendations

As noted above, improved summer-fall flow conditions in Yolo Bypass are desirable based on the need to offset net negative flows, thereby providing a more natural flow regime. However, the effects on the downstream food web are uneven, with relatively positive responses in three high-flow pulse events

(2011, 2012, 2016). The flow event in 2011 was unmanaged, the event in 2012 was hydrologically similar to previous NDFS managed actions, and 2016 was a planned management action. However, two other managed flow pulses (2018, 2019) showed only modest effects. The reasons for these differences in efficacy are unclear and worthy of continued investigation, implementation of future actions, and adaptive management.

Implementation and adaptive management of NDFS actions are now coordinated through the Delta Coordination Group (DCG) and structured decision-making (SDM). DWR is committed to the DCG collaborative SDM process; however, we would recommend the implementation of future managed NDFS actions for consideration in the SDM process. A high priority to consider is to conduct another summer action, redirecting Sacramento River flow, as in 2016. This management intervention showed promising ecological responses compared to other years that would benefit Delta Smelt. Based on our results we recommend the SDM process consider implementation of managed actions over the next few years (when hydrology is favorable), enhancing monitoring to increase our power to compare effects of how summer pulses (using Sacramento River flow) affect the food web differently from fall pulses (using agricultural return flow), and support the development of a mechanistic model approach to evaluate pulses. Alternative flow pulse types should also be evaluated by the DCG to determine if longer duration, but lower magnitude flows (as in 2011, see Chapter 2) create more optimal conditions for the food web (using Sacramento River and agriculture return water). Ultimately, after several more years of adaptive management, we hope to conclude if benefits from this strategy meet the goals of improving food availability for species conservation, or if the strategy should be off-ramped. It should be noted that regardless of food subsidies downstream, restoring net positive flow during the summer-fall is beneficial, and will likely enhance future habitat and food restoration efforts in the North Delta. Moreover, future improvements in infrastructure (e.g., Fremont Weir notch) and perhaps dedicated sources of environmental flows (e.g., Voluntary Agreements) could potentially provide additional options and flexibility for adaptive management in the region.

Chapter 7 Acknowledgements

We thank the DWR Ecosystem Monitoring, Research, and Reporting Branch and North Central Region Office colleagues and managers for their assistance with initial data wrangling, review, and feedback of the report. We thank our collaborators at US Geological Survey and San Francisco State University - Estuarine Ocean Science Center; the US Bureau of Reclamation, California Department of Fish and Wildlife, and State Water Contractors for support of previous actions; US Fish and Wildlife Service for their recent collaborations on NDFS; and the Interagency Ecology Program and long-term monitoring programs that provide usable datasets and metadata. Lastly, we thank the various operators, district managers, and landowners for their continued support and coordination of flow pulses in the Yolo Bypass.

Chapter 8 References

Anchor QEA LLC. 2020. Hydrodynamic modeling of the 2011 through 2019 north delta food web actions. Report to the California Department of Water Resources, Sacramento, CA.

Bates D, Maechler M, Bolker B, Walker S. 2021. lme4: Linear Mixed-Effects Models using 'Eigen' and S4. The Comprehensive R Archive Network (CRAN). https://cran.r-project.org/web/packages/lme4/index.html

Baxter R, Brown LR, Castillo G, Conrad L, Culberson SD, Dekar MP, Dekar M, Feyrer F, Hunt T, Jones K, Kirsch J. 2015. An updated conceptual model of Delta Smelt biology: our evolving understanding of an estuarine fish. Interagency Ecological Program, California Department of Water Resources.

Brooks ML, Fleishman E, Brown LR, Lehman PW, Werner I, Scholz N, Mitchelmore C, Lovvorn JR, Johnson ML, Schlenk D, van Drunick S. 2012. Life histories, salinity zones, and sublethal contributions of contaminants to pelagic fish declines illustrated with a case study of San Francisco Estuary, California, USA. Estuaries and Coasts. 35:603–621. https://doi.org/10.1007/s12237-011-9459-6

Brooks ME, Kristensen K, Van Benthem KJ, Magnusson A, Berg CW, Nielsen A, Skaug HJ, Machler M, Bolker BM. 2017. glmmTMB balances speed and flexibility among packages for zero-inflated generalized linear mixed modeling. The R journal. 9(2):378-400.

Brown LR, Komoroske LM, Wagner RW, Morgan-King T, May JT, Connon RE, Fangue NA. 2016. Coupled downscaled climate models and ecophysiological metrics forecast habitat compression for an endangered estuarine fish. PloS one. 11(1):e0146724. DOI:10.1371/journal.pone.0146724

Brown LR, Kimmerer W, Conrad JL, Lesmeister S, Mueller–Solger A. 2016. Food webs of the Delta, Suisun Bay, and Suisun Marsh: an update on current understanding and possibilities for management. San Francisco Estuary and Watershed Science. 14(3).

Brown L, Fleishman E, Culberson SD, Castillo G. 2010. Analysis of pelagic species decline in the upper San Francisco Estuary using multivariate autoregressive modeling (MAR). Ecological Applications. 20:1417-1430.

Brown T, Hieb KA. 2014. Status of the Siberian prawn, *Exopalaemon modestus*, in the San Francisco Estuary. San Francisco Estuary and Watershed Science. 12(1).

CDFG. 2010. State and Federally listed endangered and threatened animals of California. 771 California Department of Fish and Game, The Natural Resources Agency, North Highlands.

Cloern JE. 2019. Patterns, pace, and processes of water-quality variability in a long-studied estuary. Limnology and Oceanography. 64(S1):192-208.

Cloern JE, Foster SQ, Kleckner AE, 2014. Phytoplankton primary production in the world's estuarine-coastal ecosystems. *Biogeosciences*. 11:2477– 2501.

Cloern JE, Jassby AD. 2008. Complex seasonal patterns of primary producers at the land–sea interface. Ecology Letters. 11:1294-1303.

Cloern JE, Jassby AD. 2012. Drivers of change in estuarine-coastal ecosystems: Discoveries from four decades of study in san francisco bay. Reviews of Geophysics. 50(RG4001):1-33. http://dx.doi.org/10.1029/2012RG000397

Columbia Basin Research, University of Washington. 2020. SacPAS CDFW GrandTab Adult Escapement. Available from http://www.cbr.washington.edu/sacramento/data/query_adult_grandtab.html.

CFSM (Cramer Fish Sciences Modeling, Analysis, and Synthesis Lab). 2019. Yolo Bypass Telemetry Project: 2018 Final Report Prepared for the California Department of Water Resources. Auburn, California.

Dahm CN, Parker AE, Adelson AE, Christman MA, Bergamaschi BA. 2016. Nutrient dynamics of the Delta: effects on primary producers. San Francisco Estuary and Watershed Science. 14(4).

Delta Independent Science Board. 2016. Improving Adaptive Management in the Sacramento-San Joaquin Delta. Delta Stewardship Council, Sacramento, CA.

Dickerson KD, Medley KA, Havel JE. 2010. Spatial variation in zooplankton community structure is related to hydrologic flow units in the Missouri river, USA. River Research and Applications 26:605-618. https://doi.org/10.1002/rra.1268

Dugdale RC, Wilkerson FP, Hogue VE, Marchi A. 2007. The role of ammonium and nitrate in spring bloom development in San Francisco Bay. Estuarine Coastal and Shelf Science 73:17-29.

Emergency Drought Barrier on the Ecosystem of the California Delta. San Francisco Estuary and Watershed Science 17(3). https://doi.org/10.15447/sfews.2019v17iss3art2

Feyrer F, Slater SB, Portz DE, Odom D, Morgan-King T, Brown LR. 2017. Pelagic nekton abundance and distribution in the northern Sacramento–San Joaquin Delta, California. Transactions of the American Fisheries Society. 146(1):128-135. 10.1080/00028487.2016.1243577

Foe C, Knight A. 1985. The effect of phytoplankton and suspended sediment on the growth of Corbicula fluminea (Bivalvia). *Hydrobiologia*. *127*(2):105-115.

Foe C, Knight A. 1986. A thermal energy budget for juvenile *Corbicula fluminea*. American Malacological Bulletin*, Special Edition No. 2:143-150.*

Fox J, Weisberg S, Price B, Adler D, Bates D, et al. 2020. Package 'car'. An R Companion to Applied Regression. Comprehensive R Archive Network (CRAN). https://CRAN.R-project.org/package=car

Frantzich J, Sommer T, Schreier B. 2018. Physical and biological responses to flow in a tidal freshwater slough complex. San Francisco Estuary and Watershed Science. 16(1):1-26. https://doi.org/10.15447/sfews.2018v16iss1/art3

Frantzich J, Davis BE, MacWilliams M, Bever A, Sommer T. 2021. Use of a managed flow pulse as food web support for estuarine hish. San Francisco Estuary and Watershed Science (In Press).

Gearty AJ, Ignoffo TR, Slaughter AM, Kimmerer WJ. 2021. Growth and reproductive rates of the dominant copepod *Pseudodiaptomus forbesi* in response to environmental factors and habitat type in the northern San Francisco Estuary. Aquatic Ecology. 14:1-24. DOI: 10.1007/s10452-021-09863-4

Glibert PM. 2011. Long-term changes in nutrient loading and stoichiometry and their relationships with changes in the food web and dominant pelagic fish species in the San Francisco estuary, California. Reviews in Fisheries Science 18(2):211-232.

Hahn PKJ, Bailey RE, and Ritchie A. 2007. "Field Protocols: Beach Seining." Salmonid Field Protocols Handbook: Techniques for Assessing Status and Trends in Salmon and Trout Populations, Johnson DH, Shrier BM, O'Neal JS, Knutzen JA, Augerot X, O'Neil TA, and Pearsons TN, Published by the American Fisheries Society in association with State of the Salmon. P. 267-324 doi: https://doi.org/10.47886/9781888569926.

Hammock BG, Moose SP, Solis SS, Goharian E, Teh SJ. 2019. Hydrodynamic modeling coupled with long-term field data provide evidence for suppression of phytoplankton by invasive clams and freshwater exports in the San Francisco Estuary. Environmental management. 63(6):703-717.

Hammock BG, Slater SB, Baxter RD, Fangue NA, Cocherell D, Hennessy A, Kurobe T, Tai CY, Teh SJ. 2017. Foraging and metabolic consequences of semi-anadromy for an endangered estuarine fish. PloS one. 12(3):e0173497. 10.1371/journal.pone.0173497

Hammock BG, Hartman R, Slater SB, Hennessy A, Teh SJ. 2019. Tidal wetlands associated with foraging success of Delta Smelt. Estuaries and Coasts. 42(3):857-67. 10.1007/s12237-019-00521-5

Hartman RK, Rasmussen N, Wells E, Stewart AJ, Burdi CE, Sommer T. 2021. Interagency Ecological Program: Water quality, fish, phytoplankton, clams and zooplankton monitoring to support the Summer-Fall Suisun Marsh Salinity Control Gates Action 2018-2020 ver 1. Environmental Data Initiative. https://doi.org/10.6073/pasta/ab2fd5349925a9d28b289566a7686905 (Accessed 2021-09-27).

ICF. 2020. Effects of South Delta Temporary Barriers on Dissolved Oxygen and Water Quality. June. (ICF 00554.18.) Sacramento, CA. Prepared for California Department of Water Resources, Sacramento, CA.

Interagency Ecological Program (IEP), McKenzie R, Speegle J, Nanninga J, Cook JR, Hagen J, Mahardja B. 2020. Interagency Ecological Program: Over four decades of juvenile fish monitoring data from the San Francisco Estuary, collected by the Delta Juvenile Fish Monitoring Program, 1976-2019 ver 4. Environmental Data Initiative.

Interagency Ecological Program (IEP), Schreier B, Davis B, Ikemiyagi N. 2018. Interagency Ecological Program: Fish catch and water quality data from the Sacramento River floodplain and tidal slough, collected by the Yolo Bypass Fish Monitoring Program. Environmental Data Initiative.

Jassby AD, Cloern JE, Cole BE. 2002. Annual primary production: Patterns and mechanisms of change in a nutrient-rich tidal ecosystem. Limnology and Oceanography. 47(3):698-712.

Jassby AD. 2005. Phytoplankton Regulation in a Eutrophic Tidal River (San Joaquin River, California). San Francisco Estuary and Watershed Science, 3(1).

Johnston M, Frantzich J, Espe MB, Goertler P, Singer G, Sommer T, Klimley AP. 2020. Contrasting the migratory behavior and stranding risk of White Sturgeon and Chinook Salmon in a modified floodplain of California. Environmental Biology of Fishes. 103(5):481-93.

Jungbluth M, Lee C, Patel C, Ignoffo T, Bergamaschi B, Kimmerer W. 2021. Production of the Copepod *Pseudodiaptomus forbesi* Is Not Enhanced by Ingestion of the Diatom *Aulacoseira granulata* During a Bloom. Estuaries and Coasts. 44(4):1083-99. 10.1007/s12237-020-00843-9

Kassambara A. 2021. Package rstatix: Pipe-Friendly Framework for Basic Statistical Tests. Version 0.7.0. Comprehensive R Archive Network (CRAN). https://rpkgs.datanovia.com/rstatix/

Kuivila K, Hladik, M. 2008. Understanding the Occurrence and Transport of Current-use Pesticides in the San Francisco Estuary Watershed. *San Francisco Estuary and Watershed Science*, 6(3). doi:https://doi.org/10.15447/sfews.2008v6iss3art2

Kiernan JD, Moyle PB, Crain PK. (2012). Restoring native fish assemblages to a regulated California stream using the natural flow regime concept. Ecological Applications. 22:1472-1482. https://doi.org/10.1890/11-0480.1

Kimmerer WJ. 2002. Effects of freshwater flow on abundance of estuarine organisms: physical effects or trophic linkages? Marine Ecology Progress Series 243:39-55.

Kimmerer W, Wilkerson F, Downing B, Dugdale R, Gross ES, Kayfetz K, Khanna S, Parker AE, Thompson J. 2019. Effects of drought and the emergency drought barrier on the ecosystem of the California Delta. San Francisco Estuary and Watershed Science. 17(3).

Kimmerer WJ, Lougee L. 2015. Bivalve grazing causes substantial mortality to an estuarine copepod population. Journal of Experimental Marine Biology and Ecology. 473:53-63.

Kimmerer W, Ignoffo TR, Bemowski B, Modéran J, Holmes A, Bergamaschi B. 2018. Zooplankton Dynamics in the Cache Slough Complex of the Upper San Francisco Estuary. San Francisco Estuary and Watershed Science 16. 10.15447/sfews.2018v16iss3art4

Lasko GR, Titus RG, Ferreira JR, Coleman RM. 2014. Straying of late-fall run Chinook salmon from the Coleman National Fish Hatchery into the lower American River, California. California Fish and Game 100(4):665-682. https://nrm.dfg.ca.gov/FileHandler.ashx?DocumentID=99281

Lehman PW, Sommer T, Rivard L. 2008. The influence of floodplain habitat on the quantity and quality of riverine phytoplankton carbon produced during the flood season in San Francisco Estuary. Aquatic Ecology. 42:363-378.

Lehman PW, Kurobe T, Lesmeister S, Baxa D, Tung A, The SJ. 2017. Impacts of the 2014 severe drought on the *Microcystis* bloom in San Francisco Estuary. Harmful Algae 63(Supplement C):94-108. https://doi.org/10.1016/j.hal.2017.01.011

Lenth RV, Buerkner P, Herve M, Love J, Reibl H, Singmann H. 2020. Package 'emmeans'. Estimated Marginal Means, aka Least-Squares Means. Version 1.6.2. Comprehensive R Archive Network, CRAN. https://cran.r-project.org/web/packages/emmeans/index.html

Lopez CB, Cloern JE, Schraga TS, Little AJ, Lucas LV, Thompson JK, Burau JR. 2006. Ecological values of shallow-water habitats: Implications for the restoration of disturbed ecosystems. Ecosystems. *9*(3): 422-440.

Lotze HK, Lenihan HS, Bourque BJ, Bradbury RH, Cooke RG, Kay MC, Kidwell SM, Kirby MX, Peterson CH, Jackson JBC. 2006. Depletion, degredation, and recovery potential of estuaries and coastal seas. American Association for the Advancement of Science. 312(5781):1806-1809. http://dx.doi.org/10.1126/science.1128035

Lucas LV, Cloern JE, Thompson JK, Stacey MT, Koseff JR. 2016. Bivalve grazing can shape phytoplankton communities. Frontiers in Marine Science. 3:14.

Lucas LV, Thompson JK. 2012. Changing restoration rules: Exotic bivalves interact with residence time and depth to control phytoplankton productivity. Ecosphere. 3(12):117. http://dx.doi.org/10.1890/ES12-00251.1

Mac Nally R, Thomson J, Kimmerer W, Feyrer F, Newman K, Sih A, Bennett W, Brown L, Fleishman E, Culberson S, Castillo G. 2010. An analysis of pelagic species decline in the upper San Francisco Estuary using multivariate autoregressive modelling (MAR). Ecol Appl 20(5):1417–1430. doi: http://dx.doi.org/10.1890/09-1724.1

Mahardja B, Hobbs JA, Ikemiyagi N, Benjamin A, Finger A. 2019. Role of freshwater floodplain-tidal slough complex in the persistence of the endangered delta smelt. Plos ONE. 14(1):e0208084. 10.1371/journal.pone.0208084

McKenzie R, Mahardja B. 2021. Evaluating the Role of Boat Electrofishing in Fish Monitoring of the Sacramento–San Joaquin Delta. San Francisco Estuary and Watershed Science 19(1). https://doi.org/10.15447/sfews.2021v19iss1art4

Miner CM, Jacinto E, Holmes A, Cocherell DE, Baird SE, Schreier AM, Fangue NA, Rypel AL. 2020. Origin and Abundance of Chinook Salmon in Putah Creek: Annual Report to Solano County Water Agency. Department of Wildlife, Fish & Conservation Biology, University of California, Davis.

Moyle PB, Hobbs JA, Durand JR. 2018. Delta smelt and water politics in california. American Fisheries Society, Fisheries Magazine. 43(1). https://doi.org/10.1002/fsh.10014|

Moyle, PB. Inland fishes of California: revised and expanded. Univ of California Press, 2002.

Müller-Solger AB, Jassby AD, Müller-Navarra DC. 2002. Nutritional quality of food resources for zooplankton (Daphnia) in a tidal freshwater system (Sacramento-San Joaquin River Delta). Limnology and Oceanography. 47(5):1468-76.

Mueller–Solger A. 2001. First observation of an exotic water flea, Daphnia lumholtzi, in the Delta. IEP Newsletter 14(3):12–15. http://www.water.ca.gov/iep/newsletters/2001/IEPNewsletterSummer2001.pdf

Nagarkar M, Raulund-Rasmussen K. 2016. An appraisal of adaptive management planning and implementation in ecological restoration case studies from the San Francisco Bay Delta, USA. Ecology and Society 21(2).

Nichols FH, Cloern JE, Luoma SN, Peterson DH. 1986. The modification of an estuary. Science. 231:567-573. http://dx.doi.org/10.1126/science.231.4738.567

NMFS (National Marine Fisheries Service). 2008. "Anadromous Salmonid Passage Facility Design". NMFS, Northwest Region, Portland, Oregon.

NMFS (National Marine Fisheries Service). 2019. Biological Opinion on Long-term Operation of the Central Valley Project and the State Water Project, October 2019.

Ogle D, Doll J, Wheeler P, Dinno A. 2021. Package FSA: Simple Fisheries Stock Assessment Methods. Version 0.9.1. Comprehensive R Archive Network (CRAN). https://cran.r-project.org/package=FSA

Oksanen J, Blanchet FG, Kindt R, Legendre P, Minchin PR, O'Hara RB, Simpson GL, Solymos P. 2020. Community Ecology Package "vegan". Comprehensive R Archive Network (CRAN). https://cran.r-project.org/web/packages/vegan/index.html

Opperman JJ, Galloway GE, Fargione J, Mount JF, Richter BD, Secchi S. 2009. Sustainable floodplains through large-scale reconnection to rivers. Science. 326(5959):1487-1488.

Orlando JL, Parsia MD, Sanders C, Hladik M, Frantzich J. 2020. Pesticide Concentrations Associated with Augmented Flow Pulses in the Yolo Bypass and Cache Slough Complex, California. U.S. Geological Survey Open File Report 2020-1076.

Parker AE, Dugdale RC, Wilkerson FP. 2012. Elevated ammonium concentrations from wastewater discharge depress primary productivity in the Sacramento River and the Northern San Francisco Estuary. Marine Pollution Bulletin. 64(3): 574-586.

Poff NL, Allan JD, Bain MB, Karr JR, Prestegaard KL, Richter BD, Sparks RE, Stromberg JC. 1997. The natural flow regime: a paradigm for river conservation and restoration. BioScience. 47:769-784.

Poff NL, Zimmerman JKH. 2010. Ecological responses to altered flow regimes: a literature review to inform environmental flows science and management. Freshwater Biology. 55:194–205.

R Core Team. 2020. R: A language and environment for statistical computing. R Foundation for Statistical Computing, Vienna, Austria. URL https://www.R-project.org/.

Richter A, Kolmes SA. 2005. Maximum temperature limits for Chinook, Coho, and Chum salmon, and steelhead trout in the Pacific Northwest. Reviews in Fisheries Science. 13(1):23-49. DOI: https://doi.org/10.1080/10641260590885861

Ripley B, Venables B, Bates DM, Hornik K, Gebhardt A. 2015. Package MASS, Support Functions and Datasets for Venables and Ripley's MASS. R Project. CRAN. http://www.stats.ox.ac.uk/pub/MASS4/

Schoups G, Hopmans JW, Young CA, Vrugt JA, Wallender WW, Tanji KK, Panday S. 2005. Sustainability of irrigated agriculture in the San Joaquin Valley, California. Proceedings of the National Academy of Sciences 102:15352-15356.

Service RF. 2007. Delta blues, california style. wwwsciencemagorg. AAAS. 442 445.

Slater SB, Baxter RD. 2014. Diet, prey selection and body condition of age-0 Delta Smelt, *Hypomesus transpacificus*, in the upper San Francisco Estuary. San Francisco Estuary and Watershed Science 14. 10.15447/sfews.2014v12iss3art1

Smalling KL, Orlando JL, Kuivila KM. 2007. Occurrence of Pesticides in Water, Sediment, and Soil from the Yolo Bypass, California. San Francisco Estuary and Watershed Science. 5(1). http://dx.doi.org/10.15447/sfews.2007v5iss1art2

Sturrock AM, Satterthwaite WH, Cervantes-Yoshida KM, Huber ER, Sturrock HJ, Nusslé S, Carlson SM. 2019. Eight decades of hatchery salmon releases in the California Central Valley: factors influencing straying and resilience. Fisheries. 44(9):433-444.

Sommer TR, Harrell WC, Solger AM, Tom B, Kimmerer W. 2004. Effects of flow variation on channel and floodplain biota and habitats of the sacramento river, california, USA. Aquatic Conservation-Marine and Freshwater Ecosystems. 14(3):247-261. http://dx.doi.org/10.1002/aqc.620

Sommer TR, Armor C, Baxter RD, Breuer R, Brown LR, Chotkowski M, Culberson S, Feyrer F, Gingras M, Herbold B et al. 2007. The collapse of pelagic fishes in the upper San Francisco Estuary. Fisheries. 32(6):270-277. http://dx.doi.org/10.1577/1548-8446(2007)32[270:TCOPFI]2.0.CO;2

Sommer T, Mejia F. 2013. A place to call home: A synthesis of delta smelt habitat in the upper san francisco estuary. San Francisco Estuary and Watershed Science. 11(2). https://doi.org/10.1371/journal.pone.0234673

Sommer T, Schreier B, Conrad JL, Takata L, Serup B, Titus R. 2020. Farm to fish: Lessons from a multi-year study on agricultural floodplain habitat. San Francisco Estuary and Watershed Science. 18(3). https://doi.org/10.15447/sfews.2020v18iss3art4

Sommer TR, Harrell WC, Feyrer F. 2014. Large-bodied fish migration and residency in a flood basin of the Sacramento River, California, USA. Ecology of Freshwater Fish. 23:414-423.

Thomson JR, Kimmerer WJ, Brown LR, Newman KB, Mac Nally R, Bennett WA, Feyrer F, Fleishman E. 2010. Bayesian change point analysis of abundance trends for pelagic fishes in the upper san francisco estuary. Ecological Applications. 20(5):1431-1448. http://dx.doi.org/10.1890/09-0998.1

Twardochleb L, Maguire A, Dixit L, Bedwell M, Orlando J, MacWilliams M, Bever A, Davis B. 2021. North Delta Food Subsidies Study: Monitoring Food Web Responses to the North Delta Flow Action, 2019 Report. Department of Water Resources, Division of Environmental Services.

USFWS (United States Fish and Wildlife Service), Johnston C, Lee S, Mahardja B, Speegle J, Barnard D. 2019. U.S. Fish and Wildlife Service: San Francisco Estuary Enhanced Delta Smelt Monitoring Program data, 2016-2019 ver 1. Environmental Data Initiative. 10.6073/pasta/98bce400502fae3a6b77b3e96f6d51e7

USFWS (United States Fish and Wildlife Service). 2019. Biological Opinion for the Reinitiation of Consultation on the Coordinated Operations of the Central Valley Project and State Water Project, October 2019.

US Bureau of Reclamation [USBR]. 2019. Directed Outflow Project Technical Report 1. Available from https://www.usbr.gov/mp/bdo/index.html

van Wijngaarden RP, Belgers DJ, Zafar MI, Matser AM, Boerwinkel MC, Arts GH. 2014. Chronic aquatic effect assessment for the fungicide azoxystrobin. Environ Toxicol Chem. 33(12):2775–2785. doi: 10.1002/etc.2739.

Whitley SN, Bollens SM. 2014. Fish assemblages across a vegetation gradient in a restoring tidal freshwater wetland: diets and potential for resource competition. Environmental Biology of Fishes 97:659-674.

Willmes M, Jacinto EE, Lewis LS, Fichman RA, Bess Z, Singer G, Steel A. et al. 2021. Geochemical tools identify the origins of Chinook Salmon returning to a restored creek. Fisheries. 46(1): 22-32. https://doi.org/10.1002/fsh.10516

Wilkerson FP, Dugdale RC, Hogue VE, Marchi A. 2006. Phytoplankton Blooms and Nitrogen Productivity in San Francisco Bay. Estuaries and Coasts. 29(3):401-416.

Winder M, Jassby AD. 2011. Shifts in zooplankton community structure: implications for food web processes in the upper San Francisco Estuary. Estuaries and Coasts*. 34*(4):675-690.

Wofsy SC. 1983. A simple model to predict extinction coefficients and phytoplankton biomass in eutrophic waters. *Limnol. Oceanogr*. 28:1144–1155.

Worm B, Barbier EB, Beaumont N, Emmett Duffy J, Folke C, Halpern BS, Jackson JBC, Lotze HK, Micheli F, Palumbi SR et al. 2006. Impacts of biodiversity loss on ocean ecosystem services. Science. 314(5800). https://doi.org/10.1126/science.1132294

Yoshiyama RM, Fisher FW, Moyle PB. 1998. Historical abundance and decline of chinook salmon in the Central Valley region of California. North American Journal of Fisheries Management. 18(3):487-521.

Young M, Howe E, O'Rear T, Berridge K, Moyle P. 2021. Food Web Fuel Differs Across Habitats and Seasons of a Tidal Freshwater Estuary. Estuaries and Coasts. 44(1):286-301.

Chapter 9 Appendices

Appendix A: Operations During Flow Actions

Appendix B: Pesticides in Water and Zooplankton

Appendix C: Discrete Water Quality

Appendix D: Fish Analyses

Appendix E: Lower Trophic Analyses

Appendix F: Conceptual Summary of Flow Pulses

*Chapter 9 Appendices are provided in a separate document.